Naphthalimide, naphthaldehyde and benzaldehyde based fluorescent materials: Synthesis of 1,2-disubstituted ferrocenes from ferrocenyl *p*-tolyl sulphoxide

By

Ramu V Ranga Naidu Chinta

CHEM11201504005

National Institute of Science Education and Research,

Bhubaneswar, Odisha

A thesis submitted to the
Board of Studies in Chemical Sciences
In partial fulfillment of requirements
for the Degree of

DOCTOR OF PHILOSOPHY

Of

HOMI BHABHA NATIONAL INSTITUTE

July, 2020

Homi Bhabha National Institute [1]

Recommendations of the Viva Voce Committee

As members of the Viva Voce Committee, we certify that we have read the dissertation prepared by **Ramu V Ranga Naidu Chinta** entitled "**Naphthalimide, naphthaldehyde and benzaldehyde based fluorescent materials: Synthesis of 1,2-disubstituted ferrocenes from ferrocenyl *p*-tolyl sulphoxide**" and recommend that it may be accepted as fulfilling the thesis requirement for the award of Degree of Doctor of Philosophy.

Chairman-	Prof. A. Srinivasan	Date: 26/11/2020
Guide/ Convener-	Dr. V. Krishnan	Date: 26/11/2020
Examiner-	Prof. K. Muralidharan	Date: 26/11/2020
Member 1-	Dr. S. Peruncheralathan	Date: 26/11/2020
Member 2-	Dr. Bhargava B.L.	Date: 26/11/2020
Member 3-	Dr. Prafull Singru.	Date: 26/11/2020

Final approval and acceptance of this thesis is contingent upon the candidate's submission of the final copies of the thesis to HBNI.

I hereby certify that I have read this thesis prepared under my direction and recommend that it may be accepted as fulfilling the thesis requirement.

Date: 26/11/ 2020

Place: Bhubaneswar

(Dr. V. Krishnan)

Guide

STATEMENT BY AUTHOR

This dissertation has been submitted in partial fulfillment of requirements for an advanced degree at Homi Bhabha National Institute (HBNI) and is deposited in the Library to be made available to borrowers under rules of the HBNI.

Brief quotations from this dissertation are allowable without special permission, provided that accurate acknowledgement of source is made. Requests for permission for extended quotation from or reproduction of this manuscript in whole or in part may be granted by the Competent Authority of HBNI when in his or her judgment the proposed use of the material is in the interests of scholarship. In all other instances, however, permission must be obtained from the author.

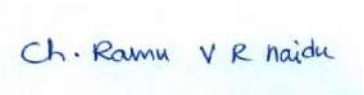

Ramu V Ranga Naidu Chinta

DECLARATION

I, hereby declare that the investigation presented in the thesis has been carried out by me. The work is original and has not been submitted earlier as a whole or in part for a degree / diploma at this or any other Institution / University.

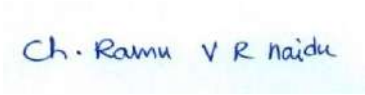

Ramu V Ranga Naidu Chinta

LIST OF PUBLICATIONS

Published

1. ***Ranga Naidu Chinta, R. V.**; Aradhyula, B. P. R; Murali, A. C; Venkatasubbaiah, K. Synthesis, photophysical and electrochemical properties of naphthaldimine based boron complexes. *J. Organomet. Chem.* **2019,** *891*, 20-27.
2. *****Sathesh, V.[1]; **Ranga Naidu Chinta, R. V.**[1]; Mamidala, R.; Mukundam, V.; Dhanunjayarao, K.; Venkatasubbaiah, K. Mercuration of ferrocenyl- *p* -tolyl sulfoxide and its conversion to 1,2-disubstituted ferrocenes. *J. Organomet. Chem.* **2017**, *853*, 74-80. (†equal contribution)
3. *****Aradhyula, B. P. R[1].; **Ranga Naidu Chinta, R. V.**[1]; Dhanunjayarao, K; Venkatasubbaiah, K. *RSC Advances*. **2020**, *10*, 13149-13154. (†equal contribution)
4. Dhanunjayarao, K; Mukundam, V; **Ranga Naidu Chinta, R. V.**;Venkatasubbaiah, K, Synthesis of highly fluorescent imidazole based diboron complex. *J. Organomet. Chem.* **2018,** *865*, 234-238.

Manuscript under preparation

1. ***Ranga Naidu Chinta, R. V.**; Venkatasubbaiah, K. Synthesis, photophysical and electrochemical properties of functionalization on the boron centre: Naphthalimide imidazole boron complexes. (Manuscript under preparation).
2. ***Ranga Naidu Chinta, R. V.**; Venkatasubbaiah, K. Synthesis and characterization of tetraaryl substituted imidazole based boron polymer. (Manuscript under preparation)

* Pertaining to thesis.

Conferences

1. Synthesis, characterization and photophysical properties of naphthalene salicyladimine-based tetra coordinate di boron complexes. **Ranga Naidu Chinta, R. V**.; Dhanunjayarao, K. Venkatasubbaiah, K. In Modern Trends in Inorganic Chemistry (MTIC) held at CSIR-NCL, Pune and IISER, Pune during 11^{th}-14^{th} December 2017 (**Poster presentation).**
2. Mercuration of ferrocenyl-*p*-tolyl sulfoxide and its conversion to 1,2-disubstituted ferrocenes. Sathesh, V.[1], **Ranga Naidu Chinta, R. V**[1], Ramesh, M.; Mukundam, V.; Dhanunjayarao, K. Venkatasubbaiah, K. In inter IISER & NISER CHEMISTRY MEET (IINCM-2017) held on (22-24)th December 2017 at NISER Bhubaneswar, India (**Poster presentation**).
3. Synthesis, characterization and photophysical properties of naphthaldimine based-tetra coordinate diboron and highly fluorescent imidazole based diboron complexes. **Ranga Naidu Chinta, R. V**.; Dhanunjayarao, K. Venkatasubbaiah, K. In ACS on campus held on 23^{rd} july, 2018 at NISER Bhubaneswar, India (**Poster presentation**).

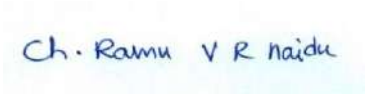

Ramu V Ranga Naidu Chinta

Dedicated to my family

ACKNOWLEDGEMENTS

I would like to express my sincere gratitude to my supervisor ***Dr. V. Krishnan*** *for his patient guidance, insightful advice and invaluable encouragementsthroughout my time as his student.*

I am thankful to ***Prof. Sudhakar panda****, Director, NISER and also* ***Prof. T. K. Chandrashekar****,* ***Prof. V. Chandrashekar*** *Founder-Directors, NISER for providing the laboratory facilities, CSIR-New Delhi for financial support.*

I would like to thank my thesis monitoring committee members ***Prof. A. Srinivasan, Dr. Bhargava B.L., Dr. S. Peruncheralathan, Dr. Praful singru*** *all other faculties in SCS NISER for their useful suggestions and* ***Dr. Upakarasamy Lourderaj, Dr. Arun Kumar*** *support on several occasions.*

I sincerely thank ***Dr. Mriganka, Mr. Deepak****,* ***Mr. Sanjaya,*** *and* ***Mr. Amit*** *forrecording the single crystal X-Ray, NMR and Mass spectral analysis.*

I am greatly indebted to ***all my teachers*** *of school (****P. Rarisinaidu sir, G. Satyannarayana sir, Baburao sir****) graduation (****Raghu sir****) and post-graduation who inculcated knowledge, discipline and encouragement.*

It gives me immense pleasure to thank all those seniors, friends and juniors who made my life at NISER really enjoyable and memorable. Special mention must be made of my labmates ***Dr. Dhanunjayarao. K, Dr. Ramesh. M, Dr. Mukundam. V, Dr. Sathish. V, Dr. Aradyula B. P. R, Dr. Joseph. P, Shreenibasa, Samser, Siva, Prakash, Priyabrata, Murali, sushanta, Ashutosh, Tharun, Sanket, Preeta, Omkar, Arihanth, Anjali, pratiksha, Bastab*** *for their support and special thanks to my seniors* ***Dr. Adhinarayana. B, Dr. Pardhasaradhisata, Dr. Chandrasekhar Reddy. G, Dr. Venkateswera rao. M.*** *Also I thank* ***Dr. Suhas. S. G, Sangya, Dr. Khokan. C, Dr. Pankaj. K, Dr. Minakdas, Dr. Dipakkumar. S, Dr. Bratati. P, Dr. Arindam. G, Dr. Narasing, Bibhu, Subhayan*** *for their help.*

I am greatly thankful to my life partner ***Rajani*** *for her understanding, support, encouragement, quite patience and unwavering love.*

I am deeply grateful to my beloved ***Amma, Nanna*** *for their unconditional love, support, sacrifices, blessings and inspiration throughout my career.*

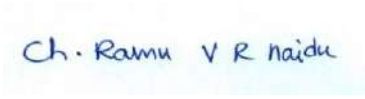

Ramu V Ranga Naidu Chinta

CONTENTS

SUMMARY

The first part of this chapter describes a brief introduction of fluorescent boron compounds. The boron based fluorescent materials classified as tri- and tetra-coordinated boron complexes (Figure 1). The vacant pz- orbital of boron atom stabilizes by adjacent aryl substituent groups in their tri coordinated boron systems. Stable tri-coordinated boron complexes are produced using the following strategies: 1) Introduction of electron releasing groups ER*n*; 2) Steric shielding by the attachment of bulky groups such as mesityl, 1,3,5-triisopropyl benzene, 1,3,5-tris(trifluoromethyl)benzene and these groups can also hinders the π-stacking of the molecules in the solid state and 3) Structural constraint by incorporation of the boron atom at a central site.

In the tri-coordinated boron compounds, the empty pz- orbital overlap with organic π-system which results exciting optoelectronic properties and enable for the detection of other anions such as fluoride and cyanide. In contrary the four-coordinated boron compounds show, better stability towards thermal, moisture and air over tri-coordinate boron compounds, even if not belong to those three strategies mentioned before. According to the chelating donor atoms, the tetra coordinate boron compounds can be classified as *N,O*-, *N,N*-, *N,C*-, and *O,O*-chelate. Among them *N,N*-chelated tetra coordinated boron complexes the dipyrromethene (BODIPY) [7] pigments have been studied extensively as these dyes are particularly used in applications as labelling reagents, laser dyes, chemo sensors, fluorescent switches and near infrared emitting materials. Narrow stokes shift and low luminescent quantum yields in the solid state limits their applications in organic light emitting diodes (OLED) and as soon.[4-6] To overcome these drawbacks different tetra coordinated boron fluorophores

have been synthesized. The strategies used in the literature will be discussed in this part.

Second part of this chapter describes a brief introduction of different probes (or) sensors for the detection of fluoride ion. Fluoride ion is one of the smallest used for the treatment of osteoporosis in human health[8]. However high doses of fluoride ion causes dental, skeletal fluorosis and many fatal diseases in human and animals,[9] hence, most of the countries focussed on control of fluoride ion consumption. Over the last few decades, large number of probes or sensors have been developed for the detection of fluoride ion, however many of them suffers from low selectivity. It is important to develop sensors with high selectivity and sensitivity[10]. In this part I will discuss about recent development in this area.

The third part of this chapter describes a brief introduction of planar chiral ferrocene derivatives. Ferrocene and its derivatives gained interest owing to their applications in material chemistry, biological studies and catalysis. Different approaches have been utilized to make planar chiral ferrocenes (Figure 2). Since the pioneering work of Ugis diastereoselective method to generate planar chirality, numerous chiral ligands based on ferrocene have been developed[11-12]. In this part of chapter, I will present different planar chiral ferrocenes reported in the literature.

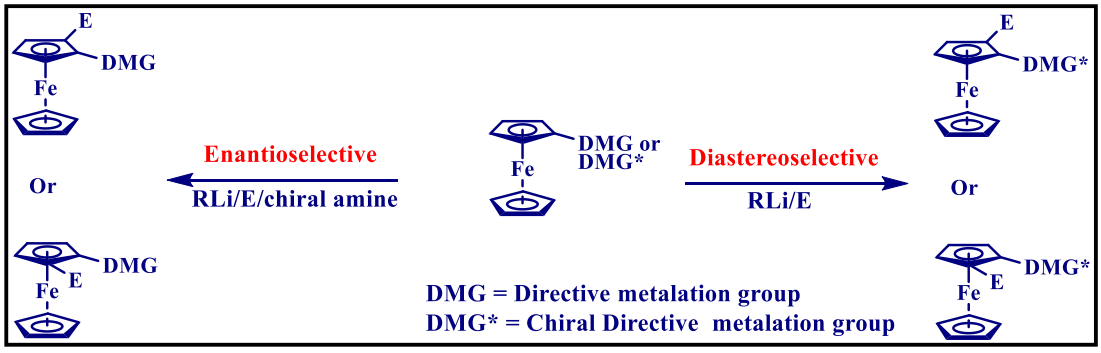

Figure: Different approaches to the synthesis of planar chiral ferrocenes.

List of tables

List of schemes

List of figures

Thesis Highlight

Name of the Student: RAMU V RANGA NAIDU CHINTA

Name of the CI/OCC: NISER **Enrolment No.: CHEM11201504005**

Thesis Title: Naphthalimide, naphthaldehyde and benzaldehyde based fluorescent materials: Synthesis of 1,2-disubstituted ferrocenes from ferrocenyl *p*-tolyl sulphoxide

Discipline: Chemical Science **Sub-Area of Discipline: Organometallics**

Date of viva voce: 26.11.2020

Innovative organic luminescent fluorophores have attracted much attention due to their numerable applications in biological as well as in optoelectronic devices. Incorporation of main-group elements into the framework of organic fluorophores has provided a new opportunity to tune the optical properties of the fluorophores. Among the many main-group incorporated fluorophores, boron-based fluorophores such as boron-dipyrromethene (BODIPY) as well as N∩O; N∩N and N∩C chelates with different ligands have gained much interest due to their attractive photo physical properties. This thesis is predominantly engrossed on such analogs. This thesis highlights the synthesis of (a) N,O-chelated naphthaldehydimine based boron complexes form their schiffbase ligands, (b) 2-butyl-5-hydroxy-6-(1,4,5-triphenyl-1H-imidazole-2-yl)-1H-benzo[de]isoquinoline-1,3(2H)-dione based *N,O*-chelated born complexes, (c) ESIPT based polymers of 2-hydroxyl-substituted tetra phenyl imidazole's and incorporation of diphenyl boron, (d) synthesis and characterization of poly(tetraphenylimidazole)s and their application in the detection of fluoride ions.

In the last part of the thesis, synthesis of 1-(aryl)-2-(p-tolylsulfinyl)ferrocenes using direct mercuration of ferrocenyl *p*-tolyl sulfoxide followed by palladium catalyzed cross-coupling of 1-(p-tolylsulfinyl)-2-(chloromercurio) ferrocene and aryl halides especially aryl iodides is described. (Figure 1).

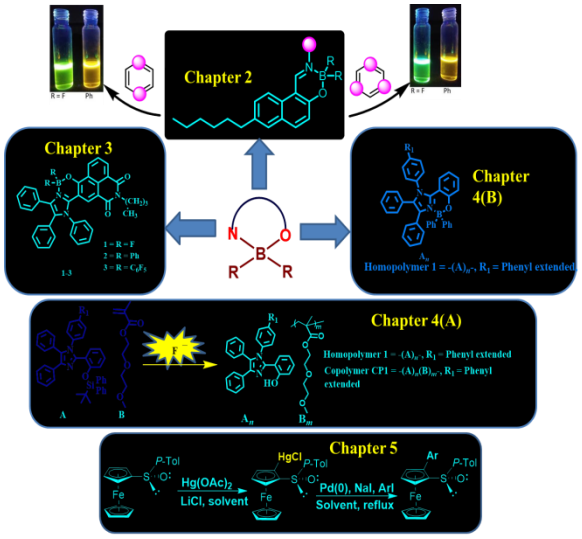

Figure 1. Representative examples of tertra coordinated boranes, fluoride ion sensing materials and synthesis of 1,2-disubstituted ferrocenes from ferrocenyl p-tolyl sulphoxide highlighted in the thesis.

Overall, the thesis describes the synthesis and tuning photophysical properties of Naphthalimide, naphthaldehyde and benzaldehyde based fluorescent materials and synthesis of 1,2-disubstituted ferrocenes from ferrocenyl *p*-tolyl sulphoxide.

1 Introduction:

This thesis deals with a) fluorescent boron compounds b) fluorescent probes for fluoride ion detection and c) planar chiral ferrocenyl compounds. A brief summary of the relevant literature is presented in this chapter.

1.1 Fluorescent Boron compounds.

Organic emissive molecules or fluorophores have drawn increasing attention due to their applications in organic light-emitting devices (OLED), nonlinear optics, organic field effect transistors (OFETs), biomolecular probes, organic solid-state lasers (OSLs), fluorescent sensors, etc[1-6]. It has been realized that incorporation of boron atom into organic framework offer development of new functional materials, with better electronic properties & stability. In general, fluorescent boron compounds have been classified into two groups, namely i) tri-coordinate boron compounds ii) tetra-coordinate boron compounds (Figure **1.1**)

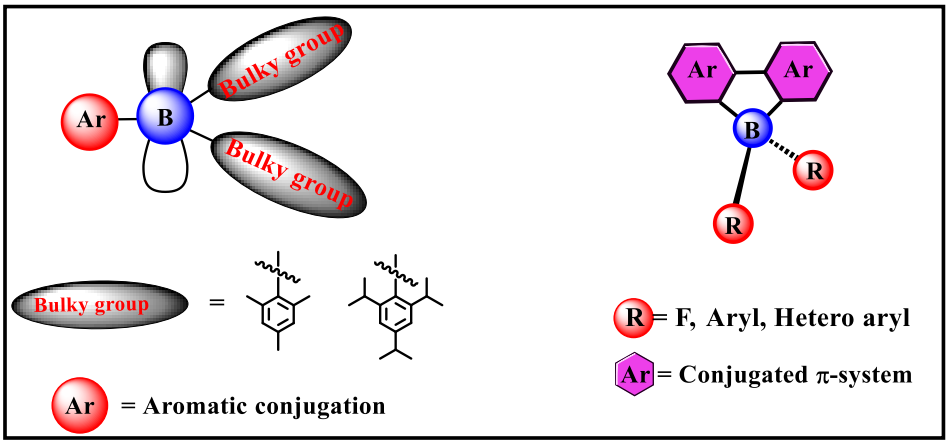

Figure 1.1: Schematic pictures of (left) tri-coordinate boron; (right) tetra-coordinate boron compounds

1.1.1 Tri-coordinate boron compounds

In general, three coordinate boron compounds are Lewis acidic due to the presence of empty pz- orbital. The presence of empty p-orbital on the boron center

makes these compounds as excellent π-accepters, which can provide significant delocalisation when conjugated with organic π-system. Owing to the vacant coordination site on the boron center, these compounds prone to attacked by Lewis bases like water, which leads bond cleavage or formation of four coordinate boron species. Stabilisation of tri-coordinated boron complexes have been made possible by use of sterically crowded aromatic groups such as mesityl, fluoro mesityl, triisopropyl phenyl (or) by use of π-donor substituents like alkoxy groups.

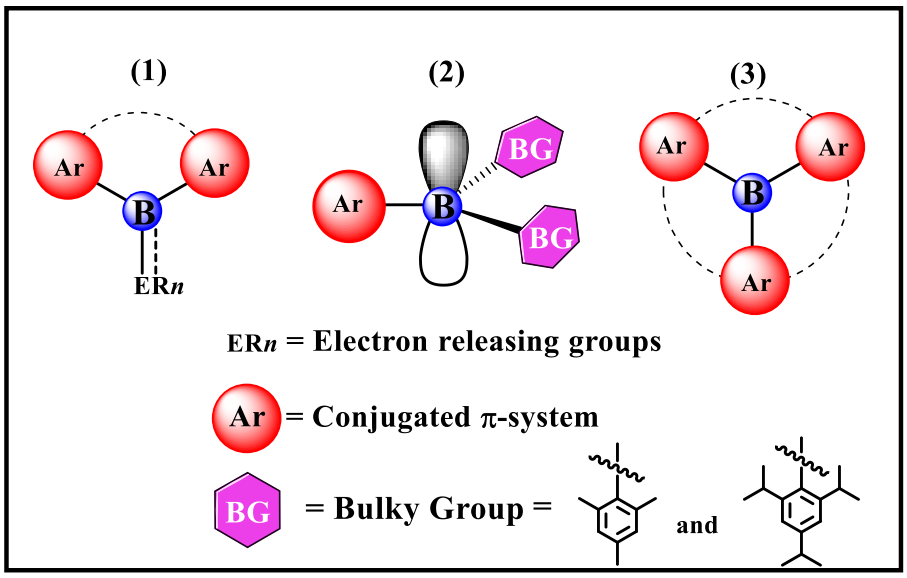

Figure 1.2: Schematic pictures of three bench-stable tri aryl boranes.

The tri-coordinated boron compounds thus obtained showed potential application in organic light emitting diodes (OLEDs), organic field effect transistors (OFETs), as sensors and as fluorescent indicators in bio imaging[7-11].

1.1.2 Tetra-coordinate boron compounds

A general representation of tetra coordinate boron compounds with π-conjugated chelate is shown in figure **1.1**. The drawbacks of tris(8-hydroxyquinolinato) aluminium (Alq_3) in optoelectronics,[12] forced researchers to

develop four coordinated boron complexes. Tetra-coordinate boron complexes can be easily tuned to get the desired luminescence and high carrier mobility which can be used in optoelectronics such as organic light-emitting diodes (OLEDs),[13-15] sensory,[16-18] organic field effect transistors[19], and imazing materials[20]. In general the chelate ligand in tetra coordinate boron compounds is mono anionic in nature which helps to produce charge neutral boron compounds. As a consequence of chelation to boron, the π-conjugation of the chelate is reinforced. Such rigid π-conjugated molecular structures not only enhances the emission intensity but also decreases the electronic state of lowest unoccupied molecular orbitals (LUMO) level to enhance the reduction potential as well as electronic affinity. Greater stabilization is accomplished by the boron coordination when the lowest unoccupied molecular orbital (LUMO) localized over chelated ligand. Nonetheless, the highest occupied molecular orbital (HOMO) of tetra coordinate boron complexes occupied on either chelating ligand or the **R** group, depending on the nature of **R** group. The photophysical and electrochemical performance of tetra coordinated boron complexes depends on either conjugated ligand or **R** groups on boron center. Based on the chelation, the tetra coordinated boron complexes can be classified as (i) *N,N*-chelated boron complex (ii) *N,C*-chelated boron complex (iii) *N,C*-chelated boron complex (iv) *C, C*-chelated boron complex (V) *C, O*-chelated boron complex (VI) *O, O*-chelated boron complex.

1.1.2.1 N,N-chelate boron (III) compounds

The N,N- chelated boron complexes can be further classified in to five categories (Figure 1.3). Type I & II, have boron five membered ring through N,N-chelation. The nitrogen atom incorporated in either one or two aromatic systems. Type III, IV, V will have boron with six membered ring with N,N- chelation. In type III both the nitrogen's are not part of aromatic systems, where as in type IV, the

nitrogen atoms is the part of one aromatic and in type V, it is part of two aromatic systems.

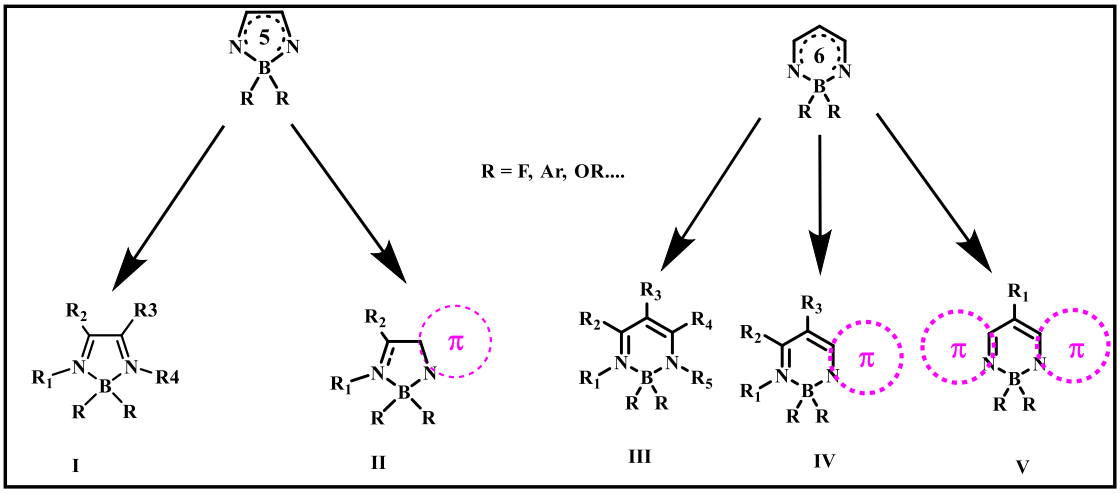

Figure 1.3: Different N,N-chelation approaches.

The 4,4-difluoro-4-bora-3a,4a-diaza-s-indacen (or) boron dipyrromethene (BODIPY) dyes [21-23]are the most well-known boron compounds with N,N-chelate ligand (Figure 1.4). In this type of compounds, out of two nitrogen atoms, one can form a covalent bond with the boron center while the other nitrogen form coordinate covalent bond by donating lone pair of electron to the empty pz- orbital of the boron centre. BODIPY dyes have excellent spectroscopic properties such as narrow absorption and emission bands, high molar extinction coefficients, high fluorescence quantum yields, strong chemical and photochemical stability in solution and solid state.

Owing to these excellent characteristics, BODIPY dyes have been studied to a greater extent in artificial light harvesters, laser dyes, fluorescent sensors, sensitizers for solar cells, molecular photonic wires and as well as in photodynamic therapy. However, the typical BODIPY dyes are weak emissive in solid state, which limits their optoelectronic applications. The luminescence quenching of BODIPYs in solid

state attributed to the undesirable π-π interactions leading to the formation of excimers and exciplexes and small Stokes shifts (400-600 cm^{-1} in most cases), which result in the self absorption of its own fluorescence. Efforts have been made to synthesise modified BODIPY fluorophores with pronounced Stokes shifts and better electroluminescent properties[24-27]. For example, solid state emissive BODIPYs has been achieved by decorating the classical BODIPY core with aryl groups[28-29].

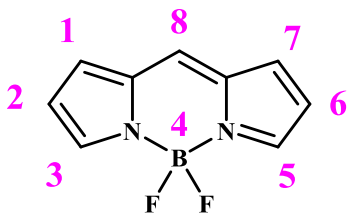

Figure 1.4: Classical BODIPY dye

Wang group reported N,N-chelate four-coordinate boron compounds **1-3** (Figure1.3). The fluorescence spectra of these complexes exhibited emission maxima at 475 nm for 7-azaindolyl (**1**), 516 nm for indolyl (**2**), and 445 nm for benzoimidazolyl (**3**) derivatives, indicating that the emission maxima of these compounds were tuned with location of the N- heteroatom in the chelating ligand[30-31]. To examine effect of substituent groups on the luminescence properties, the electron withdrawing fluoro/chloro atoms and an electron donating methoxy group were introduced to the 5-position of indole in compound **2**. The resulting compounds **4, 5** and **6** exhibited emission maxima at 490, 487 and 532 nm in solution, respectively, indicating that electron withdrawing groups blue shifted the emission maxima whereas the electron donating groups red shifted the emission maxima[32].

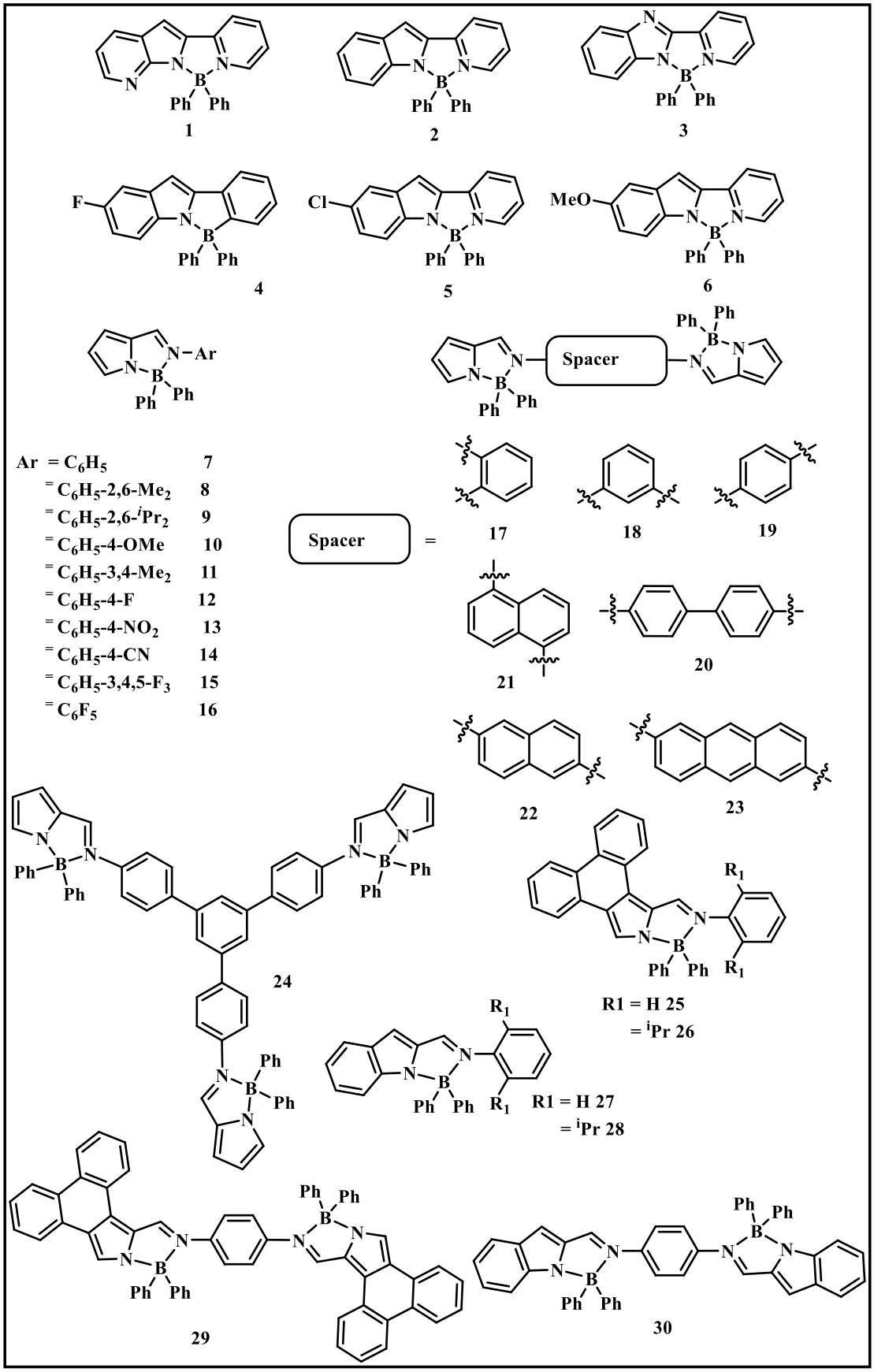

Figure 1.5: N,N-chelate tetra-coordinate boron complexes (**1**-**30**).

Gomes and co-workers synthesised several fluorescent boron compounds containing 2-(N-aryl)formiminopyrrolyl ligands. In mono nuclear compounds (**7-16**), the colour of emission could be tuned from blue to green by varying the electronic and steric nature of the N-aryl group. Further, they extended their work to synthesize bi- and tri- nuclear tetra coordinate boron complexes (**17-24**) by varying the length of π-conjugated spacer. These poly nuclear boron complexes were found to be highly fluorescent; their emission colour could be tuned from blue to orange-red depending on the π-conjugation length. The bi-nuclear compounds were successfully used as the emitting layer of non-doped OLEDs[33-35]. Recently, the same group has reported the synthesis of boron complexes **(25-30)** containing 2-(*N*-aryl)formiminophenanthro[9,10-*c*]pyrrolyl or 2-(*N*-aryl)formiminoindolyl ligands with extended π-conjugation over the pyrrole moiety. These compounds exhibited the emission colour ranged from blue to orange[36].

Chujo et al. utilized quinoline based boron framework reported to make organoboron polymers (**31-33**)[37]. Recently phenanthridinyl based azo-BF_2 complex **34** has been synthesized. Its switching capabilities (**Z⟶ E**) have been studied as a function of concentration.[38] Gomes and coworkers reported a series of fluorescent diphenyl boron compounds **(35-40)** with various substituted iminopyrrolyl ligands where substituents are phenyl (or) 9-anthracene. The fluorescence study of these complexes exhibited blue to bluish green fluorescence in solid and solution state[39]. The structural construction of category I is recently reported with different D-A-D's architecture BF_2 groups **41-44** synthesized and studied by optoelectronic properties[40].

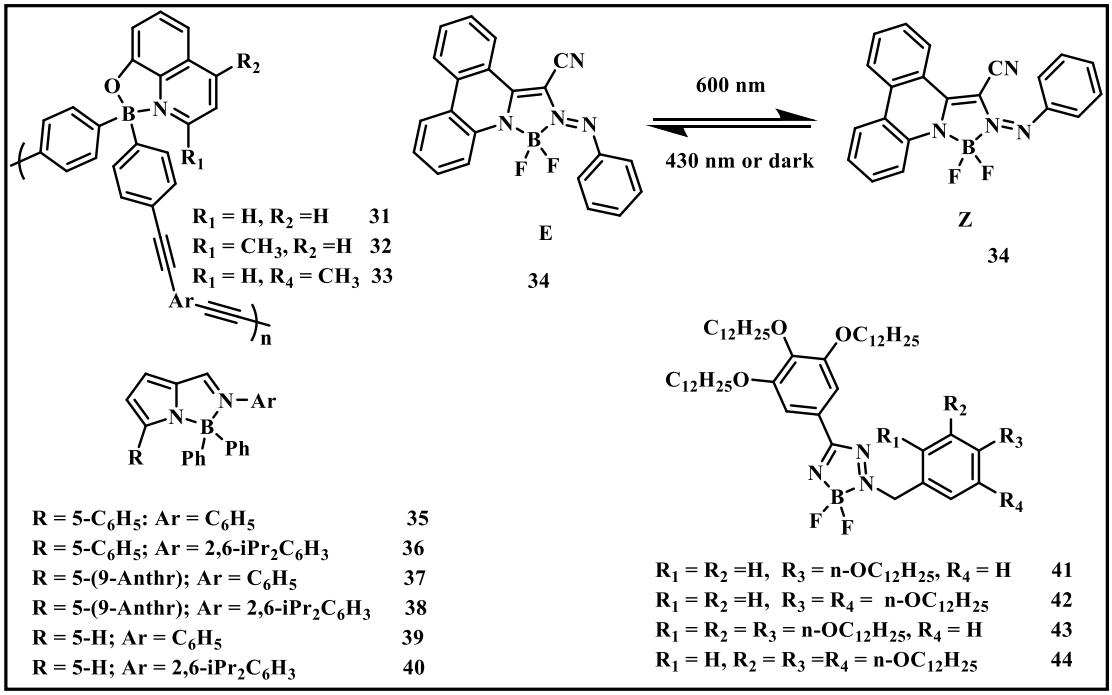

Figure 1.6: N,N-chelate tetra-coordinate boron complexes (**31**-**44**).

Gilroy and Otten groups have synthesized several boron complexes based on formazanate ligands (**45-57**) which exhibited desirable spectroscopic and electrochemical properties. Their studies revealed that electron withdrawing substituents were shown to increase reduction potentials ($E°_{red1}$ and $E°_{red2}$ become more negative) and red-shifted absorption and emission maxima[41-45]. Gilroy group also studied the effect of extended π-conjugation on the properties of BF_2 formazanate dyes (**58-63**); in their study they revealed that absorption and emission maxima were red-shifted as π-conjugation was increased, fluorescence quantum yields increased up to 10-fold[46]. More recently BF_2 formazanate dyes have been explored by the Gilroy and co-workers as an efficient electrochemiluminescent (ECL) emitters (**45-47**),[47] AIEE fluorophores (**64-66**),[48] fluorescent cell-imaging agents,[49] furthermore they have also incorporated into polymers[50].

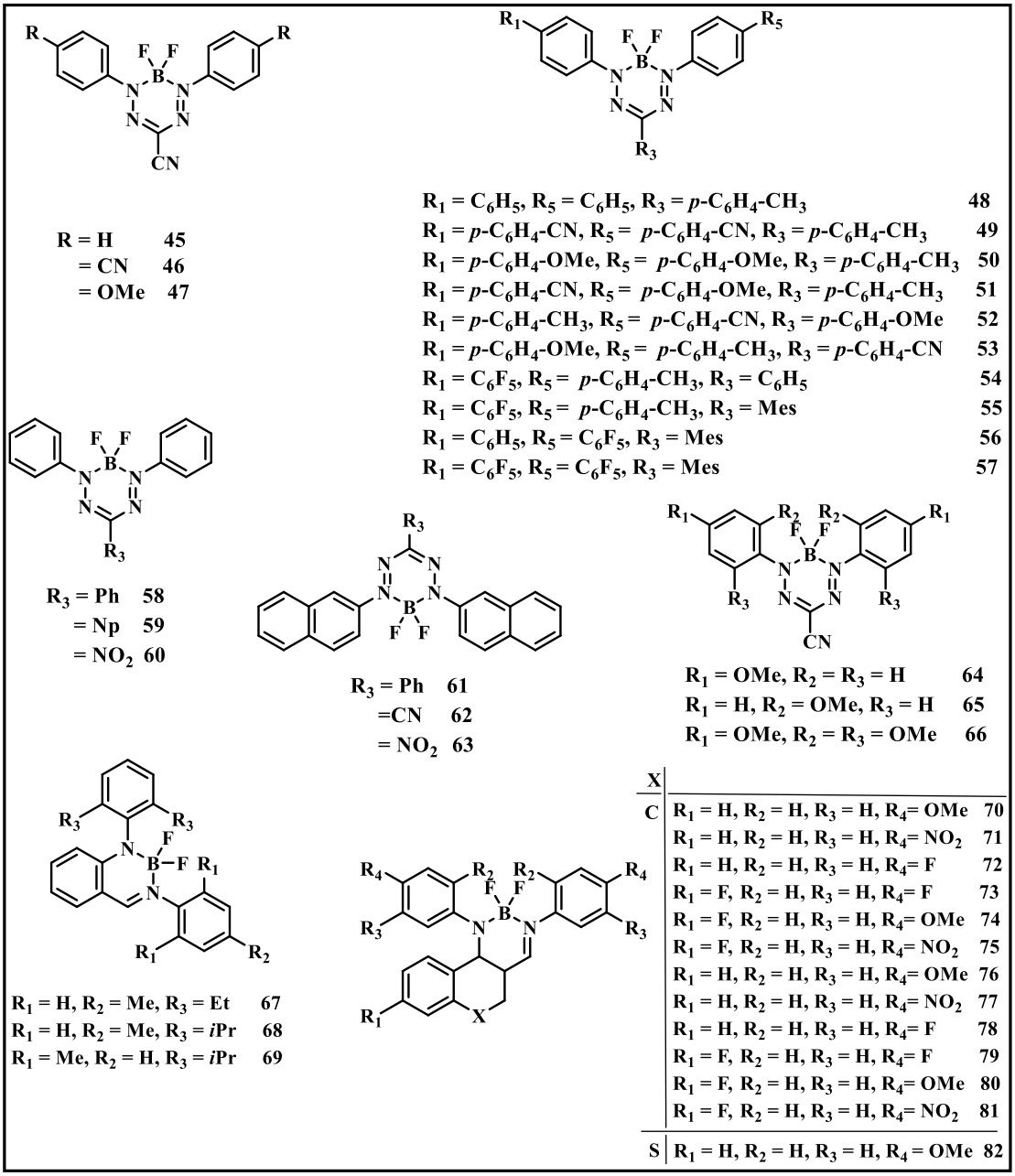

Figure 1.7: N,N-chelate tetra-coordinate boron complexes (**45-82**).

Ying Mu and coworkers reported new class of Schiff base ligands with aluminum complex as latter they inserted $–BF_2$- to synthesize difluoride boron complexes (**67-69**) with various derivatives and studied their luminescent properties in solution and solid state[51]. More recently novel β-diketoiminato boron complexes (**70-82**) with N,N-chelation were synthesized which showed large stokes shift and

solid state quantum yield. These molecules showed aggregation induced emission (AIE)[52-53].

Gardinier and co-workers reported a series colour tunable fluorophores based on the diphenylboron complexes of (2-pyrazolyl)-4-R-anilines or BORAZANS ((boron azoanilines) (**83-89**) where R is the *para* substituent on the aniline ring. In their study, it was found that BORAZANS with electron-withdrawing *para*-aniline substituents exhibit higher chemical stability and blue fluorescent emission, while the BORAZANS with the electron-donating groups shift the emission to green and destabilize the compound towards hydrolysis[54]. Piers and co-workers reported a series of anilido-pyridine boron difluorides (**90-92**), which exhibits high photostability, large Stokes shifts along with high quantum yields both in solution and in the solid state[55]. Belskaya and coworkers reported donor- accepter system type N,N-chelated six membered tetra coordinated boron complexes (**93-94**)[56]. These compounds exhibited aggregation induced emission (AIE) and aggregation induced enhanced emission (AIEE). The fluorescence get red shifted when electron donating groups present on the aromatic ring. Jun Liu and coworkers reported multiple boron-nitrogen coordination compound **95**. Due to presence of multiple borons this compound exhibit high electron affinity which was studied using electron mobility experiments. The ^{11}B NMR showed a singlet at 2.3 ppm. Which suggests that an the borons in compound **95** have similar environment[57]. Recently, Matsui and co-workers reported the synthesis of dipyridomethene-BF_2 compounds. The boron complex of dipyrido methane exhibited fluorescence in solution and in the solid state, however, the ligand dipyrromethane did not show fluorescence (**96-99**)[58]. Recently, Thomson and coworkers synthesized meso-linked dimers of boron dipyridyl mathene **100**. The

structural, photophysical and electrochemical properties of the dimers were thoroughly probed[59].

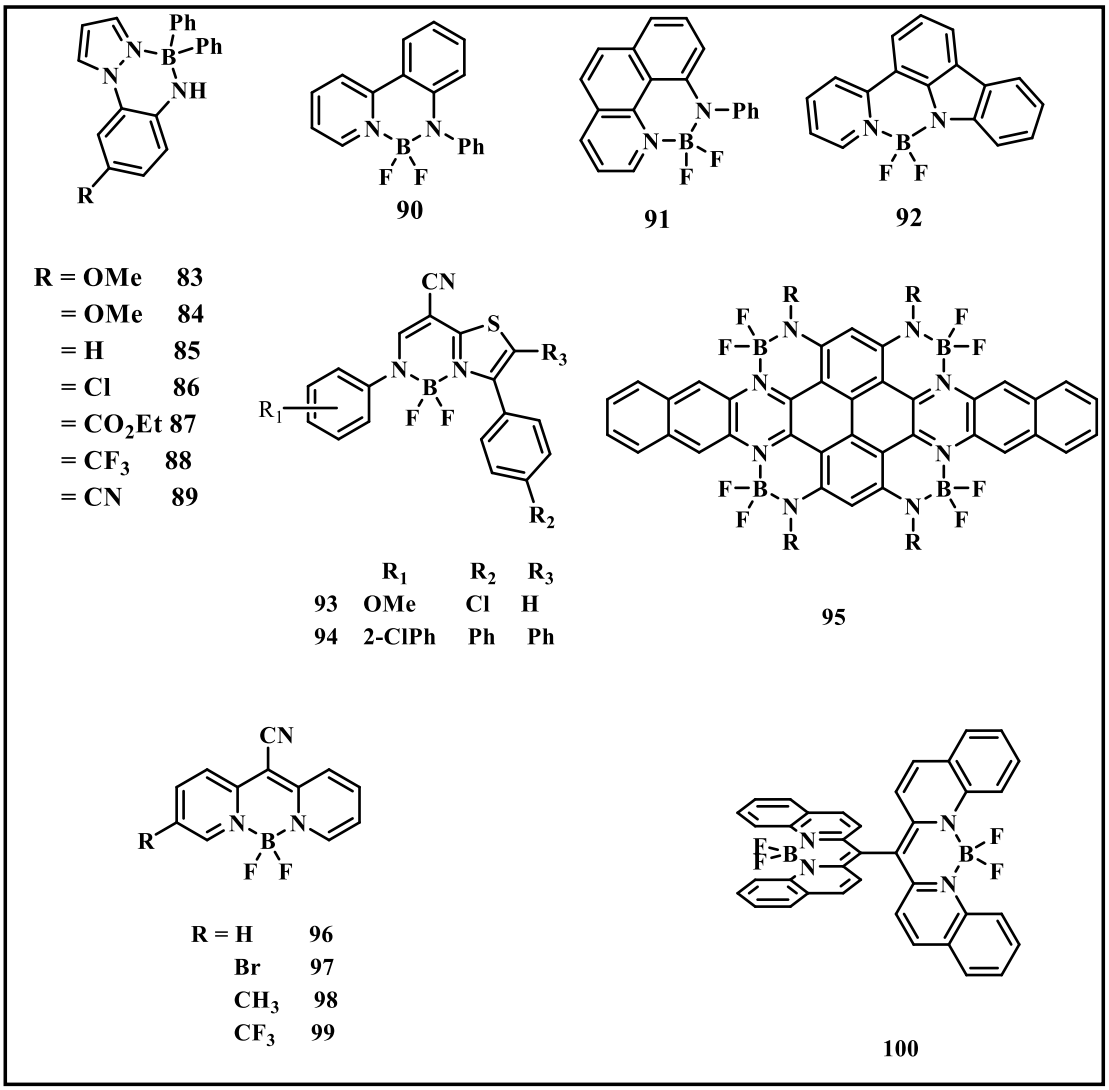

Figure 1.8: N,N-chelate tetra-coordinate boron complexes (**83-100**).

1.1.2.2 N,O-chelate boron (III) compounds

The N,O-chelated boron complexes can be further classified into five categories depending on either rigidity or close planarity (Figure 1.9). Type I & II consist nitrogen atom connected to the boron center forming five membered rings, may or may not be the part of the aromatic ring. The type III & IV The nitrogen atom

connected to the boron atom is either part of aromatic or non-aromatic system. Also, coordinated where as in type V, the nitrogen atom connected to the boron center forms a seven membered with aromatic system.

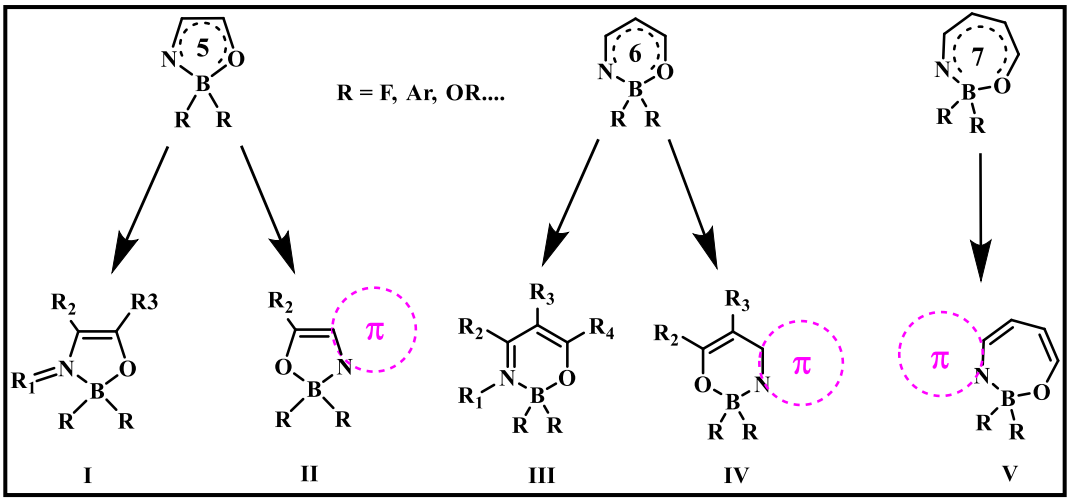

Figure 1.9: Different N,O-chelation approaches.

The condensation of aldehyde derivatives with 2-aminophenol derivatives yielded imines. The resultant imines were used to make five membered boron complexes which are studied their applications in nonlinear optics and solar cells (**101-103**)[60-62]. Wang and co-workers reported a series of 8-hydroxyquinolinate (q) boron compounds **104-107** with the general formula of BR_2q, where R = ethyl, phenyl, 1-naphthyl, and 2-naphthyl.[63] These boron compounds exhibited greenish blue emission with emission wavelength of 495–500 nm and were also investigated in OLED as emitters and electron-transporting layers. In addition to this, they reported several 8-hydroxyquinolinate based linear and star-shaped polynuclear boron compounds **108-112**, to examine the effect of extended π-conjugation and the mutual influence of multiple boron centres. These compounds exhibited emission maxima ranged from 528 to 542 nm with increased thermal stability[64]. Later, Jäkle group reported a series of emission colour tunable boron compounds **113-119** by varying the

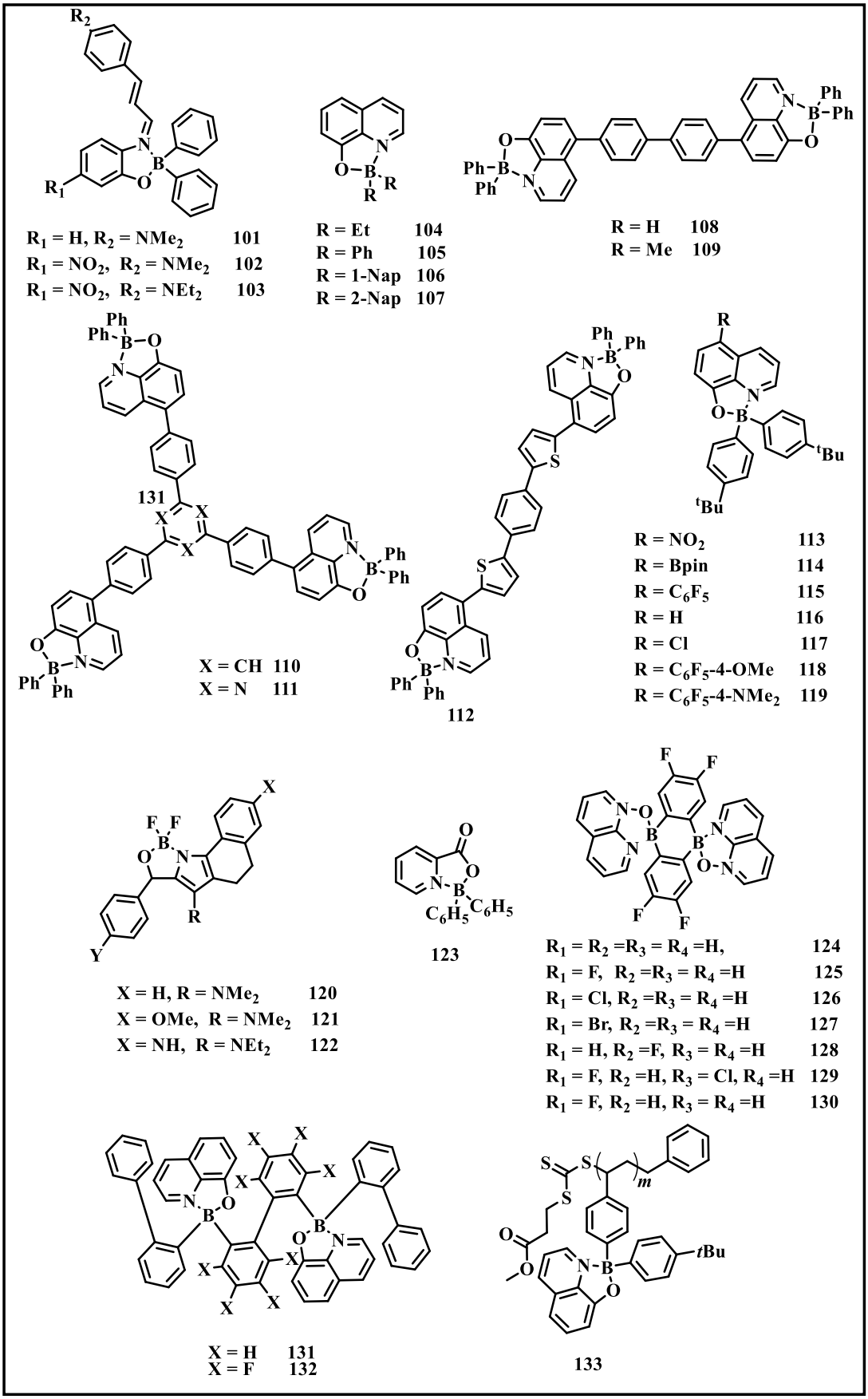

Figure 1.10: N,O-chelate tetra-coordinate boron complexes (**101-133**).

substituents at the 5th position of the quinolate ligand. They observed that, electron withdrawing groups, blue shift the emission maxima relative to the nonsubstituted one, while electron donating groups red shift the emission maxima. Recently, pyridine and ketopyrrole derivatives also used to make five membered N,O-chelated boron complexes (**120-122**)[65-66]. Lulinski and co-workers synthesized 9,10-dihydro-9,10-diboraanthracene bis(8-oxyquinolinates) derivatives **124-130** [67] and used them as green luminescent materials in OLED application. The same group reported the synthesis bis(8-oxyquinolato) diboron complexes **131-132**[68]with 2,2′-biphenyl backbone and studied the intramolecular π-stacking interactions. An N,O-chelated, 8-hydroxy quinolate based polymer was synthesized using a RAFT protocol by Jakle and Chugo. They also made block copolymer using PEO segment to make micelles (**133**) [69].

Boron compound with six-membered N,O-chelate was reported in 1980 by 'Eberhard Hohaus' **134** [70]. Recently 'Sergiusz Lulinski' and co-workers reported such kind of complexes using naphthalene core **135**[71]. Ziessel, Ulrich, and co-workers reported a new type of boron complexes **136-142**, named boranils by complexation of anils (aniline-imines) with boron (III) precursors like $BF_3.Et_2O$ or BPh_3. They found that, the photophysical properties of these compounds strongly dependent on the nature of *para* substituents on both the phenol and imine sides of the compound[72]. Later they proved that these boranil dyes (**143**) can be utilized as a interesting candidates for bio conjugation to proteins such as bovine albumin serum (BSA) in biological media[73]. Later they extended the strategy to make polyboranils (mono-, di- & tri-) with good quantum yields in the near infra-red region (534-764 nm) (**143-145)**[74-75]. From our group, we reported thermally stable salicylaldimine based diboron complexes (**147-149**) with emission maxima ranged from 460 to 494 nm[76].

Muthusubramanian reported bornil dyes **150** and **151** and explored their application as turn-on fluorescent probes for the detection of hydrogen peroxide[77].

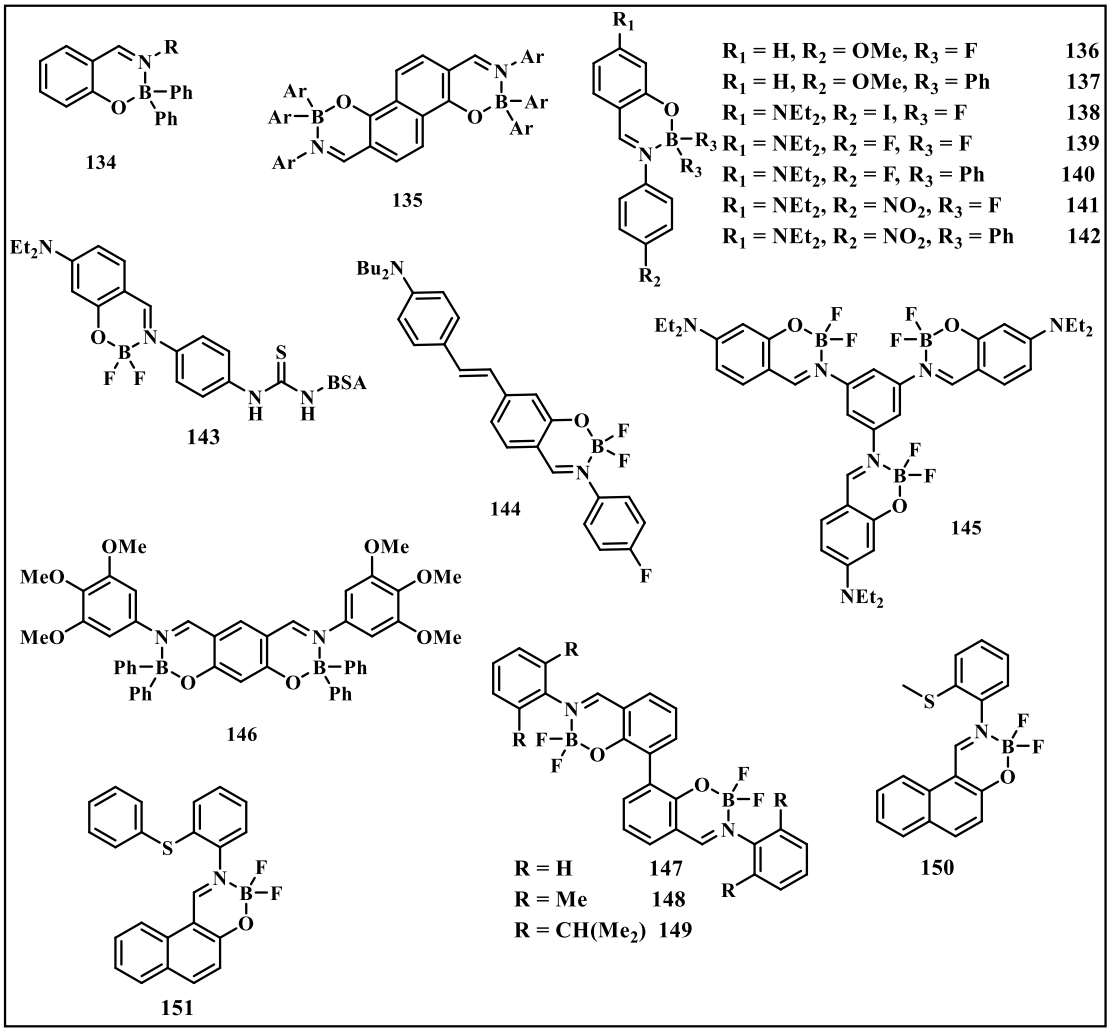

Figure 1.11: N,O-chelate tetra-coordinate boron complexes (**134-151**).

Xingliang Liu and co-workers reported triphenylamine functionalized β-ketoiminate **152** and studied its aggregation-induced emission and mechanochromism properties. Recently Ran Lu and co-workers reported new salicylaldimine boron complex **153** with D–π–A system. This molecule also exhibited both distinct mechanofluorochromic (MFC) behavior and aggregation induced emission (AIE) [78-79]. More recently Kong and co-workers reported a series of N,N-dimethyl-substituted

boron ketoiminates (NBKI) based initiators (**154-157**) and polymers/copolymers (**158-163**) which shows multicolor fluorescence [80].

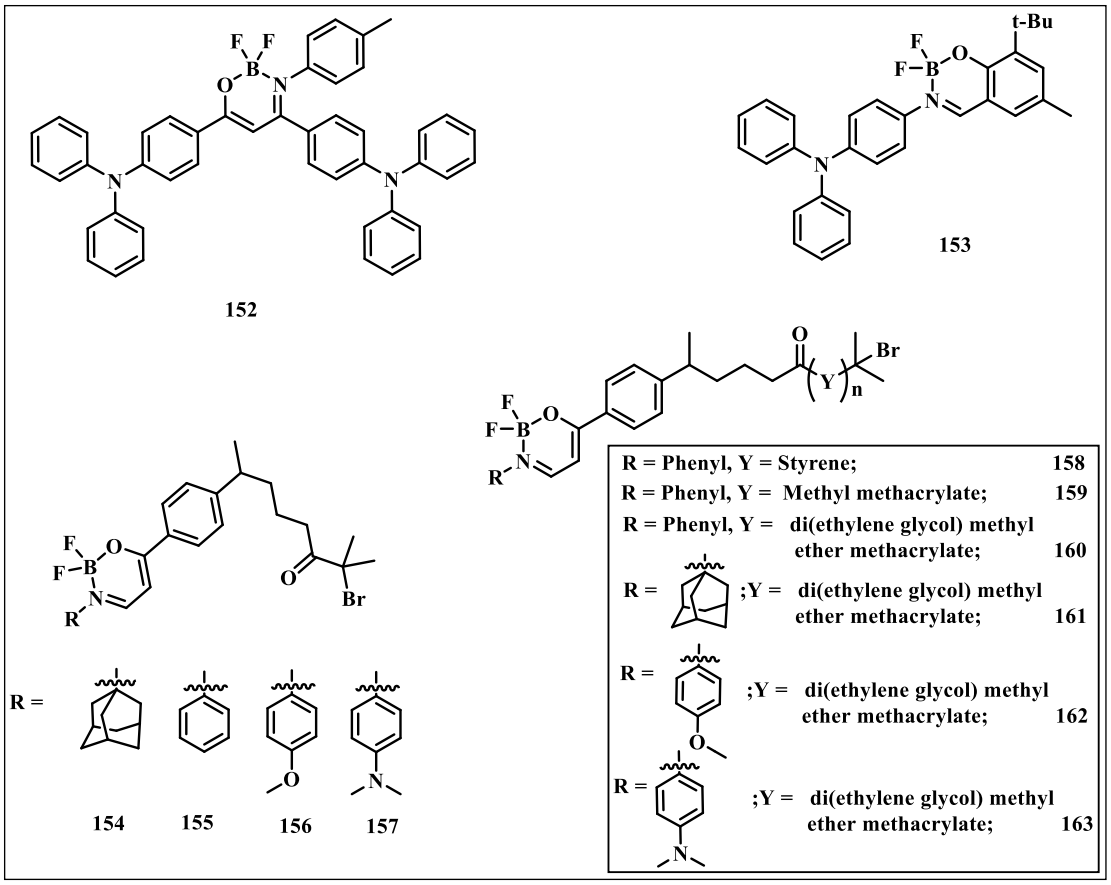

Figure 1.12: N,O-chelate tetra-coordinate boron complexes (**152-163**).

Thehydroxy benzazole (HBX)basedboron complexes such as benzimadazole (**164**) [81], benzoxazole (**165-167**) [82], benzothiozole (**168-170**) [83] derivatives also forms N,O-chelated six membered rings. Kwak and Kim synthesized difluoroboron complexes based on 2-(2′-hydroxyphenyl)benzoxazole (**171**) and 2-(2′-hydroxyphenyl)benzothiazole ligands (**172**) [84]. These boron complexes exhibited bright blue fluorescence with good thermal stability and high electron transport ability in OLEDs. Zhang, Yue Wang and co-workers reported diboron containing fused complexes **173** and **174** which exhibits good thermal stability, high electron mobility,

and intense solid state fluorescence and they also utilized them as a non doped red emitters in OLEDs [85]. Later they synthesised benzoxazole (**175**) and benzthiazole (**176-179**) boron complexes by introducing various amine groups. The emission colour of these boron complexes covered a wide range from deep blue to saturated red in both solution and the solid state [86].

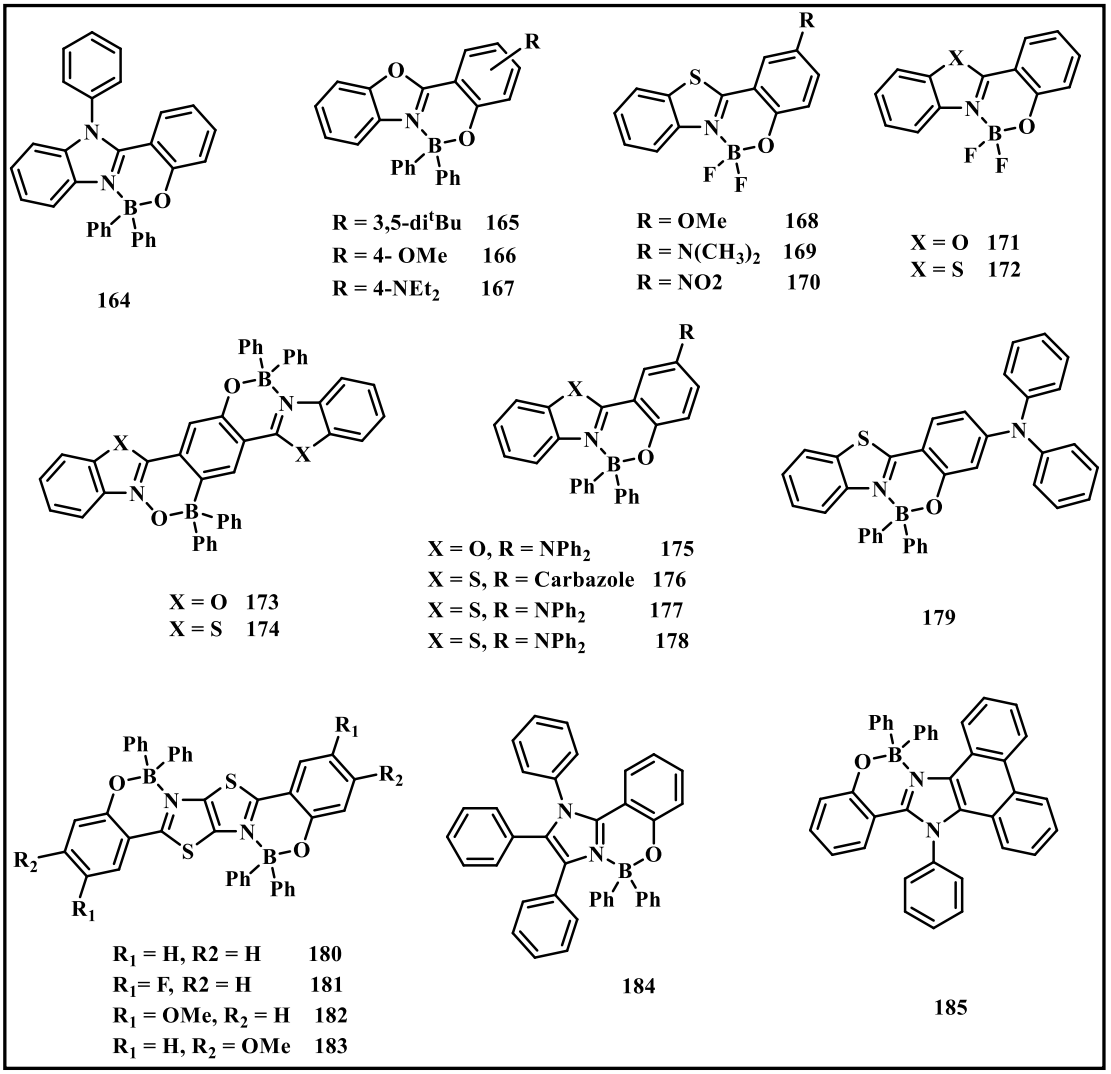

Figure 1.13: N,O-chelate tetra-coordinate boron complexes (**164-185**).

Lately, Zhang and co-workers synthesised a series of novel diboron containing π-conjugated ladders (**180-183**) from phenol substituted thiazolothiazole ligands and used them both as emitters and electron transporting materials in OLEDs. Due to the

construction of diboron ladder type skeletons, these diboron complexes exhibited high thermal stability, high fluorescence quantum yields, and strong electron affinity [87].Recently, Zang group also reported 2-(2-hydroxyphenyl) imidazole based boron complexes (**184-185**) with high thermal stability. They also studied their photoluminescence and electroluminescence properties of the materials [88].

Ziessel, Ulrich, and co-workers synthesised a series of boron complexes (**186-194**) based on electron donor/acceptor substituted 2-(2′-hydroxy phenyl)benzoxazole ligands. These boron complexes exhibited the emission wavelength ranging from 385 to 425 nm in dichloromethane [89]. Later they synthesised the ethynyl extended regioisomers of difluoro or diphenyl borate complexes (**195-205**) and electron donating groups contained diphenyl borate complexes (**206-208**) based on 2-(2′-Hydroxyphenyl)benzoxazole [90-91]

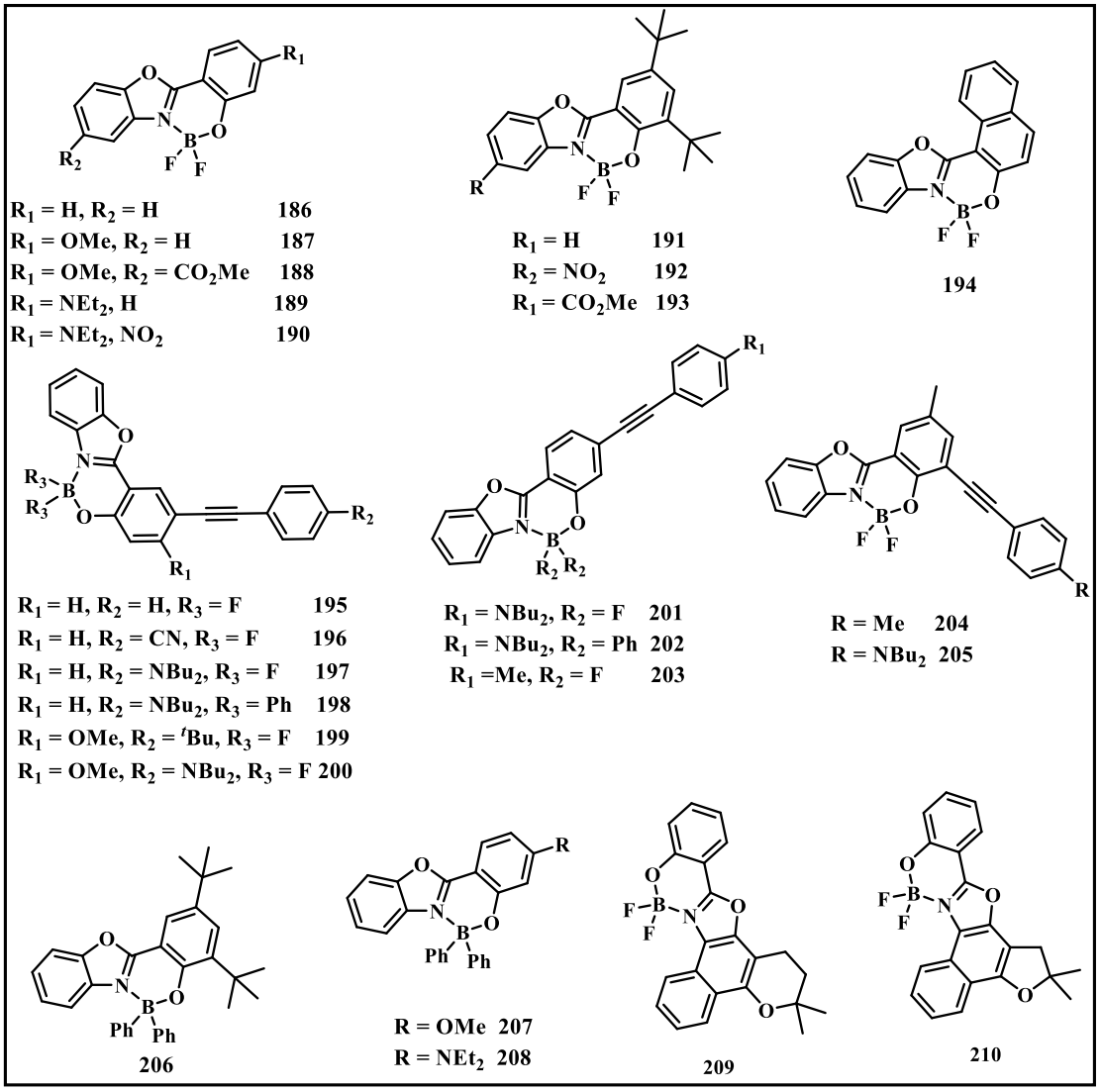

Figure 1.14: N,O-chelate tetra-coordinate boron complexes (**186-210**).

And they concluded that, the optical properties of these boron complexes highly depend on the electronic nature and position of substituents. Moreover, in all cases, as compared to BF_2 derivatives, the BPh_2 derivatives exhibited red shifted absorption and emission both in the solution and in the solid state. da Silva Ju´nior and co-workers synthesized the naphthoxazoles based boron complexes **209-210** and applied as superior and selective probes for endocytic pathway tracking in live cancer cells [92].

Yasuhiro Kubota, Masaki Matsui and co-workers reported pyrazine[93] (**211-216**) or thiazole[94] (**217-220**) boron complexes bearing a *β*-ketoiminate ligands, which

exhibits a large Stokes shifts, solid-state fluorescence and aggregation induced emission enhancement. Later, they reported solid state emissive, AIEE active pyrimidine mono and bisboron (**221-230**) complexes bearing a *β*-ketoiminate ligand. They also found that pyrimidine boron complexes bearing two phenyl groups on boron atom show more intense fluorescence than the corresponding BF_2 complexes [95]. Moreover D-π-A type pyrimidine diboron complexes **231-235** show solid state fluorescence in the NIR region[96]. Potopnyk, Grazulevicius and co-workers designed and synthesized donor-acceptor type thiozole nitrogen coordinated difluoroboron complexes (**236-240**) with electronic and photophysical properties caused by AIE effect [97]. Recently, the same group reported modified benzo[d]thiazole-based BF_2 complexes with various aryl substituents (**241-246**). Moreover, these complexes exhibited high fluorescence quantum yield in the solution state. The benzothiazole boron complex with (Ar = 4-C_6H_4CN) disclosed high fluorescence quantum yield in the solid state [98].

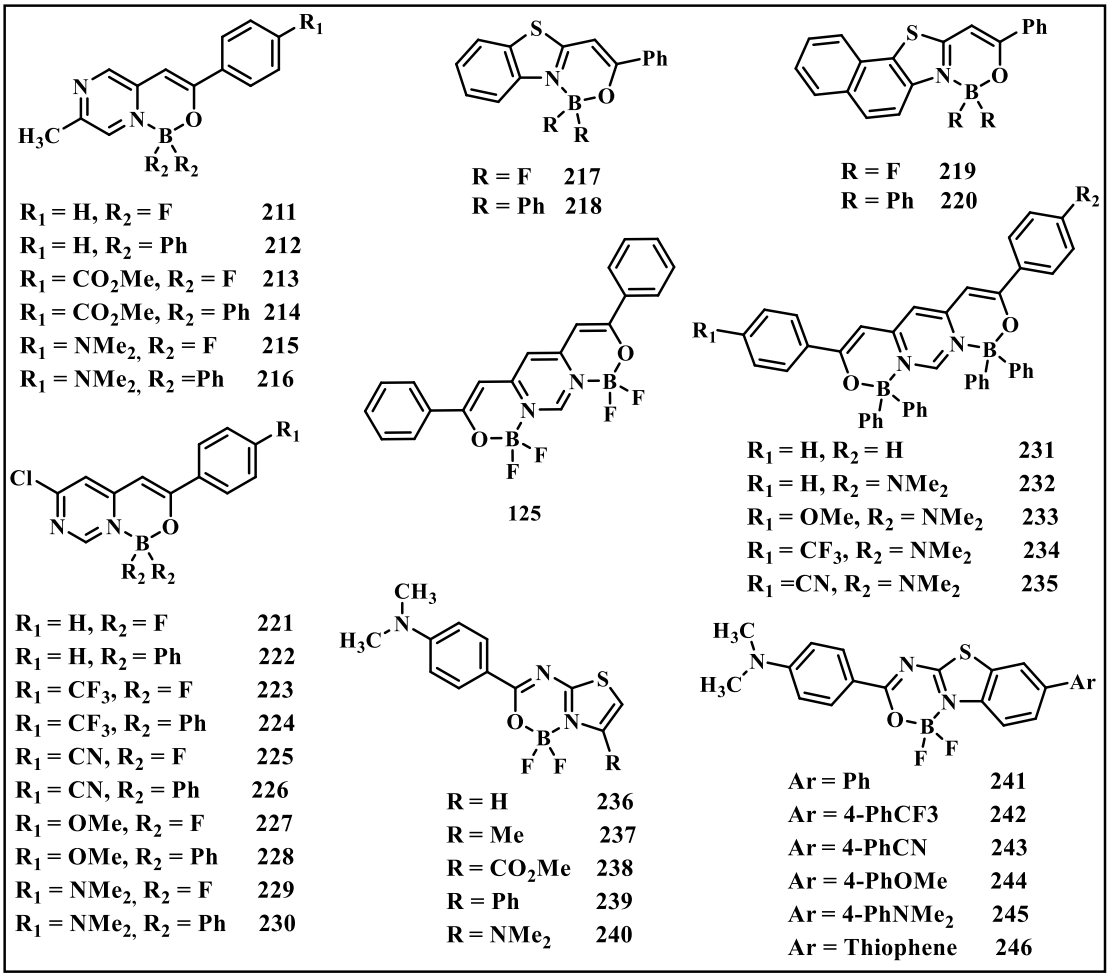

Figure 1.15: N,O-chelate tetra-coordinate boron complexes (**211-246**).

Lu and co-workers synthesised a series of carbazole[99] (**247** & **248**), triphenylamine[100] (**249**) and phenothiazine (**250-253**) functionalized *β*-iminoenolate boron complexes bearing a pyridine ligand and studied their mechanofluorochromic properties. Sun and co-workers synthesised quinoxaline-*β*-ketoiminate boron difluoride complexes **254-258** with strong luminescence both in solution and solid state. Moreover, these boron complexes exhibited reversible on-off solid state luminescence switching by acid/base fuming processes[101]. Very recently Lu and co-workers reported non-traditional π-gelators based on *β*-iminoenolate and their difluoroboron complexes (**259-264**)[102]. Most recently Pereshivko, Peshkov and co-

workers synthesized a series of N,O-chelated six membered isoquinoline-enol boron complexes (**265-270**) with tunable optical properties[103]. Kaiqi Ye and co-workers reported pyrimidine-containing *β*-iminoenolate difluoroboron complexes such as CPPAB (**271**) and TCPPAB (**272**) and studied their mechanofluorocromic behaviours. Furthermore TCPPAB can be used as a TFA probe[104].

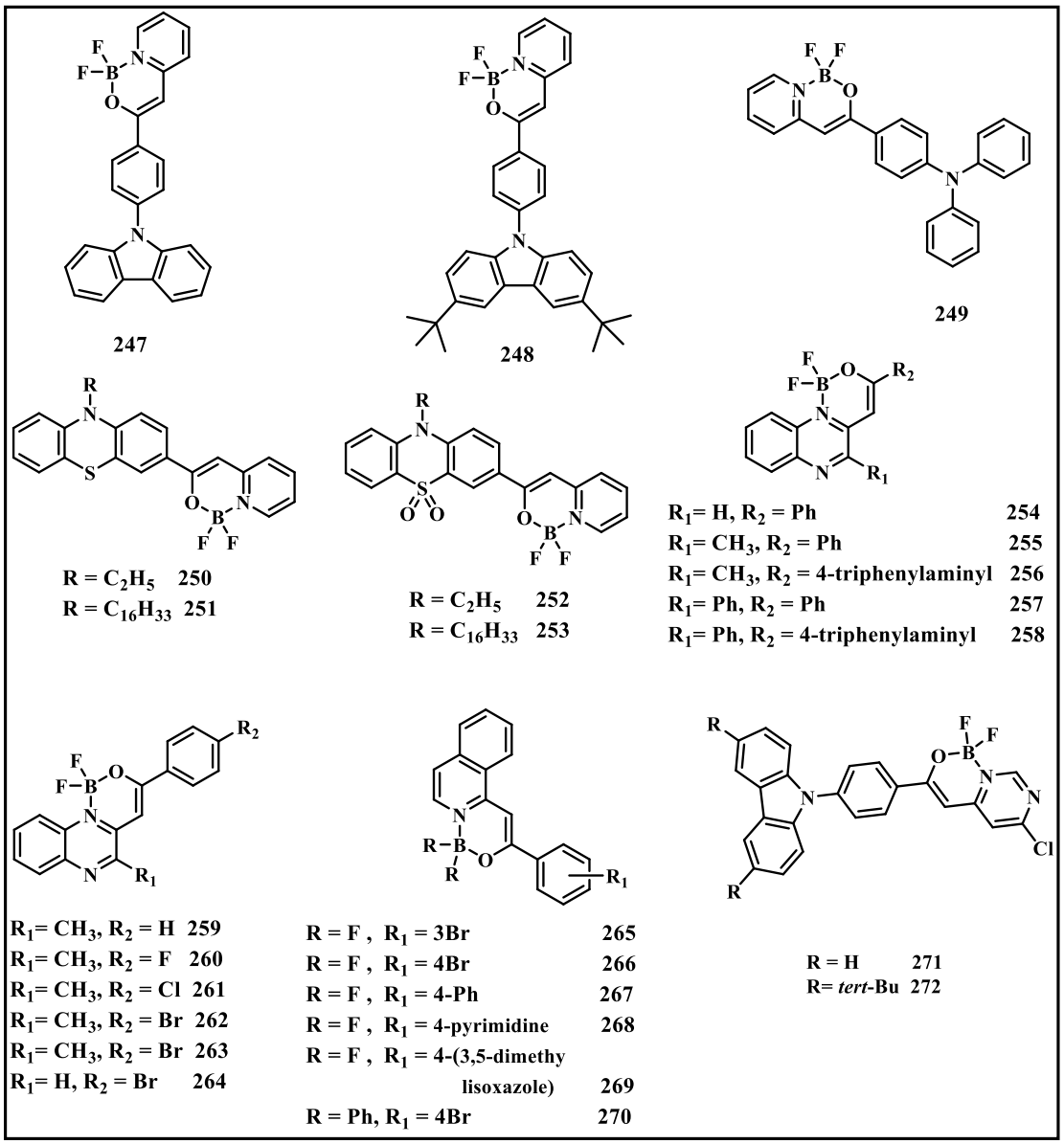

Figure 1.16: N,O-chelate tetra-coordinate boron complexes (**247-272**).

He and co-workers reported pyrimidine-based BF_2 complexes **273-274** with large Stokes shift, AIE effect, high solid-state luminescence and mechanochromic properties[105]. Later they synthesised the benzothiazole enolate ligand based boron complexes **275-278** with asymmetrical and propeller shaped structures, which exhibited large Stokes shift in solution, AIE effect and intense solid-state emission[106].

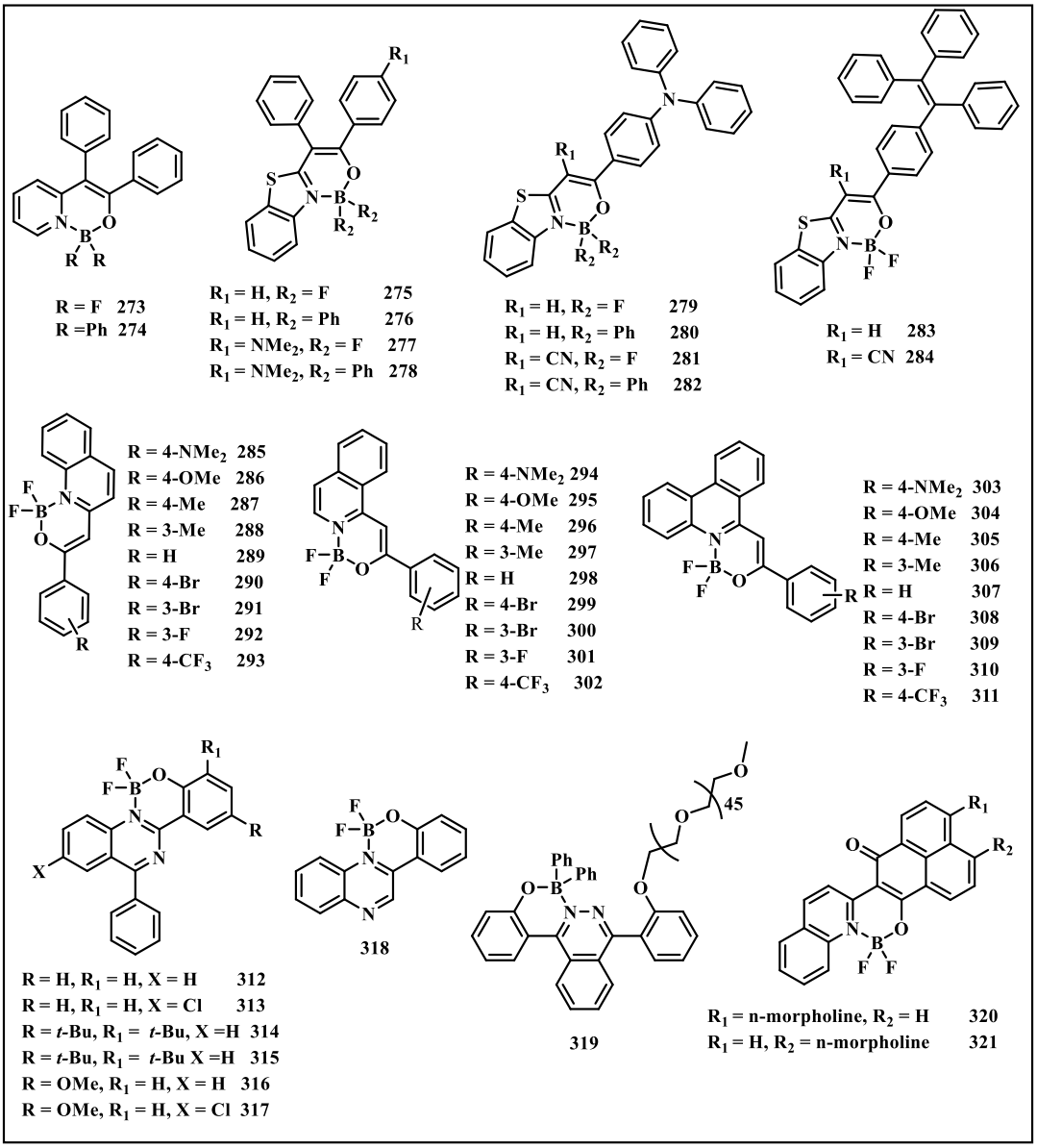

Figure 1.17: N,O-chelate tetra-coordinate boron complexes (**273-321**).

Zhao reported D-π-A type triphenylamine-functionalized thiazole based *β*-ketoiminate boron complexes (**279-282**). All these compounds exhibited strong intramolecular charge transition emission and strong cyano-dependent aggregation induced emission and mechanofluorochromic properties[107]. Li and co-workers reported D-π-A typethiazole based *β*-ketoiminate boron complexes (**283-284**) connected with tetraphenylethene, which exhibited twisted intramolecular transition emission, strong AIE phenomenon and significant mechanofluorochromic properties[108]. Ośmiałowski and co-workers reported2-benzoylmethylenequinoline[109] (**285-293**), 1-benzoylmethyleneisoquinoline[110] (**294-302**), phenacylphenantridine[111] (**303-311**) based boron complexes and studied the effect of substitution. Nosova and co-workers reported BF_2 complexes of 2-hydroxyphenyl 4-phenylquinazoline **(312-317)** and 2-(2-hydroxyphenyl)quinoxaline **(318)** with large stokes shift and highquantum yield in both solid and liquid state.[112] Sheng Han, Fan Zhang and co-workers designed and synthesized new phthalazine based tetra coordinated boron complex bearing polyethylene glycol (**319**). Compound **319** exhibits water solubility with good fluorescence performance[113]. Yi Xiao, Xuhong Qian and co-workers, lately reported novel isomeric difluoro−boron complexes **(320-321)** with strong fluorescence and large stokes shift[114].

Seven-membered boron complexes are much rare and difficult to obtain. Burgess and Wu described first report of seven membered ring with N,O-chelation **(322-326)**. The studies reveal that these compounds are weakly fluorescent compared to boraindacene, BODIPY, dyes[115]. Churchill and coworkers synthesized benzazulene based BF_2 complex with seven membered ring, which showed turn-on H^+ and F^- response **(327-331)**[116].

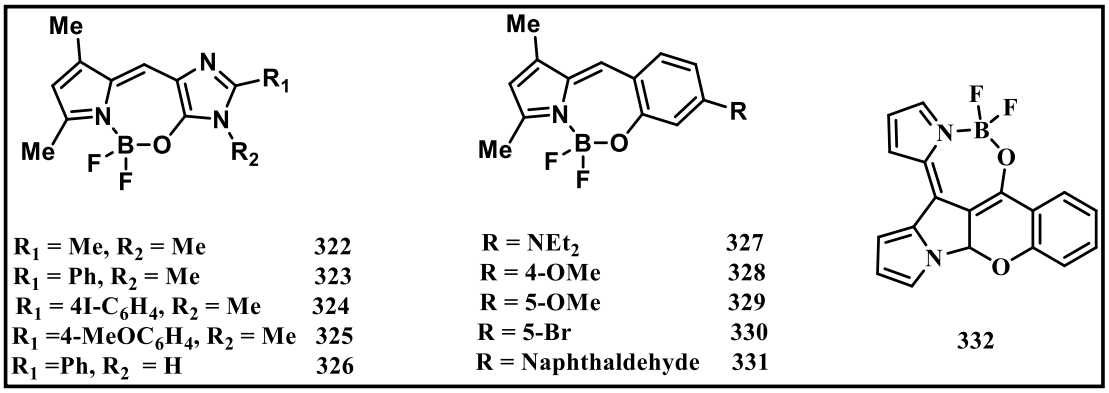

R1 = Me, R2 = Me 322
R1 = Ph, R2 = Me 323
R1 = 4I-C6H4, R2 = Me 324
R1 =4-MeOC6H4, R2 = Me 325
R1 =Ph, R2 = H 326

Figure 1.18: N,O-chelate tetra-coordinate boron complexes (**322-332**).

Pandey and co-workers synthesized thermally stable novel chroman based boron difluoride complex **(332)** which contains seven membered ring[117].

1.2 Fluorescent probes for fluoride ion sensing

1.2.1 Importance of fluoride ion

In recent years, different methods to recognize and sense biologically and environmentally important anions have become an emerging field in the area of chemical sensors[118-121]. Among the different anions, fluoride ion attracted interest in the research community. Fluoride ion play important role in human health,[122] often small amounts of fluoride ion added to tooth paste for the prevention of dental caries[123]. This anion is also administered in the treatment of osteoporosis[124-125]. However, high doses of fluoride ion can cause acute toxicity in humans and animals. There are many reports for dental and skeletal fluorosis because of the consumption of drinking water with high fluoride ion content across the world. According to the national health portal of India report 2014 over 11.7 million peoples in India from various states are at risk due to high dose of fluoride. Fluoride is easily absorbed by the body but dissipated slowly, because of this it is blamed for acute liver and kidney

diseases.[126] Therefore it is not surprising that the selective detection of fluoride ion is growing among research community[127].

1.2.2 Detection methods for fluoride ion

Many sensors based on ^{19}F NMR[128] and (or) electrochemical methods[129] have been developed. Neither NMR nor electrochemical methods can be used for intracellular fluoride ion monitoring[130]. In this circumstance colorimetric and fluorometric probes gained much attention due to their high sensitivities and the capabilities of fluoride ion monitoring in biological process[131].

Over the years a large number of optical sensor systems have been developed. Most of these methods employed hydrogen bonding interaction and interaction between fluoride and Lewis acidic boron. Apart from these methods reaction based fluorescent chemodosimeters have also been developed. In this part of the thesis, recent studies on the development of fluorescent sensors and the chemistry leading to optical responses will be presented.

1.2.2.1 Sensors based on hydrogen bonding interactions.

During the past decade many fluorescent probes utilizing hydrogen bonding interactions has been developed. Duke *et*. al developed napthalimide thiourea (**333-336**)[132-133] a fluorophore-spacer–receptor principle for fluoride ion detection. The emission intensities of **333** and **334** were quenched due to enhanced photoinduced electron transfer (PET) process from receptor to fluorophore upon addition of fluoride ion in DMSO. In case of sensors **335** and **336** the emission intensities at 528 and 533 nm got quenched upon addition of acetate, phosphate and fluoride *via* PET process. However an effective quenching was seen in the case of **335** by the addition of fluoride ion (*ca*. 90%) with no changes in absorption spectra. These results suggest that bi-directional single-electron transfer (SET) process is responsible for the

selective sensing by these napthalimide based probes. The probes **337**, **338**, **339**[134-135] also operates *via* similar SET quenching mechanism for the selective detection of fluoride ion. Thiacalix[4]arene anchored with two napthylthiourea groups, **340**[136] acts as a fluorescent sensor. The addition of fluoride ion to **340** triggers the intramolecular π-π interactions between two naphthyl groups, which leads to the formation excimer emission enhancement. It showed 1:1 complex formation between the probe **340** and F^-. Based on fluorescence resonance energy transfer (FRET) mechanism several probes have been developed for the selective detection of F^-. Pulla Rao and co-workers reported calix[4]arene based sensor **341**[137] having 7-chloro 4- nitro benzofurazan (NBD) as fluorescent sensor. This can sense fluoride ion in solution and also in the biological systems. Rajesh and co-workers designed and synthesized two colorimetric receptors (**342**, **343)**[138] for the selective detection of fluoride ion. Moreover, these receptors were also applied for fluorescence imaging of fluoride ion in HeLa cells. A colorimetric/fluorometric probe **344** was synthesized for detection of fluoride ion in DMSO/water. The probe was bound to detect F^- in 1:1 manner and showed low detection limit[139].

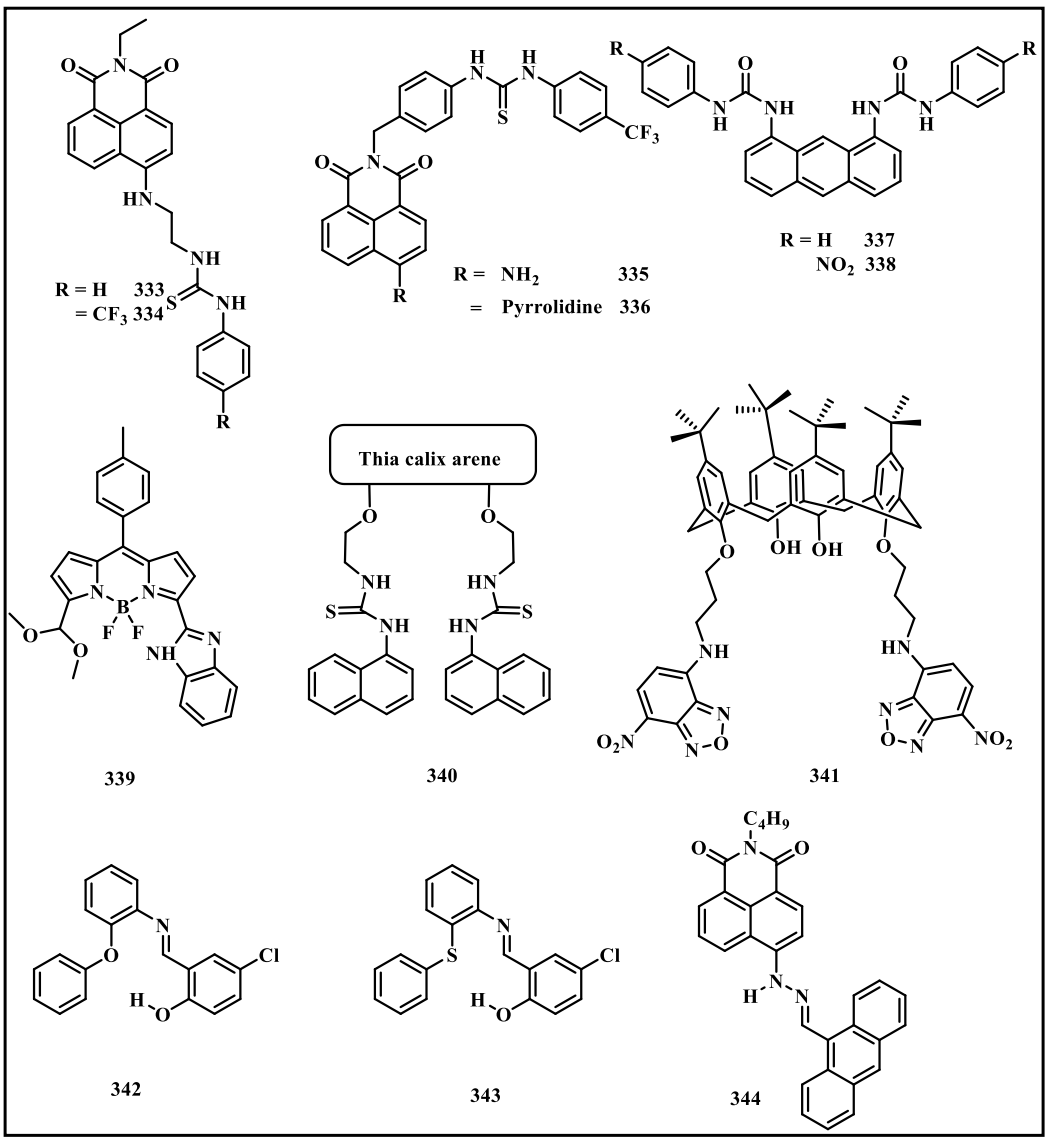

Figure 1.19: Sensors based on hydrogen bonding interactions (**333-344**).

1.2.2.2 Sensors based on interaction between Lewis acidic boron and fluoride

Triarylboranes readily reacts with small nucleophiles such as fluorides and cyanidesto give fluoroborates. This reaction occurs *via* donation of electron pair of fluoride anion to the vacant *p* orbital of the boron centre[140]. By keeping appropriate aryl substitution and steric bulk around the boron centre, the selectivity of triarylboranes for fluoride ion got achieved. Yamaguchi and coworkers has reported the boron containing π-system, tri(9-anthryl)borane (**345)** as colorimetric sensor for the detection of fluoride ion. Addition of F^- ion to **345** triggers colour changes from orange to colour less and,

in the absorption spectra, the characteristic band of **345** at 470 nm disappeared and new band around 360-400 nm appeared[141]. From the same group dibenzoborole with (*N*,*N*-diphenylamino)phenyl group at 3,7-position (**346**) has been investigated as fluorescent probe for fluoride ion. Upon complexation of **346** with F^-, the emission maxima got blue- shifted about 100 nm with 20 fold increment in quantum yield was observed *via* on/off control of the p_π-π^* conjugation of LUMO level[142]. Wang and coworkers invented two fluorescent probes **347, 345** based on charge transfer mechanism[143]. Sensor **348**, where the donor N(Ph)(1-naphthyl) and the acceptor $B(mesityl)_2$ groups in a nonplanar arrangement, showed turn on response selectively for fluoride ion. Thilagar group introduced two dissimilar acceptors (triarylborane and BODIPY) on a single donor **(349)** that operates *via* similar intramolecular charge transfer (ICT) mechanism for the selective fluoride ion detection[144]. Wang and co-workers presented two new triarylborane functionalised compounds 1-(8-(4-(dimesitylboranyl)phenyl)quinolin-2-yl)-N,N-bis(pyridin-2-ylmethyl)methanamine (**350**)[145] and 1-(6-(4-(dimesitylboryl)phenyl)pyridin-2-yl)-N,N-bis(pyridin-2-ylmethyl)methanamine (**351**). The advantage of these is that they can discriminate fluoride and cyanide ions in aqueous solutions[146].

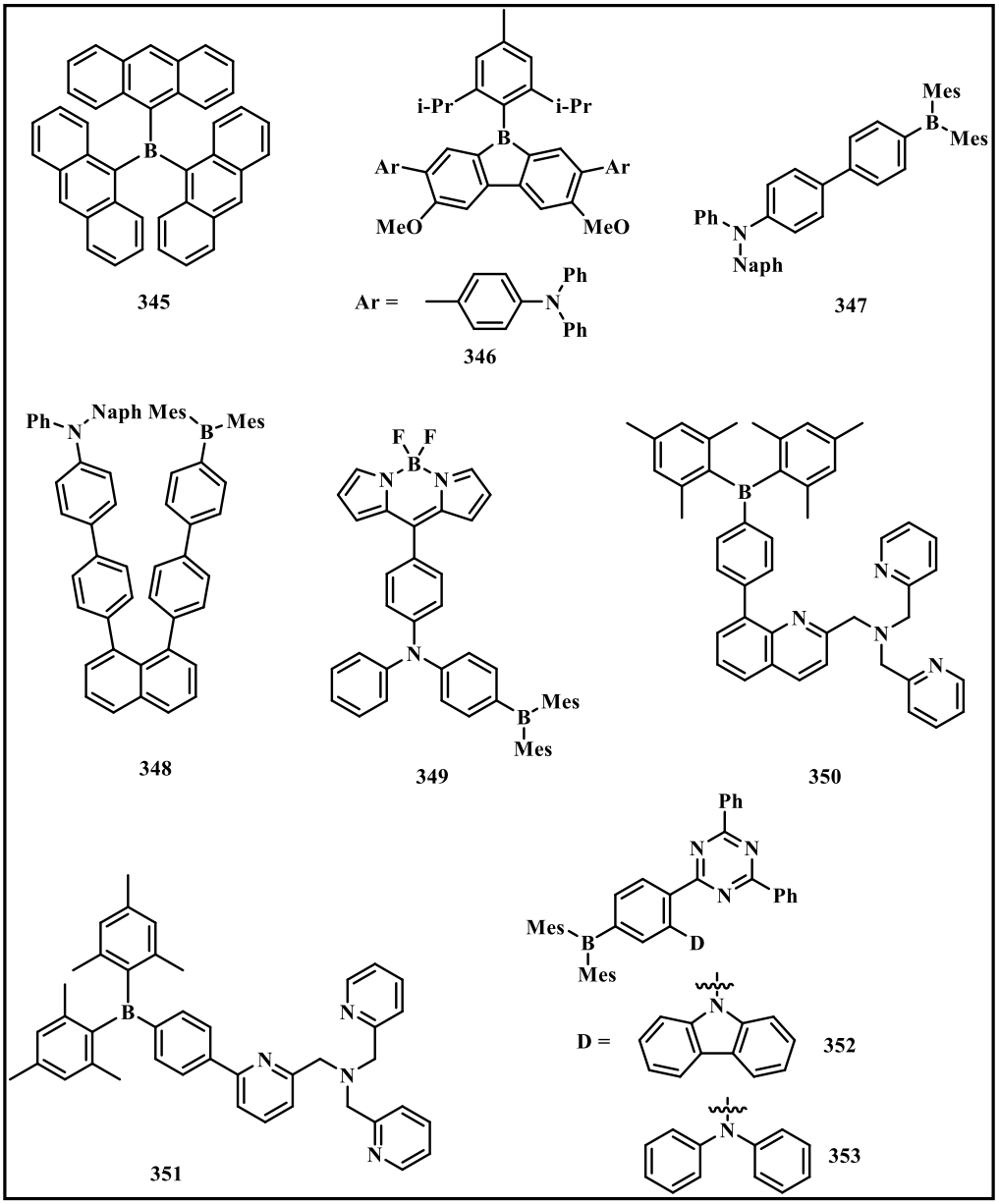

Figure 1.20: Sensors based on interaction between Lewis acidic boron and fluoride (**345-353**).

More recently Lee and co-workers reported two tri-aryl boron compounds **352-353** which contain donor-accepter units for the detection of fluoride ion though the ICT mechanism[147].

1.2.2.3 O-Si bond cleavage reactions for fluoride ion detection

In recent year's reaction based chemodosimeters are gaining attention because of their high selectivity. Silyl protection is a well known organic chemistry reaction

used for the protection of alcohols and has become key factor for the development of chemodosimeters for the selective fluoride ion detection. In 2003, Swager and co-workers developed a semiconducting polymer **354** for F^- ion detection. Fluoride ion induced lactonization triggers highly fluorescent coumarin derivatives in the side chain (**355**) which produces small band gap trapping site. The recombination of excitons in the backbone results new emission signal. This method directly interconnects the fluoride ion with polymer band structure, which serves as an alternative to FRET mechanism.[148] Jiang *etal*. developed a tris (N-salicylideneamine) based fluorophore **356** which showed emission enhancement at 460 nm[149] after addition of fluoride ion. The chemodosimeter **357** developed by Kim *et al.,* triggers Si-O bond cleavage results in phenolate anion after the addition of fluoride ion, which further undergoes cleavage to form *p*-quinomethane and resorufin. Here, resorufin acts as a fluorophore for the emission changes[150]. Two years later the same group reported coumarin based probe **358** for the detection of fluoride in HEPES buffer where TBDPS used as a silyl group. Probe **358** was also studied for fluorescence cell bioimaging for the detection of NaF in A549 human lung carcinoma cells under physiological conditions[151]. In 2010 Hu *et al*. developed probe **359** with dual wavelength emissive ability. Addition of fluoride ion triggers Si-O bond cleavage to form an ESIPT activated benzothiazole moiety which leads emission colour changes from blue-violet to bright yellow ratiometrically[152]. Si- O bond cleavage strategy was also studied on BODIPY system **(360, 361),** and were fabricated for the fluoride ion detection by Akkaya group. Addition of fluoride ion to **360** generates phenolic group on the meso position of BODIPY which leads emission quenching *via* PET quenching mechanism. Whereas in probe **361**, the addition of fluoride ion, which triggers a strong ICT process in leads emission quenching at 560 nm[153].

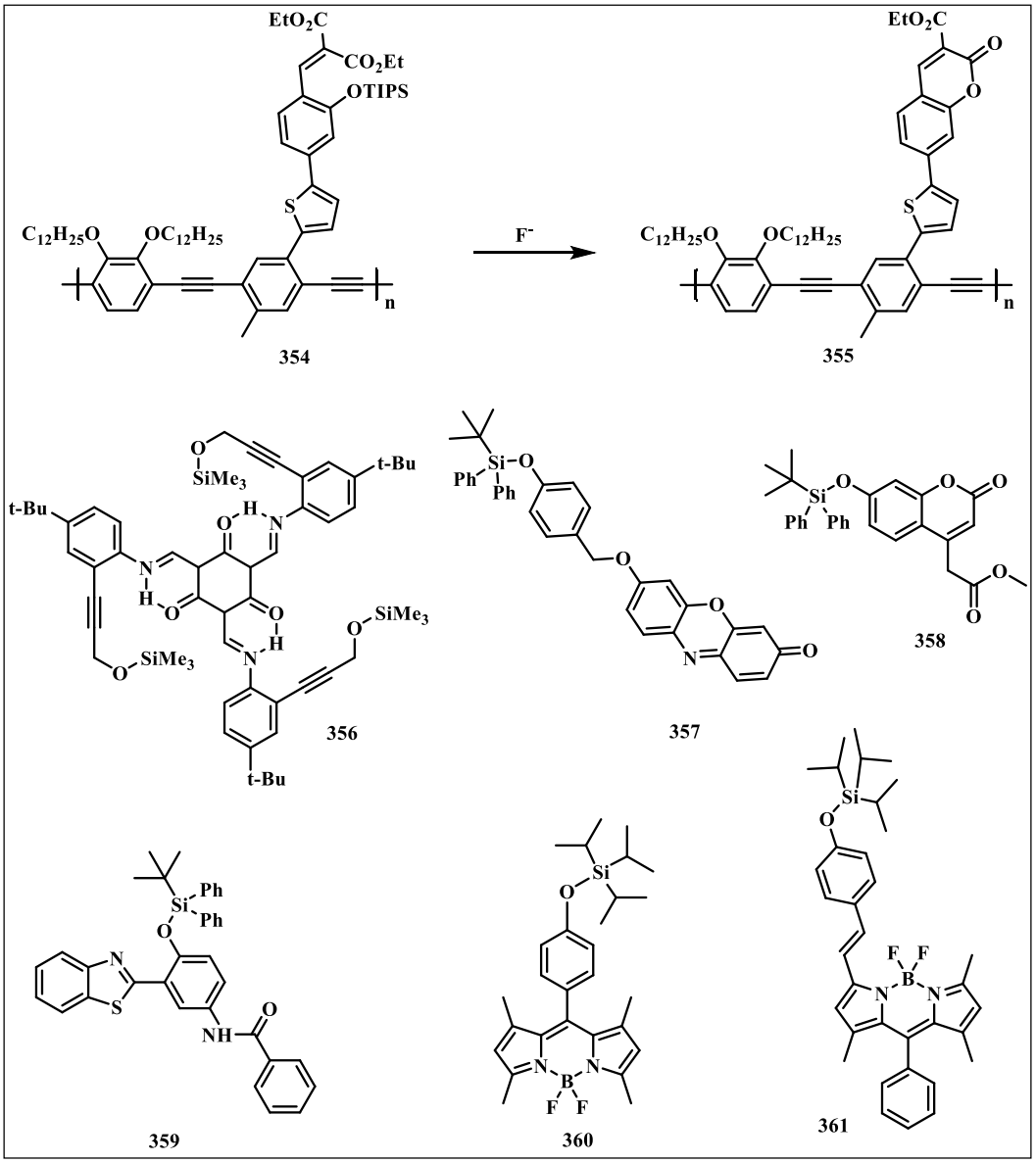

Figure 1.21: Sensors based on O-Si bond cleavage reaction (**354-361**).

In 2011, ICT based probe **362** was developed, which showed colorimetric and ratiometric emission response for fluoride ion[154]. A near infrared fluorescent probe **363** was developed by Cao et al. in 2012. Addition of 400 equiv. of fluoride to **363,** results 1000 fold emission enhancement at 718 nm in DMSO/water system[155]. A sugar modified sensor **364** was developed for fluoride ion detection in 100% water medium. This probe showed turn on emission response with detection limit as low as 1.5 mg/L with significant naked eye colour changes[156].

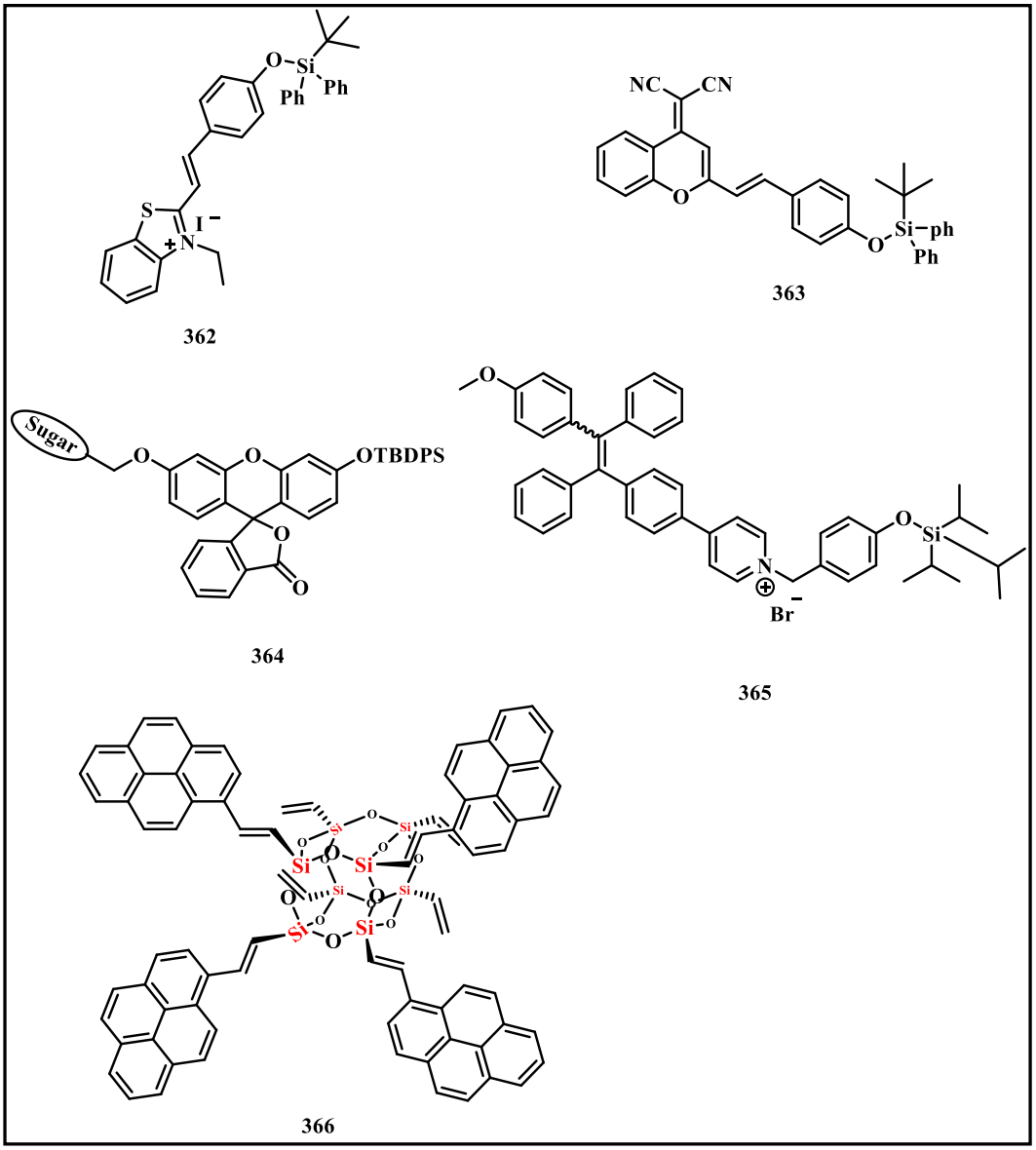

Figure 1.22: Sensors based on O-Si bond cleavage reaction (**362-366**).

Wang and co-workers developed tetraphenylethylene with a pyridinium pendant (**365**) which shows AIE property for the detection of fluoride ion in aqueous without any surfactant additives and in living cells. This probe can be spontaneously undergo 1, 6-elimination of *p*-quinone-methide to produced MOPy-TPE with poor water solubility[157]. Pyrene functionalized silsesquioxane cages **366** were exhibited different intensity of fluorescence depending on solvent polarity. Up on addition of fluoride ion

in high polar solvents (DMSO/water) exhibit enhanced emission and low polarity solvent (THF) exhibited diminished fluorescence[158].

The synthesis of novel fluorescent probe **367** reported by Xiangyang Zhang, Youyu Zhang and co-workers based on ICT strategy showed high selectivity and sensitivity for fluoride ion even in the nano molar. The probe could be used to monitor mitochondrial fluoride ion in living cells by ratiometric fluorescence imaging[159]. A novel NIR (at 665 nm) fluorescent probe **368** was synthesized by Liu group. Si-O bond was used as fluoride ion trigger, and the release of fluorophore took place after substituent reaction and subsequent 1, 6-elimination. The fluoride ion sensing was also detected in HeLa cells and zebrafish embryos through the fluorescence imaging[160]. Recently Péter Ábrányi-Balogh's group developed a new family of boroisoquinolines (BIQ) (**369-370)** for the detection of F^- in aqueous media[161]. Recently our group also developed imidazole-based fluorescent probe **371** for sensing of fluoride anion in DMSO/H_2O.[162] More recently, Fang and co-workers reported a novel homoditopic curcumin-difluoroboron based receptor **372** with triisopropylsilyl group functionalized. This is the first fluoride ion probe based on curcumin in which is highly selective with a low detection limit (0.21μM).[163]

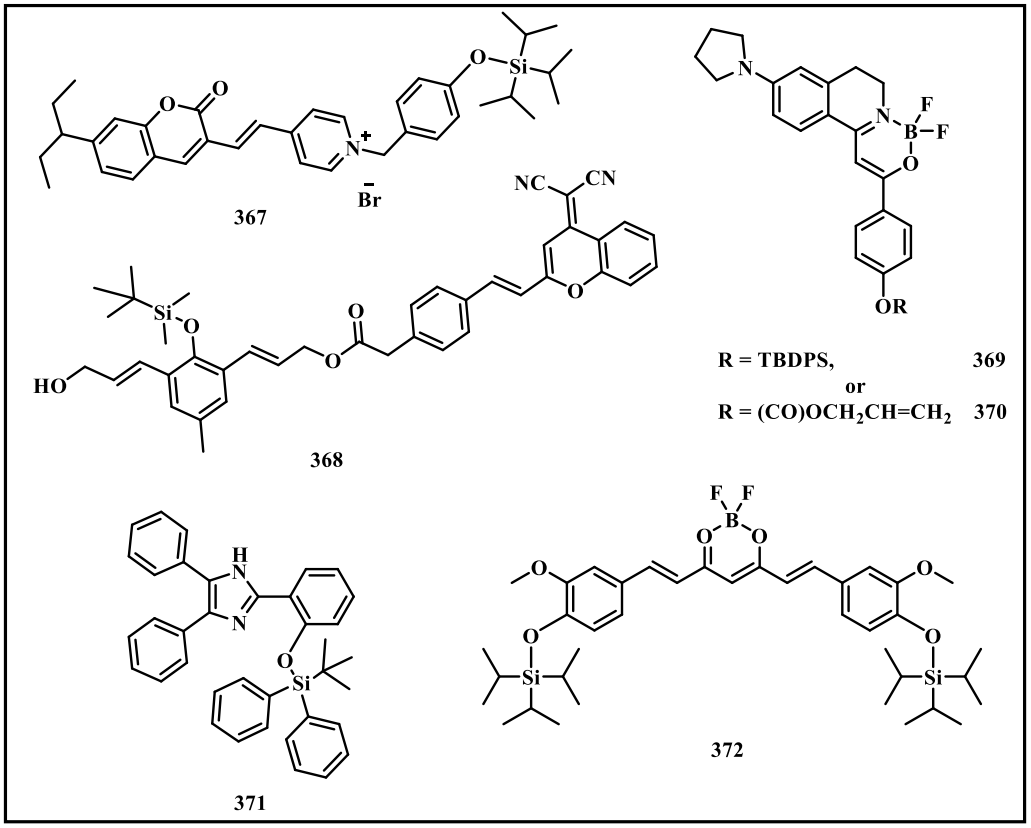

Figure 1.23: Sensors based on O-Si bond cleavage reaction (**367-372**).

1.3. Planar Chiral Ferrocene derivatives.

The organometallic chemistry has been developed dramatically since the discovery of ferrocene by Pauson and Kealy. There are many views on the topic of ferrocenes and its applications in the field of materials chemistry, catalysis, pharmaceuticals and so on. In this part of the thesis, I will present brief summary on the recent progress of planar chiral ferrocenes.

The three dimensional structure of ferrocene results planar chirality. To have planar chirality the ferrocene molecule should have at least two different substituents in the same cyclopentadiene of ferrocene[164-165]. The term planar chirality was first proposed by Cahn, Ingold and Prelog (CIP).[166] When a molecule is observed from the top of the substituted cyclopentadienyl ring of ferrocene, the planar chirality is fixed

by the order going from the substituent with higher priority to that with low priority [167-168]. If the direction is clockwise then the configuration assigned to the molecule is "*R*", otherwise "*S*" configuration. The stereo labels are "R_p" and "S_p" used to represent to the planar chirality (Figure 1.24). Additionally "*R*" and "*S*" are used to mention the central chirality.

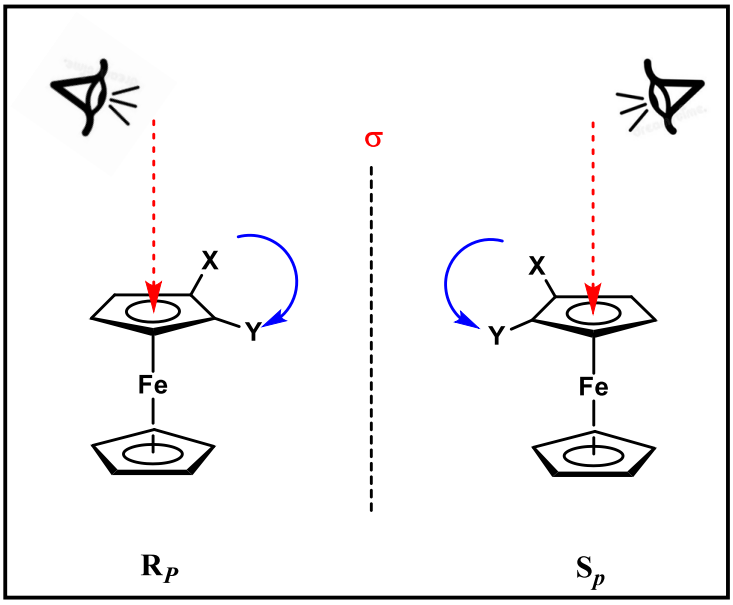

Figure 1.24: The Stereo chemistry with Schlögl model for chiral 1,2-di substituted ferrocene (priority X>Y).

Ferrocene derivatives with planar chirality products can be obtained starting from either achiral or chiral precursors. The first method (achiral) does not yield stereoselective compounds, hence chiral resolution methods should be used for the separation of individual enantiomers. For example, Fu and coworkers synthesized DMAP- fused ferrocene derivatives. However, the recemate could be resolved using chiral preparative HPLC which is a drawback of this method. The resolved chiral ferrocene used as a catalyst for asymmetric transformation[169-170] (Figure 1.25). This method has the advantage that it does not involve chiral synthesis from the precursor

and in many cases both the enantiomers can be utilized. However, the major drawback is that it relies to find suitable methods or agents to separate the enantiomers. Chiral auxiliaries methodology will overcome the drawbacks discussed in the achiral methodology. Stereo selective ortho-metalation of an enantiomerically pure, chiral ferrocene was first employed by Ugi in 1970 (Scheme 1.1). Ugis amine was resolved by complexation with R-(+)-tartaric acid[171].

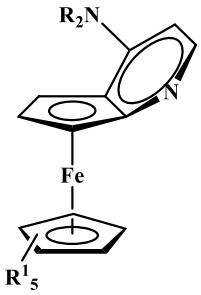

R = Me_2, -(CH_2)-
R^1 = Me, Ph

Figure 1.25: Racemic mixture of 1, 2-disubstituted ferrocene (left) and Fu's Fc-DAAPs (right).

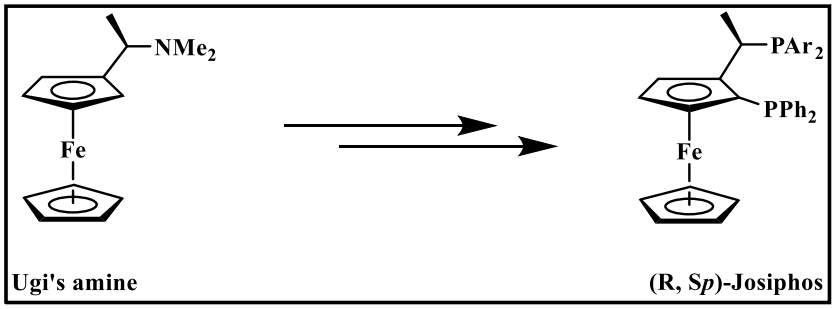

Scheme1.1: Synthesis of Ugi's amine to Josiphos ligand.

Using this method, planar chiral phosphine ligands were synthesized, namely Josiphos family [172] of ligands (Figure1.3.3) and utilized for a variety of reactions including asymmetric reduction of C=C, C=O and C=N[173-174].

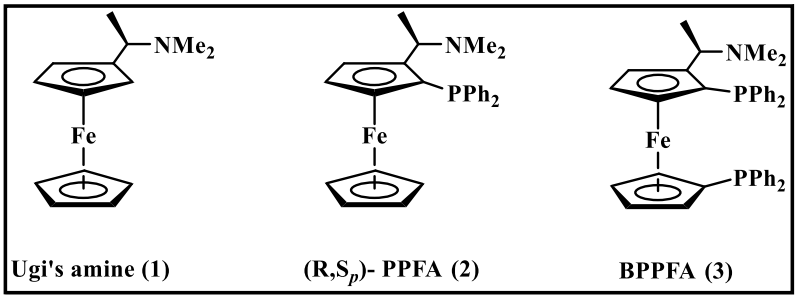

Figure 1.26: Arrangements of Ugi's amine and the first ferrocene based chiral phosphine ligands

Since this pioneering work of Ugi's amine, hundreds of chiral auxiliaries such as sulfoxides[175], oxazolines[176], sulfoximines[177], acetals[178-179], α-substituted methyl amines[171] and their congeners[180] (Figure 1.27) etc have been synthesized and utilized.

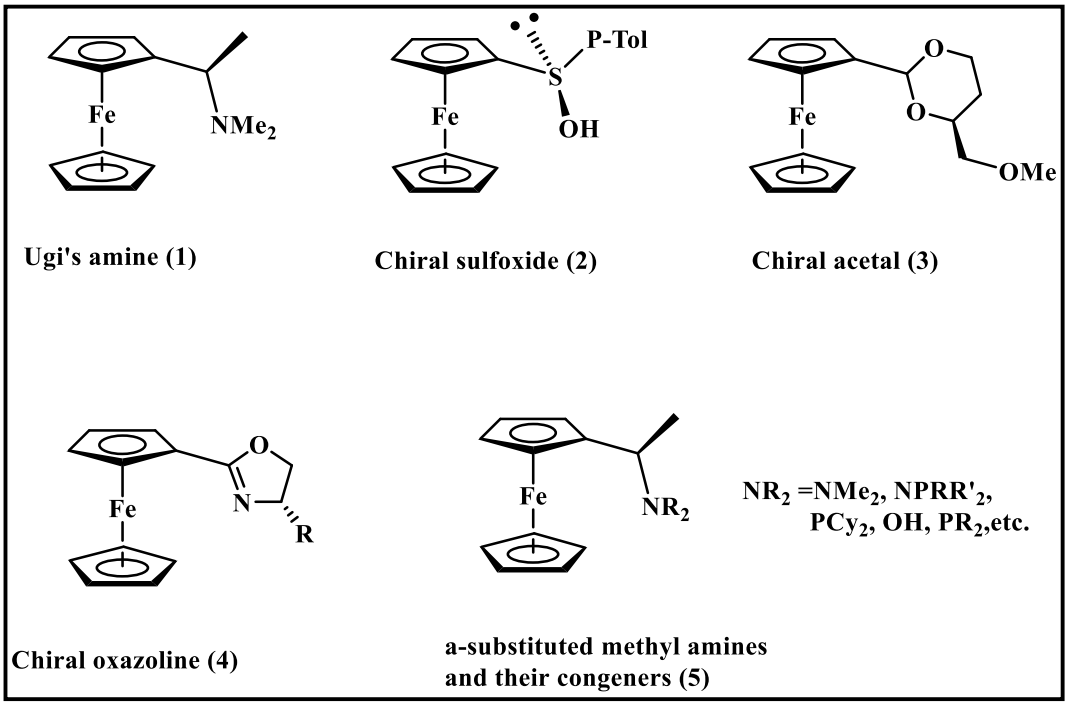

Figure 1.27: Several chiral auxiliaries used as directive metalation groups (DMG).

Among the different methods available, the sulfoxide methodology introduced by Kagan and co-workers have many advantages. The optically active ferrocenyl sulfoxide auxiliary can be prepared by quenching the lithiated ferrocene with menthyl

p-tolyl sulfonate.[181-182] (Scheme 1.2). The sulfoxide group present in the ferrocenyl sulfoxide act as an excellent ortho-directing group, can be used deprotonate the hydrogen using *n*-BuLi, which upon treatment with electrophiles will give 1,2-substituted ferrocene.

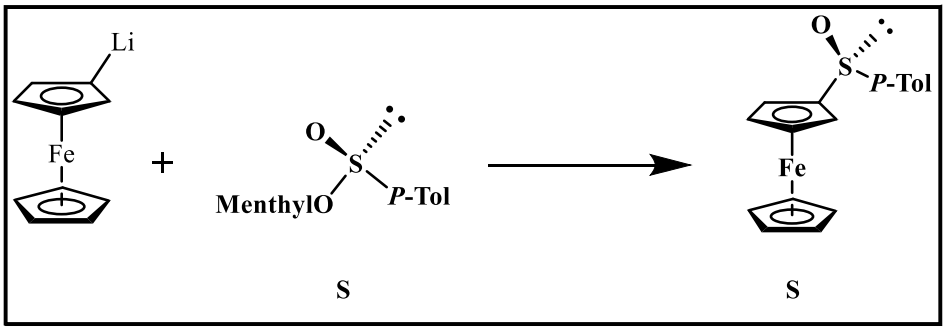

Scheme 1.2: Nucleophilic attack of monolithioferrocene on optically pure menthyl *p*-toluenesulfinate.

The chiral sulfoxide have advantage over Ugi's amine. The oxidation state of the sulfur can be readily tuned, taking this as an advantage one can easily change the central chirality[183](Scheme 1.3).

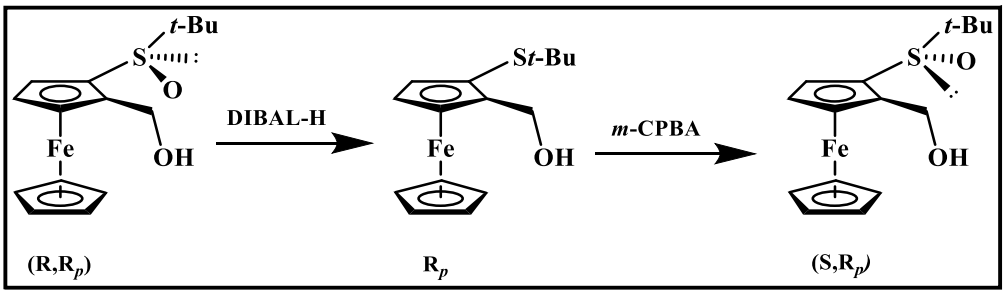

Scheme 1.3: Steric inversion arrangement at sulfur by the reduction and followed by enantioselective reoxidation.

1,2- substituted ferrocenyl sulfinate has the advantage that after derivatization of the ortho-position, the sulfinate group can be easily replaced by lithiation with tert-butyl

lithium and subsequent reaction with electrophiles will yield 1,2-substituted planar chiral compounds.[182-183] (Scheme 1.4)

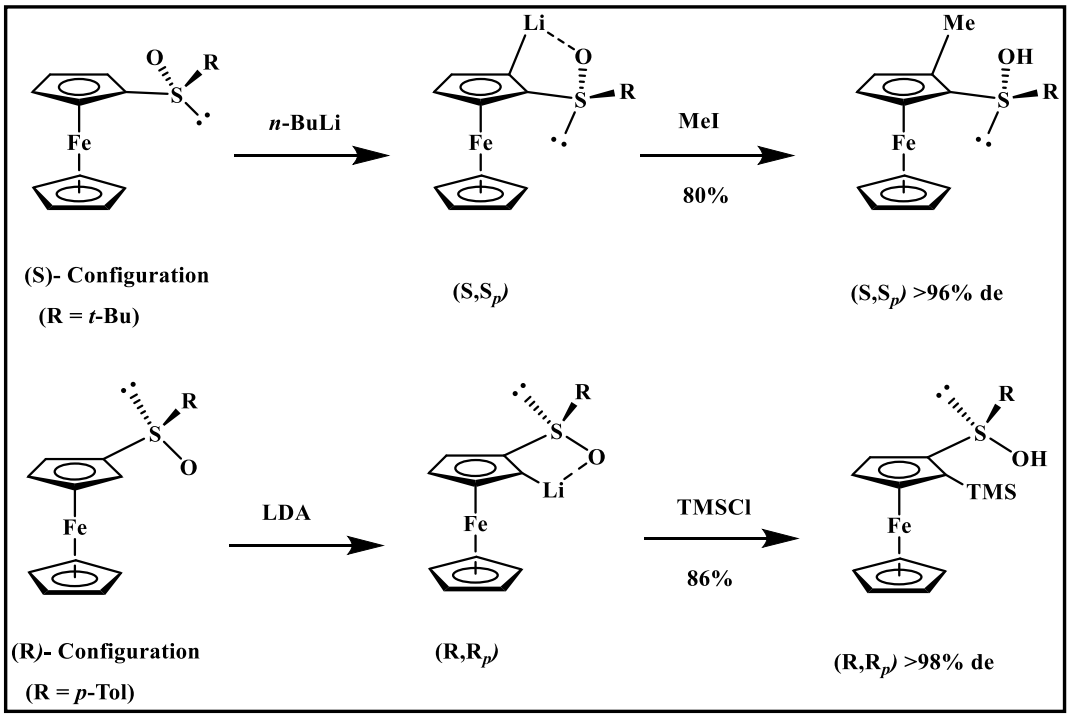

Scheme 1.4: Diastereo selective metalation of ferrocenyl *p*-tolyl sulfoxide by *n*-BuLi.

1.4 References:

(1) Anthony, J. E. *Chem. Rev*. **2006**, *106*, 5028.

(2) Coropceanu, V.; Cornil, J.; da Silva Filho, D. A.; Olivier, Y.; Silbey, R.; Brédas, J. L. *Chem. Rev*. **2007**, *107*, 926.

(3) Dalton, L. R.; Sullivan, P. A.; Bale, D. H. *Chem. Rev*. **2010**, *110*, 25.

(4) Bendikov, M.; Wudl, F.; Perepichka, D. F. *Chem. Rev*. **2004**, *104*, 4891.

(5) Hestand, N. J.; Spano, F. C. *Chem. Rev*. **2018**, *118*, 7069.

(6) Mishra, A.; Ma, C. Q.; Bäuerle, P. *Chem. Rev.* **2009**, *109*, 1141.

(7) Ji, L.; Griesbeck, S.; Marder, T. B. *Chem. Sci.* **2017**, *8*, 846.

(8) Von, G.E.; John, A.; Kaese, T.; Wagner, M. *Asian J. Org. Chem*. **2018**, *7*, 37.

(9) Hudson, Z. M.; Wang, S. *Acc. Chem. Res.* **2009**, *42*, 1584.

(10) Qin, Y.; Cheng, G.; Sundararaman, A.; Jäkle, F. *J. Am. Chem. Soc.* **2002**, *124*, 12672.

(11) Li, S.-Y.; Sun, Z.-B.; Zhao, C.-H. *Inorg. Chem.* **2017**, *56*, 8705.

(12) Tang, C. W.; VanSlyke, S. A. *Appl. Phys. Lett.* **1987**, *51*, 913.

(13) Wang, S. *Coord. Chem. Rev.* **2001**, *215*, 79.

(14) Li, D.; Zhang, H.; Wang, Y. *Chem. Soc. Rev.* **2013**, *42*, 8416.

(15) Li, P.; Chan, H.; Lai, S.-L.; Ng, M.; Chan, M.-Y.; Yam, V. W.-W. *Angew. Chem., Int. Ed.* **2019**, *58*, 9088.

(16) Maeda, H.; Fujii, Y.; Mihashi, Y. *Chem. Commun.* **2008**, 4285.

(17) Kano, N.; Yoshino, J.; Kawashima, T. *Org. Lett.* **2005**, *7*, 3909.

(18) Lamère, J. F.; Lacroix, P. G.; Farfán, N.; Rivera, J. M.; Santillan, R.; Nakatani, K. *J. Mater. Chem.* **2006**, *16*, 2913.

(19 Sun, Y.; Rohde, D.; Liu, Y.; Wan, L.; Wang, Y.; Wu, W.; Di, C.; Yu, G.; Zhu, D. *J. Mater. Chem.* **2006**, *16*, 4499.

(20) Fischer, G. M.; Jungst, C.; Isomaki-Krondahl, M.; Gauss, D.; Moller, H. M.; Daltrozzo, E.; Zumbusch, A. *Chem. Commun.* **2010**, 46, 5289.

(21) Loudet, A.; Burgess, K. *Chem. Rev.* **2007**, *107*, 4891.

(22) Carlotti, B.; Poddar, M.; Elisei, F.; Spalletti, A.; Misra, R. *Journal of Physical Chemistry C*. **2019**, *123*, 24362.

(23) Ulrich, G.; Ziessel, R.; Harriman, A. *Angew. Chem., Int. Ed.* **2008**, 47, 1184.

(24) Toyoda, M.; Imai, Y.; Mori, T. *J. Phys. Chem. Lett.* **2017**, *8*, 42.

(25) Burghart, A.; Thoresen, L. H.; Chen, J.; Burgess, K.; Bergström, F.; Johansson, L. B. Å. *Chem. Commun.* **2000**, 2203.

(26) Lakshmi, V.; Ravikanth, M. *J. Org. Chem.* **2011**, *76*, 8466.

(27) Ge, Y.; O'Shea, D. F. *Chem. Soc. Rev.* **2016**, 45, 3846.

(28) Zhang, D.; Wen, Y.; Xiao, Y.; Yu, G.; Liu, Y.; Qian, X. *Chem. Commun.* **2008**, 4777.

(29) Kubota, Y.; Kasatani, K.; Takai, H.; Funabiki, K.; Matsui, M. *Dalton Trans.* **2015**, *44*, 3326.

(30) Liu, S.-F.; Wu, Q.; Schmider, H. L.; Aziz, H.; Hu, N.-X.; Popović, Z.; Wang, S. *J. Am. Chem. Soc*. **2000**, *122*, 3671.

(31) Liang, F. S.; Cheng, Y. X.; Su, G. P.; Ma, D. G.; Wang, L. X.; Jing, X. B.; Wang, F. S. *Synth. Met.* **2003**, 137, 1109.

(32) Liu, Q.; Mudadu, M. S.; Schmider, H.; Thummel, R.; Tao, Y.; Wang, S. *Organometallics.* **2002**, *21*, 4743.

(33) Calhorda, M. J.; Suresh, D.; Gomes, P. T.; Di Paolo, R. E.; Macanita, A. L. *Dalton Trans*. **2012**, *41*, 13210.

(34) Suresh, D.; Lopes, P. S.; Ferreira, B.; Figueira, C. A.; Gomes, C. S. B.; Gomes, P. T.; Di Paolo, R. E.; MaçAnita, A. L.; Duarte, M. T.; Charas, A.; Morgado, J.; Calhorda, M. J. *Chem. -Eur. J.* **2014**, *20*, 4126.

(35) Suresh, D.; Gomes, C. S. B.; Lopes, P. S.; Figueira, C. A.; Ferreira, B.; Gomes, P. T.; Di Paolo, R. E.; Macanita, A. L.; Duarte, M. T.; Charas, A.; Morgado, J.; Vila-Vicosa, D.; Calhorda, M. J. *Chem. -Eur. J.* **2015**, *21*, 9133.

(36) Suresh, D.; Ferreira, B.; Lopes, P. S.; Gomes, C. S. B.; Krishnamoorthy, P.; Charas, A.; Vila-Vicosa, D.; Morgado, J.; Calhorda, M. J.; Macanita, A. L.; Gomes, P. T. *Dalton Trans*. **2016**, *45*, 15603.

(37) Nagata, Y.; Chujo, Y. *Macromolecules*. **2008**, *41*, 2809.

(38) Qian, H.; Wang, Y.-Y.; Guo, D.-S.; Aprahamian, I. *J. Am. Chem. Soc.* **2017**, *139*, 1037.

(39) Rodrigues, A. I.; Figueira, C. A.; Gomes, C. S. B.; Suresh, D.; Ferreira, B.; Di Paolo, R. E.; Pereira, D. d. S.; Dias, F. B.; Calhorda, M. J.; Morgado, J.; Maçanita, A. L.; Gomes, P. T. *Dalton Trans.* **2019**, *48*, 13337.

(40) Vinayakumara, D. R.; Swamynathan, K.; Kumar, S.; Adhikari, A. V. *New J. Chem.* **2019**, *43*, 7099.

(41) Barbon, S. M.; Reinkeluers, P. A.; Price, J. T.; Staroverov, V. N.; Gilroy, J. B. *Chem. -Eur. J.* **2014**, *20*, 11340.

(42) Chang, M. C.; Chantzis, A.; Jacquemin, D.; Otten, E. *Dalton Trans.* **2016**, *45*, 9477.

(43) Barbon, S. M.; Price, J. T.; Reinkeluers, P. A.; Gilroy, J. B. *Inorg. Chem.* **2014**, *53*, 10585.

(44) Chang, M. C.; Otten, E. *Chem. Commun.* **2014**, *50*, 7431.

(45) Lipunova, G. N.; Fedorchenko, T. G.; Chupakhin, O. N. *Russ. J. Gen. Chem.* **2019**, *89*, 1225.

(46) Barbon, S. M.; Staroverov, V. N.; Gilroy, J. B. *J. Org. Chem.* **2015**, 80, 5226.

(47) Hesari, M.; Barbon, S. M.; Staroverov, V. N.; Ding, Z.; Gilroy, J. B. *Chem. Commun.* **2015**, *51*, 3766.

(48) Maar, R. R.; Gilroy, J. B. *J. Mater. Chem. C.* **2016**, *4*, 6478.

(49) Maar, R. R.; Barbon, S. M.; Sharma, N.; Groom, H.; Luyt, L. G.; Gilroy, J. B. *Chem. -Eur. J.* **2015**, 21, 15589.

(50) Novoa, S.; Paquette, J. A.; Barbon, S. M.; Maar, R. R.; Gilroy, J. B. *J. Mater. Chem. C.* **2016**, 4, 3987.

(51) Ren, Y.; Liu, X.; Gao, W.; Xia, H.; Ye, L.; Mu, Y. *Eur. J. Inorg. Chem.* **2007**, *2007*, 1808.

(52) Perumal, K.; Garg, J. A.; Blacque, O.; Saiganesh, R.; Kabilan, S.; Balasubramanian, K. K.; Venkatesan, K. *Chem.-Asian J.* **2012**, *7*, 2670.

(53) Hong, Y.; Lam, J. W. Y.; Tang, B. Z. *Chem. Soc. Rev.* **2011**, *40*, 5361.

(54) Liddle, B. J.; Silva, R. M.; Morin, T. J.; Macedo, F. P.; Shukla, R.; Lindeman, S. V.; Gardinier, J. R. *J. Org. Chem.* **2007**, *72*, 5637.

(55) Araneda, J. F.; Piers, W. E.; Heyne, B.; Parvez, M.; McDonald, R. *Angew. Chem., Int. Ed.* **2011**, *50*, 12214.

(56) Lugovik, K. I.; Eltyshev, A. K.; Suntsova, P. O.; Slepukhin, P. A.; Benassi, E.; Belskaya, N. P. *Chem.-Asian J.* **2018**, *13*, 311.

(57) Min, Y.; Dou, C.; Liu, D.; Dong, H.; Liu, J. *J. Am. Chem. Soc.* **2019**, *141*, 17015.

(58) Kubota, Y.; Tsuzuki, T.; Funabiki, K.; Ebihara, M.; Matsui, M. *Org. Lett.* **2010**, *12*, 4010.

(59) Golden, J. H.; Estergreen, L.; Porter, T.; Tadle, A. C.; Sylvinson M. R, D.; Facendola, J. W.; Kubiak, C. P.; Bradforth, S. E.; Thompson, M. E. *ACS Appl. Energy Mater.* **2018**, *1*, 1083.

(60) Rodríguez, M.; Maldonado, J. L.; Ramos-Ortíz, G.; Domínguez, O.; Ochoa, M. E.; Santillan, R.; Farfán, N.; Meneses-Nava, M.-A. *Polyhedron.* **2012**, *43*, 194.

(61) Rodriguez, M.; Maldonado, J. L.; Ramos-Ortiz, G.; Lamere, J. F.; Lacroix, P. G.; Farfan, N.; Ochoa, M. E.; Santillan, R.; Meneses-Nava, M. A. *New J. Chem.* **2009**, *33*, 1693.

(62) Nolasco, J. C.; Ryan, J. W.; Rodríguez, M.; Castro-Carranza, A.; Maldonado, J. L.; Ramos-Ortiz, G.; Barbosa-Garcia, O.; Gutowski, J.; Palomares, E.; Parisi, J. *J. Mater. Sci. Mater. Electron.* **2018**, *29*, 16410.

(63) Wu, Q.; Esteghamatian, M.; Hu, N.-X.; Popovic, Z.; Enright, G.; Tao, Y.; D'Iorio, M.; Wang, S. *Chem. Mater.* **1999**, *12*, 79.

(64) Cui, Y.; Wang, S. *J. Org. Chem*. **2006**, *71*, 6485.

(65) Chen, J.; Burghart, A.; Wan, C.-W.; Thai, L.; Ortiz, C.; Reibenspies, J.; Burgess, K. *Tetrahedron Lett*. **2000**, *41*, 2303.

(66) Hohaus, E.; Umland, F. Chem. Ber. **1969**, *102*, 4025.

(67) Durka, K.; Głowacki, I.; Luliński, S.; Łuszczyńska, B.; Smętek, J.; Szczepanik, P.; Serwatowski, J.; Wawrzyniak, U. E.; Wesela-Bauman, G.; Witkowska, E.; Wiosna-Sałyga, G.; Woźniak, K. *J. Mater. Chem. C*. **2015**, *3*, 1354.

(68) Urban, M.; Górka, P.; Nawara, K.; Woźniak, K.; Durka, K.; Luliński, S. *Dalton Trans*. **2018**, *47*, 15670.

(69) Cheng, F.; Jakle, F. *Chem. Commun.* **2010**, *46*, 3717.

(70) Hohaus, E. Monatsh. Chem. **1980**, *111*, 863.

(71) Urban, M.; Durka, K.; Jankowski, P.; Serwatowski, J.; Luliński, S. *J. Org. Chem*. **2017**, *82*, 8234.

(72) Frath, D.; Azizi, S.; Ulrich, G.; Retailleau, P.; Ziessel, R. *Org. Lett.* **2011**, *13*, 3414.

(73) Frath, D.; Azizi, S.; Ulrich, G.; Ziessel, R. *Org. Lett*. **2012**, *14*, 4774.

(74) Frath, D.; Didier, P.; Mély, Y.; Massue, J.; Ulrich, G. *ChemPhotoChem*. **2017**, *1*, 109.

(75) Frath, D.; Benelhadj, K.; Munch, M.; Massue, J.; Ulrich, G. *J. Org. Chem.* **2016**, *81*, 9658.

(76) Dhanunjayarao, K.; Mukundam, V.; Ramesh, M.; Venkatasubbaiah, K. *Eur. J. Inorg. Chem.* **2014**, 539.

(77) Shanmugapriya, J.; Rajaguru, K.; Sivaraman, G.; Muthusubramanian, S.; Bhuvanesh, N. *RSC Adv*. **2016**, *6*, 85838.

(78) Zhou, L.; Xu, D.; Gao, H.; Han, A.; Liu, X.; Zhang, C.; Li, Z.; Yang, Y. *Dyes Pigm.* **2017**, *137*, 200.

(79) Sun, J.; Yang, H.; Simalou, O.; Lv, K.; Zhai, L.; Zhao, J.; Lu, R. *New J. Chem.* **2019**, *43*, 10134.

(80) Yang, D.; Liu, P.; Bai, T.; Kong, J. Macromolecules. **2020**.

(81) Lee, J. E.; Choi, G. C.; Rim, B. O.; Kim, S. M.; Park, N. G.; Ha, Y. K.; Kim, Y. S. *Mater. Sci. Eng. C*. **2004**, *24*, 269.

(82) Massue, J.; Retailleau, P.; Ulrich, G.; Ziessel, R. *New J. Chem.* **2013**, *37*, 1224.

(83) Salla, C. A. M.; Teixeira dos Santos, J.; Farias, G.; Bortoluzi, A. J.; Curcio, S. F.; Cazati, T.; Izsák, R.; Neese, F.; de Souza, B.; Bechtold, I. H. *Eur. J. Inorg. Chem*. **2019**, *2019*, 2247.

(84) Kwak, M.-J.; Kim, Y.-M. *Bull. Korean Chem. Soc.* **2009**, *30*, 2865.

(85) Li, D.; Wang, K.; Huang, S.; Qu, S.; Liu, X.; Zhu, Q.; Zhang, H.; Wang, Y. *J. Mater. Chem.* **2011**, *21*, 15298.

(86) Li, D.; Zhang, H.; Wang, C.; Huang, S.; Guo, J.; Wang, Y. *J. Mater. Chem*. **2012**, *22*, 4319.

(87) Li, D.; Yuan, Y.; Bi, H.; Yao, D.; Zhao, X.; Tian, W.; Wang, Y.; Zhang, H. *Inorg. Chem.* **2011**, *50*, 4825.

(88) Zhang, Z.; Zhang, Z.; Zhang, H.; Wang, Y. *Dalton Trans.* **2018**, *47*, 127.

(89) Massue, J.; Frath, D.; Ulrich, G.; Retailleau, P.; Ziessel, R. *Org. Lett*. **2012**, *14*, 230.

(90) Massue, J.; Frath, D.; Retailleau, P.; Ulrich, G.; Ziessel, R. *Chem. -Eur. J.* **2013**, *19*, 5375.

(91) Massue, J.; Retailleau, P.; Ulrich, G.; Ziessel, R. *New J. Chem*. **2013**, *37*, 1224.

(92) Dias, G. G.; Rodrigues, B. L.; Resende, J. M.; Calado, H. D. R.; de Simone, C. A.; Silva, V. H. C.; Neto, B. A. D.; Goulart, M. O. F.; Ferreira, F. R.; Meira, A. S.; Pessoa, C.; Correa, J. R.; da Silva Junior, E. N. *Chem. Commun*. **2015**, *51*, 9141.

(93) Kubota, Y.; Hara, H.; Tanaka, S.; Funabiki, K.; Matsui, M. *Org. Lett*. **2011**, *13*, 6544.

(94) Kubota, Y.; Tanaka, S.; Funabiki, K.; Matsui, M. *Org. Lett*. **2012**, *14*, 4682.

(95) Kubota, Y.; Ozaki, Y.; Funabiki, K.; Matsui, M. *J. Org. Chem*. **2013**, *78*, 7058.

(96) Kubota, Y.; Kasatani, K.; Niwa, T.; Sato, H.; Funabiki, K.; Matsui, M. *Chem. - Eur. J*. **2016**, *22*, 1816.

(97) Potopnyk, M. A.; Lytvyn, R.; Danyliv, Y.; Ceborska, M.; Bezvikonnyi, O.; Volyniuk, D.; Gražulevičius, J. V. *J. Org. Chem.* **2018**, *83*, 1095.

(98) Potopnyk, M. A.; Volyniuk, D.; Luboradzki, R.; Ceborska, M.; Hladka, I.; Danyliv, Y.; Gražulevičius, J. V. *J. Org. Chem.* **2019**, *84*, 5614.

(99) Zhang, Z.; Xue, P.; Gong, P.; Zhang, G.; Peng, J.; Lu, R. *J. Mater. Chem. C.* **2014**, *2*, 9543.

(100) Zhang, Z.; Wu, Z.; Sun, J.; Yao, B.; Xue, P.; Lu, R. *J. Mater. Chem. C*. **2016**, *4*, 2854.

(101) Liao, C.-W.; Rao M, R.; Sun, S.-S. *Chem. Commun*. **2015**, *51*, 2656.

(102) Wu, Z.; Sun, J.; Zhang, Z.; Yang, H.; Xue, P.; Lu, R. *Chem. -Eur. J*. **2017**, *23*, 1901.

(103) Huang, J.; Wang, Y.; Van Hecke, K.; Pereshivko, O. P.; Peshkov, V. A. *Eur. J. Org. Chem.* **2019**, *2019*, 2490.

(104) Mi, W.; Qu, Z.; Sun, J.; Zhang, F.; Zhai, L.; Zhao, J.; Ye, K. *New J. Chem.* **2018**, *42*, 12882.

(105) Wu, Y.; Li, Z.; Liu, Q.; Wang, X.; Yan, H.; Gong, S.; Liu, Z.; He, W. *Org. Biomol. Chem.* **2015**, *13*, 5775.

(106) Gong, S.; Liu, Q.; Wang, X.; Xia, B.; Liu, Z.; He, W. *Dalton Trans.***2015**, *44*, 14063.

(107) Zhou, L.; Xu, D.; Gao, H.; Han, A.; Yang, Y.; Zhang, C.; Liu, X.; Zhao, F. *RSC Adv.* **2016**, *6*, 69560.

(108) Gao, H.; Xu, D.; Liu, X.; Han, A.; Zhou, L.; Zhang, C.; Yang, Y.; Li, W. *RSC Adv.* **2017**, *7*, 1348.

(109) Zakrzewska, A.; Zaleśny, R.; Kolehmainen, E.; Ośmiałowski, B.; Jędrzejewska, B.; Ågren, H.; Pietrzak, M. *Dyes Pigm.* **2013**, *99*, 957.

(110) Ošmiałowski, B.; Zakrzewska, A.; Jędrzejewska, B.; Grabarz, A.; Zalešny, R.; Bartkowiak, W.; Kolehmainen, E. *J. Org. Chem.* **2015**, *80*, 2072.

(111) Grabarz, A. M.; Jędrzejewska, B.; Zakrzewska, A.; Zaleśny, R.; Laurent, A. D.; Jacquemin, D.; Ośmiałowski, B. *J. Org. Chem.* **2017**, *82*, 1529.

(112) Moshkina, T. N.; Nosova, E. V.; Lipunova, G. N.; Valova, M. S.; Taniya, O. S.; Slepukhin, P. A.; Charushin, V. N. *J. Fluorine Chem.* **2019**, *221*, 17.

(113) Qiu, F.; Zhang, N.; Tang, R.; Zhou, M.; Wang, Y.; Wei, W.; Bi, S.; Han, S.; Zhang, F. *J. Org. Chem.* **2018**, *83*, 12977.

(114) Zhou, Y.; Xiao, Y.; Chi, S.; Qian, X. *Org. Lett.* **2008**, *10*, 633.

(115) Wu, L.; Burgess, K. *J. Am. Chem. Soc.* **2008**, *130*, 4089.

(116) Murale, D. P.; Lee, K. M.; Kim, K.; Churchill, D. G. *Chem. Commun.* **2011**, *47*, 12512.

(117) Singh, R. S.; Yadav, M.; Gupta, R. K.; Pandey, R.; Pandey, D. S. *Dalton Trans.* **2013**, *42*, 1696.

(118) Lu, C.; Liu, Q.; Gu, P.; Chen, D.; Zhou, F.; Li, H.; Xu, Q.; Lu, J. *Polym. Chem.* **2014**, *5*, 2602.

(119) Chandrasekhar, V.; Azhakar, R.; Krishnan, V.; Athimoolam, A.; Pandian, B. M. *J. Am. Chem. Soc.* **2006**, *128*, 6802.

(120) Kubik, S. *Chem. Soc. Rev.* **2010**, *39*, 3648.

(121) Moore, J. A.; Mehta, P. G. *Macromolecules.* **1995**, *28*, 444.

(122) Kirk, K. L. *Biochemistry of the Halogens and Inorganic Halides*. **1991**, 58.

(123) Newbrun, E. *J. Public Health Dent*. **2010**, *70*, 227.

(124) Briancon, D. *Rev. Rhum*. **1997**, *64*, 78.

(125) Kleerekoper, M. *Endocrinol. Metab. Clin. North Am*. **1998**, *27*, 441.

(126) Michigami, Y.; Kuroda, Y.; Ueda, K.; Yamamoto, Y. *Anal. Chim. Acta.* **1993**, *274*, 299.

(127) Zhou, Y.; Zhang, J. F.; Yoon, J. *Chem. Rev.* **2014**, *114*, 5511.

(128) Konieczka, P.; Zygmunt, B.; Namieśnik, J. *J. Bull. Environ. Contam.Toxicol*. **2000**, *64*, 794.

(129) Cosentino, P.; Grossman, B.; Shieh, C.; Doi, S.; Xi, H.; Erbland, P. *J. Geotech. Eng.* **1995**, *121*, 610.

(130) Dhillon, A.; Nair, M.; Kumar, D. *Anal. Methods.* **2016**, *8*, 5338.

(131) Han, J.; Zhang, J.; Gao, M.; Hao, H.; Xu, X. *Dyes Pigm*. **2019**, *162*, 412.

(132) Duke, R. M.; Gunnlaugsson, T. *Tetrahedron Lett.* **2007**, *48*, 8043.

(133) Veale, E. B.; Gunnlaugsson, T. *J. Org. Chem.* **2008**, *73*, 8073.

(134) Kwon, J. Y.; Jang, Y. J.; Kim, S. K.; Lee, K.-H.; Kim, J. S.; Yoon, J. *J. Org. Chem.* **2004**, *69*, 5155.

(135) Madhu, S.; Ravikanth, M. *Inorg. Chem.* **2014**, *53*, 1646.

(136) Kumar, M.; Kumar, R.; Bhalla, V. *Tetrahedron.* **2009**, *65*, 4340.

(137) Uttam, B.; Kandi, R.; Hussain, M. A.; Rao, C. P. *J. Org. Chem.* **2018**, *83*, 11850.

(138) Kumar, G. G. V.; Kesavan, M. P.; Sivaraman, G.; Rajesh, J. *Sens. Actuators, B* **2018**, *255*, 3194.

(139) Xiao, L.; Ren, L.; Jing, X.; Li, Z.; Wu, S.; Guo, D. *Inorg. Chim. Acta.* **2020**, *500*, 119207.

(140) Wade, C. R.; Broomsgrove, A. E. J.; Aldridge, S.; Gabbaï, F. P. *Chem. Rev.* **2010**, *110*, 3958.

(141) Yamaguchi, S.; Akiyama, S.; Tamao, K. *J. Am. Chem. Soc.* **2001**, *123*, 11372.

(142) Yamaguchi, S.; Shirasaka, T.; Akiyama, S.; Tamao, K. *J. Am. Chem. Soc*. **2002**, *124*, 8816.

(143) Liu, X. Y.; Bai, D. R.; Wang, S. *Angew. Chem., Int. Ed.* **2006**, *45*, 5475.

(144) P, C. A. S.; Thilagar, P. *Inorg. Chem.* **2014**, *53*, 2776.

(145) Yuan, M.-S.; Du, X.; Liu, Z.; Li, T.; Wang, W.; Anslyn, E. V.; Wang, J. *Chem. Eur. J.***2018**, *24*, 9211.

(146) Zhang, Y.; Du, X.; Chen, L.; Li, Z.; Wang, W.; Li, T.; Yuan, M.-S. *Spectrochim. Acta, Part A.* **2019**, *218*, 119.

(147) Lee, H.; Jana, S.; Kim, J.; Lee, S. U.; Lee, M. H. *Inorg. Chem*. **2020**, *59*, 1414.

(148) Kim, T.-H.; Swager, T. M. *Angew. Chem., Int. Ed.* **2003**, *42*, 4803.

(149) Jiang, X.; Vieweger, M. C.; Bollinger, J. C.; Dragnea, B.; Lee, D. *Org. Lett*. **2007**, *9*, 3579.

(150) Kim, S. Y.; Hong, J. I. *Org. Lett*. **2007**, *9*, 3109.

(151) Kim, S. Y.; Park, J.; Koh, M.; Park, S. B.; Hong, J. I. *Chem. Commun.* **2009**, 4735.

(152) Hu, R.; Feng, J.; Hu, D.; Wang, S.; Li, S.; Li, Y.; Yang, G. *Angew. Chem., Int. Ed.* **2010**, *49*, 4915.

(153) Bozdemir, O. A.; Sozmen, F.; Buyukcakir, O.; Guliyev, R.; Cakmak, Y.; Akkaya, E. U. *Org. Lett.* **2010**, *12*, 1400.

(154) Zhu, B.; Yuan, F.; Li, R.; Li, Y.; Wei, Q.; Ma, Z.; Du, B.; Zhang, X. *Chem. Commun.* ***2011***, *47*, 7098.

(155) Cao, J.; Zhao, C.; Zhu, W. *Tetrahedron Lett.* **2012**, *53*, 2107.

(156) Wei, G.; Yin, J.; Ma, X.; Yu, S.; Wei, D.; Du, Y. *Anal. Chim. Acta.* **2011**, *703*, 219-225.

(157) Jiang, G.; Liu, X.; Wu, Y.; Wang, J.; Dong, X.; Zhang, G.; Li, Y.; Fan, X. *RSC Adv.* **2016**, *6*, 59400.

(158) Chanmungkalakul, S.; Ervithayasuporn, V.; Hanprasit, S.; Masik, M.; Prigyai, N.; Kiatkamjornwong, S. *Chem. Commun.* **2017**, *53*, 12108.

(159) Shen, Y.; Zhang, X.; Zhang, Y.; Li, H.; Chen, Y. *Sens. Actuators, B.* **2018**, *258*, 544.

(160) Feng, A.; Jia, Y.; Huang, L.; Wang, L.; Zhou, G.; Wang, S.; Liu, P. *Spectrochim. Acta, Part A.* **2019**, *220*, 117108.

(161) Sóvári, D.; Keserű, M. G.; Ábrányi-Balogh, P. *Materials*. **2020**, *13*, 199.

(162) Dhanunjayarao, K.; Mukundam, V.; Venkatasubbaiah, K. *Sens. Actuators, B* **2016**, *232*, 175.

(163) Fang, Y.; Wang, M.; Shen, Y.; Zhang, M.; Cao, Z.; Deng, Y. *Inorg. Chim. Acta.* **2020**, *503*, 119413.

(164) Hayashi, T. *Ferrocenes: Homogeneous Catalysis, Organic Synthesis, Materials Science*. **1994**, 105.

(165) Togni, A. *Metallocenes: Synthesis Reactivity Applications.* **1998**, 685.

(166) Cahn, R. S.; Ingold, C.; Prelog, V. *Angew. Chem., Int. Ed.* **1966**, *5*, 385.

(167) Schlögl, K. In *Planar chiral molecular structures*, Stereochemistry, Berlin, Heidelberg, 1984//; Vögtle, F.; Weber, E., Eds. Springer Berlin Heidelberg: Berlin, Heidelberg, **1984**; pp 27-62.

(168) Schlögl, K., Stereochemistry of metallocenes. In *Topics in stereochemistry*, Wiley Online Library: **1967**; Vol. 1, p 39.

(169) Fu, G. C. *Acc. Chem. Res.* **2000**, *33*, 412.

(170) Yoshida, K.; Liu, Q.; Yasue, R.; Wada, S.; Kimura, R.; Konishi, T.; Ogasawara, M. *ACS Catal.* **2020**, *10*, 292.

(171) Marquarding, D.; Klusacek, H.; Gokel, G.; Hoffmann, P.; Ugi, I. *J. Am. Chem. Soc*. **1970**, *92*, 5389.

(172) Colacot, T. J. *Chem. Rev.* **2003**, *103*, 3101.

(173) Sturm, T.; Weissensteiner, W.; Spindler, F. *Adv. Synth. Catal.* **2003**, *345*, 160.

(174) Boaz, N. W.; Mackenzie, E. B.; Debenham, S. D.; Large, S. E.; Ponasik, J. A. *J. Org. Chem*. **2005**, *70*, 1872.

(175) Ferber, B.; Kagan, H. B. *Adv. Synth. Catal.* **2007**, *349*, 493.

(176) Richards, C. J.; Damalidis, T.; Hibbs, D. E.; Hursthouse, M. B. *Synlett*. **1995**, *1995*, 74.

(177) Bolm, C.; Kesselgruber, M.; Muñiz, K.; Raabe, G. *Organometallics.* **2000**, *19*, 1648.

(178) Enders, D.; Peters, R.; Lochtman, R.; Raabe, G. *Angew. Chem., Int. Ed.* **1999**, *38*, 2421.

(179) Enders, D.; Peters, R.; Lochtman, R.; Runsink, J. Eur. *J. Org. Chem.* **2000**, *2000*, 2839.

(180) Blaser, H.-U.; Brieden, W.; Pugin, B.; Spindler, F.; Studer, M.; Togni, A. *Top. Catal.* **2002**, 19, 3.

(181) Guillaneux, D.; Kagan, H. B. *J. Org. Chem.* **1995**, *60*, 2502.

(182) Riant, O.; Argouarch, G.; Guillaneux, D.; Samuel, O.; Kagan, H. B. *J. Org. Chem.* **1998**, *63*, 3511.

(183) Rebière, F.; Riant, O.; Ricard, L.; Kagan, H. B. *Angew. Chem., Int. Ed.* **1993**, *32*, 568.

CHAPTER 2

Synthesis, characterization of *N,O*-chelated naphthaldimine based boron complexes, and study their photophysical and electrochemical properties

2.1 Introduction

Innovative organic luminescent fluorophores[1-2] have attracted much attention due to their numerable applications in biological as well as in optoelectronic devices[3-12]. Incorporation of main-group elements into the framework of organic fluorophores has provided a new opportunity to tune the optical properties of the fluorophores. Among the many main-group incorporated fluorophores, boron-based fluorophores such as boron-dipyrromethene (BODIPY)[13-16] as well as N∩O[17-28]; N∩N[29-35] and N∩C[36-37] chelates have gained much interest due to their attractive photophysical properties. Of these extended π-conjugated systems, the N∩O chelated boron system 'boranils' were derived from the salicylaldimine {aniline-imine (anil)} ligands[38-43]. The 'anils' were known for their behavior involving ultrafast excited state intramolecular proton transfer (ESIPT), torsional dynamics, photochromism, thermochromism, and solvatochromism[44-53].

It has been demonstrated that multi boron compounds not only increase the electron-accepting capabilities but also enhance the fluorescence quantum yields[42-43]. Recently, we have reported N∩O chelated boron compounds (boranils)[54-55] where they show tunable absorption and emission properties and moderate quantum yields in solution. In pursuit of new boron compounds with improved photophyscal properties, prompted us to prepare naphthaldimine based boron compounds. Herein, we describe the synthesis, optical and electrochemical properties of novel tetra-coordinate di- and tri-boron compounds.

2.2 Results and discussion

2.2.1 Synthesis and Characterization

The 6-hexyl-2-hydroxy-1-naphthaldehyde was made by reported synthetic procedure[56-57] (Scheme 2.1).

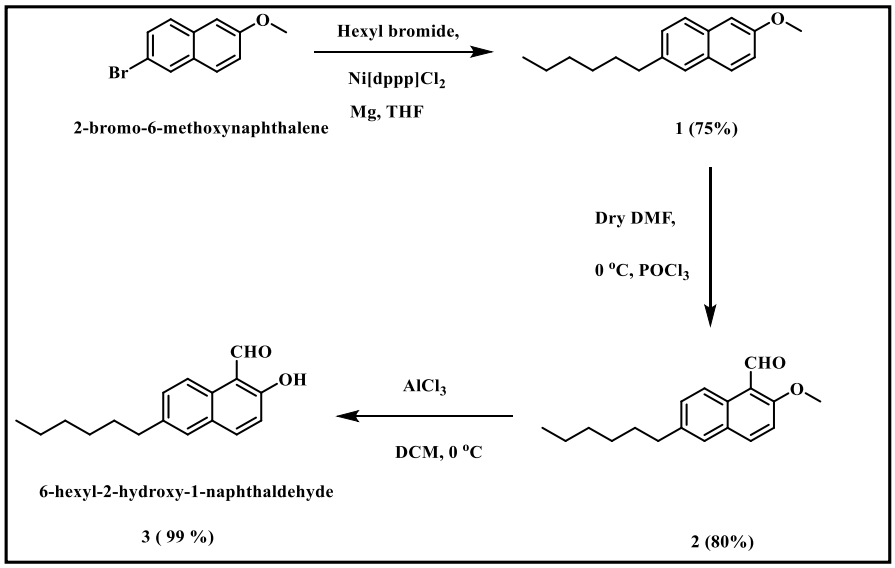

Scheme 2.1: Synthesis of compounds **1-3.**

The desired imine ligands (**4** and **5**) were synthesized in a one-step reaction by refluxing 1,4-phenylene diamine for **4** or 1,3,5-triamino benzene for **5** with 6-hexyl-2-hydroxy-1-naphthaldehyde in absolute ethanol (Scheme 2.2). The boron precursors *i.e.,* $BF_3{\cdot}OEt_2$ and BPh_3 were used to make the boron compounds using the ligands **4** and **5**. Addition of excess amount of $BF_3{\cdot}OEt_2$ to the sodium phenoxide of the ligands in dry THF yielded the difluoroborane compounds **4a** and **5a**. While the reaction of triphenylborane ($(C_6H_5)_3B$) in dry toluene under reflux conditions yielded the diphenylborane compounds **4b** and **5b** (Scheme 2.3). All the synthesized compounds were analysed by various techniques. Both the ligands (**4** and **5**) were characterized by ^1H and ^{13}C NMR spectroscopy. ^1H NMR spectrum of the ligands have shown a singlet in the far downfield region (~15 ppm) which represents the H-bonded phenolic proton.

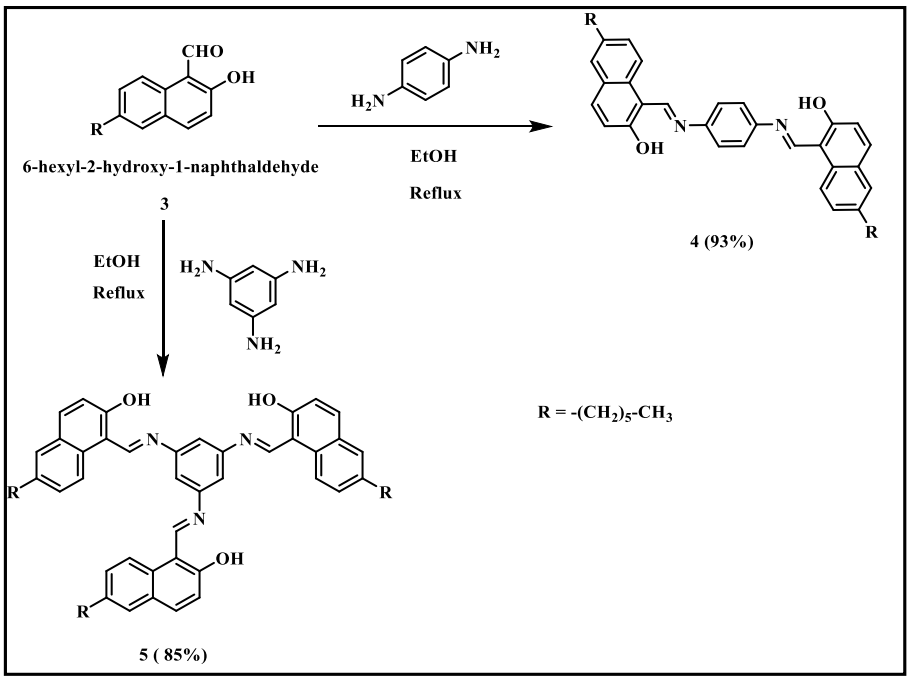

Scheme 2.2: Synthesis of compounds **4** and **5.**

A representative proton NMR spectra of ligand **4** and difluoro borane (**4a**) is shown in figure 2.1. The number of carbon signals observed in the ^{13}C NMR spectrum is well agreement with the proposed structure of the ligands. The borylated compounds were also characterized by various NMR spectroscopic techniques. Formation of the boron compounds have been readily assessed by the disappearance of the down field singlet corresponding to the H-bonded phenolic proton in the ^{1}H NMR spectroscopy (Figure 2.1). In addition to the disappearance of the phenolic proton, the shift in the peak position and the number of signals in the aromatic region with respect to aliphatic signals supports the chelation of ligand to the boron center. ^{19}F NMR exhibit

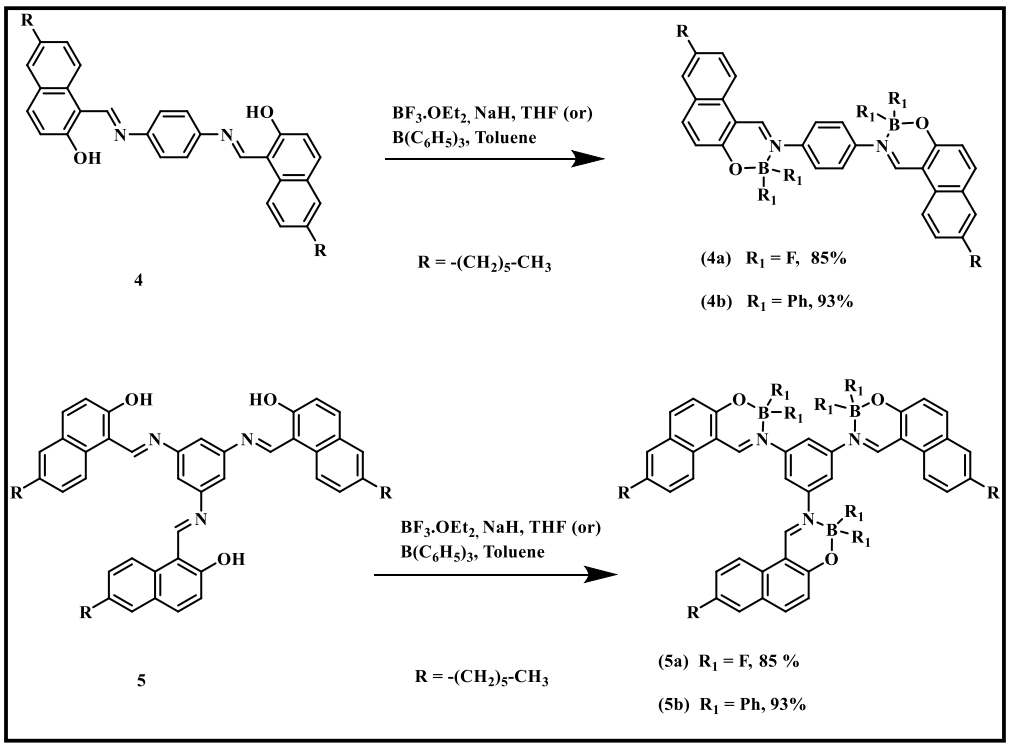

Scheme 2.3: Synthesis of compounds (**4a -5b).**

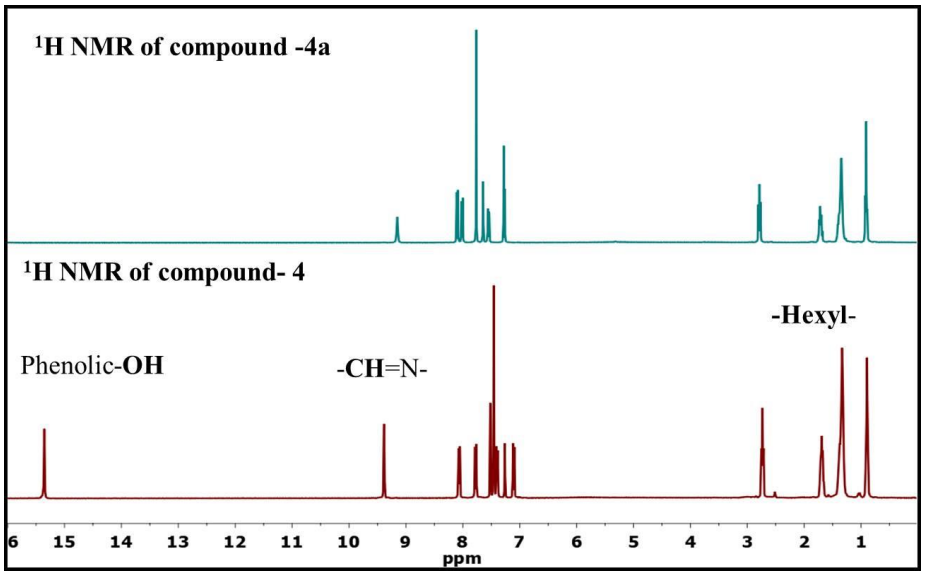

Figure 2.1: Comparison of phenolic proton and observable shift in peak position of aromatic protons form the stacked ^{1}H NMR spectrum of the ligand **4** (bottom) and its difluoro boron compound **4a** (top).

a doublet at around -133 ppm for both the compounds which is considered as the poor-resolved quartet[58]. Boron NMR spectroscopy of all the compounds exhibit a peak at around 1.00 ppm which supports the tetra-coordinate nature of the boron center. An indicative ^{19}F and ^{11}B NMR spectrum for compound **4a** is presented in figure 2.2.

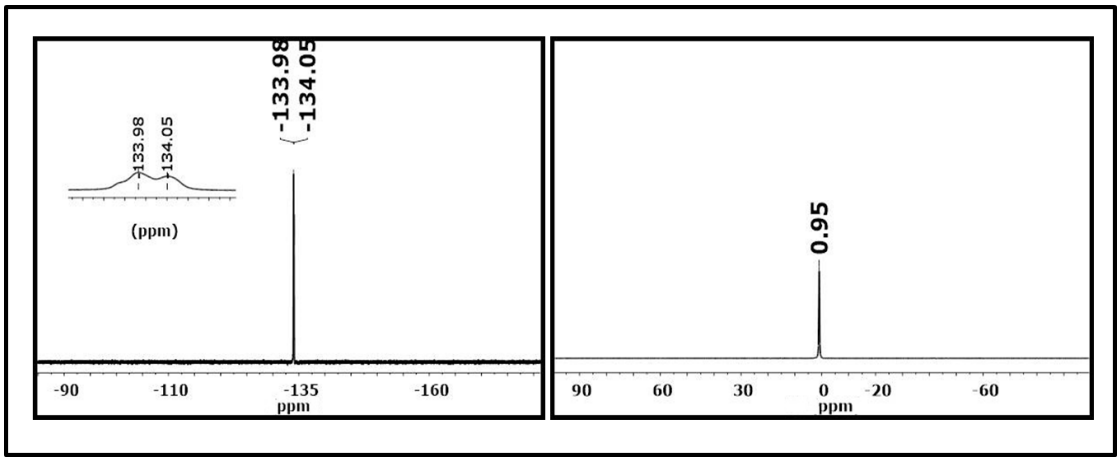

Figure 2.2: ^{19}F NMR (left) spectrum and ^{11}B NMR (right) spectrum of compound **4a.**

Furthermore all the ligands and boron compounds were identified using HRMS. Representative HRMS for compound **4b** & **5a** are represented in figure 2.3 & 2.4. All the compounds have also been characterized by infrared spectroscopy. All the compounds exhibit a typical stretching band in the range of 1620-1630 cm^{-1}, which is responsible for the characteristic C═N imine bond.

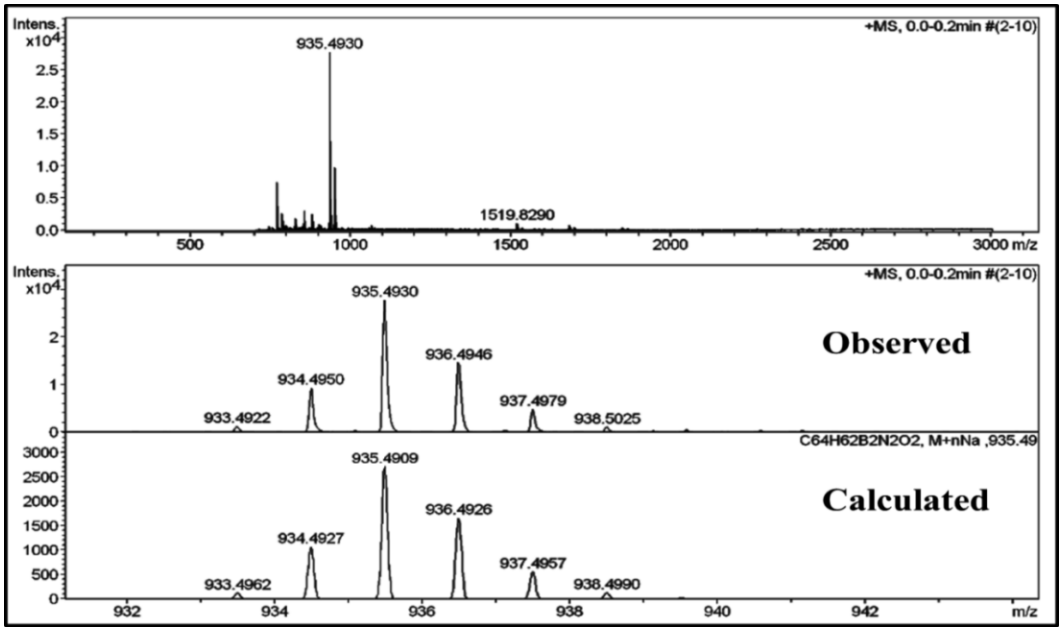

Figure 2.3: HRMS spectrum of compound **4b.**

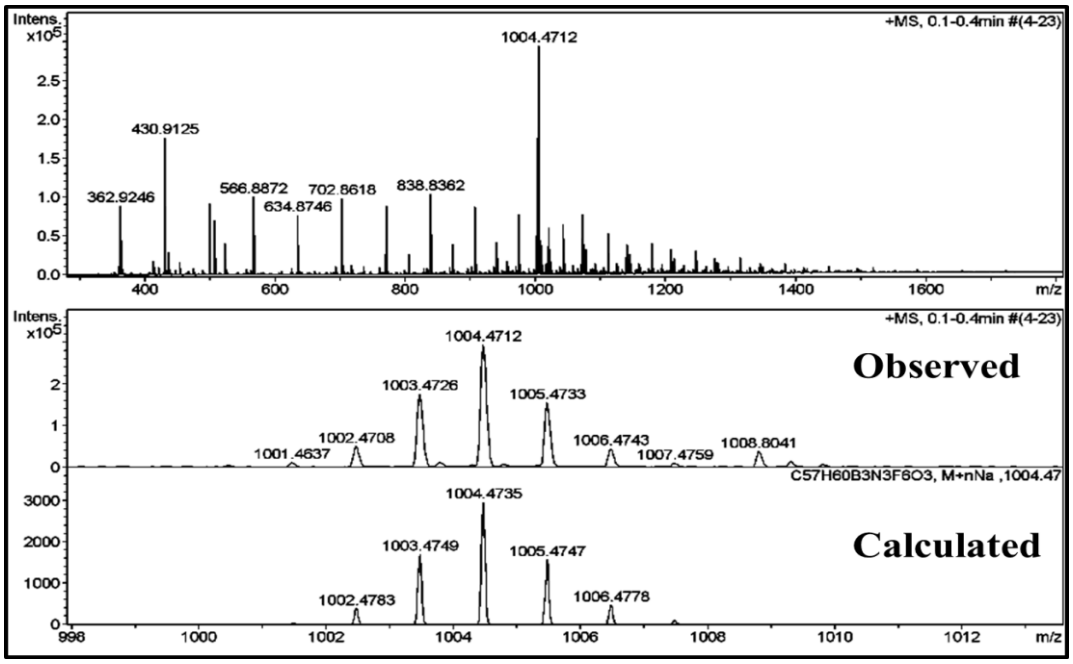

Figure 2.4: HRMS spectrum of compound **5a.**

2.2.2 Single X-ray studies

The formation of compound **4b** was further analysed by single crystal X-ray analysis. The compound has been crystalized in a triclinic system with a space group $P\bar{1}$; the

refinement data related to the same has been presented in table 2.1. Molecular structure of the compound along with important bond lengths and bond angles are represented in figure 2.5. As shown in the figure, the boron centres adopts a distorted tetrahedral geometry with N,O chelation. The B─O and B─N bond lengths and C─N─B, C─O─B and N─B─O bond angles are amenable to the other literature reported tetra-coordinate systems[59-61]. The boron atoms coordinate to the nitrogen atom to form a strain free six membered ring. Both the boron atoms deviate by 0.57 (B1) Å and 0.59 (B2) Å from the plane defined by 'naphthyl' carbon atoms, oxygen, iminocarbon and nitrogen atoms (Figure 2.5). The interplanar angles between plane 1 & plane 2 is 89.39° whereas plane 1 & plane 3 and plane 2 & plane 3 are 45.15° and 48.86° respectively.

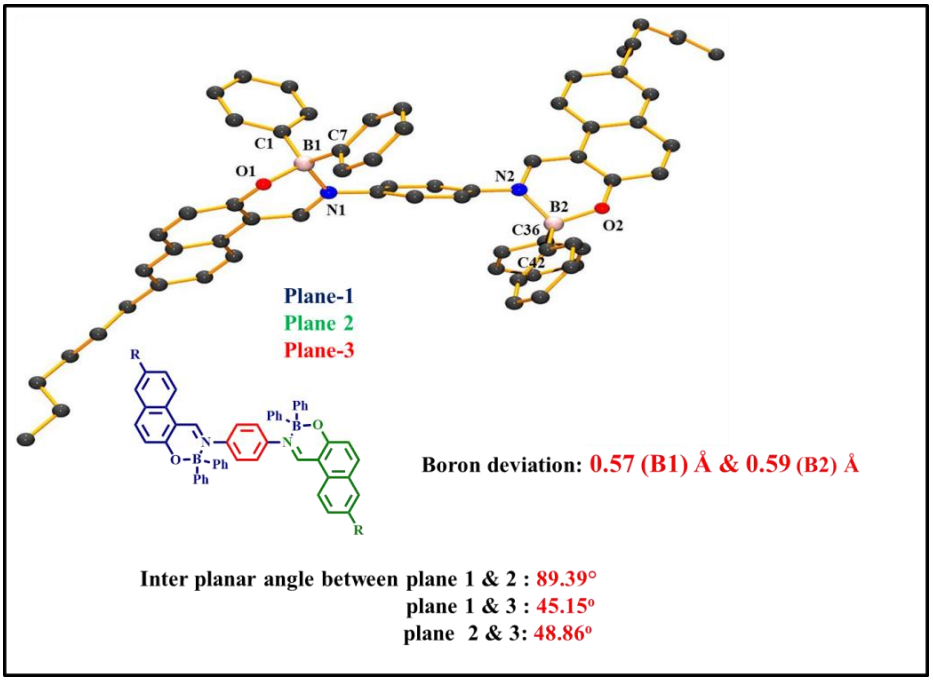

Figure 2.5: Solid state structure of the compound **4b**, hydrogen atoms omitted for the clarity (top); chemdraw structure of compound **4b** (bottom). Selected bond lengths (Å) bond angles (°) are as follows: B1─N1:1.637(4), B1─O1: 1.494(4), B1─C1: 1.619(5), B1─C7: 1.604(5), B2─N2:1.635(4), B2─O2: 1.493(4), B2─C42: 1.614(5),

B2─C36: 1.621(5), O1─B1─N1: 104.0(2), O1─B1─C7: 106.9(3), O1─B1─C1: 109.9(3), C7─B1─N1: 112.4(2), C1─B1─N1: 107.2(2), C7─B1─C1: 115.7(3), O2─B2─N2: 103.9(3), O2─B2─C42: 106.8(3), O2─B2─C36: 111.0(3), C42─B2─N2: 112.3(3), C36─B2─N2: 106.8(2), C42─B2─C36: 115.4(3).

Table 2.1: Crystal data and structure refinement parameters for compound **4b.**

Empirical formula	$C_{64}H_{51}B_2N_2O_2$
Formula weight	901.68
Temperature/K	296.15
crystal system	triclinic
space group	$P\bar{1}$
a [*Å*]	13.2400(12)
b [*Å*]	13.9352(12)
c [*Å*]	16.5750(15)
α[°]	74.994(6)
β[°]	79.001(7)
γ[°]	71.487(6)
Volume /Å^3	2781.2(5)
Z	2
ρ_{calc}[g cm^{-3}]	1.077
μ (MoKα) [mm^{-1}]	0.064
F (000)	950.0
Crystal size [mm]^3	0.15 × 0.12 × 0.09
radiation	MoKα (λ = 0.71073)
2θ range for data collection/^{o}	3.906 to 51.028
Index ranges	-15 ≤ h ≤ 15, -16 ≤ k ≤ 16, -20 ≤ l ≤ 19
reflections collected	30335
Independent reflections	10016[R_{int} = 0.0741, R_{sigma} = 0.0996]

Data/restraints/parameters	10016/19/630
Goodness-of-fit on F^2	1.003
Final R indexes [I>=2σ (I)]	R_1 = 0.0745, wR_2 = 0.1932
R indexes [all data]	R_1 = 0.1380 wR_2 = 0.2211
Largest diff.peak/hole/e $Å^{-3}$	0.89/-0.54

2.2.3Photophysical studies

The photophysical properties of the ligands (**4** and **5**) and their boron compounds **(4a-5b)** in various solvents were recorded and the results are presented in Table 2.2. As expected the imine ligands showed very weak fluorescence in solution due to their intramolecular rotations or isomerisation upon irradiation[15, 26-27, 62]. After borylation significant change to the photophysical data has been observed. Absorption and emission spectra of the synthesized boron compounds in CH_2Cl_2 solution at a concentration of 35 μM are presented in figure 2.6 and 2.7. The difluoro- and diphenyl-boron compounds (**4a-5b**) have shown better molar absorption coefficients with bathochromic shift in comparison to the free ligands in the absorption spectrum.

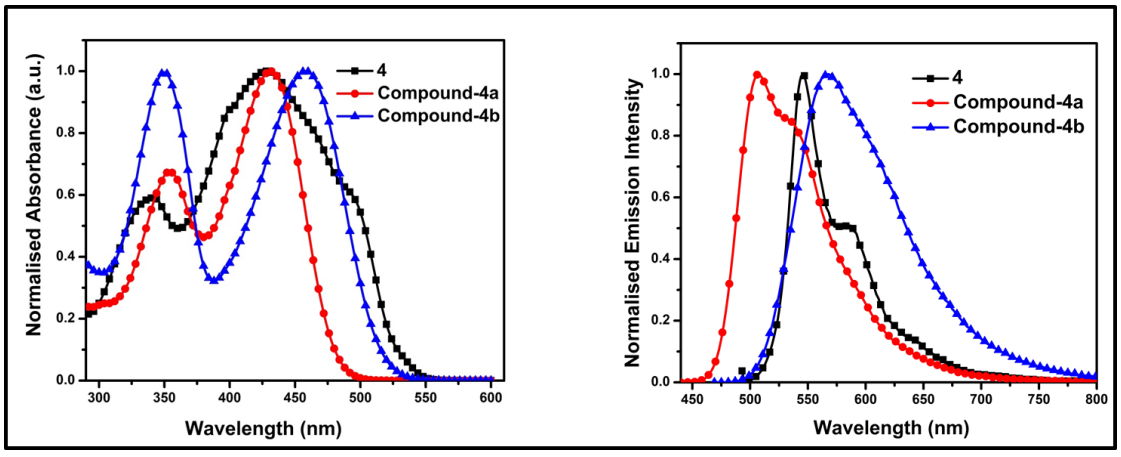

Figure 2.6: Normalized absorbance spectra (left) and emission spectra (right) of compounds (**4**, **4a** & **4b**) at a concentration of 35 μM in CH_2Cl_2 solutions.

Among the emission spectrum of boron compounds, difluoro boron compounds **4a** and **5a** (418-436 nm) have shown pronounced hypsochromic shift with respect to free ligand. The diphenyl boron analogues **4b** and **5b** showed a bathochromic shift in respect to the free ligand (440-462 nm). The molar absorption coefficient of the boron compounds ranging from 16,500 $M^{-1}cm^{-1}$ to 39,900 $M^{-1}cm^{-1}$. The molar absorption coefficient for the difluoro boron compounds (**4a** & **5a**) is much higher than their

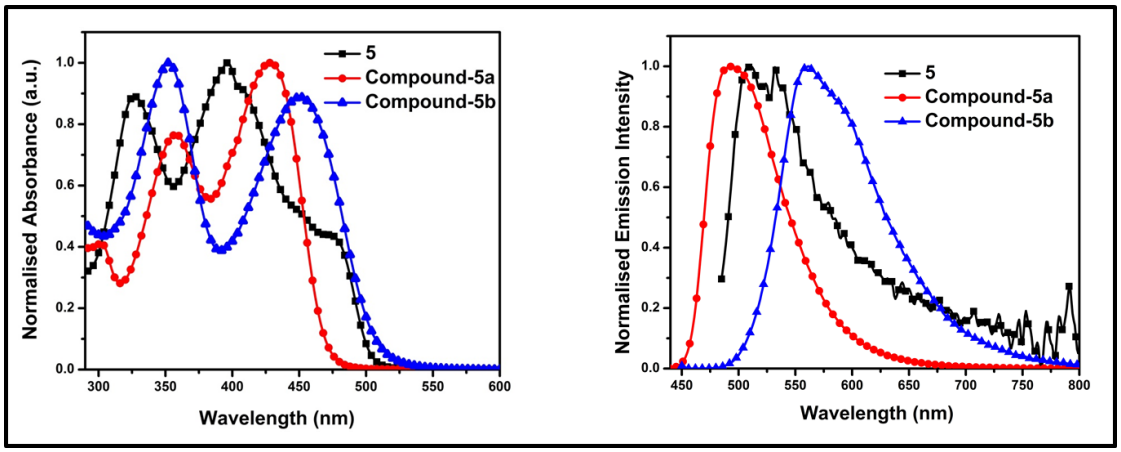

Figure 2.7: Normalized absorbance spectra (left) and emission spectra (right) of compounds (**5**, **5a** & **5b**) at a concentration of 35 μM in CH_2Cl_2.

diphenyl boron compounds (**4b** & **5b**). The fluorescence images of ligands along with their boron compounds in CH_2Cl_2 under hand held UV-Visible lamp at 365 nm are shown in figure 2.8. The emission spectra recorded for complexes **4a-5b** showed moderate fluorescence (Table 2.2) upon boron chelation. Compounds **4a-5b** exhibit moderate quantum yields and did not show drastic emission changes with solvent polarity. This proves that interaction of boron compounds with solvent molecules in the excited state is less significant[26]. Compounds **4b** & **5b** exhibit large Stokes shift over compounds **4a** & **5a**, may be associated with irregular backbone of

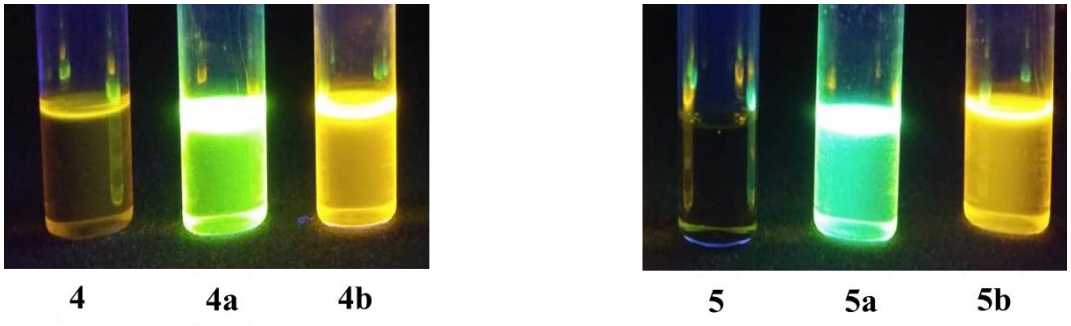

Figure 2.8: The fluorescence images of boron compounds and their ligands [**4, 4a** and **4b**] (left) & [**5, 5a** and **5b**] (right) in dichloromethane solution at 365nm.

Table 2.2: Photophysical data of imine ligands **4** and **5** and their boron compounds **4a-5b**. [a]Absorption maximum (Concentration: 3.5 x 10^{-5} M). [b]Excited at the longer wavelength absorption maximum. [c]Absolute fluorescence quantum yields were measured by integrating sphere method, [d]Shoulder peaks.

Compound	Solvent	λ_{max}[a](nm)	ε_{max} ($M^{-1}cm^{-1}$ x 10^3)	λ_{em}[a, b] (nm)	Φ_F[c] (%)	Stokes shift nm (cm^{-1})
4	Toluene	344, 423, 498[d]	12.9, 26.4, 07.3	546	<1	123 (5326)
	CH_2Cl_2	341, 428, 493[d]	14.7, 25.1, 15.1	546	<1	118 (5049)
	THF	341, 426, 497[d]	15.5, 29.6, 11.9	542	<1	116 (5024)
	CH_3CN	338, 428, 487[d]	15.2, 25.2, 17.2	539	<1	111 (4812)
5	Toluene	329, 397, 480[d]	33.1, 41.8, 08.5	507	<1	110 (5465)
	CH_2Cl_2	327, 396, 479[d]	34.8, 39.1, 16.5	511	<1	115 (5683)
	THF	326, 396, 477[d]	37.3, 43.3, 15.4	509	<1	113 (5606)
	CH_3CN	324, 396, 474[d]	36.1, 38.1, 21.7	507	<1	111 (5529)
4a	Toluene	355, 436	18.1, 30.5	508	43	72 (3251)

	CH_2Cl_2	353, 430	22.6, 33.5	507	44	77 (3532)
	THF	349, 425	19.7, 29.1	505	35	80 (3727)
	CH_3CN	348, 422	21.7, 31.2	502	30	80 (3776)
5a	Toluene	360, 433	26.4, 38.8	493	48	60 (2811)
	CH_2Cl_2	357, 428	30.6, 39.9	495	44	67 (3162)
	THF	347, 418	26.4, 33.5	490	26	72 (3515)
	CH_3CN	349, 419	28.5, 36.7	495	18	76 (3664)
4b	Toluene	352, 462	17.9, 19.5	569	35	107 (4070)
	CH_2Cl_2	350, 459	20.2, 20.3	568	47	109 (4181)
	THF	346, 455	15.9, 16.5	568	32	113 (4372)
	CH_3CN	344, 452	19.5, 19.8	561	27	109 (4299)
5b	Toluene	353, 453	23.1, 21.1	562	29	109 (4281)
	CH_2Cl_2	352, 450	23.4, 20.8	561	31	111 (4397)
	THF	348, 445	19.9, 17.4	560	21	115 (4615)
	CH_3CN	345, 440	23.3, 19.8	559	19	119 (4838)

the molecules as a consequence of crowded environment. Such a crowding may enhance the intramolecular charge transfer process which leads to large Stokes shifts. Compounds **4a** & **4b** are weekly fluorescent in the solid state, however compounds **5a** & **5b** do not fluoresce in the solid state. The observed photophysical properties are comparable with literature reported compounds of similar type[63]. Overall the emission spectra recorded for compounds **4a**-**5b** showed moderate to bright fluorescence (Table 2.2) upon boron chelation. Difluoro boron compounds (**4a** & **5a**) exhibit a hypsochromic shift in comparison with the diphenyl boron compounds (**4b** & **5b**). All the boron compounds exhibit moderate quantum yields in toluene however the

quantum yields dramatically dropped in acetonitrile which has been observed in other boron compounds of similar type[26].

2.2.4Electrochemical studies

The electrochemical behaviours of compounds **4a**-**5b** were studied by cyclic voltammetry in DME solution. The di- and tri-boron compounds exhibit two and three electron reduction waves respectively (Table 2.3 & Figure 2.9). Among the boron compounds studied (**4a**-**5b**); the reduction potentials of difluoro boron compounds (**4a & 5a**) are slightly less negative than those of diphenyl boron compounds (**4b & 5b**). This may be due to the presence of electron withdrawing fluorine in complexes **4a & 5a**.

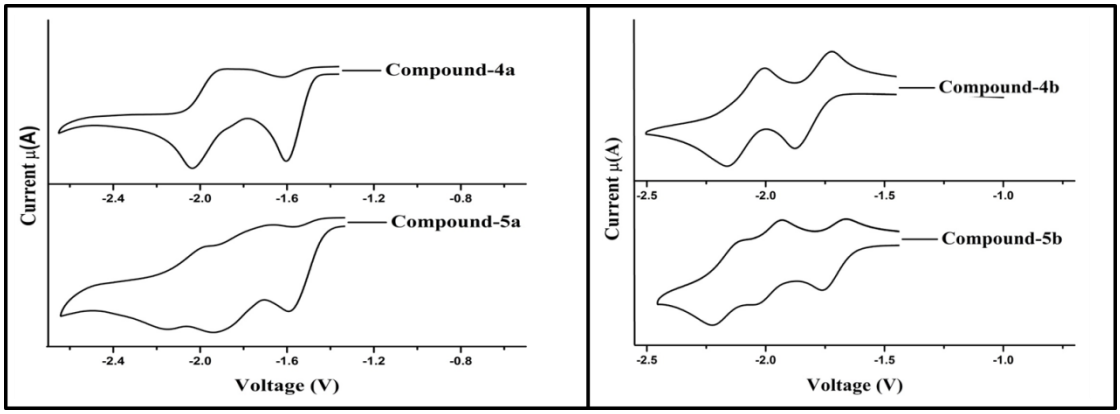

Figure 2.9: Cyclic voltammogram of **4a**-**5b**with 0.1 M $Bu_4N(PF_6)$ in DME as the supporting electrolyte (Scan rate 100 mV/s). Referenced relative to Fc/Fc^+ couple.

Table 2.3: Electrochemical data of the compounds **4a**-**5b**

Compound	4a	5a	4b	5b
1st Reduction potential	-1.53	-1.49	-1.80	-1.72
2nd Reduction potential	-1.94	-1.82	-2.08	-1.98
3rd Reduction potential	—	-2.06	—	-2.17

2.2.5 Theoretical calculations

In order to get more insights of absorption properties of compounds **4a-5b**, we carried out density functional theory (DFT) calculations[64]. As shown in figure 2.10 (Table 2.4) the HOMOs and LUMOs of compounds **4a** & **4b** delocalized over naphthyl rings and the centre phenyl ring whereas in compounds **5a** & **5b** it is limited to one (or) two naphthyl units of the molecule. Diphenyl boron compounds **4b** & **5b** have shown higher HOMO energy level which is in line with the observed red shift in comparison to the difluoro substituted compounds **4a** & **5a**. Compounds **4a** & **5a** have slightly higher LUMO energy, a possible reason for the low electron reduction potentials observed in these compounds.

Compound	4a(eV)	4b(eV)	5a(eV)	5b(eV)
LUMO+2	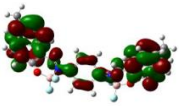 -1.1424	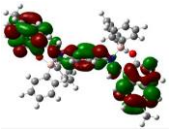 -0.8459	 -2.5296	 2.312
LUMO+1	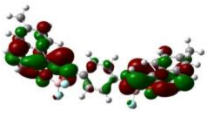 -2.584	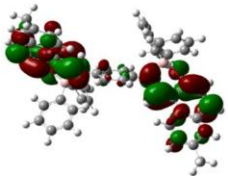 -2.312	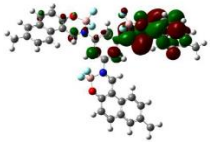 -2.7472	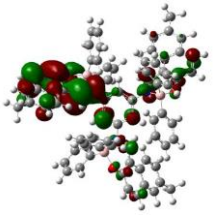 -2.3936

LUMO	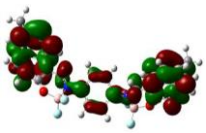 -2.8288	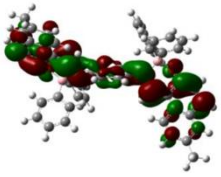 -2.4752	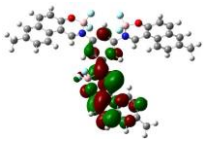 -2.9648	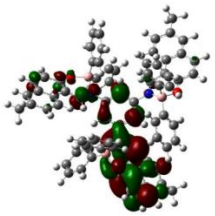 -2.5024
HOMO	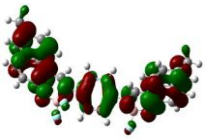 -6.12	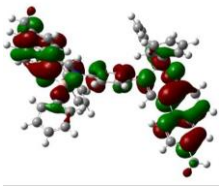 -5.712	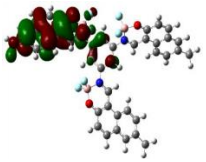 -6.0384	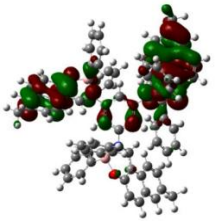 -5.6848
HOMO-1	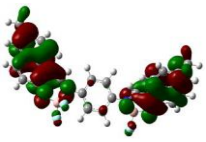 -6.3376	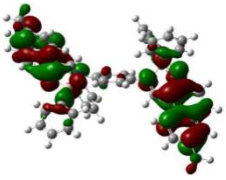 -5.8752	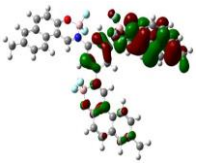 -6.2832	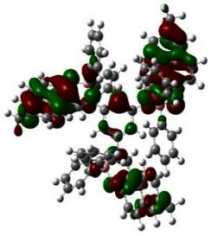 -5.7392
HOMO-2	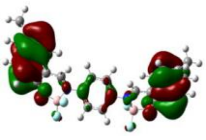 -6.8272	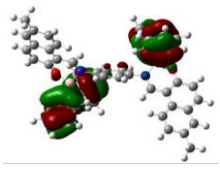 -5.9296	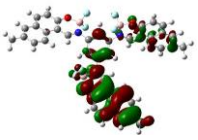 -6.4464	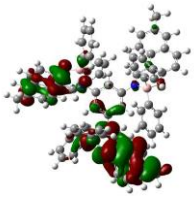 -5.8208

Figure 2.10: Computed orbitals for compounds **4a-5b.**

Table 2.4: Calculated electronic transitions for complexes **4a-5b** from TD-DFT (B3LYP) calculations.

Compound	Transition	MO contributions	Energy gap eV (nm)	Oscillator strength/f
4a	$S_0 \rightarrow S_1$	HOMO→LUMO	2.91 (425)	0.6626
	$S_0 \rightarrow S_2$	HOMO-1→LUMO HOMO→LUMO+1	3.17 (390)	0.000
	$S_0 \rightarrow S_3$	HOMO-1→LUMO HOMO→LUMO+1	3.25 (381)	0.0016
4b	$S_0 \rightarrow S_1$	HOMO-1→LUMO+1 HOMO→LUMO	2.78 (444)	0.4125
	$S_0 \rightarrow S_2$	HOMO-3→LUMO+1 HOMO-2→LUMO HOMO-1→LUMO	2.93 (424)	0.0006
	$S_0 \rightarrow S_3$	HOMO-3→LUMO HOMO-2→LUMO+1	2.93 (422)	0.0038
5a	$S_0 \rightarrow S_1$	HOMO→LUMO	2.71 (457)	0.7020
	$S_0 \rightarrow S_2$	HOMO-1→LUMO	2.94 (422)	0.0893
	$S_0 \rightarrow S_3$	HOMO→LUMO+1	2.96 (418)	0.6884

5b	$S_0 \rightarrow S_1$	HOMO-2→LUMO HOMO-1→LUMO HOMO-1→LUMO+2 HOMO→LUMO HOMO→LUMO+2	2.79 (443)	0.1460
	$S_0 \rightarrow S_2$	HOMO-2→LUMO HOMO-1→LUMO HOMO-1→LUMO+1 HOMO→LUMO HOMO→LUMO+1	2.81 (441)	0.2546
	$S_0 \rightarrow S_3$	HOMO-1→LUMO HOMO→LUMO HOMO-1→LUMO HOMO→LUMO+1 HOMO→LUMO+2	2.87 (432)	0.0933

2.3 Conclusions

In conclusion, we have isolated and characterized four new tetra coordinate boron compounds. Two of them as difluoro boron compounds (**4a** & **5a**) and the other two as diphenyl boron compounds (**4b** & **5b**). These boron compounds **4a**-**5b** have shown better quantum yields over the ligands. The increase of the number of boron *i.e.* from two boron (compound **4a** or **4b**) to three boron (compound **5a** or **5b**) center has considerable effect on the reduction potentials.

2.4 Experimental section

2.4.1 General Information

Reagents were used as received unless otherwise noted. THF and toluene were distilled from Na/benzophenone prior to use. Chlorinated solvents were distilled from CaH_2. 6-hexyl-2-hydroxy-1-naphthaldehyde was prepared by using literature reports[56-57]. NMR spectra were recorded on Bruker 700 and ARX 400 spectrometers at room temperature. All ^{1}H (700 MHz), ^{13}C (176 MHz), ^{1}H (400 MHz) and ^{13}C (100 MHz) NMR spectra were referenced internally to solvent signals. ^{11}B NMR spectra were referenced externally to $BF_3{\cdot}OEt_2$ in $CDCl_3$ (δ = 0 ppm), and ^{19}F NMR spectra were referenced to α, α, α-trifluorotoluene (0.05% in $CDCl_3$; δ = –63.73 ppm). ESI mass spectra were recorded with a Bruker microTOF-QII mass spectrometer. The absorbance spectra were recorded with a Perkin–Elmer Lambda 750 UV/Visible spectrometer. The fluorescence spectra were recorded with a Perkin–Elmer LS-55 fluorescence spectrometer and corrected for the instrumental response. Absolute fluorescence quantum yields in solution and solid state were measured by integrating sphere method using Edinburgh FS5 spectrofluorometer. Electrochemical measurements were performed with a conventional three-electrode cell and an electrochemical workstation (CH Instrument 1100A). The three-electrode system consisted of a glassy carbon working electrode, a Pt wire as the secondary electrode, and a Ag wire as the reference electrode. The voltammograms were recorded with ca. 1.0 x 10^{-3} M solutions in DME containing $Bu_4N(PF_6)$ (0.1 M) as the supporting electrolyte. The scans were referenced after the addition of a small amount of ferrocene as the internal standard. The crystals were mounted on a loop and attached to a goniometer head on a Rigaku oxford, four-circle diffractometer equipped with

graphite-monochromated Mo-K a radiation (k = 0.71073 Å). The full data sets were recorded and the images processed using the Crys Alis Pro. Structure solution by direct methods was achieved through the use of the SHELXT program, and the structural model refined by full-matrix least-squares on F^2 using SHELXL[65] by using the Olex2 software. The non-hydrogen atoms were refined with anisotropic thermal parameters expect the severely disordered hexyl. Hydrogen atoms (except for one of the hexyl group) were placed using idealized geometric positions (with free rotation for methyl groups), allowed to move in a ‘‘riding model” along with the atoms to which they were attached, and refined isotropically. The structures were optimized using 6-31G(d) (B3LYP) as the basis set. In order to reduce the computation time, “Hexyl” on the naphthyl was replaced with “Me”. The input files for **4a** and **4b** were generated using the X-ray data of compound **4b**, whereas for **5a** and **5b** the input files were generated using Gauss- View. Excitation data were determined using TD-DFT (B3LYP) calculations.

2.4.2 Synthetic procedure and spectral characterization

2.4.2.1 Synthesis of compound 1

To a solution of 2-bromo-6-methoxynaphthalene (20.00 g, 84.24 mmol) and Ni(dppp)Cl_2 (2.28 g, 3.80 mmol) in THF (30 mL) was added at room temperature *n*-hexyl magnesium bromide solution in THF, prepared from *n*-hexyl bromide (13 mL, 92.78 mmol) and Mg (2.25 gm, 92.78 mmol) in THF (15 mL), and the resulting mixture was refluxed for 19 h. After cooling, the mixture was diluted with water (20 mL) and filtered to remove unreacted Mg and other resulting solids. The filtrate was extracted with ethyl acetate (300 mL) and the combined extracts were washed with brine (10 mL × 3), dried (Na_2SO_4), and evaporated in vacuum. The resulting solid was

purified from column chromatography with hexane to give white solid. Yield: 15.30 g, (75%); mp = 48 °C; ^{1}H NMR (400 MHz, $CDCl_3$): δ = 7.67 (dd, *J* = 8.0, 4.0 Hz, 2H), 7.54 (s, 1H), 7.30 (dd, *J* = 8.0, 4.0 Hz, 1H), 7.13 (d, *J* = 4 Hz, 1H), 7.11 (s, 1H), 3.91 (s, 3H), 2.73 (t, *J* = 8.0 Hz, 2H), 1.74 – 1.63 (m, 2H), 1.40 – 1.24 (m, 6H), 0.89 (t, *J* = 8.0 Hz, 3H); ^{13}C NMR (176 MHz, $CDCl_3$): δ = 157.20, 138.29, 133.02, 129.27, 129.02, 128.08, 126.73, 126.29, 118.71, 105.79, 55.42, 36.06, 31.94, 31.62, 29.19, 22.77, 14.27 ppm; HR-MS (ESI): calcd. for $C_{17}H_{22}O$ ($[M+H]^+$): 243.1743, found: 243.1739.

2.4.2.2 Synthesis of compound 2

To a solution of 2-hexyl-6-methoxynaphthalene (**1**) (15.30 g, 63.12 mmol) in dry DMF (150 mL) at 0 °C, $POCl_3$ (20 mL, 252.51 mmol) was added drop-wise. After being stirred at 0 °C for an hour, the mixture was heated at 95 °C for 4 h. The reaction was quenched with ice-cold water, extracted with ethyl acetate (200 mL) and washed with water. Organic phase was dried with anhydrous Na_2SO_4 and concentrated in-vacuo to get a residue. The residue was purified by flash column chromatography (ethyl acetate-hexane) to get a creamy solid. Yield: 13.65 g, (80%); mp = 80 °C; ^{1}H NMR (400 MHz, $CDCl_3$): δ = 10.87 (s, 1H), 9.17 (d, *J* = 8.0 Hz, 1H), 7.98 (d, *J* = 8.0 Hz, 1H), 7.52 (s, 1H), 7.46 (d, *J* = 8.0 Hz, 1H), 7.24 (d, *J* = 2.4 Hz, 1H), 4.02 (s, 3H), 2.72(t, *J* = 8.0 Hz, 2H), 1.72 – 1.61 (m, 2H), 1.39 – 1.23 (m, 6H), 0.87 (t, *J* = 8.0 Hz, 3H);^{13}C NMR (176 MHz, $CDCl_3$): δ = 192.20, 163.63, 139.47, 137.27, 131.62, 129.98, 128.97, 126.78, 124.95, 11682, 112.63, 56.71, 35.79, 31.87, 31.34, 29.12, 22.75, 14.24; HR-MS (ESI): calcd. for $C_{18}H_{22}O_2$ ($[M+H]^+$): 271.1693, found: 271.1648.

2.4.2.3 Synthesis of compound 3

To a solution of 6-hexyl-2-methoxy-1-naphthaldehyde (**2**) (13.60 g, 50.29 mmol) in dichloromethane (200 mL) was added aluminium chloride (26.84 g, 201.16 mmol) at 0 °C. The resulting solution was warmed to room temperature with stirring. After being stirred for 24 h, the reaction mixture was cooled to 0 °C and 100 mL of water was slowly added. The aqueous layer was extracted with dichloromethane (3 × 20 mL). The combined organic phases were washed with brine and dried over Na_2SO_4. The solvent was removed under reduced pressure. The resultant crude product was purified by silica gel column chromatography using mixture of ethyl acetate and *n*-hexane as eluent to afford the corresponding product as a brown colour liquid. Yield: 12.77 g, (99 %); ^{1}H NMR (400 MHz, $CDCl_3$): δ = 13.05 (s, 1H), 10.80 (s, 1H), 8.27 (d, *J* = 12.0 Hz, 1H), 7.92 (d, *J* = 12.0 Hz, 1H), 7.57 (s, 1H), 7.47 (d, *J* = 8.0 Hz, 1H), 7.11 (d, *J* = 12.0 Hz, 1H), 2.79 – 2.71 (t, *J* = 8.0 Hz, 2H), 1.75 – 1.63 (m, 2H), 1.43 – 1.23 (m, 6H), 0.89 (t, *J* = 8.0 Hz, 3H); ^{13}C NMR (176 MHz, $CDCl_3$): δ = 193.50, 164.50, 139.33, 138.98, 131.22, 130.66, 128.23, 128.21, 119.16, 118.67, 111.48, 35.69, 31.86, 31.45, 29.10, 22.75, 14.24. HR-MS (ESI): calcd. for $C_{17}H_{20}O_2$ ($[M+H]^+$): 257.1536, found: 257.1530.

General procedure for the synthesis of Ligands 4 and 5

The precursor (aldehyde) for the ligands **4** and **5** *i.e.*,6-hexyl-2-hydroxy-1-naphthaldehyde was synthesized by following a similar procedure reported in the literature as described in the above section. Ethanol (50 mL) was added to a 250 mL round-bottomed flask containing 6-hexyl-2-hydroxy-1-naphtaldehyde and 1,4-phenylene diamine for **4** or 1,3,5-triamino benzene for ligand **5**[66]. To the reaction mixture few drops of glacial acetic acid was added. The resultant yellow mixture was stirred for overnight at reflux condition. Over the period of the time the reaction

mixture yielded cloudy precipitates. These precipitates were filtered, washed with cold methanol and dried under vacuum.

2.4.2.4 Synthesis of compound 4

The quantities involved as follows: 6-hexyl-2-hydroxy-1-naphtaldehyde (1.04 g, 4.07 mmol), 1,4-phenylene diamine (0.20 g, 1.85 mmol). Colour: Red; Yield: 1.01 g, (93%); mp = 212 °C; ^{1}H NMR (400 MHz, $CDCl_3$): δ = 15.35 (s, 2H), 9.38 (s, 2H), 8.06 (d, *J* = 8.0 Hz, 2H), 7.77 (d, *J* = 12.0 Hz, 2H), 7.52 (s, 2H), 7.45 (s, 4H), 7.40 (d, *J* = 8.0 Hz, 2H), 7.10 (d, *J* = 12.0 Hz, 2H), 2.73 (t, *J* = 8.0 Hz, 4H), 1.76 – 1.63 (m, 4H), 1.35 (m, 13H), 0.90 (t, *J* = 4.0 Hz, 6H); ^{13}C NMR (101 MHz, $CDCl_3$): δ = 168.43, 155.16, 144.55, 138.45, 136.40, 131.34, 129.54, 128.33, 127.82, 121.83, 121.65, 119.12, 109.32, 35.68, 31.91, 31.55, 29.16, 22.78, 14.26; HR-MS (ESI): calcd. for $C_{40}H_{44}N_2O_2$ ($[M+H]^+$): 585.3476, found: 585.3446.

2.4.2.5 Synthesis of compound 5

The quantities involved as follows: 6-hexyl-2-hydroxy-1-naphtaldehyde (2.18 g, 8.50 mmol), 1,3,5-tri amino benzene (0.30 g, 2.43 mmol). Colour: Brown, Yield: 1.73 g, (85%); mp = 168 °C; ^{1}H NMR (400 MHz, $CDCl_3$): δ = 15.16 (s, 3H), 9.46 (s, 3H), 8.11 (d, *J* = 8.0 Hz, 3H), 7.79 (d, *J* = 8.0 Hz, 3H), 7.52 (s, 3H), 7.41 (d, *J* = 8.0 Hz, 3H), 7.21 (s, 3H), 7.11 (d, *J* = 8.0 Hz, 3H), 2.73 (t, *J* = 8.0 Hz, 6H), 1.75 – 1.63 (m, 6H), 1.43 – 1.25 (m, 18H), 0.89 (t, *J* = 8.0 Hz, 9H); ^{13}C NMR (101 MHz, $CDCl_3$) δ = 168.36, 156.63, 148.97, 138.68, 136.86, 131.33, 129.75, 128.31, 127.89, 121.44, 119.35, 110.43, 109.35, 35.67, 31.90, 31.54, 29.16, 22.79, 14.26; HR-MS (ESI): calcd. for $C_{57}H_{63}N_3O_3$ ($[M+Na]^+$): 860.4762, found: 860.4767.

Synthesis and characterization of difluoro boron compounds

Tetrahydrofuran (20 mL) was added to a 50 mL round-bottomed flask containing ligand (**4** or **5**) and NaH under nitrogen atmosphere at 0 °C. The reaction mixture was warmed to ambient temperature and stirred at that temperature for 2h. The reaction mixture was then cooled to 0 °C and $BF_3{\cdot}OEt_2$ was added dropwise and the mixture was stirred for 24 h. The reaction mixture was filtered through celite, and the resultant filtrate was concentrated to yield a pale yellow solid, which was purified by recrystallization in diethyl ether.

2.4.2.6 Synthesis of compound 4a

The quantities involved as follows: **4** (0.20 g, 0.34 mmol), NaH (0.02 g, 0.85 mmol), $BF_3{\cdot}OEt_2$ (0.86 mL, 6.82 mmol). Yield: 0.20 g, (85%); mp = 249 °C; ^{1}H NMR (400 MHz, $CDCl_3$): δ = 9.15 (s, 2H), 8.10 (d, *J* = 12.0 Hz, 2H), 8.01 (d, *J* = 8.0 Hz, 2H), 7.76 (s, 4H), 7.64 (s, 2H), 7.55 (d, *J* = 8.0 Hz, 2H), 7.28 (s, 1H), 7.26 (s, 1H), 2.79 (t, *J* = 8.0 Hz, 4H), 1.78 – 1.64 (m, 4H), 1.48 – 1.23 (m, 12H), 0.91 (t, *J* = 8.0 Hz, 6H); ^{13}C NMR (176 MHz, $CDCl_3$): δ = 162.88, 158.54, 143.18, 141.81, 140.46, 131.34, 129.73, 128.70, 128.48, 125.24, 120.38, 119.31, 109.02, 35.71, 31.85, 31.45, 29.10, 22.75, 14.24; ^{11}B NMR (128 MHz, $CDCl_3$): δ = 0.95; ^{19}F NMR (377 MHz, $CDCl_3$): δ = -134.0 (d, *J* = 26.4 Hz) ; IR (KBr): $\bar{\nu}$ = 2926 (m), 2855 (m), 1609 (s), 1557 (s), 1503 (s), 1467 (s), 1409 (s), 1386 (s), 1355 (s), 1309 (s); HR-MS (ESI): calcd. for $C_{40}H_{42}B_2F_4N_2O_2$ ($[M+Na]^+$): 703.3274, found: 703.3270.

2.4.2.7 Synthesis of compound 5a

The quantities involved as follows: **5**(0.30 g, 0.30 mmol), NaH (0.03 g, 1.25 mmol), $BF_3{\cdot}OEt_2$ (1.35 mL, 10.74 mmol). Yield: 0.30 g, (85%); mp = 258 °C; ^{1}H NMR (700 MHz, $CDCl_3$): δ = 9.24 (s, 3H), 8.11 (d, *J* = 9.1 Hz, 3H), 8.03 (d, *J* = 8.5 Hz, 3H), 7.96 (s, 3H), 7.62 (s, 3H), 7.55 (d, *J* = 8.4 Hz, 3H), 7.27 (s, 2H), 7.25 (s, 1H), 2.77 (t,

J = 4.0 Hz, 6H), 1.74 – 1.65 (m, 6H), 1.40 – 1.21 (m, 18H), 0.89 (t, *J* = 8.0 Hz, 9H); ^{13}C NMR (101 MHz, $CDCl_3$): δ = 163.39, 159.31, 144.89, 142.58, 140.66, 131.64, 129.70, 128.66, 128.45, 120.20, 119.59, 119.46, 109.16, 35.67, 31.84, 31.37, 29.09, 22.75, 14.23; ^{11}B NMR (128 MHz, $CDCl_3$): δ = 0.97;^{19}F NMR (377 MHz, $CDCl_3$): δ = -133.1 (d, *J* = 22.6 Hz); IR (KBr): $\bar{\nu}$ = 2927 (m), 2854 (m), 1614 (s), 1600 (s), 1553 (s), 1466 (s), 1413 (s), 1388 (s), 1355 (s), 1311 (s); HR-MS (ESI): calcd. for $C_{57}H_{60}B_3N_3F_6O_3$ ($[M+Na]^+$): 1004.4735, found: 1004.4712.

Synthesis and characterization of phenyl boron compounds

Ligand (**4** or **5**) was taken in a sealed tube to that triphenylborane was added under nitrogen atmosphere followed by dry toluene (5 mL). The reaction mixture was refluxed for 12 h under nitrogen atmosphere. The reaction mixture was cooled and the solvent was evaporated by vacuum distillation leaving behind a glassy residue. To the resultant residue dry *n*-hexane (5mL) was added under nitrogen atmosphere and the mixture was heated with vigorous stirring for 30 minutes. After cooling to room temperature, the solvent was decanted off the insoluble precipitate was dried under vacuum. Crystallization was done using CH_2Cl_2/*n*-hexane.

2.4.2.8 Synthesis of compound 4b

The quantities involved are as follows: **4**(0.20 g, 0.34 mmol), triphenyl borane (0.21 g, 0.85 mmol). Yield: 0.29 g, (93%); mp = 219 °C; ^{1}H NMR (400 MHz, $CDCl_3$): δ = 8.81 (s, 2H), 7.87 (d, *J* = 8.0 Hz, 2H), 7.78 (d, *J* = 8.0 Hz, 2H), 7.49 (s, 2H), 7.39 (d, *J* = 8.0 Hz, 10H), 7.16 (dd, *J* = 4.0, 12.0 Hz, 14H), 6.95 (s, 4H), 2.71 (t, *J* = 8.0 Hz, 4H), 1.65 (m, 4H), 1.32-1.27 (m, 12H), 0.89 (t, *J* = 8.0 Hz, 6H); ^{13}C NMR (101 MHz, $CDCl_3$): δ = 165.22, 157.49, 145.41, 140.69, 139.33, 133.78, 130.54, 130.52, 128.53, 128.01, 127.18, 126.64, 125.18, 121.48, 119.24, 111.48, 35.69, 31.86, 31.54, 29.07,

22.75, 14.24; ^{11}B NMR (128 MHz, $CDCl_3$): δ = 5.19; IR (KBr): $\bar{\nu}$ = 2925 (m), 2853 (m), 1607 (s), 1550 (s), 1498 (s), 1459 (s), 1431 (s), 1403 (s), 1385 (s), 1347 (s); HR-MS (ESI): calcd. for $C_{64}H_{62}B_2N_2O_2$ ($[M+Na]^+$): 935.4909, found: 935.4930.

2.4.2.9 Synthesis of compound 5b

The quantities involved as follows: **5** (0.30 g, 0.36 mmol), triphenyl borane (0.32 g, 1.32 mmol). Yield: 0.45 g, (93%); mp = 137 °C; ^{1}H NMR (700 MHz, $CDCl_3$): δ = 8.26 (d, *J* = 7.7 Hz, 2H), 8.12 (s, 2H), 7.86 (d, *J* = 9.1 Hz, 2H), 7.68 (d, *J* = 9.1 Hz, 2H), 7.61 (t, *J* = 7.7 Hz, 2H), 7.52 (t, *J* = 7.7 Hz, 2H), 7.48 – 7.46 (m, 5H), 7.29 (d, *J* = 9.1 Hz, 9H), 7.21 – 7.17 (m, 15H), 7.08 (d, *J* = 9.1 Hz, 3H), 6.77 (s, 2H), 2.74 (t, *J* = 7.7 Hz, 6H), 1.70-1.66 (m, 6H), 1.39 – 1.32 (m, 18H), 0.90 (d, *J* = 7.0 Hz, 9H); ^{13}C NMR (176 MHz, $CDCl_3$): δ = 165.62, 157.68, 146.12, 141.29, 139.64, 135.80, 133.78, 132.86, 130.30, 128.43, 128.15, 127.98, 127.43, 126.78, 121.29, 120.34, 120.23, 112.08, 35.72, 31.88, 31.60, 29.09, 22.77, 14.26; ^{11}B NMR (128 MHz, $CDCl_3$): δ = -0.18; IR (KBr): $\bar{\nu}$ = 2924 (m), 2853 (m), 1609 (s), 1544 (s), 1513 (w), 1455 (s), 1431 (s), 1380 (s), 1345 (s), 1308 (s); HR-MS (ESI): calcd. for $C_{93}H_{90}B_3N_3O_3$ ($[M+Na]^+$): 1352.7164, found: 1352.7113.

2.5 References

(1) Yan, Y.; Zhao, Y. S. *Chem. Soc. Rev.* **2014**, *43*, 4325.

(2) Liang, J.; Tang, B. Z.; Liu, B. *Chem. Soc. Rev.* **2015**, *44*, 2798.

(3) Weil, T.; Vosch, T.; Hofkens, J.; Peneva, K.; Mullen, K. *Angew. Chem., Int. Ed.* **2010**, *49*, 9068.

(4) Kobayashi, H.; Ogawa, M.; Alford, R.; Choyke, P. L.; Urano, Y. *Chem. Rev.* **2009**, *110*, 2620.

(5) Yuan, L.; Lin, W.; Zheng, K.; He, L.; Huang, W. *Chem. Soc. Rev.* **2013**, *42*, 622.

(6) Lee, M. H.; Kim, J. S.; Sessler, J. L. *Chem. Soc. Rev.* **2015**, *44*, 4185.

(7) Climent, E.; Biyikal, M.; Gawlitza, K.; Dropa, T.; Urban, M.; Costero, A. M.; Martinez-Manez, R.; Rurack, K. *Chem. Eur. J.* **2016**, *22*, 11138.

(8) Lin, Y.; Li, Y.; Zhan, X. *Chem. Soc. Rev.* **2012**, *41*, 4245.

(9) Hains, A. W.; Liang, Z.; Woodhouse, M. A.; Gregg, B. A. *Chem. Rev.* **2010**, *110*, 6689.

(10) Mishra, A.; Bauerle, P. *Angew. Chem. Int. Ed.* **2012**, *51*, 2020.

(11) Zhu, M.; Yang, C. *Chem. Soc. Rev.* **2013**, *42*, 4963.

(12) Zhu, X. H.; Peng, J.; Cao, Y.; Roncali, J. *Chem. Soc. Rev.* **2011**, *40*, 3509.

(13) Boens, N.; Leen, V.; Dehaen, W. *Chem. Soc. Rev*. **2012**, *41*, 1130.

(14) Lu, H.; Mack, J.; Yang, Y.; Shen, Z. *Chem. Soc. Rev*. **2014**, *43*, 4778.

(15) Frath, D.; Massue, J.; Ulrich, G.; Ziessel, R. *Angew. Chem. Int. Ed.* **2014**, *53*, 2290.

(16) Thorat, K. G.; Chowdhary, G.; Isar, P.; Ravikanth, M. *Eur. J. Org. Chem*. **2018**, *2018*, 5389.

(17) Zhou, Y.; Kim, J. W.; Kim, M. J.; Son, W.-J.; Han, S. J.; Kim, H. N.; Han, S.; Kim, Y.; Lee, C.; Kim, S.-J. *Org. Lett*. **2010**, *12*, 1272.

(18) Zhou, Y.; Xiao, Y.; Chi, S.; Qian, X. *Org. Lett*. **2008**, *10*, 633.

(19) Massue, J.; Frath, D.; Ulrich, G.; Retailleau, P.; Ziessel, R. *Org. Lett*. **2011**, *14*, 230.

(20) Benelhadj, K.; Massue, J.; Ulrich, G. *New J. Chem*. **2016**, *40*, 5877.

(21) Kubota, Y.; Niwa, T.; Jin, J.; Funabiki, K.; Matsui, M. *Org. Lett*. **2015**, *17*, 3174.

(22) Urban, M.; Durka, K.; Jankowski, P.; Serwatowski, J.; Luliński, S. *J. Org. Chem*. **2017**, *82*, 8234.

(23) Frath, D.; Didier, P.; Mély, Y.; Massue, J.; Ulrich, G. *ChemPhotoChem.* **2017**, *1*, 109.

(24) Frath, D.; Azizi, S. b.; Ulrich, G.; Retailleau, P.; Ziessel, R. *Org. Lett*. **2011**, *13*, 3414.

(25) Frath, D.; Azizi, S.; Ulrich, G.; Ziessel, R. *Org. Lett.* **2012**, *14*, 4774.

(26) Dobkowski, J.; Wnuk, P.; Buczyńska, J.; Pszona, M.; Orzanowska, G.; Frath, D.; Ulrich, G.; Massue, J.; Mosquera-Vázquez, S.; Vauthey, E. *Chem. Eur. J.* **2015**, *21*, 1312.

(27) Wesela-Bauman, G.; Urban, M.; Luliński, S.; Serwatowski, J.; Woźniak, K. *Org. Biomol. Chem*. **2015**, 13, 3268.

(28) Zhang, P.; Liu, W.; Niu, G.; Xiao, H.; Wang, M.; Ge, J.; Wu, J.; Zhang, H.; Li, Y.; Wang, P. *J. Org. Chem*. **2017**, *82*, 3456.

(29) Araneda, J. F.; Piers, W. E.; Heyne, B.; Parvez, M.; McDonald, R. *Angew. Chem. Int. Ed*. **2011**, *50*, 12214.

(30) Curiel, D.; Más-Montoya, M.; Usea, L.; Espinosa, A.; Orenes, R. A.; Molina, P. *Org. Lett*. **2012**, *14*, 3360.

(31). Fischer, G. M.; Daltrozzo, E.; Zumbusch, A. *Angew. Chem. Int. Ed*. **2011**, *50*, 1406.

(32) Li, W.; Lin, W.; Wang, J.; Guan, X. *Org. Lett*. **2013**, *15*, 1768.

(33) Zhao, D.; Li, G.; Wu, D.; Qin, X.; Neuhaus, P.; Cheng, Y.; Yang, S.; Lu, Z.; Pu, X.; Long, C. *Angew. Chem. Int. Ed*. **2013**, *52*, 13676.

(34) Gao, N.; Cheng, C.; Yu, C.; Hao, E.; Wang, S.; Wang, J.; Wei, Y.; Mu, X.; Jiao, L. *Dalton Trans*. **2014**, *43*, 7121.

(35) Yoshino, J.; Kano, N.; Kawashima, T. *Tetrahedron*. **2008**, *64*, 7774.

(36) Baranov, M. S.; Lukyanov, K. A.; Borissova, A. O.; Shamir, J.; Kosenkov, D.; Slipchenko, L. V.; Tolbert, L. M.; Yampolsky, I. V.; Solntsev, K. M. *J. Am. Chem. Soc*. **2012**, *134*, 6025.

(37) Pais, V. F.; Alcaide, M. M.; López-Rodríguez, R.; Collado, D.; Nájera, F.; Pérez-Inestrosa, E.; Álvarez, E.; Lassaletta, J. M.; Fernández, R.; Ros, A. *Chem. Eur. J.* **2015**, *21*, 15369.

(38) Frath, D.; Benelhadj, K.; Munch, M.; Massue, J.; Ulrich, G. *J. Org. Chem.* **2016**, *81*, 9658.

(39) Zhou, Y.; Kim, J. W.; Nandhakumar, R.; Kim, M. J.; Cho, E.; Kim, Y. S.; Jang, Y. H.; Lee, C.; Han, S.; Kim, K. M. *Chem. Commun*. **2010**, *46*, 6512.

(40) Gong, P.; Yang, H.; Sun, J.; Zhang, Z.; Sun, J.; Xue, P.; Lu, R. *J. Mater. Chem. C.* **2015**, *3*, 10302.

(41) Riddle, J. A.; Lathrop, S. P.; Bollinger, J. C.; Lee, D. *J. Am. Chem. Soc*. **2006**, *128*, 10986.

(42) Zhang, Z.; Bi, H.; Zhang, Y.; Yao, D.; Gao, H.; Fan, Y.; Zhang, H.; Wang, Y.; Wang, Y.; Chen, Z. *Inorg. Chem*. **2009**, *48*, 7230.

(43) Li, D.; Yuan, Y.; Bi, H.; Yao, D.; Zhao, X.; Tian, W.; Wang, Y.; Zhang, H. *Inorg. Chem*. **2011**, *50*, 4825.

(44) Hadjoudis, E.; Mavridis, I. M. *Chem. Soc. Rev*. **2004**, *33*, 579.

(45) Ziółek, M.; Cohen, B.; Yang, X.; Sun, L.; Paulose, M.; Varghese, O. K.; Grimes, C. A.; Douhal, A. *Phys. Chem. Chem. Phys*. **2012**, *14*, 2816.

(46) Sekikawa, T.; Schalk, O.; Wu, G.; Boguslavskiy, A. E.; Stolow, A. *J. Phys. Chem. A.* **2013**, *117*, 2971.

(47) Spörkel, L.; Cui, G.; Thiel, W. *J. Phys. Chem. A.* **2013**, *117*, 4574.

(48) Ziółek, M.; Burdziński, G.; Douhal, A. *Photochem. Photobiol. Sci*. **2012**, *11*, 1389.

(49) Ziółek, M.; Martín, C.; Navarro, M. T.; Garcia, H.; Douhal, A. *J. Phys. Chem. C* **2011**, *115*, 8858.

(50) Grabowska, A.; Kownacki, K.; Karpiuk, J.; Dobrin, S. *Chem. Phys. Lett.* **1997**, *267*, 132.

(51) Kownacki, K.; Mordzinski, A.; Wilbrandt, R.; Grabowska, A. *Chem. Phys. Lett*. **1994**, *227*, 270.

(52) Otsubo, N.; Okabe, C.; Mori, H.; Sakota, K.; Amimoto, K.; Kawato, T.; Sekiya, H. *J. Photochem. Photobiol., A.* **2002**, *154*, 33.

(53) Fabian, W. M.; Antonov, L.; Nedeltcheva, D.; Kamounah, F. S.; Taylor, P. J. *J. Phys. Chem. A.* **2004**, *108*, 7603.

(54) Dhanunjayarao, K.; Mukundam, V.; Ramesh, M.; Venkatasubbaiah, K. *Eur.J. Inorg. Chem.* **2014**, *2014*, 539.

(55) Dhanunjayarao, K.; Mukundam, V.; Ranga Naidu Chinta, R, V.; Venkatasubbaiah, K. *Organomet. Chem.* **2018**, *865*, 234.

(56) Niimi, K.; Kang, M. J.; Miyazaki, E.; Osaka, I.; Takimiya, K. *Org. Lett*. **2011**, *13*, 3430.

(57) Kumar, B. S.; Ravi, K.; Verma, A. K.; Fatima, K.; Hasanain, M.; Singh, A.; Sarkar, J.; Luqman, S.; Chanda, D.; Negi, A. S. *Bioorg. Med. Chem*. **2017**, *25*, 1364.

(58) This is presumably caused by the fast ring-flipping associated with the complex in solution at room temperature.

(59) Moeller, A.; Bleckenwegner, P.; Monkowius, U.; Mohr, F. *J. Organomet. Chem*. **2016**, *813*, 1.

(60) Mtiraoui, H.; Gharbi, R.; Msaddek, M.; Bretonniere, Y.; Andraud, C.; Renard, P.-Y.; Sabot, C. *RSC Adv*. **2016**, *6*, 86352.

(61) Shanmugapriya, J.; Rajaguru, K.; Sivaraman, G.; Muthusubramanian, S.; Bhuvanesh, N. *RSC Adv*. **2016**, *6*, 85838.

(62) Grabarz, A. M.; Laurent, A. l. D.; Jedrzejewska, B.; Zakrzewska, A.; Jacquemin, D.; Ośmiałowski, B. *J. Org. Chem*. **2016**, *81*, 2280.

(63) Frath, D.; Benelhadj, K.; Munch, M.; Massue, J.; Ulrich, G. *J. Org. Chem*. **2016**, *81*, 9658.

(64) Gaussian, F., MJ et al. Gaussian 09, (*revision 02*), *Gaussian. Inc.: Wallingford, CT* **2009**.

(65) Sheldrick, G. M. *Acta Crystallogr. Sect. A: Found. Adv.* **2015,** *71*, 3.

(66) Hexyl-group was introduced on the naphthyl in order to increase the solubility; without "hexyl" the products showed limited solubility.

CHAPTER 3

Synthesis, photophysical and electrochemical properties of naphthalimide imidazole boron complexes

3.1 Introduction

Tetra-coordinate boron compounds are a class materials gained attention owing to their greater stability and wide applications in biological as well as optoelectronic devices[1-4]. Possible ways for obtaining various tetra-coordinate boron complexes with the desired properties are tuning the ligand with different chelates (*N,N-; N,O-; N,C-*; *O,O-*; etc) and (or) changing the substituents on boron atoms[5-8]. Among the different chelates N,N-chelate tetra coordinate boron complexes especially boron dipyrromethane (BODIPY)s have been studied extensively. However, small stokes shift and weak solid-state emission[9-14]. Therefore, made thus not suitable for specific applications efferts have been made to synthesis tetra-coordinated boron complexes with relatively high fluorescence quantum yields and large stokes shifts[15-16].

1,8-Naphthalimide and its derivatives are known for their potential applications ranging from OLEDs to bioimaging materials[17-25]. Like any other planar chromophores these naphthalimides are also suffer from aggregation caused quenching (ACQ) phenomenon[26]. In order to avoid ACQ effect, N-functionalisation and (or) substitutions at the fourth position of the naphthalimide moiety were performed[27-30]. Recently, Pandey and co-workers have tuned the naphthalimide moiety at the fourth position with BODIPY moiety and seen their potential applications in live the cell lysosomal tracking[31]. In the present study we have chosen fused phenolic group (2-butyl-6-hydroxy-1,3-dioxo-2,3-dihydro-1H-benzo[*de*]isoquinoline-5-carbaldehyde) as the building block to make N∩O chelate tetracoordinate boron complexes and studied their photophysical properties.

3.2 Results and discussion

3.2.1 Synthesis and characterization

The ligand 2-butyl-5-hydroxy-6-(1,4,5-triphenyl-1H-imidazole-2-yl)-1H-benzo[*de*]isoquinoline-1,3(2H)-dione **(L)** was synthesized using one-step condensation reaction following the reported procedure[32]. The aldehyde of 1,8-naphthalimide was prepared by adopting the literature reported procedure[33] The difluoro boron complex **1** was synthesized by treating the ligand **L** with boron trifluoride etherate using diisopropylethylamine as a base, whereas aryl boron complexes **2** and **3** were synthesized by treating the ligand **(L)** with respective triphenyl boron and pentafluorotriphenyl boron respectively (Scheme 3.1).

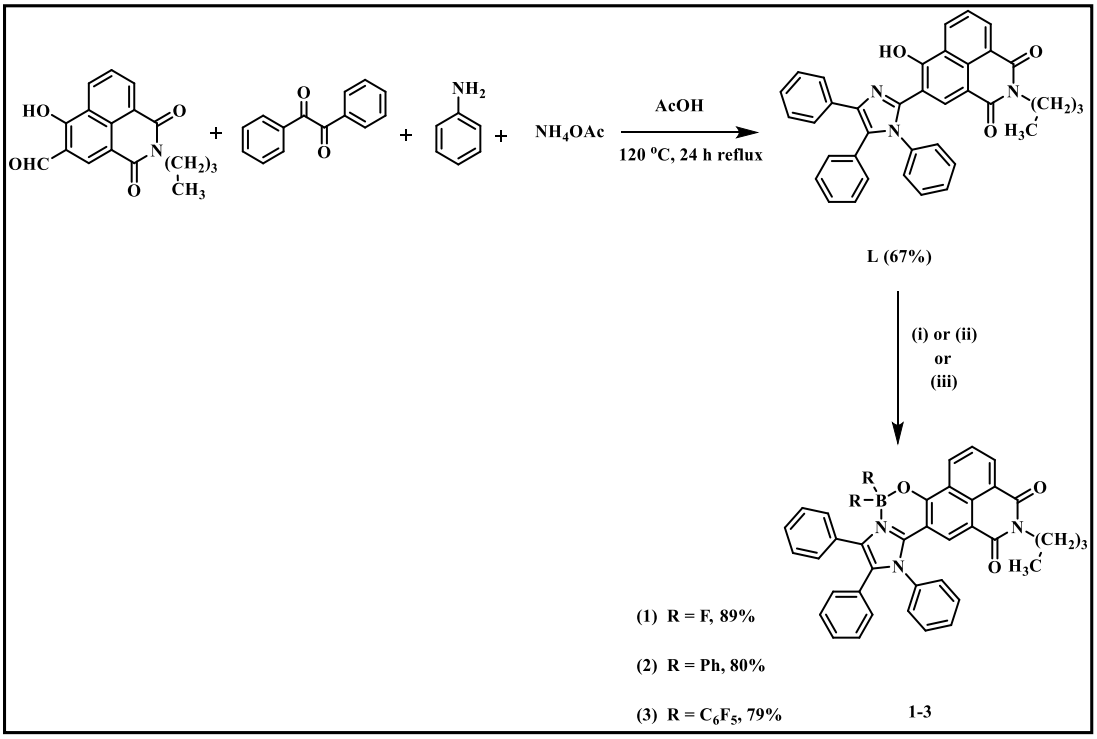

Scheme 3.1: Synthesis of boron complexes **1-3**: (i) N,N-diisopropylethylamine, $BF_3{\cdot}OEt_2$, 1,2-dichloroethane (ii) $B(C_6H_5)_3$ in toluene (iii) $B(C_6F_5)_3$ in toluene.

The ligand (**L**) and the complexes were purified by using column chromatography and (or) recrystallization and conformed by multinuclear magnetic resonance

spectroscopy (^{1}H NMR, ^{13}C NMR, ^{11}B NMR, ^{19}F NMR) and high-resolution mass spectrometry. The^{1}H NMR of complexes **1-3** shows distinct peaks in the aromatic region compared to the ligand. The ratio between the aliphatic proton signals *vs* the aromatic signals matches with proposed structure (Figure 3.1). As expected, the ^{11}B NMR of complexes **1-3** resonates at 0, 6.7 & 4.7 ppm respectively. A representative ^{11}B NMR spectrum (Complex **1**) is shown in Figure 3.2.

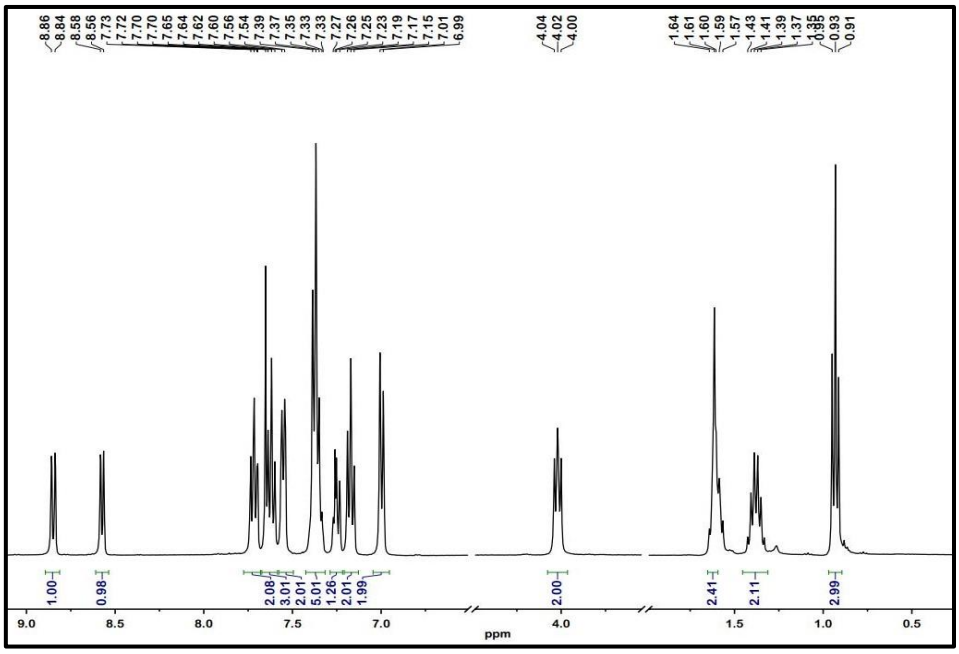

Figure 3.1: ^{1}H NMR spectrum of complex **1** recorded in $CDCl_3$

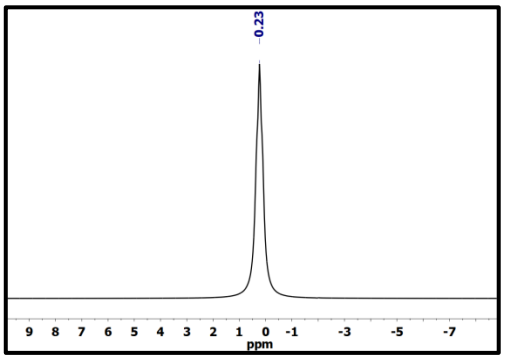

Figure 3.2: ^{11}B NMR spectrum of complex **1** recorded in $CDCl_3$**.**

Complexes **1** and **3** were further characterized by ^{19}F NMR. For complex **1** the ^{19}F chemical shift appears at -135 ppm and for complex **3** the chemical shift appears at -135ppm (doublet), -156ppm(triplet), -164ppm (doublet of triplet) (Figure 3.3).

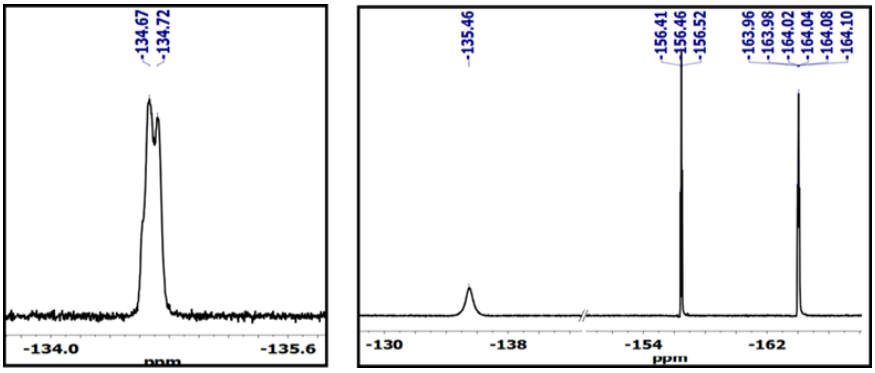

Figure 3.3: ^{19}F NMR spectrum of complex **1** (left) and complex **3** (right) recorded in $CDCl_3$.

All the boron complexes show distinctive $[HRMS]^+$ ions in HRMS analysis. Characteristic HRMS spectra of complexes **2** & **3** are given in figure 3.4 and 3.5.

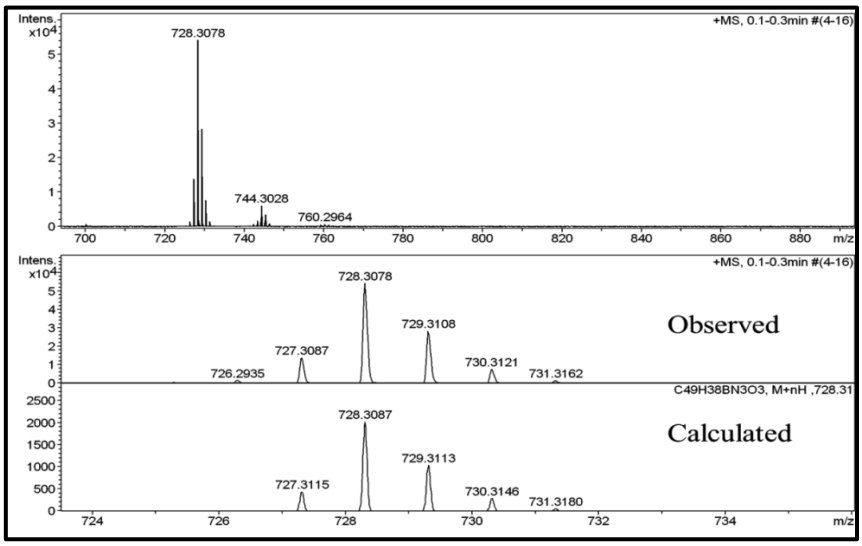

Figure 3.4: HRMS spectrum of complex **2.**

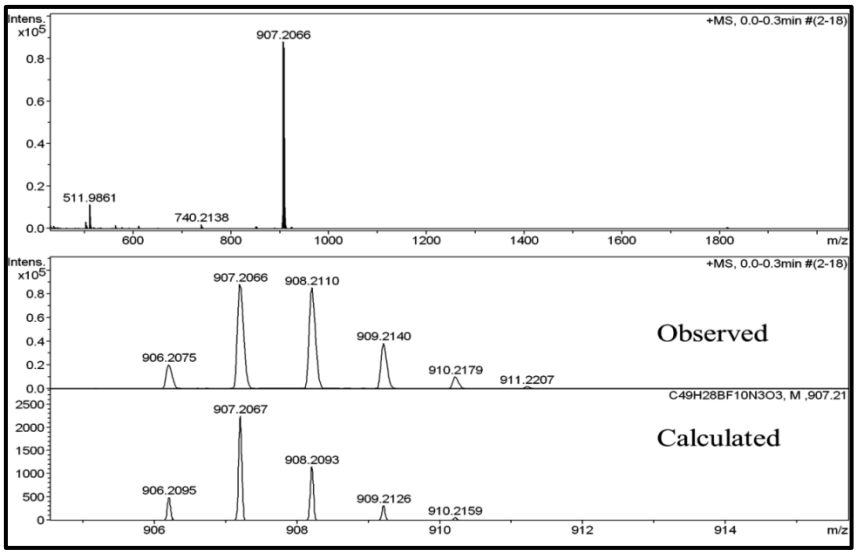

Figure 3.5: HRMS spectrum of complex **3**

3.2.2 Single crystal X-ray studies

Molecular structures of complexes **1**-**3** were also confirmed by single crystal X-ray diffraction studies. Well diffracting single crystals of complexes **1-3** suitable for X-ray analysis were obtained by passing vapours of *n*-hexane into saturated chloroform solution at -15 ºC. The molecular structures of complexes **1**-**3** are shown in figure 3.6 and the structure refinement parameters are given in table 3.1. The tetra coordinate boron centres of complexes **1-3** adopt a tetrahedral or distorted tetrahedral geometry to form N∩O chelate rings, which leads to form a six membered ring. Important bond lengths and bond angles for the complexes **1-3** are tabulated in table 3.2. The bond lengths and bond angles of N,O-chelate ligand around the vicinity of the boron atom effected by the electronic nature of the groups present on the boron atom. Complexes **1** & **3** have shorter B-O & B-N bond length over complex **2** due to the electron withdrawing nature of the fluorine and pentafluoro phenyl attached to the boron atom**.** Phenyl groups around the imidazole moiety are arranged in a propeller manner. Chelation of the ligand to the boron atom has brought the rigidity to the

structure of the molecule. Such a rigidity has been explained form the torsion angle of the planes constructed by the imidazole moiety and naphthalimide moiety of the complexes (table 3.3). Higher torsion angle has been noted when the size of the 'R' group on the boron atom is bulkier and it has followed the order: complex **3** > complex **2** > complex **1** with a torsion value of 16.156 (145),14.289 (71) and 7.577 (69) respectively (Figure 3.6).

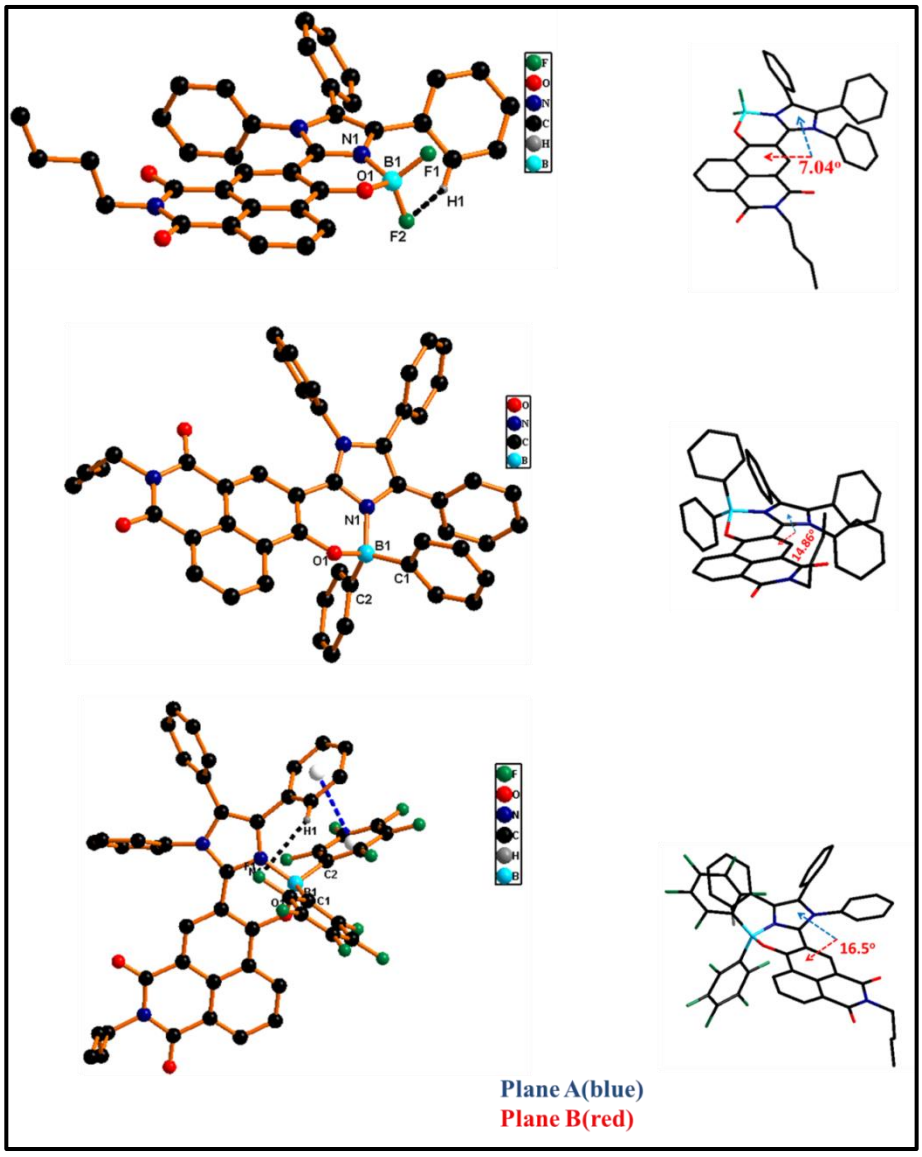

Figure 3.6: Molecular structure of complex **1** (top), complex **2** (middle) and complex **3** (bottom). Hydrogen atoms are removed for clarity.

Table 3.1: Crystallographic information and refinement parameters for complexes **1-3.**

Crystal data and structure refinement parameters			
	1	**2**	**3**
Empirical formula	$C_{37}H_{28}BF_2N_3O_3.CHCl_3$	$C_{49}H_{38}BN_3O_3.(CHCl_3)_2$	$C_{49}H_{28}BF_{10}N_3O_3$
Formula weight	730.80	966.37	907.55
Temperature/K	277(20)	293(2)	130(20)
crystal system	Triclinic	Triclinic	Triclinic
space group	$P\bar{1}$	$P\bar{1}$	$P\bar{1}$
a [*Å*]	11.5584(4)	10.7782(2)	10.8114(3)
b [*Å*]	12.9493(5)	11.7248(2)	12.1670(3)
c [*Å*]	13.6334(5)	20.6634(2)	20.5830(4)
α[°]	100.768(3)	84.1411(11)	84.2837(19)
β[°]	97.117(3)	86.9468(12)	86.457(2)
γ[°]	113.238(3)	65.9107(18)	63.952(3)
Volume /Å^3	1797.32(12)	2371.23(7)	2419.93(12)
Z	2	2	2
ρ_{calc}[g cm^{-3}]	1.350	1.353	1.246
μ (CuK$_\alpha$) [mm^{-1}]	2.740	3.671	0.899
F (000)	752.0	996.0	924.0
Crystal size [mm]^3	0.15 × 0.12 × 0.09	0.16 × 0.13 × 0.11	0.17 × 0.15 × 0.12
θ range [°]	3.382- 75.614	4.146-74.503	4.057-74.5
Index ranges	-14 ≤ h ≤ 14, -16 ≤ k ≤ 16, -17 ≤ l ≤ 15	-13 ≤ h ≤ 13, -14 ≤ k ≤ 14, -25 ≤ l ≤ 19	-13 ≤ h ≤ 13, -15 ≤ k ≤ 14, -25 ≤ l ≤ 20
reflections collected	25959	34005	31298
Independent reflns	7250 [R_{int} = 0.0694]	9463 [R_{int} = 0.0537]	9720 [R_{int} =

			0.2134]
data/restraints/parameters	7250/0/452	9463/0/578	9720/0/596
Goodness-of-fit on F^2	1.080	1.076	1.572
Final R indexes [I>=2σ (I)]	R_1 = 0.0868,wR_2 = 0.2676	R_1 = 0.0790,wR_2 = 0.2442	R_1 = 0.1292,wR_2 = 0.3629
R indexes [all data]	R_1 = 0.0984,wR_2 = 0.2802	R_1 = 0.0854,wR_2 = 0.2528	R_1 = 0.1554,wR_2 = 0.3899
Largest diff.peak/hole/e $Å^{-3}$	0.69/-0.95	0.81/-0.77	0.90/-0.76

Table 3.2: List of selected bond lengths [Å] and bond angles [°] for complexes**1-3**.

	1	**2**	**3**
B1-F1	1.373 (4)	—	—
B1-F2	1.367 (4)	—	—
B1-O1	1.448 (4)	1.513 (3)	1.468(6)
B1-N1	1.572 (4)	1.604 (3)	1.575 (5)
B1-C38	—	1.613(3)	1.637 (7)
B1-C44	—	1.614 (4)	1.640 (6)
F2-B1-F1	111.4 (2)	—	—
O1-B1-F1	109.1 (3)	—	—
O1-B1-F2	109.8(2)	—	—
N1-B1-F1	108.9 (2)		
N1-B1-F2	109.1 (3)		
N1-B1-O1	108.4 (2)	104.52 (16)	107.9 (3)
C38-B1-C44	—	117.38 (18)	115.8 (4)
O1-B1-C44	—	108.71 (18)	105.5 (4)
O1-B1-C38	—	106.03 (18)	107.3 (3)
N1-B1-C38	—	109.14 (18)	112.1 (4)
N1-B1-C44	—	110.21 (18)	107.8 (3)

Table 3.3: Comparison of deviation of boron atom from C_3NBO plane [Å] and interplanar angles [°] for complexes **1-3.**

	1	**2**	**3**
Deviation of B from C_3NBO plane (Å)	0.1527	0.3180	0.2491
Imidazole//plane A (°)	7.193	14.870	16.631
Imidazole//plane B (°)	86.139	68.45	71.516
Imidazole//plane C (°)	52.336	56.398	57.570
Imidazole//plane D (°)	50.39	62.965	61.432

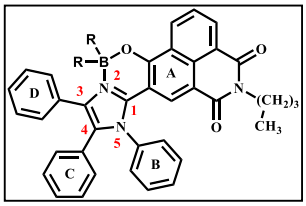

3.2.3 Photophysical studies

The solvent effect on the absorption and fluorescence properties of the synthesized boron complexes (**1-3**) were examined and the corresponding data is summarised in table 3.4. All the complexes **1-3** contains two absorption bands in all the solvents. The first absorption band (longer wavelength) spread around at λ_{max} = 362-375 nm (49450 $M^{-1}cm^{-1}$ to 41470 $M^{-1}cm^{-1)}$, whereas, the second band appeared at around λ_{max} = 319-325 nm (16150 $M^{-1}cm^{-1}$ to9700 M^{-1} cm^{-1}) for compounds **1-3**. The fluorescence spectra of boron chelated compounds were displayed deep blue intense emission. The boron complexes **1** & **3** showed blue shifted emissions in comparison to ligand (λ^{em}_{max}= 471(for ligand), 450 (for **1**), 458 (for **3**), however complex **2** showed a red shifted emission (λ^{em}_{max}= 485). This may be attributable owing to the presence of electron withdrawing nature of –F and $–C_6F_5$ attached to the boron atom. Normalized absorption and emission spectra of the synthesized ligand and boron complexes in dichloromethane have shown in figure 3.7. The fluorescence images of boron complexes (**1-3**) in CH_2Cl_2 under hand held UV-visible lamp at 365 nm are shown in figure 3.8.

Table 3.4: Photophysical data for imidazole boron complexes **1-3**.

Compound	Solvent	λ_{max}[a] (nm)	ε_{max} ($M^{-1}cm^{-1}$ X 10^3)	λ_{em}[a,b] (nm)	Φ_F[c] (%)	Stokes shift nm (cm^{-1})
1	Toluene	321, 367	45.18, 14.75	421, 441	45	74 (4572)
	CH_2Cl_2	319, 365	46.17, 14.83	450	56	84 (5175)
	THF	319, 349, 364	46.12, 12.1, 14.6	453	65	89 (5397)
	CH_3CN	315, 362	49.45, 13.34	468	66	106(6256)
	Solid	319,365			8	
	TLF	319,365		502	37	137(7476)
2	Toluene	325, 364	42.16, 9.7	471	64	107(6241)
	CH_2Cl_2	325, 356, 375	45.22,10.92,16.15	485	87	110(6048)
	THF	323, 372	42.01, 13.3	472	86	100(5695)
	CH_3CN	321, 369	41.47, 9.75	495	78	126(6898)
	Solid	325, 356, 375			15	
	TLF	325, 356, 375		493	58	118(6383)
3	Toluene	322, 371	42.12, 14.42	428, 448	31	77 (4633)
	CH_2Cl_2	322, 371	42.64, 14.32	458	56	87 (5120)
	THF	320, 369	44.9, 14.7	455	43	86 (5122)
	CH_3CN	319, 369	44.36, 13.42	467	69	98 (5687)
	Solid	322, 371			23	
	TLF	322, 371		454	31	83 (4928)

[a]Absorption maximum (Concentration: 2 x 10^{-5} M). [b]Excited at the longer wavelength absorption maximum. [c]Absolute fluorescence quantum yields were measured by integrating sphere method.

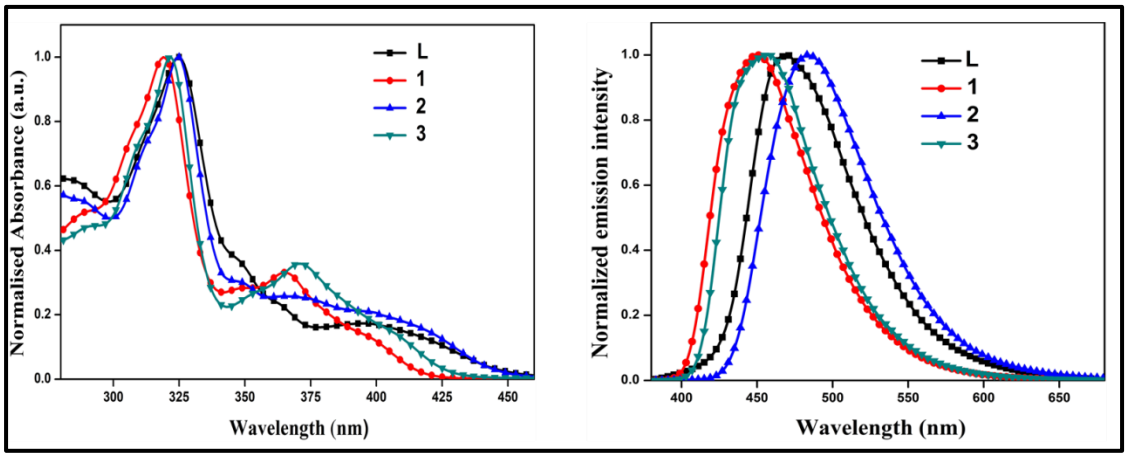

Figure 3.7: Normalized absorbance (left) and fluorescence (right) spectra of the ligand and boron complexes (**1-3**) at a concentration of 20 µM in CH_2Cl_2 solution.

The absorption maxima of complexes **1-3** have shown slight solvent dependent while fluorescence have shown around 20 nm red shift with increase of solvent polarity (Figure 3.9). For instance, the emission value of complex **1** in toluene is 441 nm but in acetonitrile it is at 468 nm. As a consequence, there is an increment in the value of stokes shift with the increasing in solvent polarity. All these properties of absorption, emission and stokes shift with the increase of solvent polarity indicating that the permanent dipole moments of the complexes in the ground and the exited states may not be similar. All these complexes have shown moderate fluorescence quantum yields ranging from 35-80 % in the chosen solvents.[34-35]

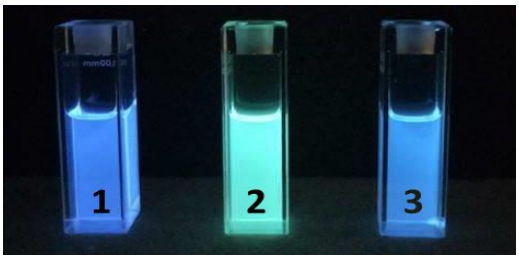

Figure 3.8: The fluorescence images of complexes **1-3** in dichloromethane solution. Boron complexes were under hand held UV lamp of 365 nm in dichloromethane.

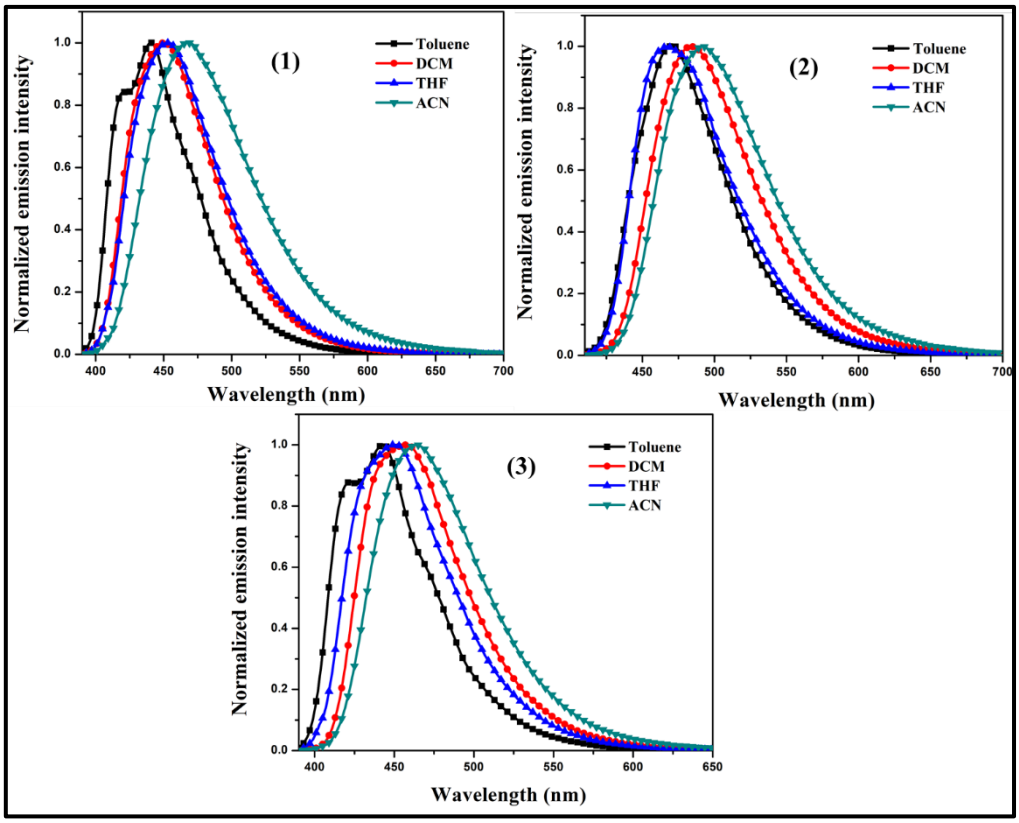

Figure 3.9: Normalized fluorescence spectra of the boron complexes **1-3** with increasing solvent polarity at concentration of 20 µM.

The solid-state quantum yields of complexes **1-3** were also measured in the powder form and as a thin layer film using integrating sphere method. The clear homogenous films were prepared by co-dissolving the complexes **1-3** with PMMA in CH_2Cl_2 (0.4 %, complex/PMMA, w/w), followed by drying in a glass plate**.** The quantum yields of the powder are much less than their solution state and thin film form. The fluorescence images of boron complexes (**1-3**) in thin film state under hand held UV-visible lamp at 365 nm are shown in figure 3.10.

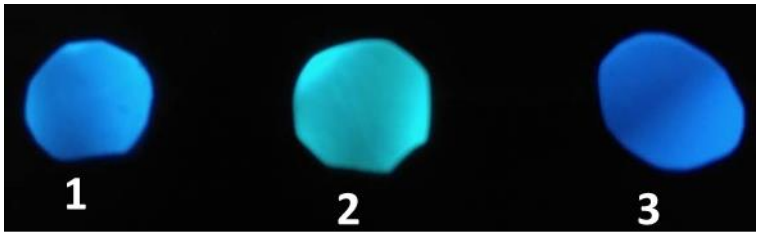

Figure 3.10: The fluorescence images of complexes **1-3** as thin film. Boron complexes were under hand held UV lamp of 365 nm.

3.2.4 Electrochemical properties

The electrochemical performances of complexes **1-3** were studied by cyclic voltammetry in DME solution using Bu_4NPF_6 as the supporting electrolyte. The observed electrochemical data is summarized in table 3.5.Imidazole skeleton shows two irreversible reduction waves at $E_{1/2}$ = −2.0 and −2.60 V (vs Fc/Fc^+). Tetra coordinated difluoride boron complex **1** showed three irreversible reduction potential waves at $E_{1/2}$ = −1.97, −2.56 V and −2.87 V (vs Fc/Fc^+). Complexes **2** & **3** showed similar trend (Table 3.5). Among the boron complexes, the third reduction potential of **1** is slightly less than **2** and **3**. This may be due to the electron with drawing nature of fluorine (Figure 3.11).

Table 3.5: Electrochemical data of ligand (**L**) and boron complexes **1-3.**

Compound	1^{st} reduction Potential	2^{nd} reduction potential	3^{rd} reduction potential
L	-2.0 V	-2.60 V	-----
1	-1.97 V	-2.56 V	-2.87 V
2	-1.99 V	-2.57 V	-2.95 V
3	-1.96 V	-2.65 V	-2.92 V

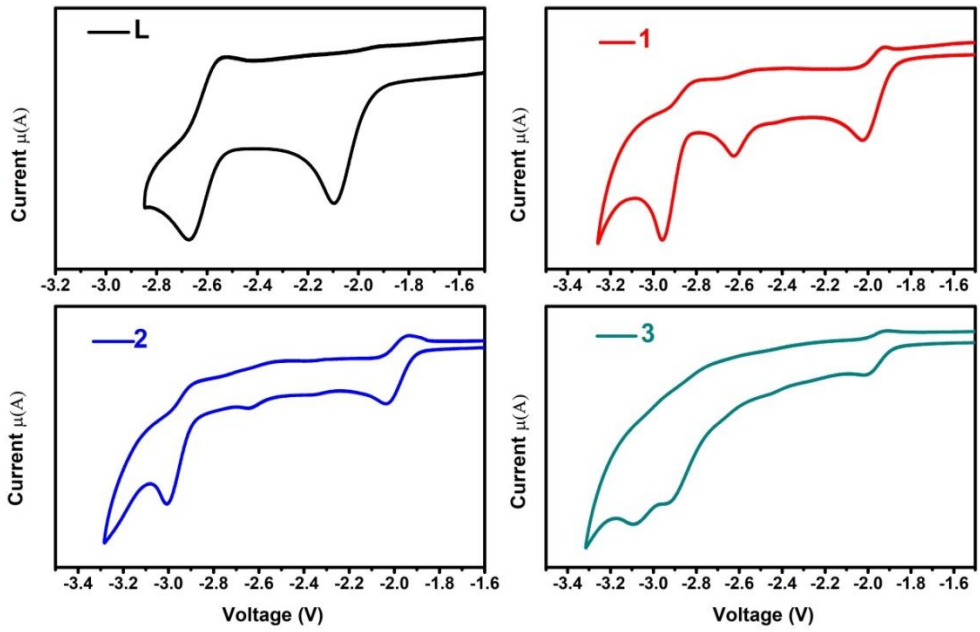

Figure 3.11: Cyclic voltammogram of ligand **L** and **1-3** with 0.1M $Bu_4N(PF_6)$ in DME as the supporting electrolyte (Scan rate 100 mV/s). The potentials are referenced to ferrocene.

3.3 Conclusions

In conclusion we have designed and synthesized three new N,O-chelate tetra coordinate boron complexes. The UV-Visible absorbance studies reveal that, all the compounds showed good molar absorption coefficient and does not show any solvatochromism. All three complexes showed good solution state quantum yields, and moderate solid state quantum yields. The electrochemical behaviour reveals that these boron complexes exhibit three one electron reductions. All these studies indicate that these complexes may find applications in making OLEDs and fluorescent probes.

3.4 Experimental section

3.4.1 General Information

Vacuum line techniques were used for handlings air and moisture sensitive compounds. All reagents and metal precursors used for the reactions were purchased from spectrochem, Alfa-aesar and Sigma-Aldrich otherwise mentioned. The 2-butyl-6-hydroxy-1,3-dioxo-2,3-dihydro-1H-benzo[de]isoquinoline-5-carbaldehyde was synthesized by adopting the literature procedure[33]. Acetic acid, dichloromethane (DCM), tetrahydrofuran (THF), and toluene were purchased from Spectrochem India. Toluene and THF were distilled from Na/benzophenone prior to use. Chlorinated solvents were distilled from CaH_2.^{1}H NMR (400 MHz, 700 MHz), ^{13}C NMR (100 MHz, 176 MHz), ^{11}B NMR (128 MHz), ^{19}F NMR (376 MHz) spectra were recorded on a Bruker ARX 400 and 700 spectrometers operating at 400 MHz and 700 MHz respectively. All ^{1}H and ^{13}C NMR spectra were referenced internally to residual solvent signals namely chloroform (δ = 7.26 ^{1}H; δ = 77.16 ^{13}C in ppm), ^{11}B NMR spectra were referenced externally to $BF_3{\cdot}OEt_2$ in $CDCl_3$ (δ= 0), and ^{19}F NMR was recorded with reference to α,α,α-trifluorotoluene. All NMR spectra were recorded at ambient temperature. Chemical shifts in all the NMR spectra are reported in ppm (δ) with the multiplicities represented by singlet (s), doublet (d), triplet (t), quartet (q), muliplet (m), doublet of doublet (dd) and broad (br). Coupling constants (*J*) are reported in Hertz. Melting points for the solid compounds were measured on a Fischer-John's melting point apparatus and mentioned as obtained. ESI-MS spectra were obtained from Bruker, microTOF-QII mass spectrometer. Infrared (IR) spectrum of compounds were recorded on Perkin Elmer FT-IR spectrometer in the solid state using KBR pellet. Distilled and degassed solvents used for photophysical properties. UV-Visible spectral measurements were performed using Jasco Lambda 750 UV/Visible spectrometer. All the fluorescence spectral measurements, absolute fluorescence quantum yields in solution and solid-state were performed with Edinburg

fluorescence FS5 spectrophotometer and the instrumental response corrected for each experiment. Integrating sphere method was used for calculating the quantum yields. Cyclic Voltammetry studies were performed using (CH Instrument 1100A) by employing a traditional three-electrode cell which comprises of working electrode (glassy carbon), auxillary (Pt wire) electrode, and reference electrode (Ag). The voltammograms were recorded with ca. 1 mM solutions in 1,2-dimethoxy ethane containing TBAP (0.1M) as the supporting electrolyte and referred to ferrocene as the internal standard.

Single crystal X-ray diffraction data were collected on Rigaku diffractometer at 277K , 293K and 130K for compounds 1-3 respectively using Cu-Kα radiation (λ = 1.54184. SHELXT program was used for solving the crystal structures and simultaneous refinement was done[36] with least-squares minimization using SHELXL incorporated in Olex2[37]. In order to refine non-hydrogen atoms anisotropic displacement coefficients were used and the hydrogen atoms were placed at calculated positions and were refined as riding atoms.

3.4.2 Synthetic procedure and spectral characterization

3.4.2.1 Synthesis of 2-butyl-6-hydroxy-1,3-dioxo-2,3-dihydro-1H-benzo[de]isoquinoline-5-carbaldehyde (L)

A mixture of benzil (1.15 g, 5.5 mmol) and 2-butyl-5-hydroxy-1,3-dioxo-2,3-dihydro-1H-benzo[de]isoquinoline-6-carbaldehyde (1.50 g, 5 mmol) and aniline (0.65 g, 7 mmol) were taken in acetic acid, to this mixture ammonium acetate (1.156 g, 15 mmol) were added and refluxed for 24 h. The reaction mixture was cooled to room temperature, evaporates the acetic acid and separated by separating funnel using

dichloromethane and water. The product was purified by silica packed column chromatography using dichloromethane and *n*-hexane as solvent. The yellow colour solid was recrystallized from ethyl acetate to get the pure product. Yield: 1.9 g, 67 %; ^{1}H NMR (700 MHz, $CDCl_3$): δ = 8.75 (d, *J* = 7.0 Hz, 1H), 8.53 (d, *J* = 7.0 Hz, 1H), 7.79 (s, 1H), 7.68 (t, *J* = 7.0 Hz, 1H), 7.56 (dd, *J* = 14.0, 7.0 Hz, 3H), 7.50 (t, *J* = 7.0 Hz, 2H), 7.32 – 7.23 (m, 8H), 7.17 (d, *J* = 7.0 Hz, 2H), 4.00 (t, *J* = 7.0 Hz 2H), 1.61 – 1.54 (m, 2H), 1.39 – 1.31 (m, 2H), 0.90 (t, *J* = 7.0 Hz, 3H); ^{13}C NMR (176 MHz, $CDCl_3$): δ = 164.74, 163.69, 162.93, 144.76, 136.51, 134.60, 132.56, 132.30, 131.63, 131.21, 130.54, 130.31, 129.54, 129.44, 129.26, 129.15, 128.96, 128.82, 128.74, 127.81, 127.22, 126.06, 124.20, 122.57, 112.20, 107.76, 40.30, 30.53, 20.70, 14.20; HR-MS (ESI):calcd.for $C_{37}H_{29}N_3O_3$ $[M+H]^+$: 564.2282, found: 564.2274.

3.4.2.2 Synthesis of boron difluoride complex 1

The anhydrous 1,2-dichloroethane (20 ml) under an inert atmosphere was added to a 50 ml round-bottomed flask containing imidazole **L** (0.30 g, 0.53 mmol), $BF_3{\cdot}Et_2O$ (0.39 mL, 3.19 mmol.) was added. To this reaction mixture N,N-diisopropylethylamine (DIPEA) (0.87 mL, 3.19 mmol) was poured and the as obtained mixture was kept for stirring while heating at 40 °C for 1h and followed by heating at 27 °C for 12h. The crude mixture was passed through a basic Al_2O_3 eluting with dichloromethane. The collected solution was reduced under pressure which yielded a yellow solid. Yield: 0.29 g, 89%; mp: > 300°C; ^{1}H NMR (400 MHz, $CDCl_3$): δ = 8.85 (d, *J* = 8.0 Hz, 1H), 8.57 (d, *J* = 8.0 Hz, 1H), 7.71 (m, 2H), 7.63 (m, 3H), 7.55 (d, *J* = 8.0 Hz, 2H), 7.42 – 7.32 (m, 5H), 7.25 (dd, *J* = 8.0, 5.0 Hz, 1H), 7.17 (t, *J* = 8.0 Hz, 2H), 7.00 (d, *J* = 8.0 Hz, 2H), 4.02 (t, *J* = 8.0 Hz, 2H), 1.65 – 1.59 (m, 2H), 1.45 – 1.31 (m, 2H), 0.93 (t, *J* = 8.0 Hz, 3H); ^{13}C NMR (100 MHz, $CDCl_3$): δ =

164.27, 163.23, 159.68, 140.68, 134.70, 133.34, 132.64, 131.68, 131.36, 131.21, 131.13, 130.70, 130.18, 129.55, 129.43, 128.81, 128.53, 128.24, 128.17, 127.72, 126.89, 126.45, 124.66, 122.51, 113.89, 105.02, 40.40, 30.42, 20.64, 14.15; ^{19}F NMR (376 MHz, $CDCl_3$): δ = -134.66 (d, *J* = 26.39 Hz, 2F); ^{11}B NMR (128 MHz, $CDCl_3$): δ = 0.23 (s); HR-MS (ESI): calcd.for $C_{37}H_{28}BF_2N_3O_3$ [M]: 611.2193, found: 611.2216.

General procedure for the synthesis of boron complexes 2 & 3

The ligand and triphenyl borane or tris(pentafluorophenyl)borane were taken in a sealed tube. To this dry toluene (5ml) was added under inert atmosphere. The reaction mixture was refluxed for 12 h and then cooled to room temperature and the solvent was dried by vacuum distillation which left a glassy residue. Dry *n*-hexane (5 ml) was added to the resultant residue under inert atmosphere and the resulting solution was refluxed vigorously. After 30 min the solution was brought to room temperature and the solvent was decanted and the resulted precipitate was dried. Both the compounds were crystallized by slow evaporation of solution from a mixture of CH_2Cl_2/*n*-hexane.

3.4.2.3 Synthesis of complex 2

The quantities involved as follows: Imidazole **L** (0.30 g, 0.532 mmol), triphenyl borane (0.15 g, 0.638 mmol). Yield: 0.31 g, (80%); mp: 293-295 °C; ^{1}H NMR (400 MHz, $CDCl_3$): δ = 8.76 (d, *J* = 8.0 Hz, 1H), 8.51 (d, *J* = 8.0 Hz, 1H), 7.67 (t, *J* = 8.0 Hz, 1H), 7.64 – 7.55 (m, 4H), 7.41 (d, *J* = 8.0 Hz, 2H), 7.28 (m, 4H), 7.15 (t, *J* = 8.0 Hz, 1H), 7.09 (m, 2H), 7.06 – 7.02 (m, 6H), 7.02 – 6.92 (m, 3H), 6.88 – 6.78 (m, 4H), 4.00 (t, *J* = 8.0 Hz, 2H), 1.61 – 1.49 (m, 2H), 1.41 – 1.23 (m, 2H), 0.90 (t, *J* = 8.0 Hz, 3H); ^{13}C NMR (176 MHz, $CDCl_3$): δ = 164.63, 164.59, 163.61, 140.76, 135.36,

135.05, 134.78, 133.86, 133.39, 133.02, 131.39, 131.31, 131.26, 130.95, 130.57, 129.07, 128.75, 128.73, 128.46, 128.44, 128.29, 128.26, 127.71, 127.02, 126.87, 126.37, 126.30, 125.77, 122.58, 112.19, 107.22, 40.27, 30.50, 20.66, 14.19; ^{11}B NMR (128 MHz, $CDCl_3$): δ = 6.77 (s); HR-MS (ESI): calcd.for $C_{49}H_{38}BN_3O_3$ ($[M+H]^+$): 728.3087, found: 728.3078.

3.4.2.4 Synthesis of complex 3

The quantities involved as follows: Imidazole **L** (0.40 g, 0.709 mmol), tris(pentafluorophenyl)borane (0.54 g, 1.06 mmol). Yield: 0.51 g, (79%); mp: 308-310 °C; ^{1}H NMR (400 MHz, $CDCl_3$): δ = 8.67 (d, *J* = 8.0 Hz, 1H), 8.57 (d, *J* = 8.0Hz, 1H), 7.70 (m, 2H), 7.62 (m, 3H), 7.39 (d, *J* = 8.0 Hz, 2H), 7.20 (t, *J* = 6.4 Hz, 2H), 7.16 – 7.08 (m, 1H), 7.06 (t, *J* = 8.0 Hz, 1H), 6.98 (d, *J* = 7.2 Hz, 2H), 4.01 (t, *J* = 8.0 Hz, 2H), 1.57 – 1.51 (m, 2H), 1.41 – 1.28 (m, 2H), 0.90 (t, *J* = 8.0 Hz, 3H); ^{13}C NMR (100 MHz, $CDCl_3$): δ = 163.99, 163.02, 161.25, 140.00, 134.36, 133.80, 133.25, 132.90, 131.42, 130.95, 130.85, 130.63, 130.30, 130.18, 129.23, 129.09, 128.35, 128.03, 128.00, 127.65, 126.90, 125.75, 125.07, 122.46, 113.58, 105.92, 40.07, 30.17, 20.31, 13.84; ^{19}F NMR (376 MHz, $CDCl_3$): δ = -135.46 (s), -156.46 (t, *J* = 21.6 Hz), -164.03 (td, *J* = 24, 8.0 Hz); ^{11}B NMR (128 MHz, $CDCl_3$): δ = 0.50 (s); HR-MS (ESI): calcd.for $C_{49}H_{28}BF_{10}N_3O_3$ ([M]): 907.2067, found: 907.2066.

3.5 References

(1) Liu, Y.; Guo, J.; Zhang, H.; Wang, Y. *Angew. Chem., Int. Ed.* **2002,** *41*, 182.

(2) Qin, Y.; Pagba, C.; Piotrowiak, P.; Jäkle, F. *J. Am. Chem. Soc.* **2004**, *126*, 7015.

(3) Ibarra-Rodríguez, M.; Muñoz-Flores, B. M.; Gómez-Treviño, A.; Chan-Navarro, R.; Berrones-Reyes, J. C.; Chávez-Reyes, A.; Dias, H. V. R.; Sánchez Vázquez, M.; Jiménez-Pérez, V. M. . *Appl. Organomet. Chem.* **2019**, *33*, 4718.

(4) Li, D.; Zhang, H.; Wang, Y. *Chem. Soc. Rev.* **2013**, *42*, 8416.

(5) Maeda, C.; Suka, K.; Nagahata, K.; Takaishi, K.; Ema, T. *Chem. Eur. J.* **2020**, *26*, 4261..

(6) Chan, J. Y. M.; Kawata, T.; Kobayashi, N.; Ng, D. K. P. *Angew. Chem., Int. Ed.* **2019**, *58*, 2272.

(7) Rodrigues, A. I.; Figueira, C. A.; Gomes, C. S. B.; Suresh, D.; Ferreira, B.; Di Paolo, R. E.; Pereira, D. d. S.; Dias, F. B.; Calhorda, M. J.; Morgado, J.; Maçanita, A. L.; Gomes, P. T. *Dalton Trans.* **2019**, *48*, 13337.

(8) Pammer, F.; Schepper, J.; Glöckler, J.; Sun, Y.; Orthaber, A. *Dalton Trans.* **2019**, *48*, 10298.

(9) Ni, Y.; Lee, S.; Son, M.; Aratani, N.; Ishida, M.; Samanta, A.; Yamada, H.; Chang, Y. T.; Furuta, H.; Kim, D. *Angew. Chem., Int. Ed.* **2016**, *55*, 2815.

(10) Bonnier, C.; Piers, W. E.; Al-Sheikh Ali, A.; Thompson, A.; Parvez, M. *Organometallics.* **2009**, *28*, 4845.

(11) Bozdemir, Ö. A.; Al-Sharif, H. H. T.; McFarlane, W.; Waddell, P. G.; Benniston, A. C.; Harriman, A *Chem. Eur. J.* **2019**, *25*, 15634.

(12) Avellanal-Zaballa, E.; Ventura, J.; Gartzia-Rivero, L.; Bañuelos, J.; García-Moreno, I.; Uriel, C.; Gómez, A. M.; Lopez, J. C. *Chem. Eur. J.* **2019**, *25*, 14959.

(13) Sun Choung, K.; Teets, T. S. *ChemPhotoChem.* **2019**, *3*, 86.

(14) Hu, R.; Lager, E.; Aguilar-Aguilar, A.; Liu, J.; Lam, J. W. Y.; Sung, H. H. Y.; Williams, I. D.; Zhong, Y.; Wong, K. S.; Peña-Cabrera, E.; Tang, B. Z. *J. Phys. Chem. C.* **2009**, *113*, 15845.

(15) Yu, C.; Hao, E.; Fang, X.; Wu, Q.; Wang, L.; Li, J.; Xu, L.; Jiao, L.; Wong, W.-Y. *J. Mater. Chem. C.* **2019**, *7*, 3269.

(16) Rihn, S.; Retailleau, P.; De Nicola, A.; Ulrich, G.; Ziessel, R. *J. Org. Chem.* **2012**, *77*, 8851.

(17) Zhang, W.; Huo, F.; Liu, T.; Yin, C. *J. Mater. Chem. B.* **2018**, *6*, 8085.

(18) Jia, H.; Xia, S.; Feng, H.; Meng, Q.; Duan, C.; Zhang, Z.; Zhang, R. *Org. Biomol. Chem.* **2018**, *16*, 2074.

(19) Havlík, M.; Talianová, V.; Kaplánek, R.; Bříza, T.; Dolenský, B.; Králová, J.; Martásek, P.; Král, V. *Chem. Commun.* **2019**, *55*, 2696.

(20) Xing, P.; Feng, Y.; Niu, Y.; Li, Q.; Zhang, Z.; Dong, L.; Wang, C. *Chem. Eur. J.* **2018**, *24*, 5748.

(21) Reddy, T. S.; Shin, S. H.; Choi, M. S. *Dyes Pigm.* **2019**, *160*, 483.

(22) Banerjee, S.; Veale, E. B.; Phelan, C. M.; Murphy, S. A.; Tocci, G. M.; Gillespie, L. J.; Frimannsson, D. O.; Kelly, J. M.; Gunnlaugsson, T. *Chem. Soc. Rev.* **2013**, *42*, 1601.

(23) Maiti, K.; Ghosh, D.; Maiti, R.; Vyas, V.; Datta, P.; Mandal, D.; Maiti, D. K. *J. Mater. Chem. A.* **2019**, *7*, 1756.

(24) Xing, P.; Shi, Y.; Li, Q.; Feng, Y.; Dong, L.; Wang, C. *Talanta.* **2018**, *179*, 326.

(25) Xiong, H.; He, L.; Zhang, Y.; Wang, J.; Song, X.; Yang, Z. *Chin. Chem. Lett.* **2019**, *30*, 1075.

(26) Gopikrishna, P.; Meher, N.; Iyer, P. K. *ACS Appl. Mater. Interfaces*. **2017**, *10*, 12081.

(27) Gudeika, D. *Synth. Met.* **2020**, *262*, 116328.

(28) Coronado, J. G.; Martín, E.; Montero, L.; Fierro, J.; de la Vega, J. G. *J. Phys. Chem. A*. **2007**, *111*, 9724.

(29) Hu, G.; Jia, H.; Hou, Y.; Han, X.; Gan, L.; Si, J.; Cho, D.-H.; Zhang, H.; Fang, J. *Anal. Chem.* **2020**, *92*, 4371.

(30) Li, G.; Chen, Y.; Qiao, Y.; Lu, Y.; Zhou, G. *J. Org. Chem.* **2018**, *83*, 5577.

(31) Dwivedi, B. K.; Singh, R. S.; Ali, A.; Sharma, V.; Mobin, S. M.; Pandey, D. S. *Analyst.* **2019**, *144*, 331.

(32) Aradhyula, B. P. R.; Ranga Naidu Chinta, R. V.; Dhanunjayarao, K.; Venkatasubbaiah, K. *RSC Adv.* **2020**, *10*, 13149.

(33) zhang, H.; Yin, C.; Liu, T.; Chao, J.; Zhang, Y.; Huo, F. *Dyes Pigm.* **2017**, *146*, 344.

(34) Mukundam, V.; Dhanunjayarao, K.; Chuang, C.-N.; Kang, D.-Y.; Leung, M.-k.; Hsieh, K.-H.; Venkatasubbaiah, K. *Dalton Trans.* **2015**, *44*, 10228.

(35) Mukundam, V.; Dhanunjayarao, K.; Samal, S.; Venkatasubbaiah, K. *Asian J. Org. Chem.* **2017**, *6*, 1054.

(36) Sheldrick, G. M. *Acta Crystallogr. Sect. A: Found. Crystallogr.* **2008**, *64*, 112.

(37) Allen, A. J.; Hajdu, J.; McIntyre, G. J. *J. Appl. Crystallogr.* **2018**, *51*, 233.

CHAPTER 4A

Synthesis and characterization of poly(tetraphenylimidazole)s and their application in the detection of fluoride ions

4A.1 Introduction

The development of selective and efficient sensors is of prime importance owing to their applications in biological, and analytical processes[1-8]. A number of sensors or probes have been reported for the detection of different analytes based on intramolecular charge transfer,[9,10] photoinduced electron transfer,[11-15] fluorescence resonance energy transfer,[16-20] excimer/exciplex formation,[21-23] metal-ligand charge transfer,[24-27]twisted intramolecular transfer[28]. Another unique process known as excited state intramolecular proton transfer (ESIPT) have given promising materials with applications ranging from organic light emitting diodes to fluorescent probes[29-34]. Among the different ESIPT molecules, imidazoles (or) imidazole analogues containing 2-hydroxyphenyl have been studied to a greater extent due to their potential application in electroluminescent, laser dyes and as chemosensor materials[34-38]. Using this unique process of 2-hydroxyphenyl imidazoles (or) imidazole analogues, several anion probes have been developed[39-43]. The respective imidazole polymers are particularly interesting due to their high thermal stability, the opportunity of using solution processing techniques for device fabrication and so on. Recently, Lin and co-workers[44] synthesized thieno-imidazole based polymers and used as probes for the detection of iron, mercury or zinc. Mallavia and co-workers[45] have synthesized new fluorescent conjugated polymer microsphere for sensing copper in aqueous solution. Several methodologies have been reported for the incorporation of imidazole moieties into the backbone of the polymers[46-50]. However, in comparison with polymers that contain imidazoles in the main chain, polymers with imidazoles especially tetraarylimidazoles as side-chain have received far less attention and the side chain functionalization of imidazoles has not been systematically studied[51-55]. Recently, Lu and co-workers[56] have reported long fluorescence lifetime

europium-complexes of imidazole. Inspite of these recent encouraging results, the use of imidazoles in side chain polymers especially for sensing applications are scarcely studied.

Fluoride ion, play an important role in human health where it is primarily used for the treatment of osteoporosis, prevention of dental caries and enamel demineralization[57]. Although low doses of fluoride is beneficial, high doses of fluoride ion is dangerous and can cause acute toxicity in humans and animals[58]. Hence control of fluoride consumption is a great concern in most of the countries. Over the last few decades, a number of fluoride ion sensors have been reported,[59-62] however most of them were based on small molecules. Recently, polymer based sensors/probes gained attention owing to their advantageous features over small-molecule based sensors. For example, Kim and Swager described a novel method for the detection of fluoride ion taking advantage of fluorine affinity towards silicon[63]. Jäkle and co-workers[64] reported an elegant boron based block co-polymer method for the detection of fluoride ion. With the aim to develop ESIPT based polymers for the detection of fluoride ion we report design and synthesis of silyl protected imidazole based polymers and their sensing ability towards fluoride anion.

4A.2 Results and discussion

4A.2.1 Synthesis and characterization of probe 1 & probe 2

We synthesized silylated imidazole monomer (compound **2)** in three step reaction process as shown in scheme 4A.1. The first step is ESIPT based brominated tetraarylimidazole (compound **1a)** was synthesized using one-pot reaction with condensation of by reported literature procedures [65-66]. In a second step styryl containing compound **1** was synthesized through Suzuki–Miyaura crosscoupling

between 4-vinylphenylboronic acid and compound **1a** in 70% yield. Also, compound **1** treated with tert-butyl(chloro)diphenylsilane in the presence of a base (DBU) to obtained silylated compound **2** [67] with good yield 89% in a third step. Synthesized homo polymer (probe **1,** 84%) has been made when compound **2** was polymerized using 2,2'-azobis(isobutyronitrile) (AIBN) as the initiator under typical free radical polymerization conditions. We also made block co-polymer (probe **2**) in 74% yield, when using di(ethylene glycol) methyl ether methacrylate as the second monomer with compound **2** to have better solubility in organic solvents (Scheme 4A.2).

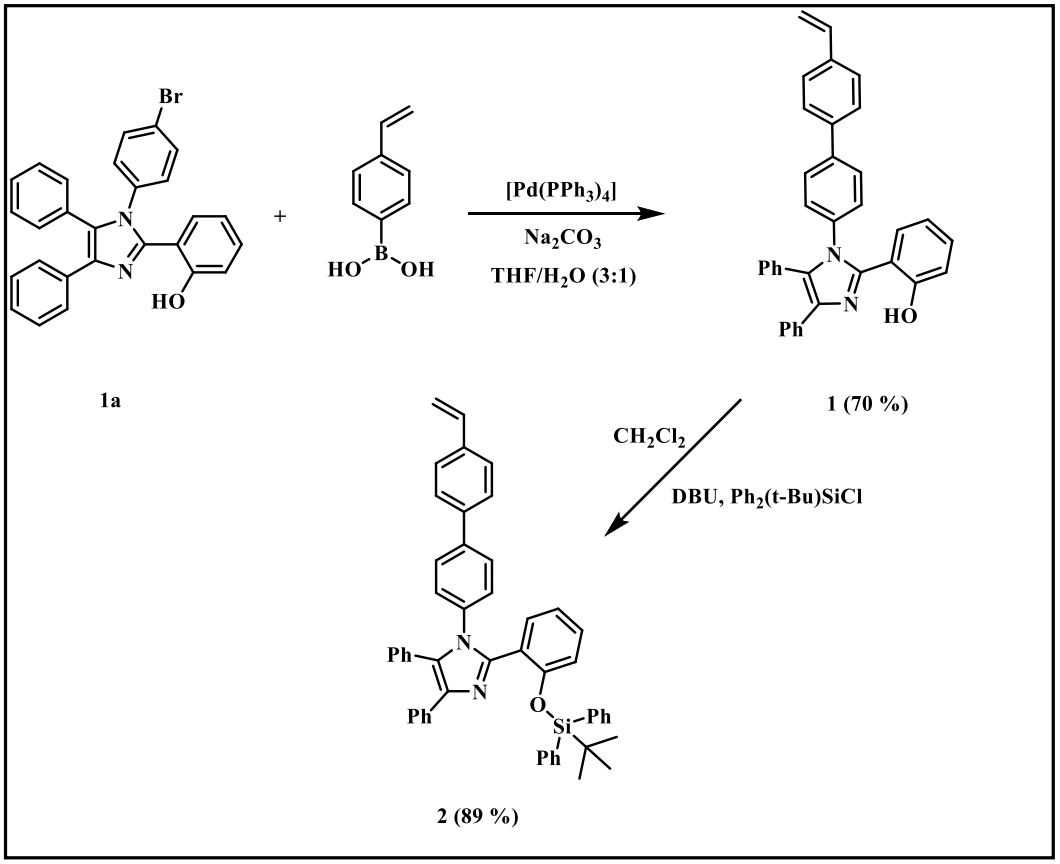

Scheme 4A.1: Synthetic route to the monomer.

All the synthesized compounds were analyzed by various techniques. Both the compounds (**1** and **2**) were characterized by ^{1}H, ^{13}C and ^{29}Si NMR spectroscopy in $CDCl_3$ solvent. The purification of polymerised polymers performed in reprecipitation

of dichloromethane solution of polymers in *n*-hexane. The resultant polymers were fully characterized by multi nuclear NMR (^{1}H, ^{13}C and ^{29}Si) spectroscopy techniques in $CDCl_3$ solvent. ^{1}H NMR spectrum of the polymers has shown characteristic broadening features in their peaks and complete disappearance of the AMX patterned vinyl protons (Figure 4A.1). Furthermore, the ratio of the repeat unit of compound **2** to di(ethylene glycol) methyl ether methacrylate in the block copolymer was found to be 1 : 1, as elucidated using ^{1}H NMR (Figure 4A.2). Additionally, ^{29}Si NMR comparison of monomer and block copolymer are showed in $CDCl_3$ (Figure 4A.3).The representative mass spectrum of compound **2** is shown in figure 4A.4.

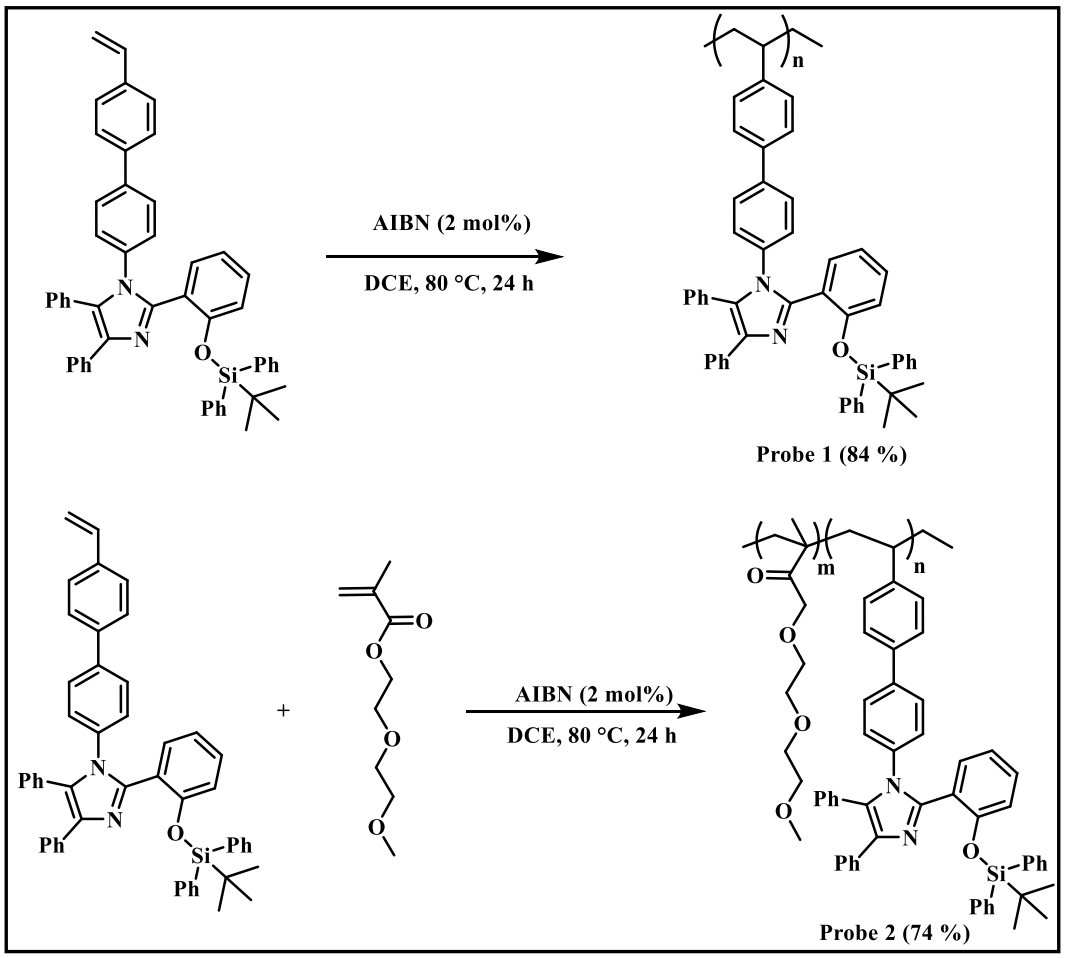

Scheme 4A.2: Synthetic route to the homo-(probe **1**) and random co-polymer (probe **2**).

The molecular weights of the polymers were studied by gel permeation chromatography (GPC) in tetrahydrofuran using narrow polystyrene standards. The weight-average molecular weights of the homo- and random co-polymer are 16700 and 25400 with polydispersity indices (Đ) of 2.51 and 1.95 respectively as shown in table 4A.1. The enhancement of molecular weight in copolymer has resulted less retention time i.e. 6.434 min. in comparison with the homopolymer retention time i.e. 6.571 min as shown in figure 4A.5.Based on the GPC and the ^{1}H NMR data, the composition of the block co-polymer was assumed as m : n = 14 : 14.

Monomer was further confirmed by single crystal X-ray crystallography which crystallizes in a monoclinic system with a space group P21/c (Figure 4A.6). The crystallographic data for monomer is given in table 4A.2. The phenyls attached to the imidazole ring are arranged in a propeller fashion with a torsion angle ranging from 24.37 to 78.11º.

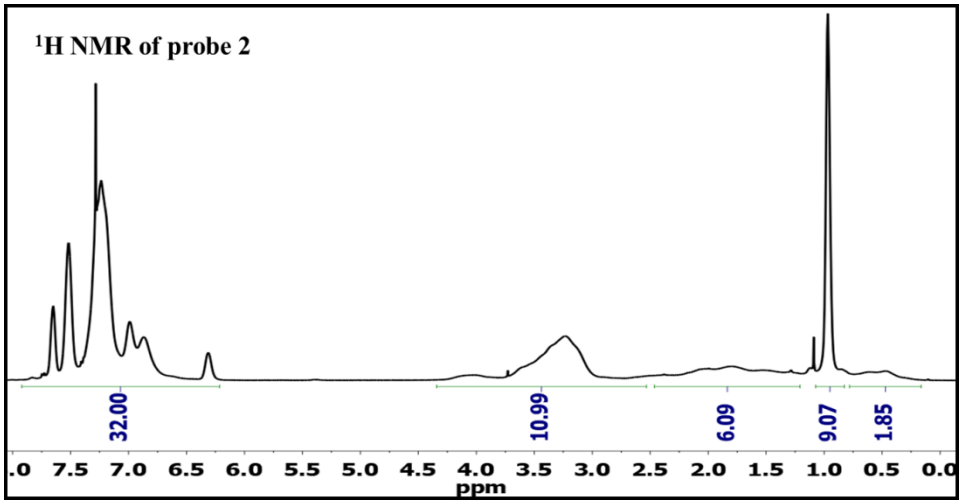

Figure 4A.1: ^{1}H NMR spectrum of block co-polymer (probe **2**).

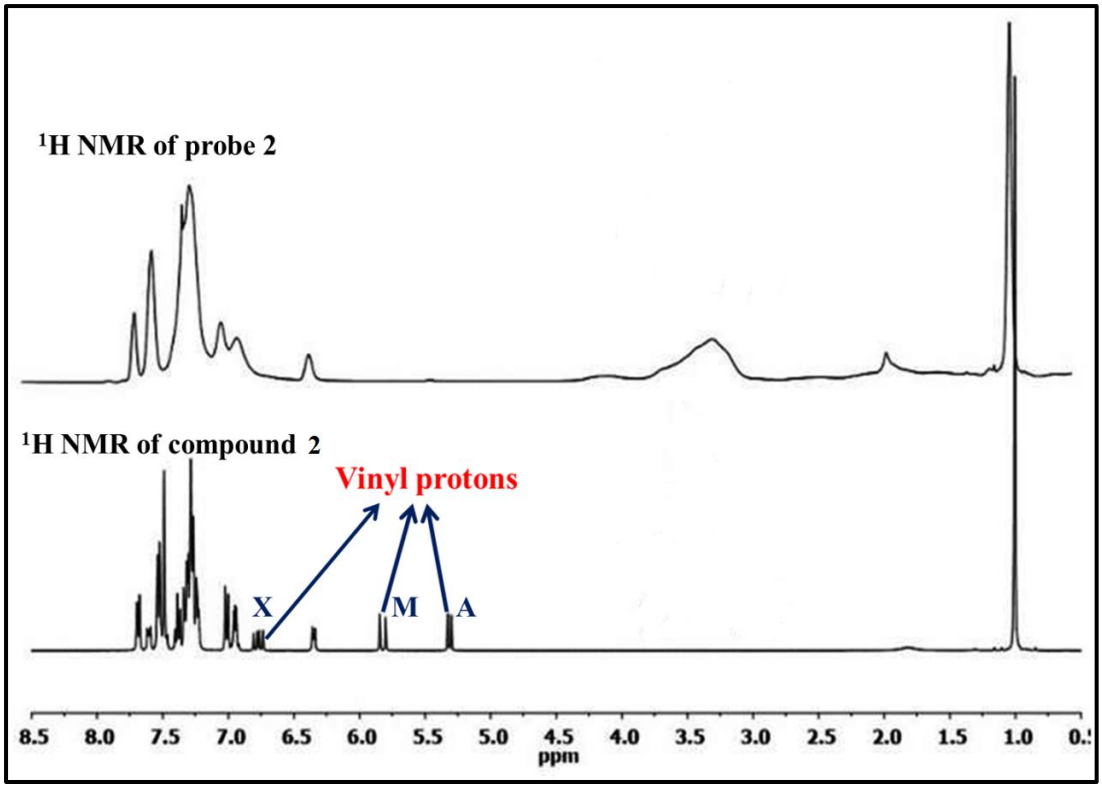

Figure 4A.2: ^{1}H NMR spectrum of compound **2** and block co-polymer (probe **2**).

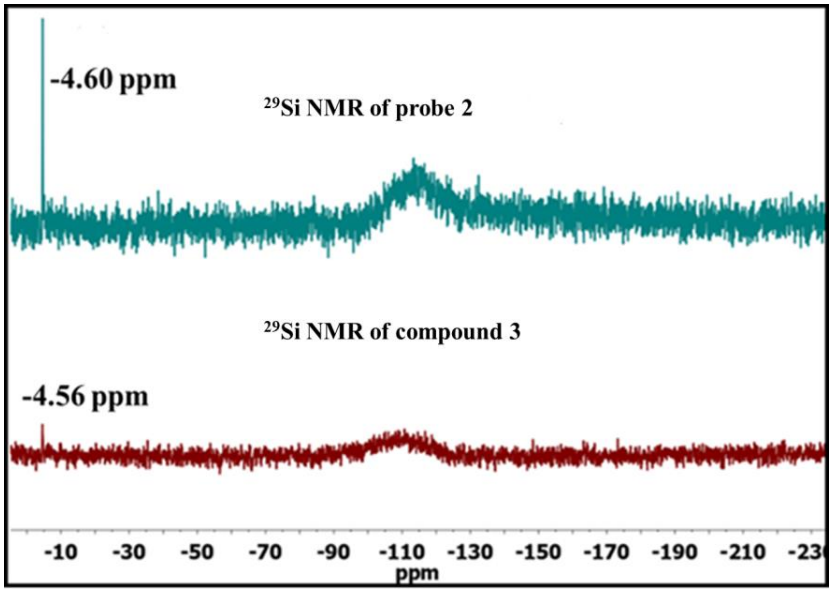

Figure 4A.3: ^{29}Si NMR spectrum of compound **2** and co-polymer (probe **2**).

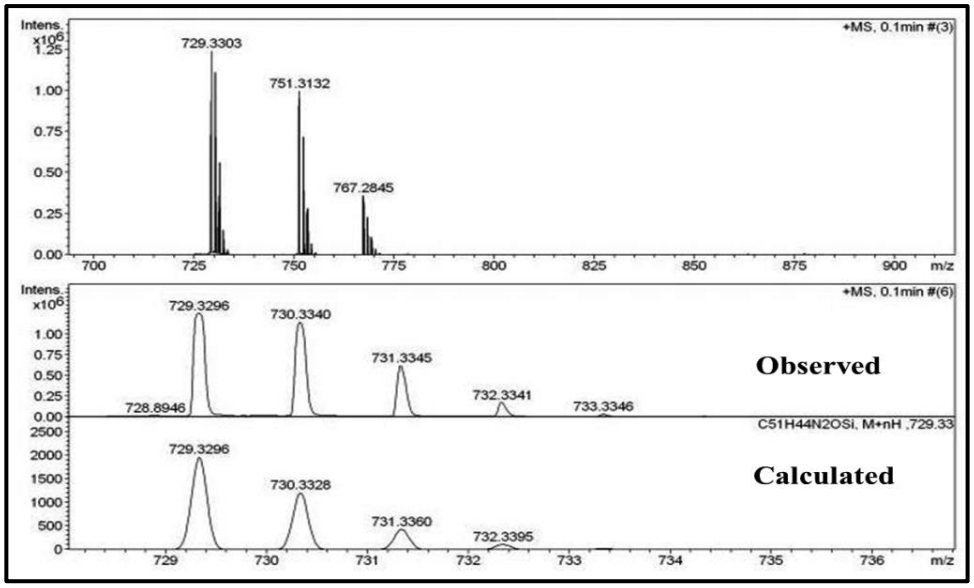

Figure 4A.4: HRMS spectrum of compound **2.**

Table 4A.1: Molecular weight data for polymers (probe **1** and probe **2**).

Polymer	M_w, **Da**[a]	M_n, **Da**[a]	**PDI**[a]
Homo	16750	6665	2.51
Copolymer	25457	13058	1.95

[a] GPC-RI in THF *vs* polystyrene standards, PDI-polydispersity index (PDI = M_w/M_n)

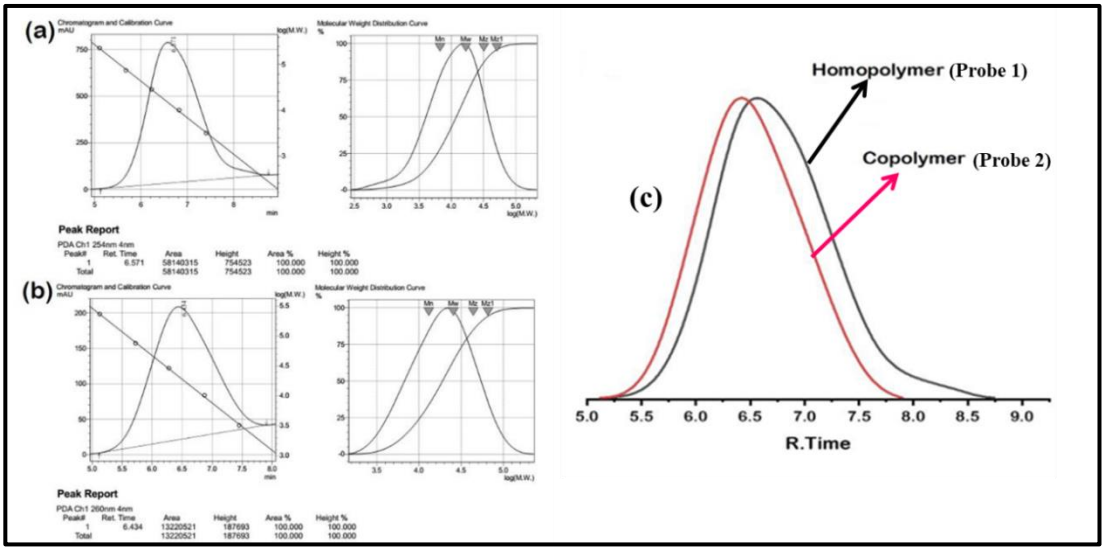

Figure 4A.5: GPC traces of the (a) Homopolymer (probe **1**) (b) Copolymer (probe **2**) (c) Comparison of retention time of both the probes. Plot represent normalized RI intensities vs elution time, where THF used as eluent and polystyrene standards were used for calibration.

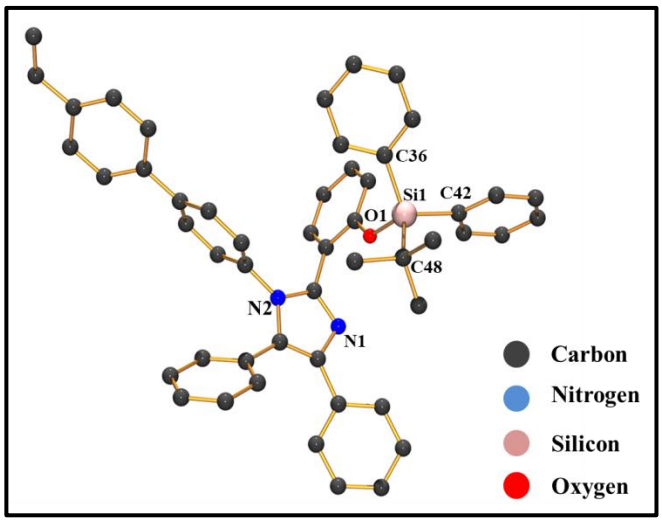

Figure 4A.6: Molecular structure of the silyl protected monomer (2). Ball and stick model (hydrogen atoms are omitted for the clarity). Selected bond lengths (Å) and bond angles (°) are as follows: Si1-O1 1.6484(12), Si1-C36 1.866(2), Si1-C42 1.867(2), Si1-C48 1.8807(18), O1-Si1-C36 107.97(9), O1-Si1-C42 108.36(8), O1-Si1-C48 103.53(7), C36-Si1-C42 112.68(9). Angle between the plane constructed by the imidazole ring and the neighbouring phenyl groups are 24.37, 49.03, 74.45 and 78.11.

Table 4A.2: Crystal data and structure refinement parameters for compound **2.**

Compound	**2**
Empirical formula	$C_{51}H_{44}N_2OSi$
Formula weight	728.97
Temperature/K	293(2)
Crystal system	Monoclinic

Space group	*P*2/*c*
a/Å	14.7258(2)
b/Å	17.0253(2)
c/Å	17.5571(3)
α/°	90
β/°	105.6548(18)
γ/°	90
Volume/Å^3	4238.49(13)
Z	4
ρ_{calcd}/g cm^{-3}	1.142
μ(MoKα) /mm^{-1}	0.777
F(000)	1544.0
2θ range for data collection/°	6.234 to 148.984
Index ranges	-18 ≤ h ≤18, -21 ≤ k ≤ 15, -19 ≤ l ≤ 21
Reflns. collected	25771
Independent reflns	8533[R_{int} = 0.0317, Rsigma = 0.0275]
Data/restraints/parameters	8533 / 0 / 507
GOF on F^2	1.087
Final R indices [$I > 2\sigma(I)$]	R_1 = 0.0535, wR_2 = 0.1564
R indices (all data)	R_1 = 0.10601,wR_2 = 0.1627
Largest diff. peak /hole [e Å^{-3}]	0.29/ -0.30

4A.2.2 Thermal studies

The thermal stability of the resultant polymers were analysed using thermogravimetric analysis (TGA) and differential scanning calorimetry (DSC). The relevant data are summarized in table 4A.3. TGA study reveals that the probes are thermally stable up to 320 ºC. Furthermore, differential scanning colorimetric studies reveals that probes **1** & **2** have high glass transition temperatures (Tg).

Table 4A.3: Thermal data for polymers (probe **1** and probe **2**).

Polymer	**PDT, °C**	**T_g, °C**
Probe 1	380	155
Probe 2	320	120

PDT-polymer decomposition temperature, T_g-glass transition temperature

4A.2.3 Probes for fluoride ion sensing

In order to study their application as a fluoride ion sensing ability by obtained polymers were used in organic solvents. Both the polymers displayed one absorption band at 275 nm and an emission band at around 382 nm in THF solution. When we added different equivalents of tetra butyl ammonium fluoride and the response was observed by absorption as well as emission spectroscopy (Figure 4A.7).

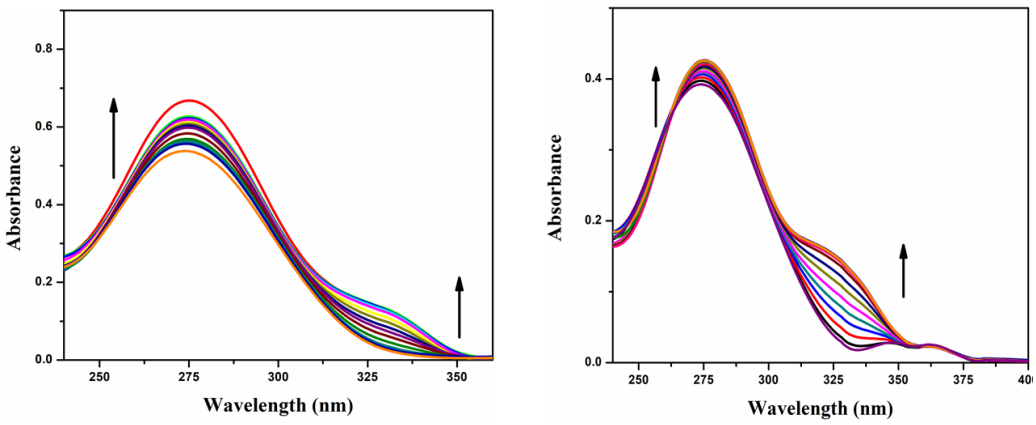

Figure 4A.7: Absorption spectra for 10 µm of probe **1** (left) and probe **2** (right) upon gradual addition 0.1 eqv. (1 µm) of TBAF (0 to 1.3 eqv.) in THF solution.

On incremental addition of fluoride ions to the THF solution of both the probes, resulting new absorption bands has not been observed. But the structured emission

intensity band of the probe **1** showed at 381 nm gradually decreases with steadily appearance of new band at 485 nm with Iso bestic point at 443 nm. Probe **2** emission intensity band showed at 382 nm gradually decreases along with the appearance of a new red-shifted emission 488 nm with Isisbestic point at 447 nm (Figure 4A.8).

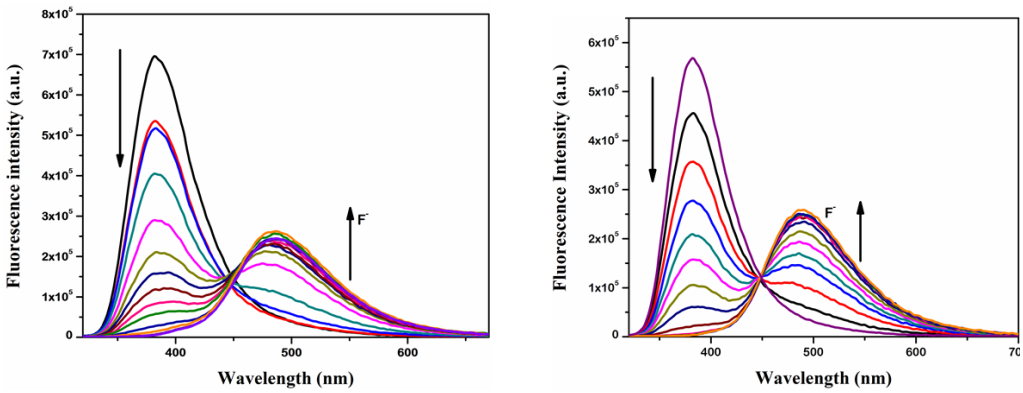

Figure 4A.8: Emission spectra for 10 µm of probe **1** (left) and probe **2** (right) upon gradual addition 0.1 eqv. (1 µm) of TBAF (0 to 1.3 eqv.) in THF when excited at 275 nm.

Asdemonstrated by us and others,[2,3,5,6,62,63,65,66](probes **1** & **2**) showed normal stokes shifted emission(silylated compounds)and the desilylated compounds showed ESIPT emission(Figure 4A.9). The Stokes shift of the desilylated probes are around 100 nm.

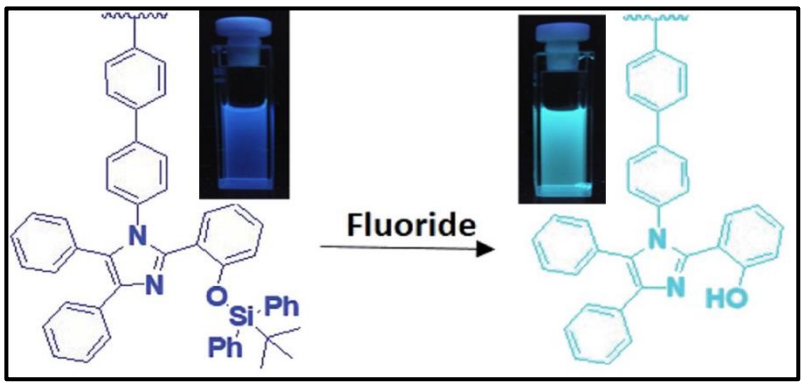

Figure 4A.9: Schematic representation of sensing mechanism.

The plot of ratios of fuorescence intensities i.e. I_{485} nm/I_{381} nm vs. fluoride ion concentration for probe **1** shows a linear increase between 0–9 µM of fluoride ions with a detection limit of 0.003 µm but for the probe II it is 0–7 µM with a detection limit of 0.177 µm. The ratio of emission intensities varies from 9 to 19 for probe **1** whereas for probe **2** it is 11 to 39 (Figure 4A.10).

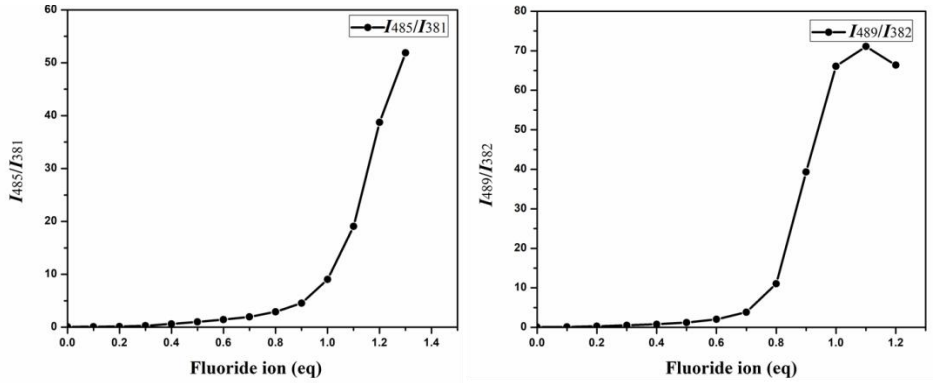

Figure 4A.10: Plots of fluorescence intensities ratios of probes **1 (**left**)** & probes **2 (**right**)** sensing with TBAF (0 to 1.3 eqv.).

To realize the effect of time on sensing the fluoride ion, we monitored the fluorescence intensity for 60 min. These experiments shows that our probes got quenched ≈ 90% (92% for probe **1** and 93% for probe **2**) within five minutes which suggest that our probes are highly sensitive (Figure 4A.11).

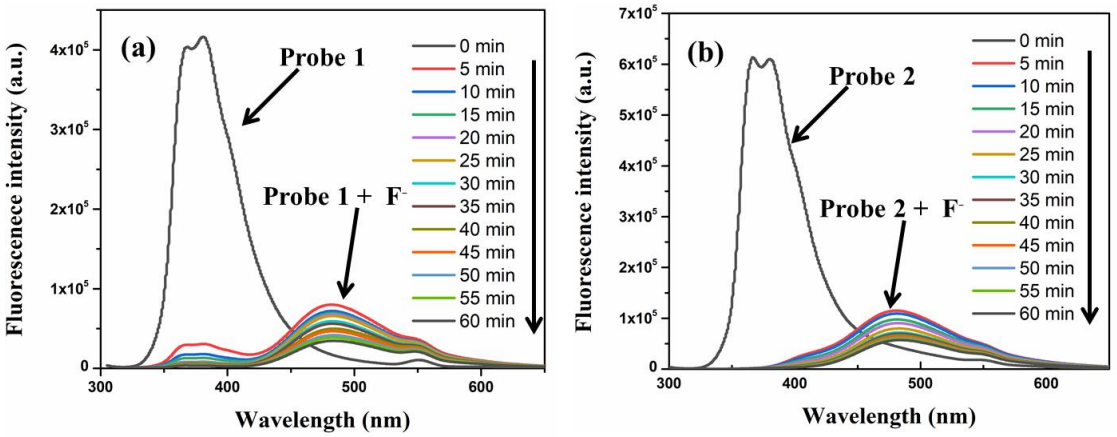

Figure 4A.11: Fluorescence response of both the probes (10 μmol) (a) Probe **1** (homo-polymer) and (b) Probe **2** (random co-polymer) with equimolar fluoride ion (10 μmol) over a period of 60 min.

Selectivity is an important parameter for the success of a chemical probe, to investigate the selectivity of the probes for fluoride ion, we measured the fluorescence spectra of our probes with various other anions such as Cl^-, Br^-, CN^-, I^-, NO_2^-, OAc^-, HSO_4^-, $H_2PO_4^-$, OH^- and ClO_4^-. As shown in Figure 4A.12, addition of other anions does not results any significant change in the fluorescence behaviour of probe **1** & **2,** especially there is no emission band at ≈ 485 nm. This comparative study indicates that our polymeric probes (both probe **1** and probe **2**) displayed excellent selectivity for the detection of fluoride ion over other anions.

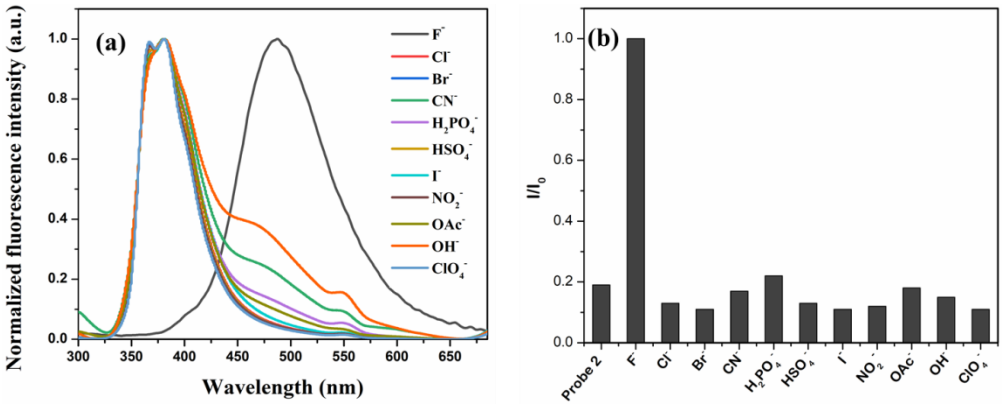

Figure 4A.12: Normalized emission spectra of probe **1** (left) and Selectivity of fluoride ion by monitoring the fluorescence intensities of probe (right)**2** at 488 nm upon incubation with 10 eqv. of F^-, Cl^-, Br^-, CN^-, I^-, NO_2^-, OAc^-, HSO_4^-, $H_2PO_4^-$, OH^- and ClO_4^- for 15 min.

We further treated our probes with fluoride ion in the presence of different anions to probe the competition of fluoride over other ions which shows that our probes are highly selective even in the presence of different anions (Figure 4A.13†).

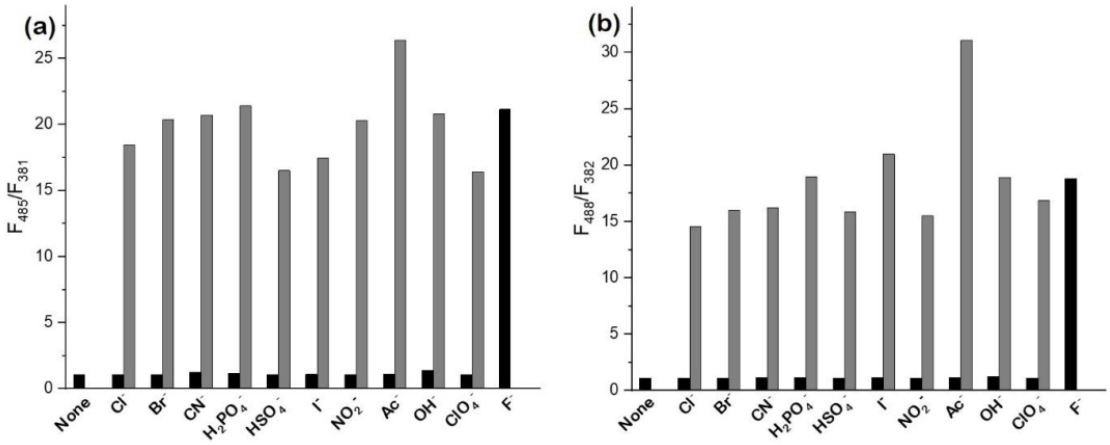

Figure 4A.13: Fluorescence response of both probes (10 μmol) towards various analytes in THF solution. All the data represents the fluorescence intensity ratio (F_{485}/F_{381} for probe **1** (left) and F_{488}/F_{382} for probe **2** (right)). Black bars represent the addition of single analyte including 100 μmol anions (Cl^-, Br^-, CN^-, $H_2PO_4^-$, HSO_4^-, I^-, NO_2^-, Ac^-, OH^- and ClO_4^-). Light gray bars represent the subsequent addition of F^-, to the mixture. Each data was obtained after various analytes addition at ambient temperature for 15 min.

Our efforts to evaluate the fluoride ion sensing using ^1H NMR titrations did not yield any fruitful results (Figure 4A.14). Control experiments were performed to know the stability of the monomer and the probes **1** & **2** in solution.

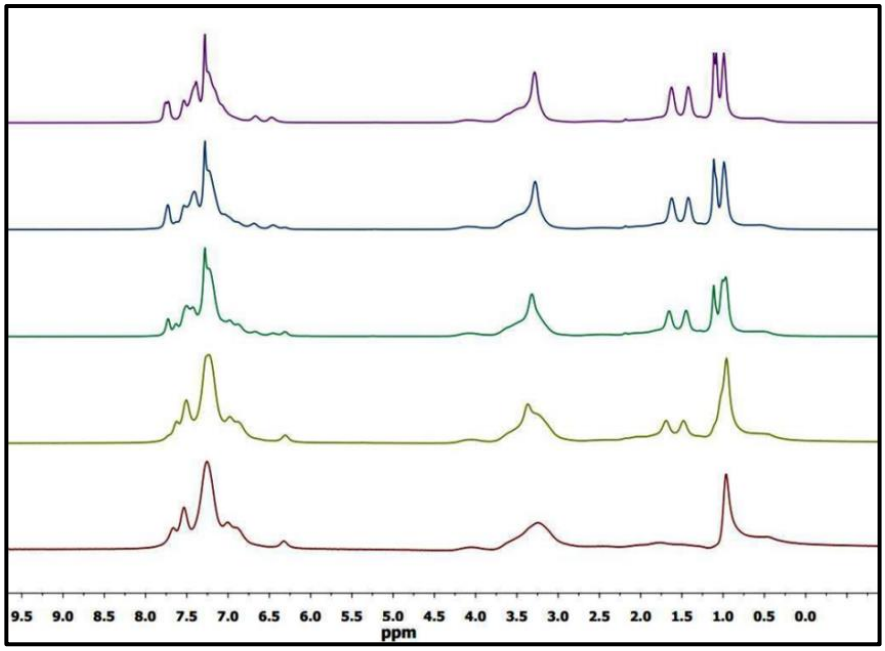

Figure 4A.14: ^{1}H NMR titration spectrum of random co-polymer (probe **2**) 54 mmol with 14, 28, 42 and 56 mmol of fluoride ions in $CDCl_3$ (bottom to top).

These studies reveal that the monomer and the probes **1** & **2** are stable in solution at least for 24 h (Figure 4A.15).

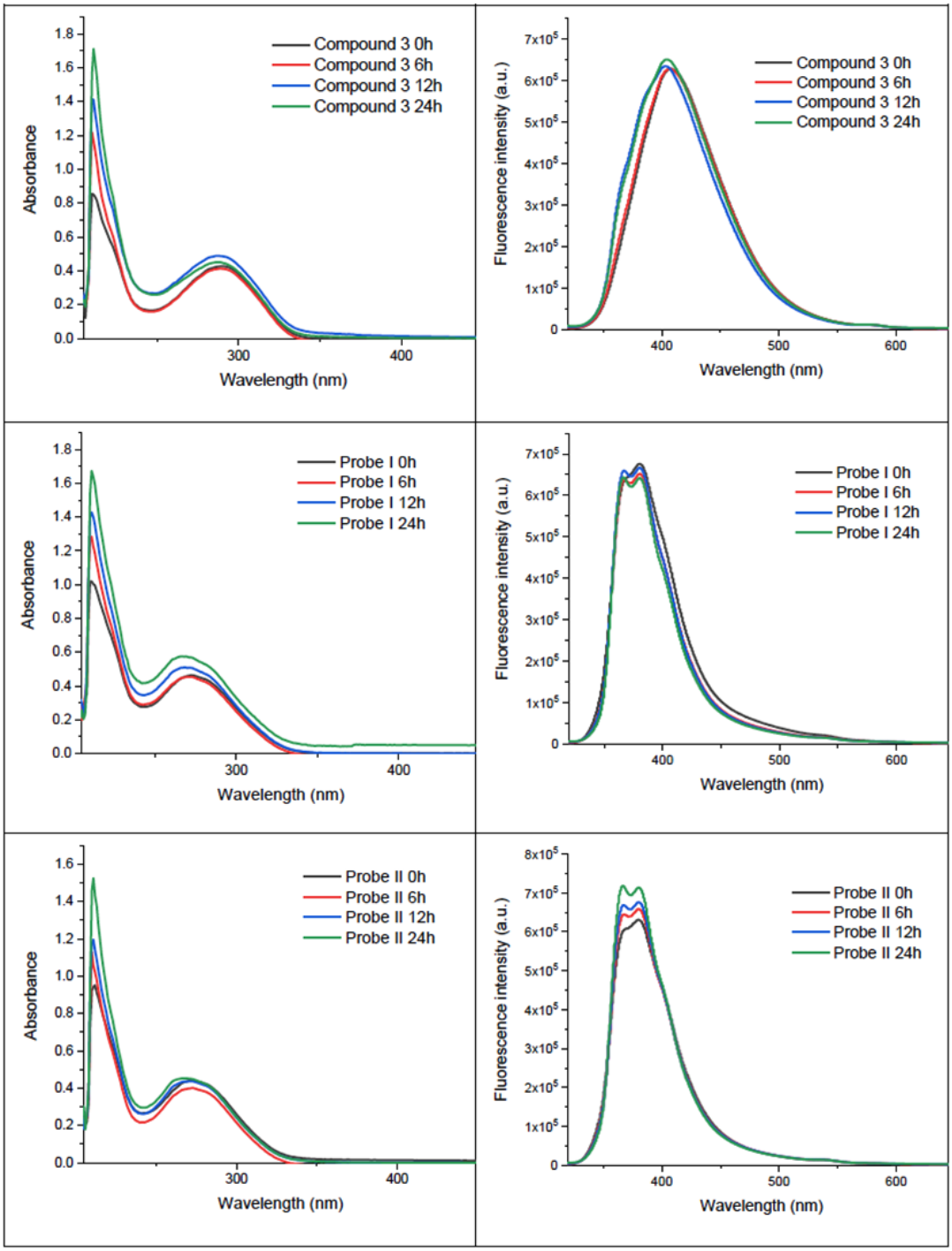

Figure 4A.15: UV-Vis and emission spectra of monomer and the probes **1** & **2** in THF solution at different interval of time.

We also tested the effect of concentration and temperature of our probes along with different ions like Cl^-, NO_2^-, HSO_4^-. These results reveals that there is no

appreciable change in the peak position of the emission (Figure 4A.16 & 4A.17), which indicates that the probes are stable at different temperature and concentration.

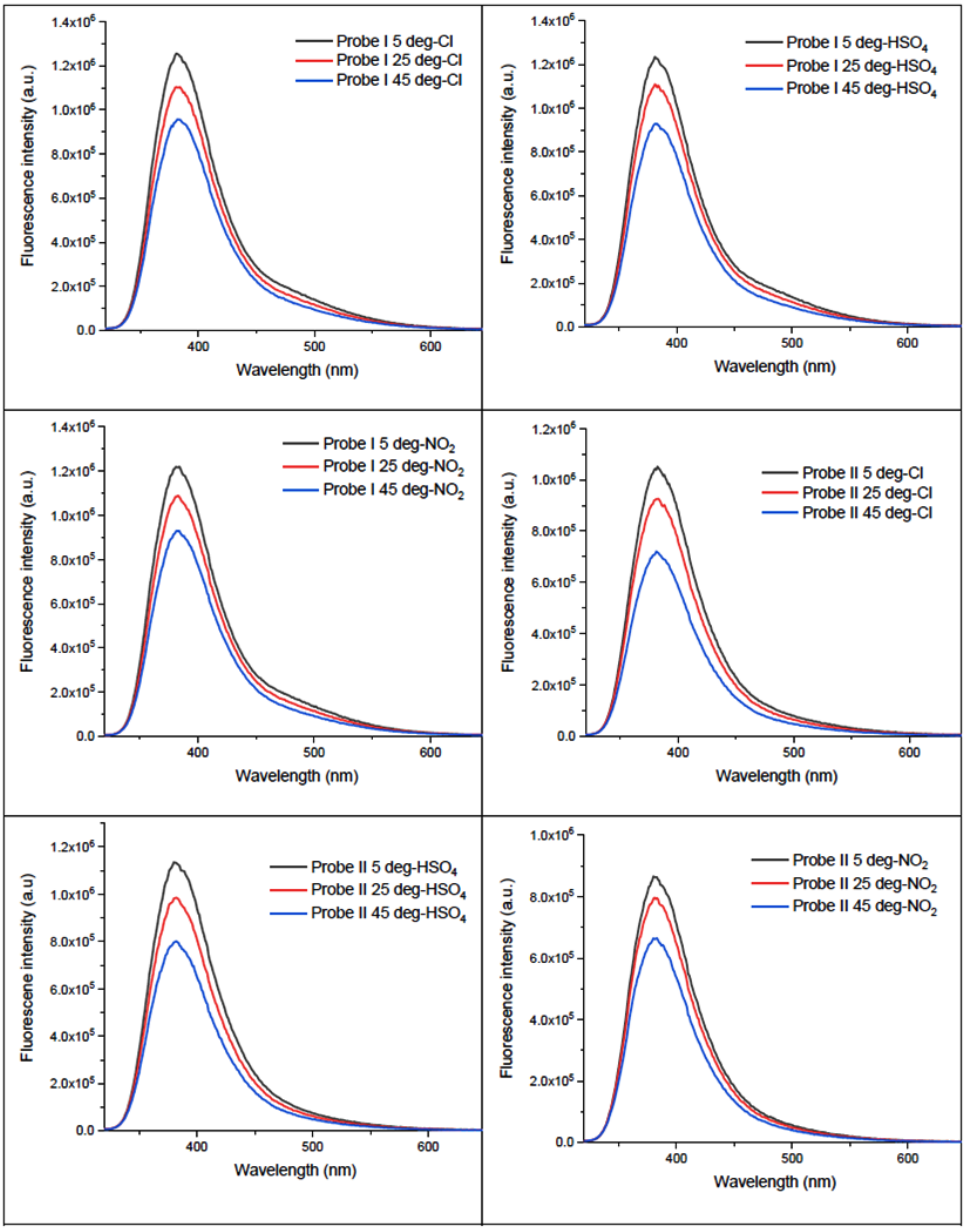

Figure 4A.16: Emission spectra of probes **1** & **2** along with different ions in THF solution at different three different temperatures.

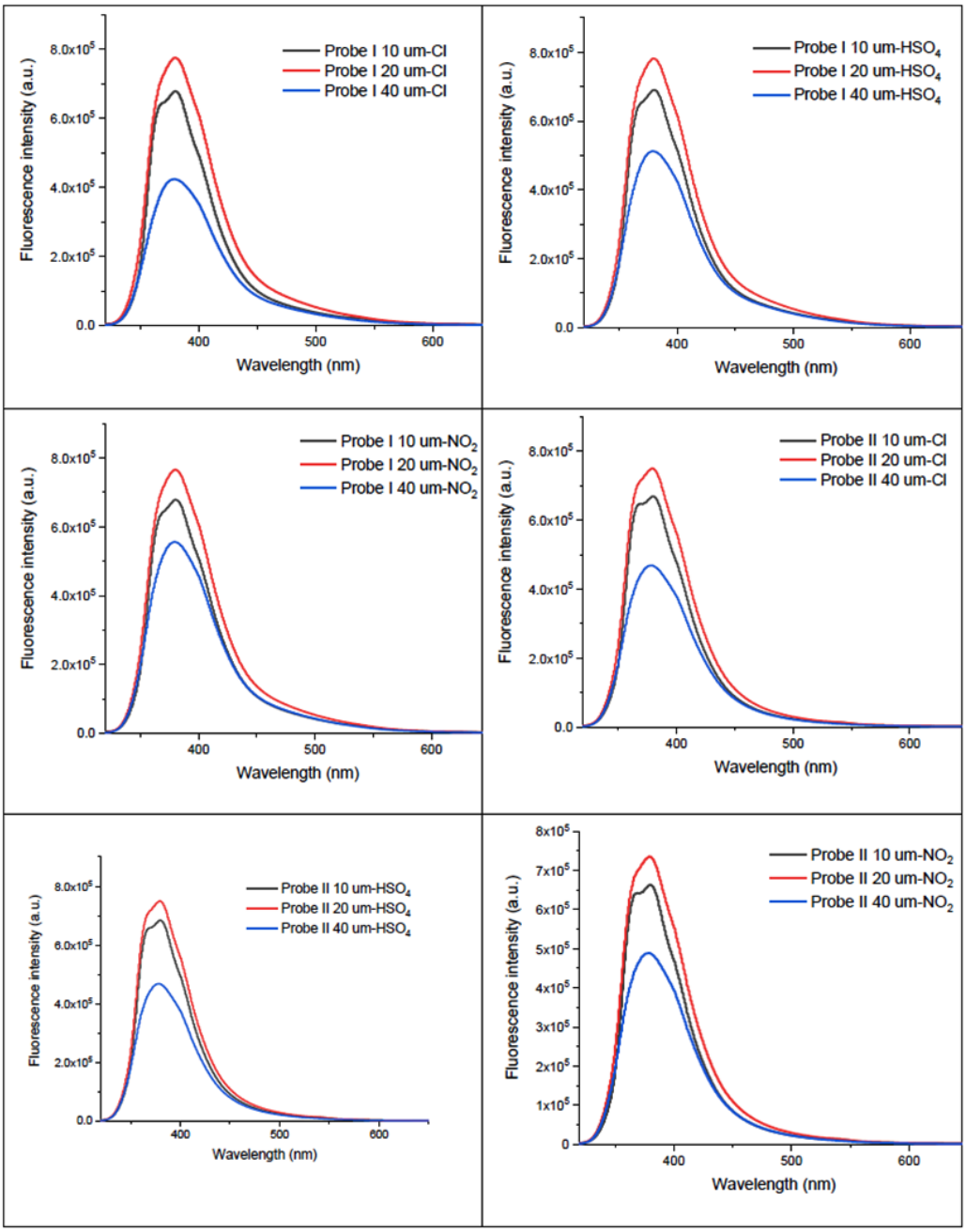

Figure 4A.17: Emission spectra of probes **1** & **2** along with different ions in THF solution at different concentrations.

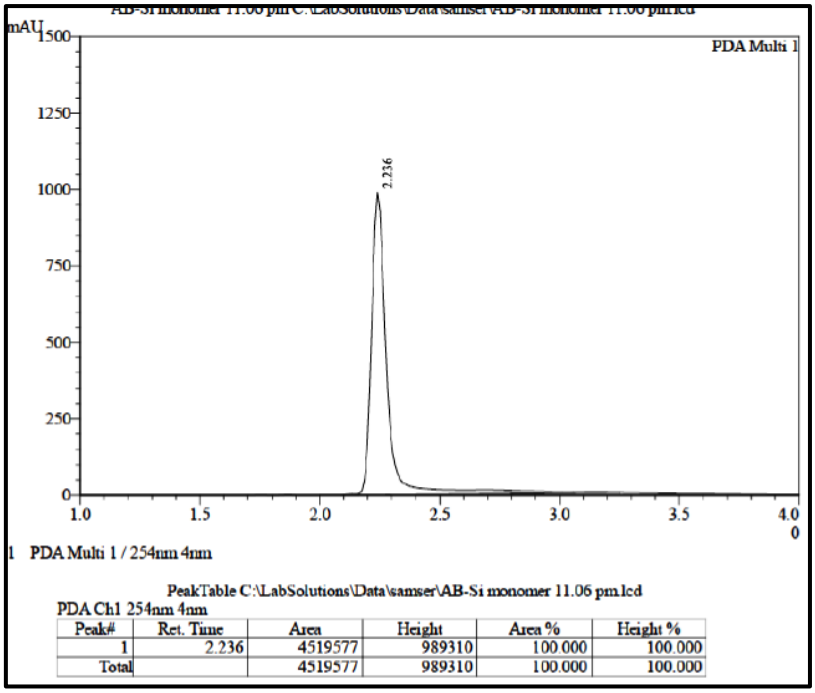

Figure4A.18: HPLC trace of compound 2.

4A.3 Conclusions

In summary, ESIPT masked tetraaryl substituted imidazole polymers (homo and copolymer) have been successfully synthesized using classic free radical polymerization method. Upon addition of fluoride ion both the polymers exhibited large Stokes shift which is an ESIPT emission. Most importantly both the probes showed high selectivity for fluoride ion over other ions. We expect our results will have significant impact in developing luminescent polymers for biological imaging and organic electronics. Further studies to tune the solubility of the polymers in aqueous medium are ongoing in our group.

4A.4 Experimental section

4A.4.1 General Information

Solvents and other general reagents were purified according to standard procedures. Benzil, 4-bromoaniline, 4-vinylphenylboronicacid, di(ethylene glycol) methyl ether methacrylate and ammonium acetate were purchased from Sigma-Aldrich. 1,8-Diazabicyclo [5.4.0]undec-7-ene (DBU), tert-butyl(chloro)diphenylsilane

and salicylaldehyde were purchased from Alfa-Aesar. Glacial acetic acid and 2,2'-azobis(isobutyronitrile) were obtained from Spectrochem. All 400 MHz ^{1}H, 100 MHz ^{13}C, and 79 MHz ^{29}Si, spectra were recorded on a Bruker ARX 400 spectrometer operating at 400 MHz. All ^{1}H and ^{13}C NMR spectra were referenced internally to solvent signals. ^{29}Si NMR spectra were referenced externally to TMS in $CDCl_3$ (δ = 0). All NMR spectra were recorded at ambient temperature. ESI mass spectra were recorded on a Bruker, microTOF-QII mass spectrometer. The absorbance spectra were recorded on JASCO V-730 UV-visible spectrometer. The fluorescence spectra were recorded using Edinburgh FS5 spectrofluorometer. The fluorescence spectra were corrected for the instrumental response. Thermogravimetric analyses (TGA) were recorded on a perkinElmer pyris 6 TGA model in nitrogen condition at a heating rate of 20 ^{o}C min^{-1}. Differential scanning calorimetric (DSC) analyses were recorded on a PerkinElmer Pyris 6 DSC model in nitrogen atmosphere at a heating rate of 20 °C min^{-1}. Gel-permeation chromatography (GPC) analyses were performed on a Shimadzu-LC20AD system referenced to poly(styrene) standards. THF was used as the mobile phase with a flow rate of 1.0 mL min^{-1}. Single-crystal X-ray diffraction data was collected on a Rigaku Oxford X-ray diffractometer. The data was collected at 293 K using Cu-Kα radiation (1.54184 Å). Crystallographic data for **2**, details of X-ray diffraction experiments and crystal structure refinements are given in table 4A.2. The structures were solved and refined with SHELX suite of programs. All non-hydrogen atoms were refined with anisotropic displacement coefficients. The H atoms were placed at calculated positions and were refined as riding atoms. Crystallographic data for the structure **2** has been deposited with the Cambridge Crystallographic Data Center.

4A.4.2 Synthetic procedure and spectral characterization

4A.2.2.1 Synthesis of 2-(4,5-diphenyl-1-(4'-vinyl-[1,1'-biphenyl]-4-yl)-1H-imidazol-2-yl)phenol (1):

Under nitrogen, a biphasic solution of imidazole (1.00 g, 2.14 mmol), 4-styrene boronic acid (0.38 g, 2.57 mmol), sodium carbonate (0.68 g, 6.42 mmol) and [$Pd(PPh_3)_4$] (3 mol%) in tetrahydrofuran (THF) and water (20:8; 56 mL) was heated at reflux for 12 hours. The organic layer was separated and the aqueous layer was extracted twice (20 mL) with ethyl acetate. The combined organic phase was dried with sodium sulphate and concentrated under vacuum. The product was purified by column chromatography to afford off-white compound. Yield: 0.74 g (70%). ^{1}H NMR (400 MHz, $CDCl_3$) δ 5.33 (d, *J* = 12 Hz, 1H), 5.84 (d, *J* = 20 Hz, 1H), 6.53 (t, *J* = 8 Hz, 1H), 6.71 (d, *J* = 8 Hz, 1H), 6.78 (dd, *J* = 12 & 20 Hz, 1H), 7.12 – 7.32 (m, 12H), 7.52 (d, *J* = 8 Hz, 2H), 7.57-7.64 (m, 6H), 13.39 (s, 1H); ^{13}C NMR (101 MHz, $CDCl_3$): δ 112.88, 114.55, 117.94, 118.16, 126.42, 126.81, 127.05, 127.15, 127.24, 127.80, 128.37, 128.62, 128.91, 130.25, 130.49, 131.35, 136.15, 137.38, 138.55, 141.31, 144.84, 158.32; IR (KBr): υ(cm^{-1}) = 3057 (s), 1602 (m), 1588 (m), 1527 (s), 1485 (m), 1443 (s), 1415 (s), 1384 (m), 1294 (s), 1261 (m), 1184 (s), 1161 (s), 1139 (s), 1074 (s), 1027 (s), 994 (s), 973 (s), 915 (s), 838 (m), 783 (m), 756 (m), 734 (m), 724 (m), 714 (m), 702 (m), 654 (s); HR-MS (ESI): calcd. for $C_{35}H_{26}N_2O$ ([M + H]$^+$): 491.2118, found: 491.2133.

4A.4.2.2 Synthesis of 2-(2-((tert-butyldiphenylsilyl)oxy)phenyl)-4,5-diphenyl-1-(4'-vinyl-[1,1'-biphenyl]-4-yl)-1H-imidazole (2):

To a solution of imidazole (1.00 g, 2.04 mmol) in dichloromethane, 1,8-diazabicyclo[5.4.0]undec-7-ene (DBU) (0.61 mL, 4.08 mmol) was added at -20 ˚C and stirred for 20 min. at this temperature, then *tert*-butyl(chloro)diphenyl silane (1.1 mL, 4.08 mmol) was added and the solution was allowed to warm up to room temperature and stirred at the same temperature for 12 h. After water workup, the organic layer was separated and dried over sodium sulphate and concentrated using rotary evaporator. The product was separated by silica gel column chromatography using ethyl acetate and *n*-hexane (20:80) mixture as the eluent. Yield: 1.32 g, 89 %. ^{1}H NMR (400 MHz, $CDCl_3$): δ 1.00 (s, 9H), 5.32 (d, *J* = 12 Hz, 1H), 5.82 (d, *J* = 16 Hz, 1H), 6.35 (d, *J* = 8 Hz, 1H), 6.77 (dd, *J* = 12 & 16 Hz, 1H), 6.94 – 6.96 (m, 2H), 7.01 (d, *J* = 8 Hz, 2H), 7.23 – 7.34 (m, 14H), 7.39 (t, *J* = 8 Hz, 2H), 7.46 – 7.62 (m, 8H), 7.59 – 7.62 (m, 1H), 7.68 (d, J = 4 Hz, 2H); ^{13}C NMR (101 MHz, $CDCl_3$): δ 19.54, 26.62, 114.22, 117.33, 119.27, 119.50, 120.80, 126.58, 126.70, 126.99, 127.74, 127.78, 128.09, 128.14, 129.56, 129.80, 129.89, 130.24, 130.98, 132.09, 132.30, 132.53, 135.28, 135.39, 136.28, 136.97, 138.42, 145.67, 154.20; ^{29}Si NMR (79 MHz, $CDCl_3$): δ -4.53; IR (KBr): υ(cm^{-1}) = 3448 (s), 3068 (s), 3043 (s), 2956 (s), 2929 (s), 2856 (s), 1496 (m), 1472 (m), 1441 (m), 1429 (m), 1396 (m), 1280 (m), 1255 (m), 1108 (m), 922 (m), 824 (m), 749 (m), 698 (m), 502 (m); HR-MS (ESI): calcd. for $C_{51}H_{44}N_2OSi$ ($[M + H]^+$): 729.3296, found: 729.3299.

General procedure for the synthesis of homo- and co-polymers:

Schlenk tube was charged with the monomers and the free radical initiator 2,2'-azobis(isobutyronitrile) (2 mol%). The system was purged with nitrogen and degassed dichloroethane (DCE) 1.0 mL was added. The reaction mixture was stirred at 80 °C for 24 h. The mixture was then slowly added to *n*-hexane to

precipitate the polymers. The resulting solid was redissolved in dichloroethane (1 mL) and reprecipitated from *n*-hexane. The precipitation was repeated three times. The solid was collected and dried under high vacuum to obtain the polymers as a white solid.

4A.4.2.3 Synthesis of homo-polymer (probe 1):

The quantity of the silylated monomer (compound **2**) (0.729 g, 1.00 mmol). Yield: 0.635 g (84 %), ^{1}H NMR (400 MHz, $CDCl_3$): 0.90 (s, ^{t}Bu-H) ppm, 1.14-2.13 (polymer backbone), 6.16-7.87 (aromatic H). ^{13}C NMR (101 MHz, $CDCl_3$) δ 19.48, 26.49, 40.59, 40.45, 119.21, 122.93, 123.27, 123.87, 125.26, 126.55, 127.77, 128.25, 128.46, 129.24, 129.87, 130.82, 132.27, 132.42, 135.32, 138.42, 145.22, 154.23. ^{29}Si NMR (79 MHz, $CDCl_3$): δ -4.55; IR (KBr): υ(cm^{-1}) = 3422 (s), 3049 (s), 2930 (s), 2857 (s), 1604 (s), 1577 (s), 1525 (m), 1499 (m), 1428 (m), 1391 (s), 1364 (s), 1282 (s), 1252 (s), 1112 (m), 1006 (s), 917 (m), 823 (m), 754 (m), 702 (m), 652 (s), 613 (s), 540 (s), 502 (m). GPC (in tetrahydrofuran against polystyrene standards): M_n = 6,600, PDI = 2.51.

4A.4.2.4 Synthesis of co-polymer (probe 2):

The quantities of the monomers are as follows: Silylated monomer (compound **2**) (0.729 g, 1.00 mmol) and di(ethylene glycol) methyl ether methacrylate (0.18 mL, 1.00 mmol). Yield: 0.698 g (74 %), ^{1}H NMR (400 MHz, $CDCl_3$): 0.98 (s, 9 H, ^{t}Bu-H) ppm, 1.24-2.33 (polymer backbone), 2.88-4.38 (CH, CH_2 & CH_3), 6.16-8.04 (aromatic H). ^{13}C NMR (101 MHz, $CDCl_3$) δ 19.53, 26.57, 40.61, 41.06, 59.01, 61.93, 68.54. 68.87, 70.32, 71.88, 119.18, 120.71, 123.11, 126.40, 126.51, 127.65, 127.75, 128.12, 128.45, 129.33, 129.43, 130.13, 130.94, 132.21, 132.53, 134.71, 135.36, 135.52, 137.34, 138.11, 138.32, 139.40, 145.58, 154.23. ^{29}Si NMR (79 MHz, $CDCl_3$): δ -4.60; IR (KBr): υ(cm^{-1}) = 3422 (s), 3049 (s), 2930 (m), 2858 (s), 1726 (s), 1604 (s),

1577 (s), 1525 (s), 1499 (m), 1471 (m), 1448 (m), 1428 (s), 1391 (m), 1364 (s), 1282 (m), 1252 (m), 1196 (s), 1111 (m), 1029 (s), 1006 (s), 961 (s), 919 (m), 823 (m), 754 (m), 700 (m), 653 (s), 613 (s), 539 (s), 502 (s). GPC (in tetrahydrofuran against polystyrene standards): M_n = 13,000, PDI = 1.95.

4A.5 References

(1) Galbraith, E.; James, T. D. *Chem. Soc. Rev.* **2010**, *39*, 3831.

(2) Chen, P.; Bai, W.; Bao, Y. *J. Mater. Chem. C.* **2019**, *7*, 11731.

(3) Gai, L.; Mack, J.; Lu, H.; Nyokong, T.; Li, Z.; Kobayashi, N.; Shen, Z. *Coord. Chem. Rev.* **2015**, *285*, 24.

(4) Kobayashi, H.; Ogawa, M.; Alford, R.; Choyke, P. L.; Urano, Y. *Chem. Rev.* **2010**, *110*, 2620.

(5) Lee, M. H.; Kim, J. S.; Sessler, J. L. *Chem. Soc. Rev.* **2015**, *44*, 4185.

(6) Dhiman, S.; Ahmad, M.; Singla, N.; Kumar, G.; Singh, P.; Luxami, V.; Kaur, N.; Kumar, S. *Coord. Chem. Rev.* **2020**, *405*, 213138.

(7) Wang, D.; Tang, B. Z. *Acc. Chem. Res.* **2019**, *52*, 2559.

(8) Shunmugam, R.; Gabriel, G. J.; Smith, C. E.; Aamer, K. A.; Tew, G. N. *Chem.Eur. J.* **2008**, *14*, 3904.

(9) Zhou, G.; Baumgarten, M.; Müllen, K. *J. Am. Chem. Soc.* **2008**, *130*, 12477.

(10) Li, S.-Y.; Sun, Z.-B.; Zhao, C.-H. *Inorg. Chem.* **2017**, *56*, 8705.

(11) Sun, W.; Li, M.; Fan, J.; Peng, X. *Acc. Chem. Res.* **2019**, *52*, 2818.

(12) Madhu, S.; Ravikanth, M. *Inorg. Chem.* **2014**, *53*, 1646.

(13) Mawai, K.; Nathani, S.; Roy, P.; Singh, U. P.; Ghosh, K. *Dalton Trans.* **2018**, *47*, 6421.

(14) Xu, X.-H.; Liu, C.; Mei, Y.; Song, Q.-H. *J. Mater. Chem. B.* **2019**, *7*, 6861.

(15) Pang, X.; Ge, J.; Yu, X.; Li, Y.; Shen, F.; Wang, Y.; Ren, J. *New J. Chem.* **2019**, *43*, 10554.

(16) Xu, W.; Liu, S.; Sun, H.; Zhao, X.; Zhao, Q.; Sun, S.; Cheng, S.; Ma, T.; Zhou, L.; Huang, W. *J. Mater. Chem.* **2011**, *21*, 7572.

(17) Qiu, B.; Zeng, Y.; Hu, R.; Chen, L.; Chen, J.; Yu, T.; Yang, G.; Li, Y. *ACS Omega.* **2018**, *3*, 18153.

(18) Chang, M. J.; Kim, K.; Park, K. S.; Kang, J. S.; Lim, C. S.; Kim, H. M.; Kang, C.; Lee, M. H. *Chem. Commun.* **2018**, *54*, 13531.

(19) Zhao, C.; Zhang, X.; Li, K.; Zhu, S.; Guo, Z.; Zhang, L.; Wang, F.; Fei, Q.; Luo, S.; Shi, P.; Tian, H.; Zhu, W.-H. *J. Am. Chem. Soc.* **2015**, *137*, 8490.

(20) Xu, K.; He, L.; Yang, X.; Yang, Y.; Lin, W. *Analyst.* **2018**, *143*, 3555.

(21) Song, Q.; Bamesberger, A.; Yang, L.; Houtwed, H.; Cao, H. *Analyst.* **2014**, *139* , 3588.

(22) Gai, L.; Chen, H.; Zou, B.; Lu, H.; Lai, G.; Li, Z.; Shen, Z. *Chem. Commun.* **2012**, 48, 10721.

(23) Kim, S. K.; Bok, J. H.; Bartsch, R. A.; Lee, J. Y.; Kim, J. S. *Org. Lett.* **2005**, *7*, 4839.

(24) Kurishita, Y.; Kohira, T.; Ojida, A.; Hamachi, I. *J. Am. Chem. Soc.* **2010**, *132*, 13290.

(25) Sun, Y.; Ross, N.; Zhao, S.-B.; Huszarik, K.; Jia, W.-L.; Wang, R.-Y.; Macartney, D.; Wang, S. *J. Am. Chem. Soc.* **2007**, *129*, 7510.

(26) Ko, S.-B.; Lu, J.-S.; Kang, Y.; Wang, S. *Organometallics*. **2013**, *32*, 599.

(27) Vadavi, R. S.; Kim, H.; Lee, K. M.; Kim, T.; Lee, J.; Lee, Y. S.; Lee, M. H. *Organometallics.* **2012**, *31*, 31.

(28) Che, W.; Li, G.; Zhang, J.; Geng, Y.; Xie, Z.; Zhu, D.; Su, Z. *J. Photochem. Photobiol. A.* **2018**, *358*, 274.

(29) Kwon, J. E.; Park, S. Y. *Adv. Mater.* **2011**, *23*, 3615.

(30) Chou, P.; McMorrow, D.; Aartsma, T. J.; Kasha, M. *J. Phys. Chem.* **1984**, *88*, 4596.

(31) Suzuki, N.; Fukazawa, A.; Nagura, K.; Saito, S.; Kitoh-Nishioka, H.; Yokogawa, D.; Irle, S.; Yamaguchi, S. *Angew. Chem., Int. Ed.* **2014**, *53*, 8231.

(32) Zhao, J.; Ji, S.; Chen, Y.; Guo, H.; Yang, P. *Phys. Chem. Chem. Phys*. **2012**, *14*, 8803.

(33) Suzuki, N.; Suda, K.; Yokogawa, D.; Kitoh-Nishioka, H.; Irle, S.; Ando, A.; Abegão, L. M. G.; Kamada, K.; Fukazawa, A.; Yamaguchi, S. *Chem. Sci.* **2018**, *9*, 2666.

(34) Sedgwick, A. C.; Wu, L.; Han, H.-H.; Bull, S. D.; He, X.-P.; James, T. D.; Sessler, J. L.; Tang, B. Z.; Tian, H.; Yoon, J. *Chem. Soc. Rev.* **2018**, *47*, 8842.

(35) Kwon, J. E.; Park, S.; Park, S. Y. *J. Am. Chem. Soc.* **2013**, *135*, 11239.

(36) Kim, C. H.; Park, J.; Seo, J.; Park, S. Y.; Joo, T. *J. Phys. Chem. A.* **2010**, *114*, 5618.

(37) Lim, S.-J.; Seo, J.; Park, S. Y. *J. Am. Chem. Soc.* **2006**, *128*, 14542.

(38) Kim, S.; Chang, D. W.; Park, S. Y.; Kawai, H.; Nagamura, T. *Macromolecules.* **2002**, *35*, 2748.

(39) Chu, Q.; Medvetz, D. A.; Pang, Y. *Chem. Mater.* **2007**, *19*, 6421.

(40) Singh, N.; Kaur, N.; Mulrooney, R. C.; Callan, J. F. *Tetrahedron Lett.* **2008**, *49*, 6690.

(41) Kim, T.-I.; Kang, H. J.; Han, G.; Chung, S. J.; Kim, Y. *Chem. Commun*. **2009**, 5895.

(42) Xu, Y.; Pang, Y. *Chem. Commun.* **2010**, *46*, 4070.

(43) Xu, Z.; Xu, L.; Zhou, J.; Xu, Y.; Zhu, W.; Qian, X. *Chem. Commun.* **2012**, *48*, 10871

(44) Satapathy, R.; Wu, Y.-H.; Lin, H.-C. *Org. Lett.* **2012**, *14*, 2564.

(45) Salinas-Castillo, A.; Camprubí-Robles, M.; Mallavia, R. *Chem. Commun.* **2010**, *46*, 1263.

(46) Toba, M.; Nakashima, T.; Kawai, T. *Macromolecules.* **2009**, *42*, 8068.

(47) Bao, Y.; Wang, H.; Li, Q.; Liu, B.; Li, Q.; Bai, W.; Jin, B.; Bai, R. *Macromolecules.* **2012**, *45*, 3394.

(48) Wang, F.; Ren, F.; Ma, D.; Mu, P.; Wei, H.; Xiao, C.; Zhu, Z.; Sun, H.; Liang, W.; Chen, J.; Chen, L.; Li, A. *J. Mater. Chem. A.* **2018**, *6*, 266.

(49) Kumar B, S.; Sana, B.; Unnikrishnan, G.; Jana, T.; Kumar K. S, S. *Polym. Chem.* **2020**, *11*, 1043.

(50) Neophytou, M.; Ioannidou, H. A.; Ioannou, T. A.; Chochos, C. L.; Economopoulos, S. P.; Koutentis, P. A.; Itskos, G.; Choulis, S. A. *Polym. Chem.* **2012**, *3*, 2236.

(51) Overberger, C. G.; Vorchheimer, N. *J. Am. Chem. Soc.* **1963**, *85*, 951.

(52) Zeng, Q.; Cai, P.; Li, Z.; Qin, J.; Tang, B. Z. *Chem. Commun.* **2008**, 1094.

(53) Dong, S.; Ou, D.; Qin, J.; Li, Z. *J. Polym. Sci., Part A: Polym. Chem.* **2011**, *49*, 3314.

(54) Chen, X.; Kang, S.; Kim, M. J.; Kim, J.; Kim, Y. S.; Kim, H.; Chi, B.; Kim, S.-J.; Lee, J. Y.; Yoon, J. *Angew. Chem. Int. Ed.* **2010**, *49*, 1422.

(55) Pu, H.; Qin, Y.; Wan, D.; Yang, Z. *Macromolecules.* **2009**, *42*, 3000.

(56) Yang, C.; Xu, J.; Ma, J.; Zhu, D.; Zhang, Y.; Liang, L.; Lu, M. *Polym. Chem.* **2012**, *3*, 2640.

(57) Kirk, K. L. *Biochemistry of the Elemental Halogens and Inorganic Halides*, Plenum Press, New York, **1991**.

(58) Kleerekoper, M. *Endocrinol. Metabol. Clin*, **1998**, *27*, 441.

(59) Zhou, Y.; Zhang, J. F.; Yoon, J. *Chem. Rev.* **2014**, *114*, 5511.

(60) Wade, C. R.; Broomsgrove, A. E. J.; Aldridge, S.; Gabbaï, F. P. *Chem. Rev.* **2010**, 110, 3958.

(61) Yamaguchi, S.; Akiyama, S.; Tamao, K. *J. Am. Chem. Soc.* **2001**, *123*, 11372.

(62) Dhanunjayarao, K.; Mukundam, V.; Venkatasubbaiah, K. *J. Mater. Chem. C.* **2014**, *2*, 8599.

(63) Kim, T.-H.; Swager, T. M. *Angew. Chem. Int. Ed.* **2003**, *42*, 4803.

(64) Cheng, F.; Bonder, E. M.; Jäkle, F. *J. Am. Chem. Soc.* **2013**, *135*, 17286.

(65) Park, S.; Kwon, O.-H.; Kim, S.; Park, S.; Choi, M.-G.; Cha, M.; Park, S. Y.; Jang, D.-J. *J. Am. Chem. Soc.* **2005**, *127*, 10070.

(66) Dhanunjayarao, K.; Mukundam, V.; Venkatasubbaiah, K. *Sens. Actuators, B.* **2016**, *232*, 175.

(67) The purity of the monomer was further confirmed using HPLC. The HPLC data reveal that the monomer is extremely pure (Fig. S20).

CHAPTER 4B

Synthesis and characterization of tetraaryl substituted imidazole based boron polymer

4B.1 Introduction

Tri- and tetra-coordinated boron fluorophores have been explored for their implementation in various fields such as light-emitting diodes (LEDs), non-linear optics (NLOs), sensing such as anions fluoride and cyanide etc[1-16]. Complexation of boron with organic fluorophores results in new hybrid materials with different electronic and photophysical properties. The respective boron containing polymers widely found applications in variety of fields. Recently, Jackle and co-workers have reported polymeric analogous of boron-quinolates complexes by the reaction of 8-hydroxy quinoline with thienyl substituted boron polymers.[5, 17-20] A similar boron-quinolate containing block co-polymer system with green emission was latter reported by Weck and co-workers[21]. Here we report, boron embedded poly(Tetra phenyl imidazole) through N,O-chelation.

4B.2 Results and discussion

4B.2.1 Synthesis and characterization

The starting imidazole, compound **1a** and monomer **1** were synthesized as described in the previous chapter [22]. In order to get polymer $\mathbf{P_1}$, traditional polymerization conditions were employed on monomer **1** using 2,2'-azobis(isobutyronitrile (AIBN) as an initiator. The obtained polymer was purified by precipitate of dichloromethane solution of polymer in *n*-hexane. The borylated polymer $\mathbf{P_1BPh_2}$ was synthesized by reacting $\mathbf{BPh_3}$ in THF. All the newly synthesized compounds were characterized by various techniques.

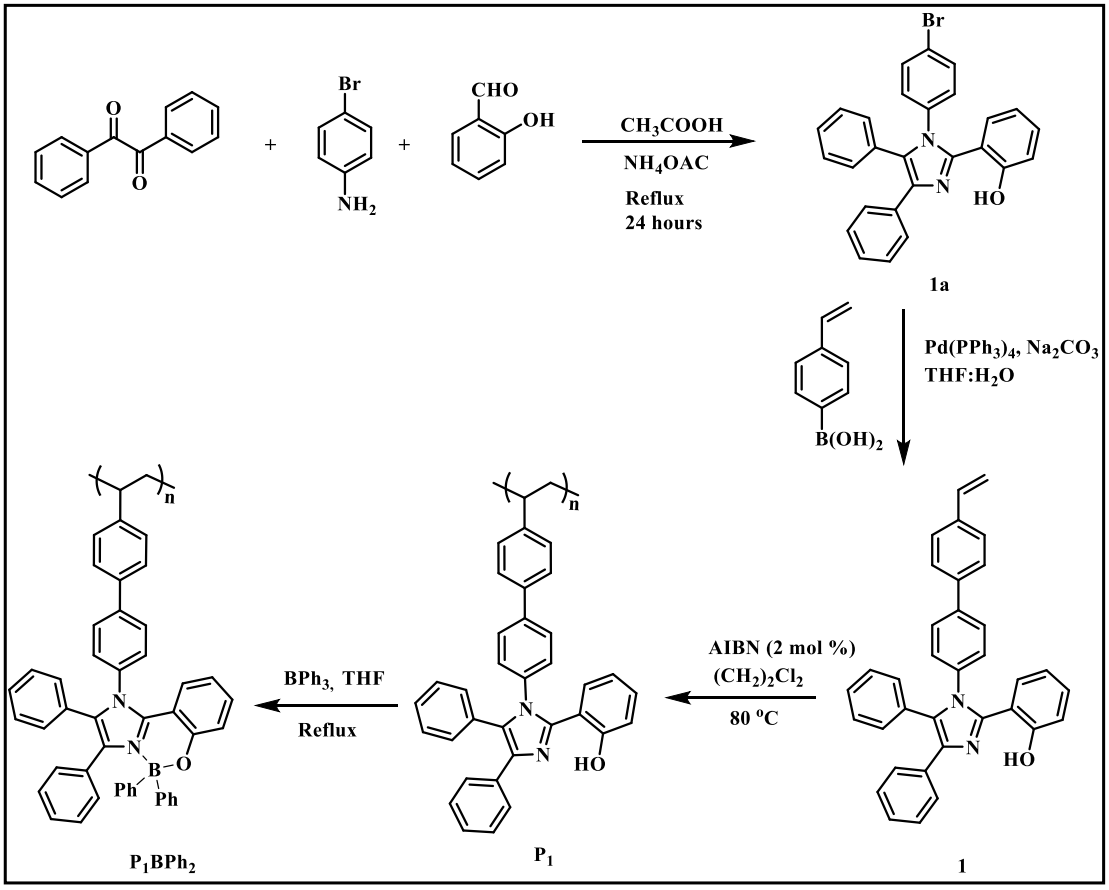

Scheme 4B.1: Synthetic route to the borylated homo polymer.

The following observations are found from ^{1}H NMR spectrum of the polymer **P_1** i) distinct broadening in their peaks and ii) absence of the AMX splitting type of vinyl protons in compound **1** (Figure 4B.1). Formation of monomer, compound **1** was confirmed by HRMS as shown in figure 4B.2. gel permeation chromatography (GPC) analysis reveal the molecular weights of the polymers which were recorded using narrow polystyrene standards in THF. The polymer **P_1** and **P_1BPh_2** exhibited weight-average molecular weight as 52841 and 54586 respectively with polydispersity indices (Đ) of 2.85 and 2.68 respectively and the values are provided in table 4B.1.

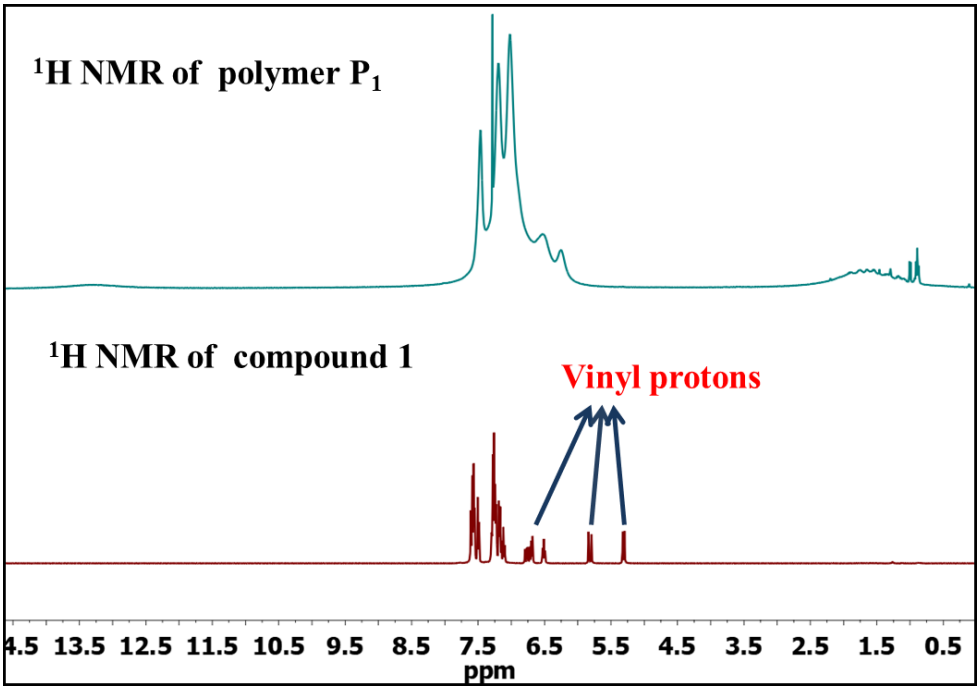

Figure 4B.1: ^{1}H NMR spectrum of compound **1** (top) and polymer **P_1** (bottom) in $CDCl_3$.

Table 4B.1: Molecular weight data for polymer **P_1** & **P_1BPh_2**.

Polymer	***M*$_w$, Da[a]**	***M*$_n$, Da[a]**	**PDI[a]**
P_1	52841	18519	2.85
P_1BPh_2	54586	20326	2.68
[a] GPC-RI in THF *vs* polystyrene standards, PDI-polydispersity index (PDI = M_w/M_n)			

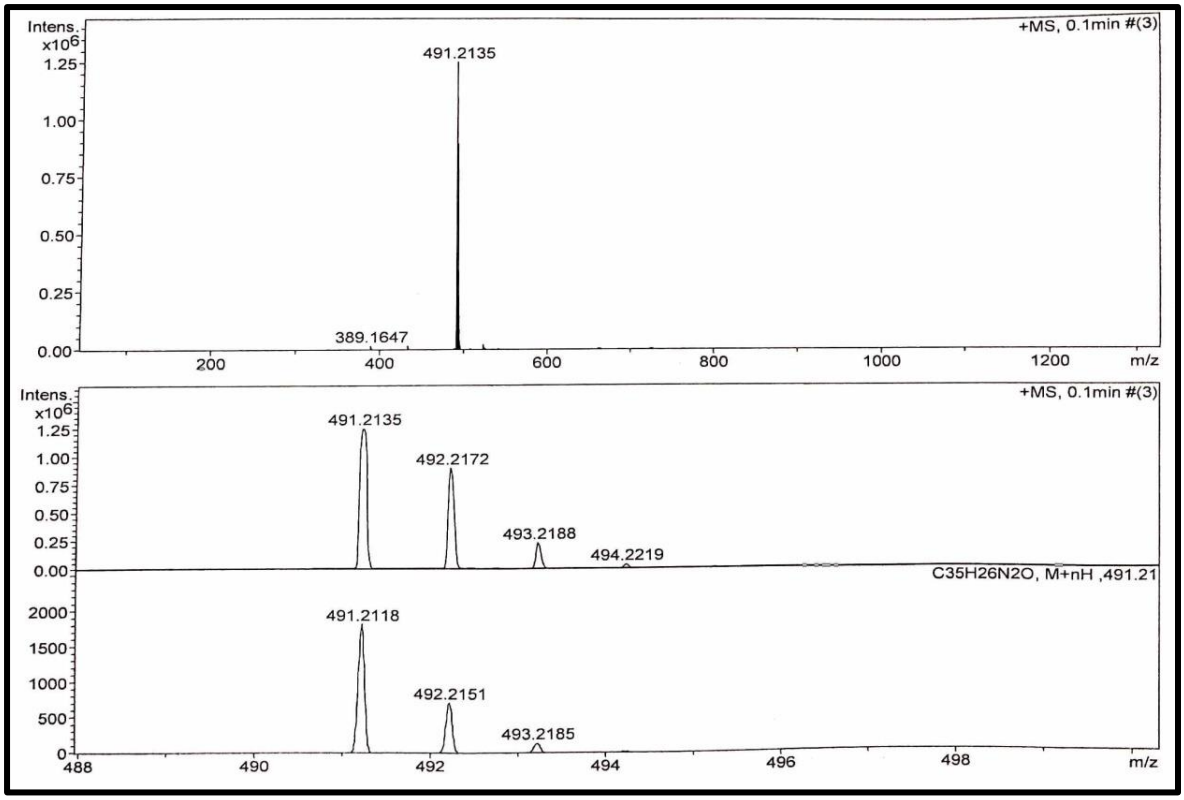

Figure 4B.2: HRMS spectrum of compound **1**.

4B.2.2 Photophysical studies

The photophysical data of the synthesized polymersare summarized in table 4B.2. Both the polymers contain two absorption bands in the absorption spectra in THF solution. The absorption bands of borylated polymer **P_1BPh_2** is red shifted [329 nm ($10830M^{-1}cm^{-1}$) and 283 nm ($30620M^{-1}cm^{-1}$)] compared to polymer **P_1** (321 nm ($16777M^{-1}cm^{-1}$) and 275 nm ($40463M^{-1}cm^{-1}$)). The fluorescence spectra of boron chelated polymer **P_1BPh_2** (λ^{em}_{max}= 421 nm) exhibited deep blue emission in comparison to ligand polymer **P_1** (λ^{em}_{max}= 483 nm). Normalized absorption and emission spectra of the synthesized ESIPT polymer and boron compound in tetrahydrofuran is presented in figure 4B.3 and the fluorescence images under hand held UV-visible lamp at 365 nm are shown in figure 4B.4.

Table 4B.2: Photophysical data for imidazole polymer and its boron complex.

Compound	Solvent	λ_{max}[a] (nm)	ε_{max} ($M^{-1}cm^{-1}$ X 10^3)	λ_{em}[a,b] (nm)	Φ_F[c] (%)	Stokes shift nm (cm^{-1})
P_1	THF	275, 321	40.46, 16.77	485	7	164 (10534)
P_1BPh_2		285, 329	30.62, 10.83	421	17	92 (6642)

[a]Absorption maximum (Concentration: 2 x 10^{-5} M). [b]Excited at the longer wavelength absorption maximum. [c]Quantum yield were measured by using quinine sulphate as reference in 1N H_2SO_4.

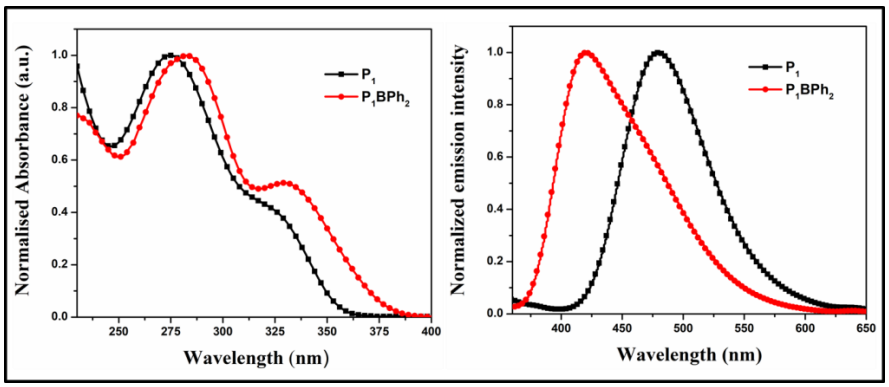

Figure 4B.3 Normalized absorbance (Left) and fluorescence (right) spectra of the ligand polymer and borylated polymer at a concentration of 20 µM in tetrahydrofuran solution.

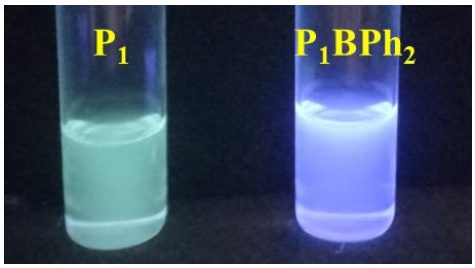

Figure 4B.4: Fluorescence images of poly boron compound and their poly ligand under hand held UV lamp of 365 nm in THF solution.

4B.3 Conclusions

In conclusion, tetraaryl substituted imidazole based ESIPT polymer (**P_1**) and its respective borylated N,O-chelated polymer (**P_1BPh_2**) have been synthesized. The photophysical properties of polymer **P_1** & **P_1BPh_2** have been studied in THF solution. Polymer **P_1BPh_2** exhibited blue fluorescence when excited at the absorption maxima and showed moderate quantum yields.

4B.4 Experimental section

4B.4.1 General Information

Solvents and other general reagents were purified according to standard procedures. Benzil, $Pd(PPh_3)_4$ and 4-bromoaniline were purchased from Sigma Aldrich. Ammonium acetate was purchased from spectrochem. Salicylaldehyde, sodium carbonate, 4-vinylbenzeneboronic acid, aniline, triphenylborane, were purchased from Alfa Aesar. All 400 MHz ^1H spectra were recorded at ambient temperature on a Bruker ARX 400 spectrometer operating at 400 MHz. For all ^1H (400 MHz), ^{13}C (100 MHz) internal reference was used for solvent signals whereas $BF_3{\cdot}OEt_2$was used as external reference in ^{11}B NMR spectra (δ = 0 ppm). ES-MS spectra were collected using with a Bruker microTOF-QII mass spectrometer. The electronic spectra were recorded on JASCO V-730 UV-visible spectrometer. The fluorescence spectra were recorded using SHIMADZU, RF-6000 spectrofluorometer. The fluorescence spectra were corrected for the instrumental response. Gel Permeation Chromatography was done using Shimadzu prominence GPC system.

4B.4.2 Synthetic procedure and spectral characterization:

4B.4.2.1 Synthesis of compound 1a

To 150 mL of glacial acetic acid, a mixture of benzil (6.00 g, 28.52 mmol), 4-bromoaniline (6.38 g, 37.10 mmol), salicylaldehyde (3.49 g, 28.52 mmol) and ammonium acetate (11 g, 142.72 mmol) was added and refluxed for 24 hours. The product formed (as precipitate) was filtered and dried under vacuum. Yield: 8.00 g (60%); ^{1}H NMR (400 MHz, $CDCl_3$):δ = 7.53 (dd, *J* = 8.0, 4.0 Hz, 2H), 7.48 – 7.46 (m, 2H), 7.31 – 7.21 (m, 6H), 7.18 – 7.11 (m, 3H), 7.09 – 7.02 (m, 3H), 6.61 (dd, *J* = 8.0, 2.0 Hz, 1H), 6.55 – 6.51 (m, 1H);^{13}C NMR (101 MHz, $CDCl_3$): δ = 158.55, 146.82, 145.09, 136.21, 135.41, 133.16, 132.60, 131.61,130.78, 130.56,130.43, 129.56, 129.15, 129.06, 128.70, 128.68, 127.67, 127.34, 127.32,126.72, 123.64, 118.54, 118.26, 114.36, 112.80 ppm. HR-MS (ESI): calcd. for $C_{27}H_{19}BrN_2O$ ($[M+H]^+$): 467.0754, found: 467.0718.

4B.4.2.2 Synthesis of compound 1

A mixture of compound **1** (4.40 g, 9.42mmol), 4-vinylbenzene boronic acid (1.67 g, 11.30mmol), sodium carbonate (3.42 g, 32.25mmol) and palladium tetrakistriphenyl phosphine (0.32 g, 0.28mmol) was taken. A mixture of THF and water (THF:H_2O = 4:1) was degassed for 30 minutes and then added to the reaction mixture under nitrogen atmosphere. The reaction mixture was refluxed for 24h. After completion of the reaction, the compound was extracted with water and dichloromethane (3 x 50 mL). The organic phase was collected and dried using Na_2SO_4. The solvent was evaporated using rota vapour and the product was purified using silica gel column (100-200) using *n*-hexane and ethyl acetate (90:10) as eluant. Yield = 3.25 g, (70%); ^{1}H NMR (400 MHz, $CDCl_3$): δ = 7.58 (dd, *J* = 16.0, 8.0 Hz, 6H), 7.50 (d, *J* = 8.0 Hz, 2H), 7.33 – 7.21 (m, 8H), 7.20 – 7.08 (m, 4H), 6.76 (dd, *J* = 20 Hz, 8 Hz 1H), 6.69 (d, *J* = 8 Hz, 1H), 6.51 (t, *J* = 8.0 Hz, 1H), 5.82 (d, *J* = 20 Hz, 1H), 5.31 (d, *J* = 8 Hz, 1H); ^{13}C NMR (101 MHz, $CDCl_3$): δ = 158.75, 145.28, 141.53, 138.90, 137.67,

136.48, 135.61, 133.40, 131.66, 130.79, 130.28, 130.12, 130.12, 129.27, 128.87, 128.82, 128.61, 128.10, 127.44, 127.35, 127.26, 127.11, 126.44, 118.29, 118.03, 114.82, 113.32 ppm. HR-MS (ESI): calcd. for $C_{35}H_{26}N_2O$ ($[M+H]^+$): 491.2118, found: 491.2054.

4B.4.2.3 Synthesis of compound P_1

A sealed tube was charged with compound **2** (2.50 g, 5.10 mmol) and 2,2'-azobis(isobutyronitrile (0.017g, 2mol%) and degassed ethylenedichloride (4 mL) was added under inert conditions. The above reaction mixture was refluxed at 80 °C for 24 h. The mixture was then slowly poured into *n*-hexane and the polymer was obtained as precipitate. The as obtained solid was redissolved in dichloromethane (4 mL) and precipitated again from *n*-hexane. The precipitation process was repeated three times in hexane and followed by once in methanol. Eventually, the white solid polymer $\mathbf{P_1}$ was accomplished by drying under high vacuum. Yield = 2.1 g (84%). ^{1}H NMR (400 MHz, $CDCl_3$): δ = 13.22 (s, 1H), 8.2 – 5.93 (m, 22H), 2.37 – 0.94 (m, 3H); ^{13}C NMR (101 MHz): δ = 158.91, 145.11, 141.70,141.10, 137.13, 136.50, 136.10, 133.74, 133.03, 131.59, 130.43, 130.21, 130.07, 129.35, 128.69, 127.63, 127.40, 126.84, 126.32, 118.26,117.89, 115.84, 113.58, 113.31, 40.83ppm.

M_w= 52841 and M_n= 18519; M_w/ M_n= 2.85.

4B.4.2.4 Synthesis of compound P_1BPh_2

The compound $\mathbf{P_1}$ (0.50 g, 1.00 mmol) and triphenyl borane (0.37 g, 1.50 mmol) were taken in sealed tube. To this dry THF was added under argon atmosphere. As obtained reaction mixture was refluxed for 12 h at 65 ^{o}C followed by cooled to room temperature. When obtained mixture was gently transferred into *n*-hexane upon which

borylated polymer got precipitated. The gained solid was redissolved in methylene dichloride (DCM) (2 mL) and made to precipitate from *n*-hexane and the process is repeated for three cycles in *n*-hexane. The white solid polymer **P_1BPh_2** was collected after drying under high vacuum. Yield = 0.41 g (61%); ^{1}H NMR (400 MHz, DMSO): δ = 8.5 – 5.5 (m, 32H), 2.2 – 1.25 (m, 3H).

M_w= 54586 and M_n= 20326; M_w/ M_n= 2.68.

4B.5 References

(1) Entwistle, C. D.; Marder, T. B. *Chem. Mater.* **2004,** *16*, 4574.

(2) Hudnall, T. W.; Chiu, C.-W.; Gabbaï, F. P. *Acc. Chem. Res.* **2009,** *42*, 388.

(3) Rao, Y.-L.; Amarne, H.; Wang, S. *Coord. Chem. Rev.* **2012,** *256*, 759.

(4) Hudson, Z. M.; Wang, S. *Acc. Chem. Res.* **2009,** *42*, 1584.

(5) Jäkle, F. *Coord. Chem. Rev.* **2006,** *250*, 1107.

(6) Lorbach, A.; Hübner, A.; Wagner, M. *Dalton Trans.* **2012,** *41*, 6048.

(7) Araneda, J. F.; Piers, W. E.; Heyne, B. *Angew. Chem., Int. Ed.* **2011,** *50*, 12214.

(8) Shigehiro, Y.; Atsushi, W. *Pure Appl. Chem.* **2006,** *78*, 1413.

(9) Wade, C. R.; Broomsgrove, A. E. J.; Aldridge, S.; Gabbaï, F. P. *Chem. Rev.* **2010,** *110*, 3958.

(10) Wade, C. R.; Gabbaï, F. P. *Inorg. Chem.* **2010,** *49*, 714.

(11) Tay, A. C. Y.; Frogley, B. J.; Ware, D. C. *Dalton Trans.* **2018,** *47*, 3388.

(12) Shiu, Y.-J.; Cheng, Y.-C.; Tsai, W.-L.; Wu, C.-C.; Chao, C.-T.; Lu, C.-W.; Chi, Y.; Chen, Y.-T.; Liu, S.-H.; Chou, P.-T. *Angew. Chem., Int. Ed.* **2016,** *55*, 3017.

(13) Zhang, Z.; Zhang, Z.; Zhang, H.; Wang, Y. *Dalton Trans.* **2018,** *47*, 127.

(14) Sarkar, S. K.; Kumar, G. R.; Thilagar, P. *Chem. Commun.* **2016,** *52*, 4175.

(15) Kobayashi, H.; Choyke, P. L. *Acc. Chem. Res.* **2011,** *44*, 83.

(16) Kölmel, D. K.; Hörner, A.; Castañeda, J. A.; Ferencz, J. A. P.; Bihlmeier, A.; Nieger, M.; Bräse, S.; Padilha, L. A. *J. Phys. Chem. C.* **2016,** *120*, 4538.

(17) Qin, Y.; Pagba, C.; Piotrowiak, P.; Jäkle, F. *J. Am. Chem. Soc.* **2004,** *126*, 7015.

(18) Qin, Y.; Kiburu, I.; Shah, S.; Jäkle, F. *Macromolecules.* **2006,** *39*, 9041.

(19) Li, H.; Jäkle, F. *Macromolecules.* **2009,** *42*, 3448.

(20) Jäkle, F. *Chem. Rev.* **2010,** *110*, 3985.

(21) Wang, X.-Y.; Weck, M. *Macromolecules.* **2005,** *38*, 7219.

(22) Aradhyula, B. P. R.; Ranga Naidu Chinta, R. V.; Dhanunjayarao, K.; Venkatasubbaiah, K. *RSC Adv.* **2020,** *10*, 13149.

CHAPTER 5

Synthesis of planar chiral cyclomercurated ferrocenyl *p*-tolyl sulfoxide and its conversion to diastereopure 1, 2-substituted ferrocenes

5.1 Introduction

Ferrocene and its derivatives are of great interest in the fields of materials science, catalysis, biomedical research and so on[1-3]. The interest in ferrocene continues to grow owing to its versatility in the synthesis of numerous derivatives, reversible redox properties and thermal stability[4-6]. Since the pioneering work of Ugi's diastereoselective generation of planar chirality[7], hundreds of chiral ligands based on ferrocene have been synthesized and utilized in asymmetric catalysis. Among the different methods available for the synthesis of planar chiral ferrocenes, the stereoselective *ortho*-metallation introduced by different chiral auxiliaries such as oxazolines[8,9], hydrazones[10,11], sulfoxides[12], sulfoximines[13], pyrrolidines[14] and acetals[15,16] have been most widely used (Scheme 5.1).

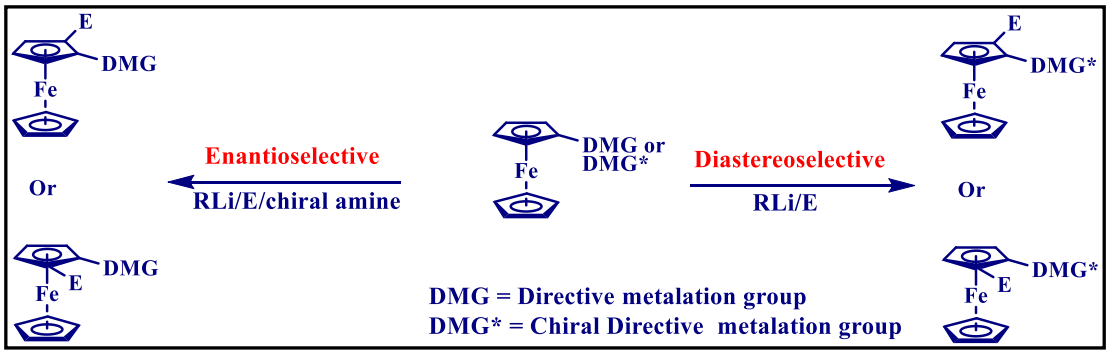

Scheme 5.1: Different approaches to the synthesis of planar chiral ferrocenes.

The sulfoxide methodology introduced by Kagan and co-workers have the advantage to act as (1) an excellent diastereoselective *ortho*-directing group to make planar chiral compounds, (2) the sulfoxide group can be replaced by different substituents to make 1,2-disubstituted compounds and (3) the absolute configuration of the resultant 1,2-substituted ferrocenes are always predictable[12]. However, most of the achiral and chiral 1,2-disubstituted ferrocenes synthesized using this methodology involved

organolithium reagents for the deprotonation of the *ortho*-position of the ferrocenyl ring[16-24]. Here, we report the synthesis of diastereomrically pure (S_p,*S*)-1-(aryl)-2-(*p*-tolylsulfinyl) ferrocenes using direct mercuration of ferrocenyl *p*-tolyl sulfoxide followed by palladium-catalysed cross-coupling of (S_p,*S*)-1-(*p*-tolylsulfinyl)-2-(chloromercurio)ferrocene and aryl iodide.

5.2 Results and discussion

5.2.1 Synthesis and characterization

Following the literature procedure[15] as shown in Scheme 5.2. The ferrocenyl *p*-tolylsulfoxide **(±)2** was synthesized through transmetalation of **1** and 1.1 equivalent of DL-menthyl *p*-tolylsulfinate in 72% yield, using the well-established report by Kagan and co-workers methodology[25].

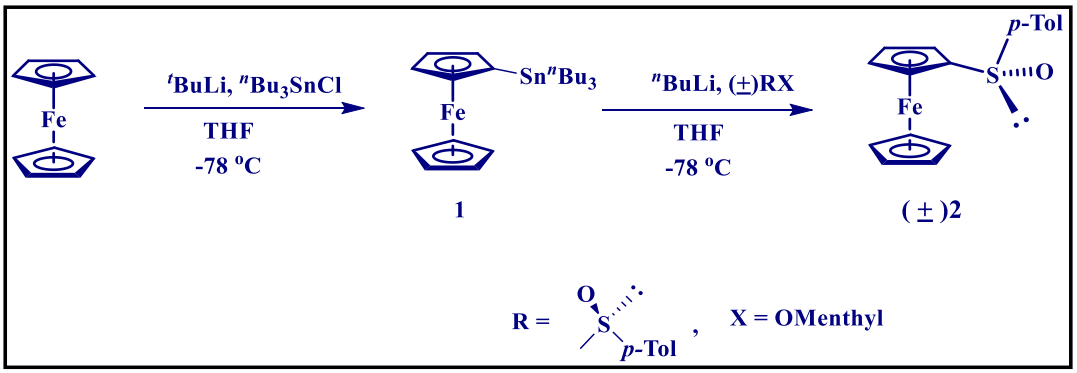

Scheme 5.2: Synthetic route to compound **(±)2**.

Ortho-mercuration of substituted ferrocenes[26] attracts a great deal of interest owing to the fact that they can be used a) to synthesis other organometallic compounds through trasmetallation and b) as reagents in organic synthesis. Although, syntheses of *ortho*-mercury ferrocene using different functionalities like azobenzenes, benzylideneanilines, phenylhydrazenes, *etc*. have been reported[26]; however, to the best of our knowledge, there are no reports on the *ortho*-mercuration of ferrocenyl *p*-

tolyl sulfoxide. *Ortho*mercuration of the sulfinyl ferrocene proceeded smoothly to produce 2-chloromercurated ferrocenylsulfoxide **(±)3** in moderate yield (Scheme 5.3).

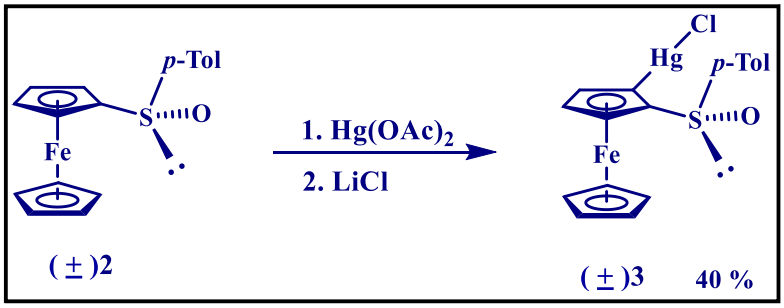

Scheme 5.3: Synthesis of 1-(*p*-tolylsulfinyl)-2-(chloromercurio)ferrocene **(±)3**.

The ^{1}H NMR of compound **(±)3** shows three signals of equal intensity for the substituted Cp ring (δ = 4.81, 4.56, & 4.33 ppm) and one signal for the unsubstituted Cp ring at δ = 4.43 ppm, which is consistent with a 1,2-disubstituted ferrocene (Figure 5.1). The representative mass spectrum of compound **(±)3** is shown in figure 5.2.

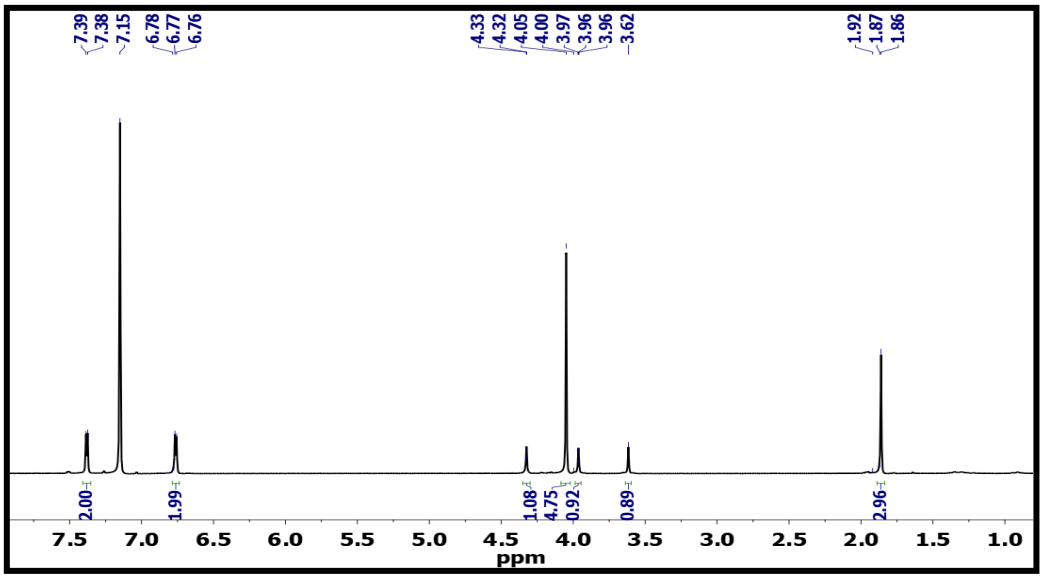

Figure 5.1: ^{1}H NMR spectrum of compound **(±)3** recorded in C_6D_6.

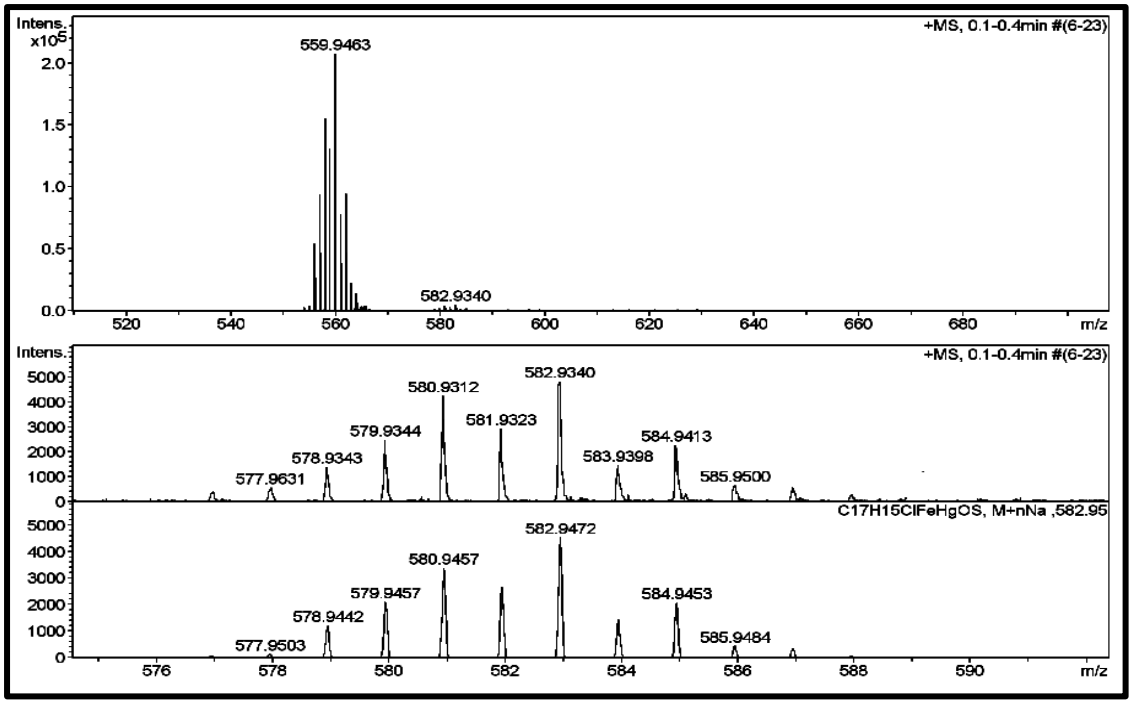

Figure 5.2: HRMS of compound **(±)3.**

5.2.2 Reaction of compound (±)3 to form compound (±)4

It is interesting to note that this step can be performed at room temperature in open air unlike *ortho*-lithiation, which requires low temperature and inert atmosphere**.** Inspired by Beletskaya and co-workers[27] work, we tested cross-coupling of 1-(*p*-tolylsulfinyl)-2-(chloromercurio)ferrocene (**±3**) with 4-iodobenzonitrile as the model substrate. We first studied the reaction using 1.5 eqv. of CuO as an oxidant in the presence of 5 mol % $PdCl_2$(dppf) in anhydrous dimethylformamide (DMF) at 100 °C under argon atmosphere but failed to get the desired product (Table 5.1, entry 1). Various palladium based catalysts, solvents, additives were screened and found that the reaction proceeded smoothly with 2 mol % of $Pd(PPh_3)_4$ (Table 5.1, entry 6) in a mixture of solvents (THF/acetone) at reflux condition. Under optimized reaction conditions the scope of DL-substrates were investigated. To our delight the desired product was obtained with a 90% isolated yield using 2 mol% of catalyst loading.

Table 5.1: Cross-coupling reaction between 4-iodobenzonitrile and compound **±3**[a]

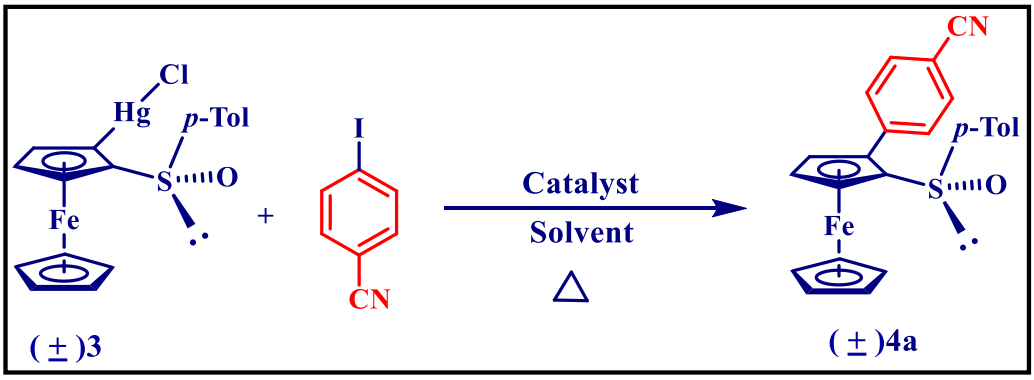

S. No	Catalyst	Cat. Loading (mol %)	Additives (eqv.)	Solvents[b]	Temp. (°C)	Yield (%) [c]
1	$PdCl_2(dppf)$	5	CuO (1.5)	DMF	100	-
2	$Pd(dba)_2$	5	$ZnCl_2$ (1.5)	THF	80	-
3	$Pd(PPh_3)_4$	5	K_2CO_3 (4)	THF	80	-
4	$Pd(PPh_3)_4$	5	NaI (4)	THF/Acetone	80	95
5	$Pd(PPh_3)_4$	5	-	THF/Acetone	80	-
6	$Pd(PPh_3)_4$	2	NaI (4)	THF/Acetone	80	90

[a]Reaction conditions: Compound **(±)3** (0.50 mmol), 4-iodobenzonitrile (1.25 mmol). [b]All reactions were carried out under inert atmosphere. [c]Isolated yield.

As shown in Table 5.2, various substituted aryl iodides bearing electron withdrawing groups were converted to the corresponding products with good to moderate isolated yields. The reaction of 4-iodobromobenzene with compound **±3** resulted in 1-(4-bromophenyl)-2-(*p*-tolylsulfinyl) ferrocene **(±4d)** in 85% yield.

Table 5.2: Cross-coupling reaction between different aryl halides and compound **(±)3.**

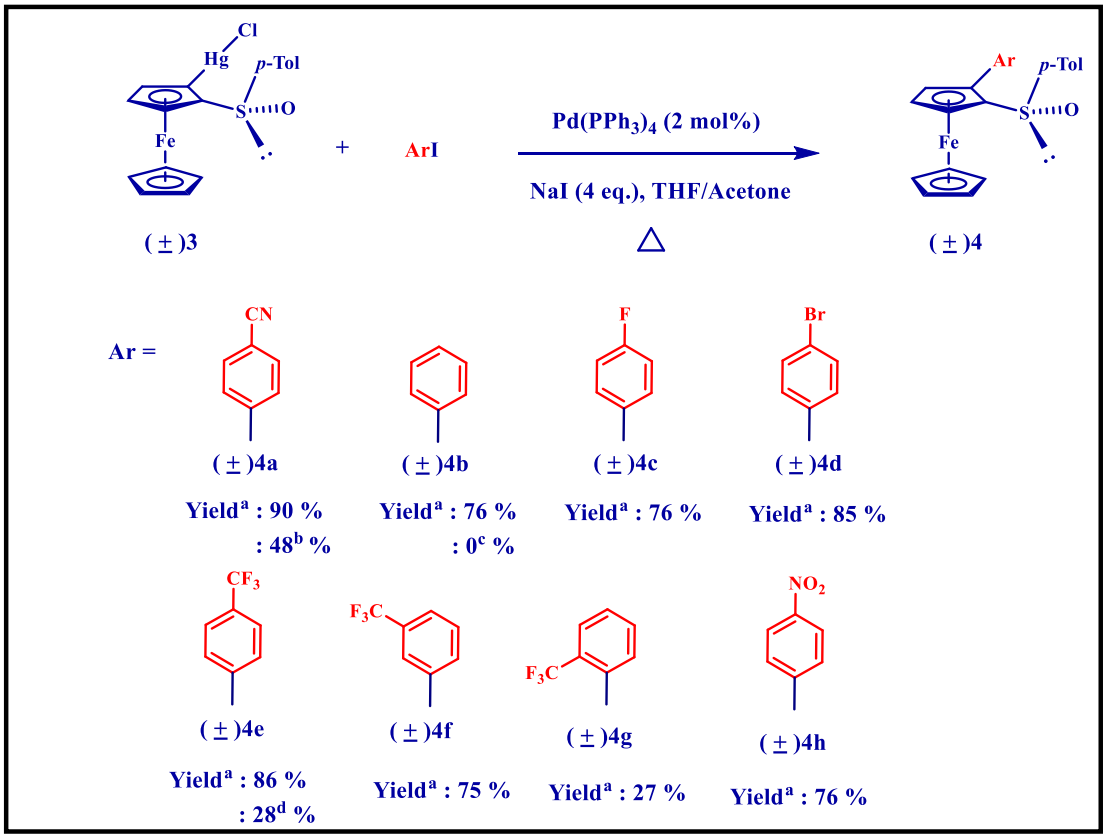

[a]Reaction conditions: Compound **±3** (0.10 mmol), aryl iodides (0.25 mmol), $Pd(PPh_3)_4$ (2 mol %), and NaI (0.40 mmol) in 1 mL dry acetone and 2 mL of dry THF at reflux condition. [b]Isolated yield after flash column chromatography. [c]4-bromobenzonitrile is used. [d]bromobenzene is used. [e]4-bromobenzotrifluoride is used.

o-Iodobenzotrifluorides were converted to the corresponding products (**±4e, ±4f** & **±4g**) with moderate yields. However, the *o*-iodobenzotrifluoride afforded only low yield (27%). Aryl bromides such as 4-bromobenzonitrile and 4-bromobenzotrifluoride got converted to their respective products in 48% and 28% respectively, however bromobenzene was not active enough to give the desired

product under the experimental conditions. Moreover, aryl chlorides failed to afford the respective products under the optimized conditions.

Product **±4a** was further confirmed using single crystal X-ray analysis. The X-ray analysis revealed one molecule is present in the asymmetric unit. The Cp//Cp tilt angles are 0.89° for **±4a**. The angle between cyclopentadienyl (Cp) and the X-phenyl group is 37.68° respectively. The oxygen atom on sulfur (-SO-) points upwards and the tolyl points away from the CN-Phenyl (Figure 5.3). All coupled products (**±4a** - **±4h**) were confirmed using ^{1}H, ^{13}C and HRMS.

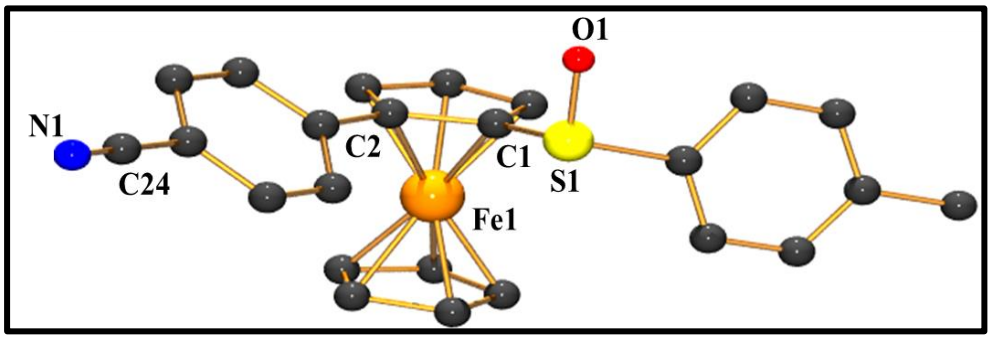

Figure 5.3: Molecular structure of **±4a** (ball and stick). Hydrogen atoms are omitted for clarity. Selected bond lengths (Å) and bond angles (°): C1-S1 1.776(3), S1- O1 1.494(2), C1-C2 1.449(3), C24-N1 1.139(4), C1-S1-O1 105.7(1), C1-S1-C11 106.9(1), C2-C1-S1 123.3(2), N1-C24-C21 177.2(3).

We also synthesized *S*-ferrocenyl-*p*-tolyl sulfoxide **(2)** following similar procedure starting from *S*-menthyl *p*-tolyl sulfonate. As mentioned before the mercuration reaction was performed which resulted in compound **(R_p,*S*)-3**. As this compound decomposed in HPLC column the diastereoselectivity of the same was not measured, however its optical rotation was measured $[\alpha]^{22}_{D}$ = +266 (c = 0.05, $CHCl_3$) using polarimeter.

In order to confirm the absolute configuration of compound **3**, a single crystal X-ray diffraction analysis was carried out. The oxygen (O) atom points towards the mercury (Hg) atom. The distance between O and Hg atom (2.875 (5) Å) is shorter than the sum of the Van der Waals radii (for Hg 1.73-2.00 Å[28]; for O 1.54 Å[29]), thus indicating an interaction between the oxygen and the mercury atom (Figure 5.4). Such type of weak interactions has been reported in the literature[19, 30-32]. We believe that this oxygen mercury interaction is responsible for the diastereoselective *ortho*-mercuration of compound **2** into compound **3** with R_p,*S* -configuration.

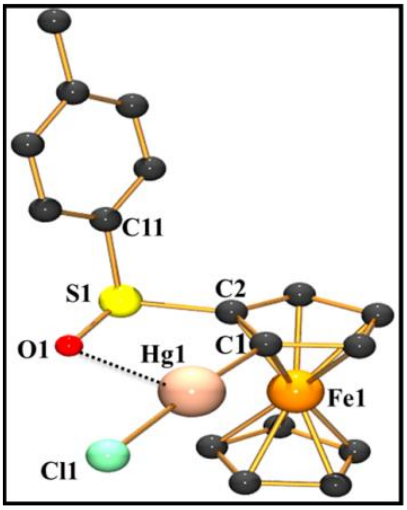

Figure 5.4: Molecular structure of compound **(R_p,*S*)-3** (ball and stick). Hydrogen atoms are omitted for clarity. Selected bond lengths (Å) and bond angles (°): Hg1-C1 2.035(5), Hg1-O1 2.875(5), Hg1-Cl1 2.308(1), S1-O1 1.489(3), C1-Hg1-Cl1 178.9(1).

Using the mercurated compound **3**, as the starting material the scope of substrates were explored with the optimized reaction conditions. As shown in Table 5.3. *p*, *m*, *o*-Iodobenzotrifluorides were converted to the corresponding chiral products **4f**, **4g** & **4h** with good diastereoselectivities (de: 99 for **4f**, 82 for **4g**, & 96 for **4h**).

Table 5.3: Cross-coupling reaction between different aryl iodides and compound **(R_p,*S*)-3**[a].

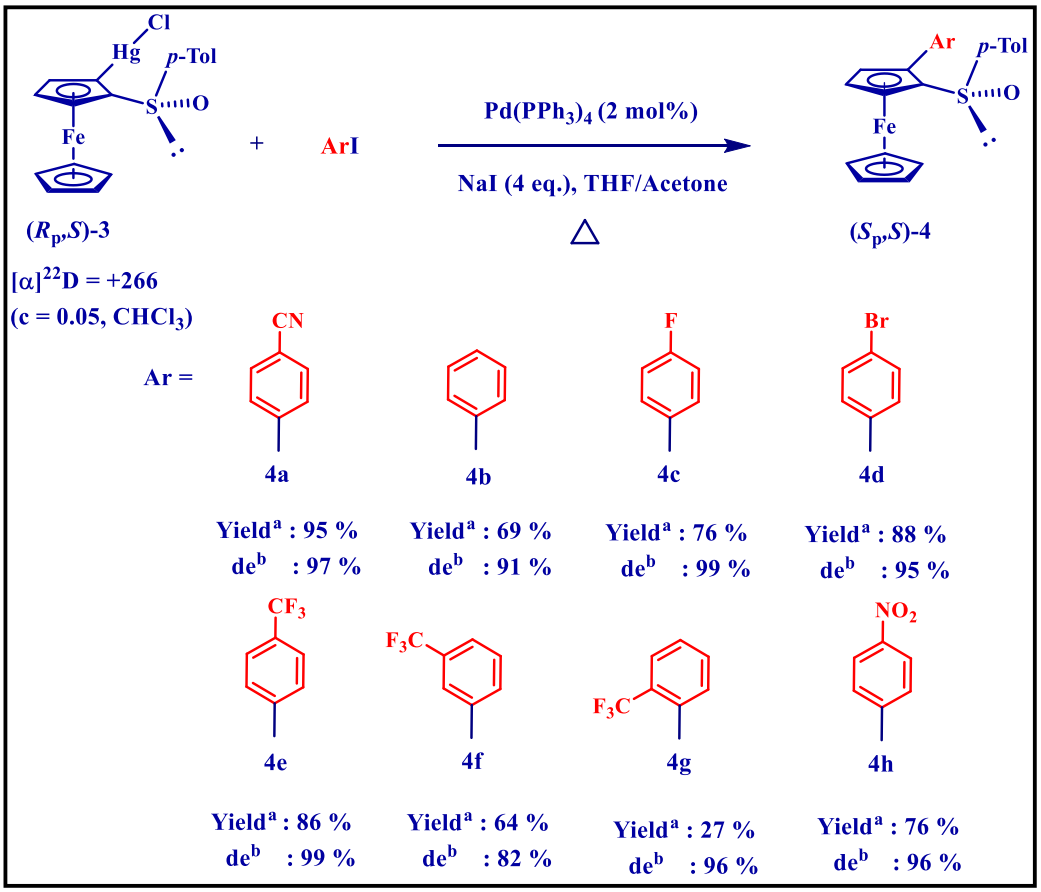

[a]Reaction conditions: Compound **(R_p,*S*)-3** (0.10 mmol), aryl iodides (0.25 mmol), $Pd(PPh_3)_4$ (2 mol %), and NaI (0.40 mmol) in 1 mL dry acetone and 2 mL of dry THF at reflux condition. [b]Isolated yield after flash column chromatography. [c]The (diastereomeric excess) de was determined by HPLC analysis (Column: OD-H, solvent: *n*-hexane /*i*PrOH, flow 1 mL/min.).

However, the *o*- iodobenzotrifluoride afforded only a low yield (27%) with good diastereoselectivity. The HPLC traces of compound **4d,** have been shown in figure 5.5.

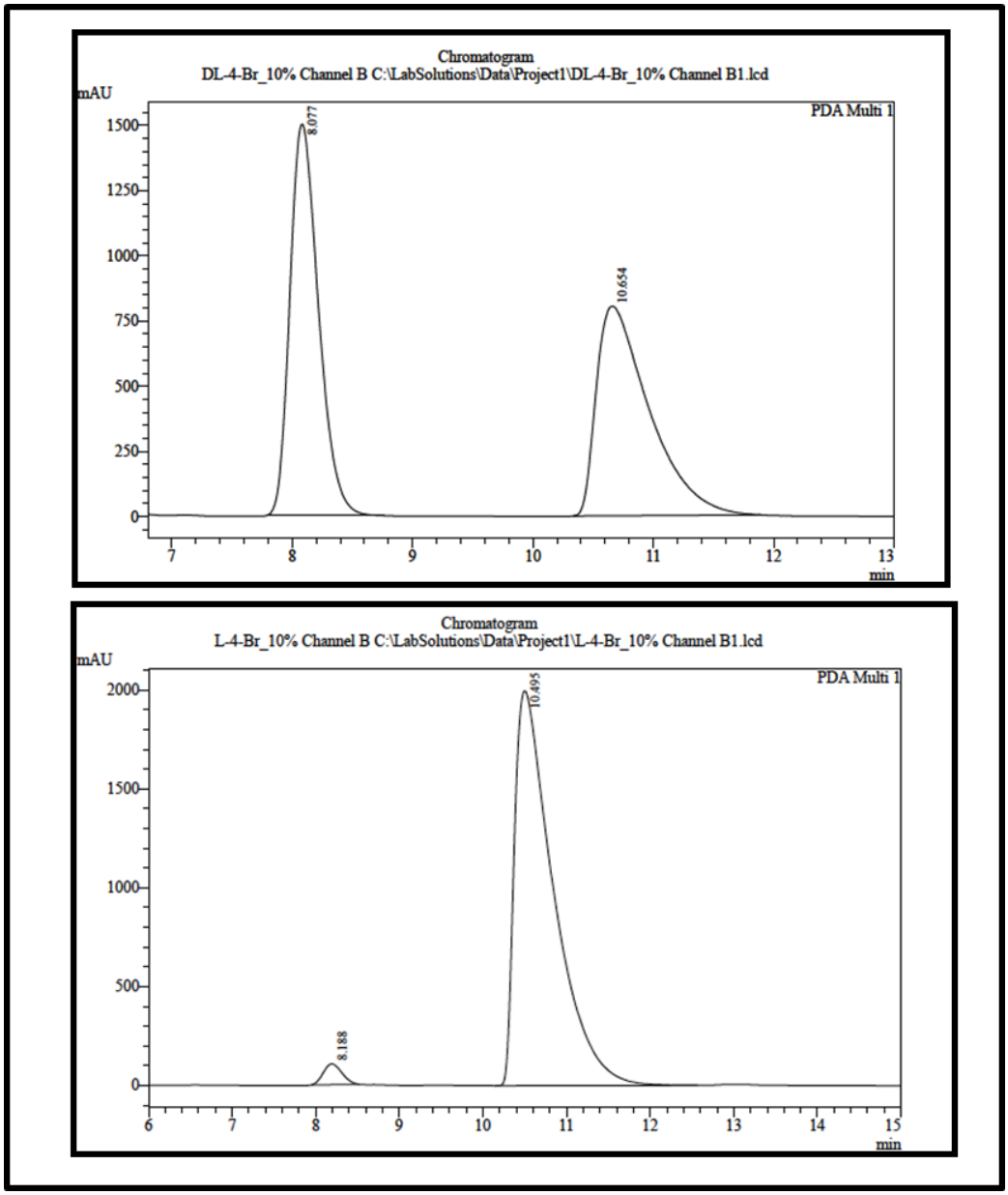

Figure 5.5: HPLC for **±4d** (top) and **(**S_p,*S*)**4d (**bottom) of 1-(4-bromophenyl)-2-(*p*-tolylsulfinyl)ferrocene.

The molecular structure of product **4c** confirmed that the expected S_p,*S* stereochemistry is preserved after the cross-coupling reaction**.** The X-ray analysis revealed one molecule is present in the asymmetric unit. The Cp//Cp tilt angle is 0.69° for **4c**. The angle between (Cp) and X-phenyl group is 47.14°. The oxygen atom on

sulfur (-SO-) points upwards and the tolyl points down to the bottom Cp ring for **4c**. See the angles in figure 5.6.

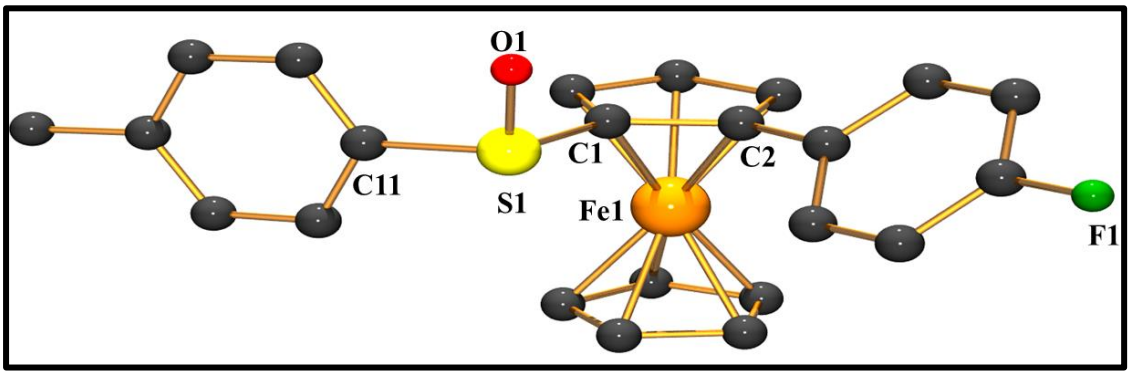

Figure 5.6: Molecular structure of **4c** (ball and stick). Hydrogen atoms are omitted for clarity. Selected bond lengths (Å) and bond angles (°): C1-S1 1.774(25), S1- O1 1.482(24), C1-C2 1.442(35), C1-S1-O1 107.53(13), C11-S1-O1, 107.00(13), C2-C1-S1 123.56(19), Cp//Cp tilt angle is 0.69° and Cp and X-phenyl group angle is 47.14°.

We propose a plausible mechanism based on LC/MS and X-ray analysis and based on the previous literature [27]. As shown in Scheme 5.4, the mechanism for the

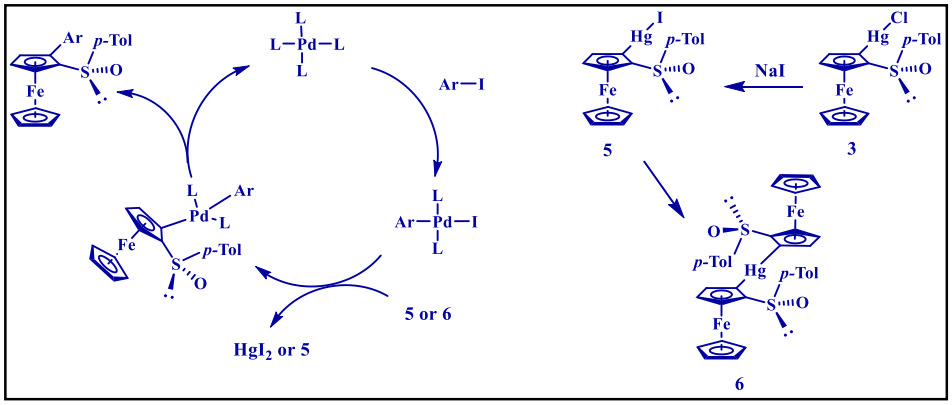

Scheme 5.4: Proposed mechanism for the palladium-catalyzed cross-coupling of compound **3** with aryl halides.

cross- coupling of aryl iodide and 1,2-substituted mercury compound (**3**) is analogous to other organometallic coupling reactions. To examine the species involved during

transformation; we recorded the ESI of the reaction mixture of one of the reactions and found fragment ion of m/z = 651.9037 and m/z = 848.0237 which corresponds to compound **5** and **6** respectively (See figure 5.7).

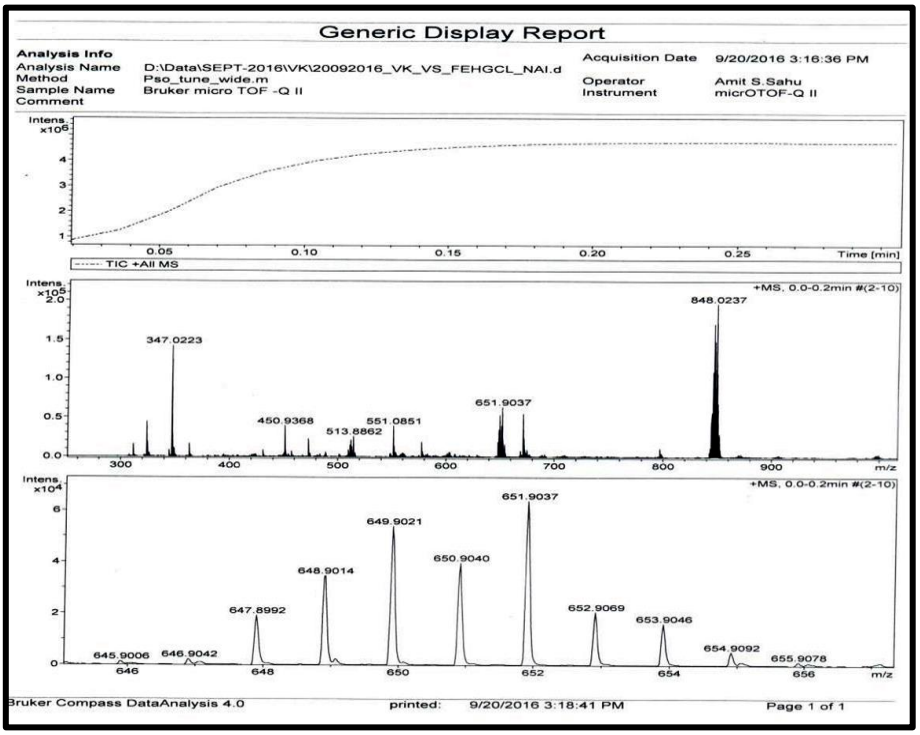

Figure 5.7: ESI-Mass of compound **5.**

We have found the formation of symmetrized (Fc-SO-tolyl))$_2$Hg (**6**) as a side product under our optimized reaction conditions without the use of aryl iodide and palladium catalyst. It has been reported in literature[33] that the treatment of chloro mercury organic compounds in the presence of sodium iodide results in symmetrization or dimerization or cyclization depending on the starting materials. To know the role of compound **6**, a control experiment was carried out using compound **6** as the substrate and 4-fluorophenyl iodide as the arylating agent. We found a higher yield of product **4c** under similar conditions discussed *vide supra*. We were lucky enough to have the crystal structure of **6** also. As shown in figure 5.8, two (tolyl sulfoxide)ferrocenyl moieties are linked through a mercury atom. The Hg1-C1 (2.051

(6) Å) and Hg1-C18 (2.056(6) Å) bond lengths are comparable to those found in related organomercury compounds.[19, 30, 31]

Table 5.4: Crystal data and structure refinement parameters for compounds **3, 4a** and **4c.**

Crystal parameters	**3**	**4a**	**4c**
Empirical formula	$C_{17}H_{15}ClFeHgOS$	$C_{24}H_{19}FeNOS$	$C_{23}H_{19}FFeOS$
Formula weight	559.24	425.31	418.29
Wavelength, Å	0.71073 Å	0.71073 Å	0.71073 Å
Temperature/K	296	296	296
Crystal system	Monoclinic	Triclinic	Orthorhombic
Space group	*C*2/c	$P\bar{1}$	*P*212121
a [*Å*]	28.4638(6)	8.8248(4)	8.0903(3)
b [*Å*]	7.7315(2)	9.2364(4)	14.5388(6)
c [*Å*]	18.9428(5)	11.9724(5)	16.1475(6)
α[°]	90	97.062(3)	90
β[°]	126.330(3)	92.011(3)	90
δ[°]	90	93.221(3)	90
Volume/$Å^3$	3358.38(9)	966.06(7)	1899.32 (13)
Z	8	2	4
ρ_{calc}[g cm^{-3}]	2.212	1.462	1.463
μ (MoKα) [mm^{-1}]	10.276	0.903	0.923
F (000)	2112.0	440.0	864.0
Crystal size [mm]	0.25 × 0.24 × 0.2	0.2 × 0.18 × 0.17	0.25 × 0.16 ×0.14
θ range for data collection/°	2.669-28.25	1.715-28.833	2.523–27.907
Limiting indices	-37 ≤ h ≤ 37 -10 ≤ k ≤ 8 -25 ≤ l ≤ 24	-11 ≤ h ≤ 11 -12 ≤ k ≤ 12 -16 ≤ l ≤ 16	-9 ≤ h ≤ 10 -19 ≤ k ≤ 19 -21 ≤ l ≤ 21
Reflns. Collected	23199	16973	15611

Independent reflns	4160 [*R*int = 0.0561]	5003 [*R*int = 0.0521]	4478 [*R*int = 0.0268]
Data/restraints/parameters	4160/0/201	5003/0/254	4478/0/246
Goodness-of-fit on F^2	1.026	1.042	1.017
Final R indexes [I>=2σ (I)]	*R1* = 0.0319, *wR2* = 0.0755	*R1* = 0.0460, *wR2* = 0.1005	*R1* = 0.0284, *wR2* = 0.0641
R indexes [all data]	*R1* = 0.0441, *wR2* = 0.0813	*R1* = 0.0632, *wR2* = 0.1073	*R1* = 0.0373, *wR2* = 0.0680
Largest diff. peak /hole [e $Å^{-3}$]	2.06/-1.88	0.65/-0.38	0.18/-0.22

The molecular structure of compound **6** also shows the coordination to one of the oxygen atoms with mercury atom. The Hg1…O1 (2.824(4) Å) bond length is shorter than the sum of the Van der Waals radii of Hg and O, whereas the Hg1…C18 bond length (3.374(6) Å) shows a very weak interaction between O and Hg. The $Cp_{centroid}$-Hg-C angles of 176.5° and 177.7° indicates almost linear coordination geometry at Hg, however C1-Hg1-C18 angle of 173.6° reveals a slight tilting toward O1 atom associated with binding of the –SO ligand.

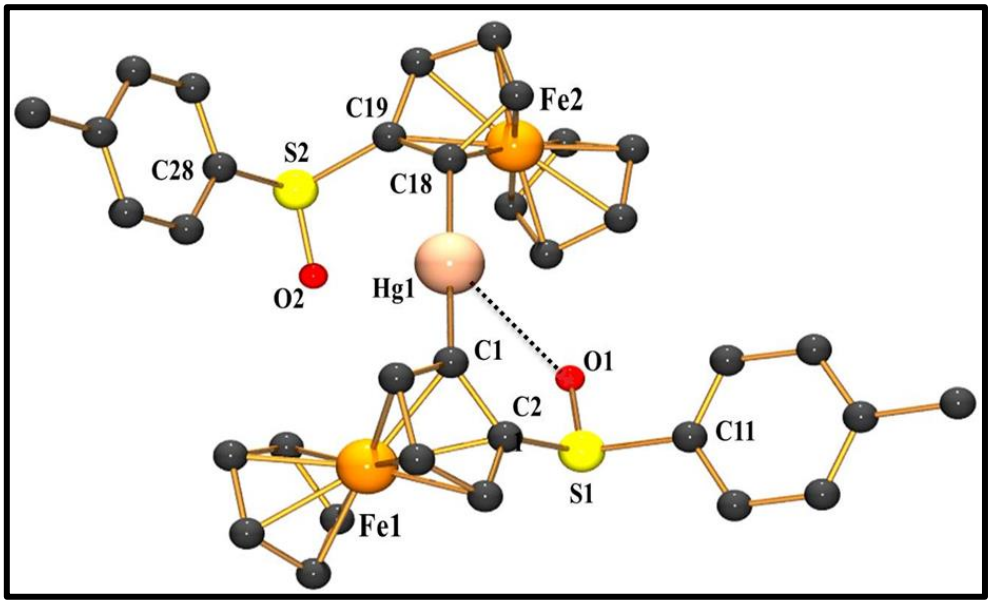

Figure 5.8: Molecular structure of **6** (ball and stick). Hydrogen atoms are omitted for clarity. Selected bond lengths (Å) and bond angles (°): Hg1-C1 2.051(6), Hg1-C18 2.056(6), S1-O1 1.493(5), S2-O2 1.478(5), C1-Hg1-C18 173.7(2), $Cp_{centroid}$-Hg-C1 176.5, $Cp_{centroid}$-Hg-C18 177.7.

Table 5.5: Crystal data and structure refinement parameters for compound **6**

Compound	**6**
Empirical formula	$C_{34}H_{30}Fe_2HgO_2S_2$
Formula weight	846.99
Wavelength, Å	0.71073 Å
Temperature/K	296
Crystal system	Monoclinic
Space group	$P2_1/n$
a/Å	10.8322(2)
b/Å	12.7489(3)
c/Å	10.9538(3)
α[°]	90
β[°]	92.464(2)
γ[°]	90
Volume/Å^3	1511.31(7)
Z	2
ρ_{calcd}/g cm^{-3}	1.861
μ(MoK$_\alpha$) /mm^{-1}	6.183
F(000)	828.0
θ range for data collection/°	1.861-28.313
Index ranges	$-14 \leq h \leq 14$, $-16 \leq k \leq 17$, $-14 \leq l \leq 14$
Reflns. Collected	27868
Independent reflns	6730[R_{int}= 0.0482]
Data/restraints/ Parameters	6730/1/372
Goodness-of-fit on F^2	0.892
Final R indices [$I > 2\sigma(I)$]	*R1* = 0.0288, *wR2* = 0.0491

R indices (all data)	*R1* = 0.0367, *wR2* = 0.0513
Largest diff. peak /hole [e $Å^{-3}$]	0.68/-0.42

5.3 Conclusions

In summary, we have developed a new methodology for the synthesis of planar chiral ferrocenes from ferrocenyl *p*-tolyl sulfoxide. This protocol furnished excellent levels of diastereoselectivity with moderate to good yield. We have also shown that sulfoxide moiety (FcSO) acts as a versatile functional group to direct mercury to form (R_p,*S*)-1-(*p*-tolylsulfinyl)- 2-(chloromercurio)ferrocene (**3**) as an isolable air and moisture stable compound. Unlike *ortho*-lithiation, the mercuration does not require low temperature.

5.4 Experimental section

5.4.1. General Information

All chemicals were used as received from commercially available sources. DL-menthol, ferrocene, *t*-Bu_3SnCl were procured from Sigma-Aldrich. All solvents were purified and dried according to standard procedures. Ferrocenyl *p*-tolyl sulfoxide was prepared according to literature procedure using menthyl-*p*-toluenesulfinate prepared from DL-menthol [16, 17]. NMR spectra were recorded on Bruker 700 and ARX 400 spectrometers at room temperature. ^1H (700 MHz), ^{13}C (176 MHz), ^1H (400 MHz) and ^{13}C (100 MHz) NMR chemical shifts in ppm were referenced internally to its proton resonance of incomplete deuterated solvent signals. In case of compounds **±3**, **±4c**, **±4d** & **±4h** the splitting for Cp protons were not observed due to the fluxional behavior of the sulfoxide. HPLC analyses were performed on a Shimadzu-LC20AD system using Daicel chiralpak OD-H or Daicel chiralpak AD-H columns.

Optical rotation was obtained with a Rudolph, Autopl-IV polarimeter. Electrospray ionization (ESI) mass spectra were recorded on a Bruker microTOF QII spectrometer. Single crystal X-ray diffraction data were collected on a Bruker APEX-II diffractometer. The data were collected at 296 K using, Mo-K_α radiation (0.71073 Å). Crystallographic data for **3, ±4a, 4c** & **6** and details of X-ray diffraction experiments and crystal structure refinements are given in Table 5.4 and 5.5. Using Olex2, the structures were solved with the ShelXS structure solution program using Direct Methods and refined with the ShelXL refinement package using Least Squares minimization. All nonhydrogen atoms were refined with anisotropic displacement coefficients. The H atoms were placed at calculated positions and were refined as riding atoms.

5.4.2 Synthetic procedure and spectral characterization

5.4.2.1 Synthesis of 1-(*p*-tolylsulfinyl)-2-(chloromercurio)ferrocene (±)3

Ferrocenyl *p*-tolyl sulfoxide **(±)2** (0.320 g, 1.0 mmol) was dissolved in 5 mL of dichloromethane in100 mL, two necked round bottom flask fitted with a magnetic stirrerand an equilibrated addition funnel. $Hg(OAc)_2$ (0.320 g, 1.0mmol) was dissolved in a sufficient amount of MeOH. This solutionwas added dropwise to compound **1**, over a period of 25 minutes intheopen air. Then, 0.080 g of LiCl (2.0 mmol) dissolved in MeOH, hasbeen added through addition flask over 20 minutes and the stirring was continued for 24 hours. Finally the solvents were evaporated under reduced pressure and the resulting crude mixture was dissolved in dichloromethane (10 mL), filtered through frit to remove the insoluble salts. The solution was transferred into separating funnel, and then 50 mL of water was added. The organic layer was separated and the process was repeated twice. The collected organic

fractions were dried over Na_2SO_4. The resulting solution was evaporated *in vacuo* and subjected to a flash column chromatography on silica gel, eluted with *n*-hexane/ethylacetate (4:1 ratio). The first band was collected and afforded the title compound **(±)3** in 40% yield (0.22 g, 0.4 mmol). The crude yellow solid was recrystallized from dichloromethane and *n*-hexane 1:0.2 ratio to afford the corresponding compound **(±)3** as a reddish-yellow crystals, mp = 159-160 °C; ^{1}H NMR (700 MHz, Benzene-d_6): δ = 7.38 (d, *J* = 7.9 Hz, 2H, ArH), 6.76 (d, *J* = 7.9 Hz, 2H, ArH), 4.32 (s, 1H, Cp), 4.05 (s, 5H, Cp), 3.96 (s, 1H, Cp), 3.62 (s, 1H, Cp), 1.86 (s, 3H, CH_3); ^{13}C NMR (176 MHz, Benzene-d_6): δ = 144.9, 141.1, 130.3, 123.9, 99.6 (Cp), 76.6 (Cp), 75.1 (Cp), 73.0 (Cp), 70.8 (Cp), 69.0 (Cp), 21.2(CH_3) ppm; HR-MS (ESI): calcd. for $C_{17}H_{15}ClFeHgSO$([M]$^+$): 559.9656, found: 559.9628.

5.4.2.2 (*R*$_p$,*S*)-1-(*p*-tolylsulfinyl)-2-(chloromercurio)ferrocene 3

(*S*)-ferrocenyl *p*-tolyl sulfoxide **2** (0.320 g, 1.0 mmol), $Hg(OAc)_2$ (0.320 g, 1.0mmol), LiCl (0.080 g, 2.0 mmol) dissolved in MeOH, has been added through addition flask over 20 minutes and the stirring was continued for 24 hours. Compound is reddish-yellow crystals with 40% yield (0.22 g, 0.4 mmol). $[\alpha]^{22}_D$ = +266 (c = 0.05, $CHCl_3$).

General procedure for Cross-coupling reaction between 1-(*p*-tolylsulfinyl)-2 (chloromercurio)ferrocene (±)3 and aryl iodides catalyzed by Pd(0

In a Schlenk tube 0.5 mmol of compound **(±)3**, 1.25 mmol of ArI, 2.0 mmol of NaI and $Pd(PPh_3)_4$ (2 mol %) wereplaced. Subsequently 3 mL of dry THF and 2 mL of dry acetone were added and the reaction mixture was refluxed for the time mentionedin the procedure. After completion of the reaction the resulting product was filtered through a pad of silica, washed with 2x20mL of THF and the resultant filtrate was concentrated. The crude product was purified by flash column chromatography

using *n*-hexane and ethyl acetate as an eluent to afford the desired 1,2-disubstituted ferrocenyl product.

5.4.2.3 1-(4-Cyanophenyl)-2-(*p*-tolylsulfinyl)ferrocene ±4a

The quantities involved are as follows. Compound **(±)3** (0.200 g, 0.36 mmol), 4-iodobenzonitrile (0.204 g, 0.89 mmol), sodium iodide (0.214 g, 1.43 mmol) and $Pd(PPh_3)_4$ (0.012 g, 2.0 mol %). After refluxing for 2 h the title compound was purified by flash column chromatography (*n*-hexane: EtOAc 4:1). Yield = 0.138 g (90%), mp = 189-190 °C. ^{1}H NMR (700 MHz, Benzene-d_6): δ = 7.69 (d, *J* = 7.0 Hz, 2H, ArH), 7.44 (d, *J* = 7.0 Hz, 2H, ArH), 7.01 (d, *J* = 7.0 Hz, 2H, ArH), 6.73 (d, *J* = 7.0 Hz, 2H, ArH), 4.22 (dd, *J* = 2.7, 1.6 Hz, 1H, Cp), 4.15 (dd, *J* = 2.6, 1.6 Hz, 1H, Cp), 4.00 (s, 5H, Cp), 3.95 (t, *J* = 2.6 Hz, 1H, Cp),1.85 (s, 3H, CH_3) ppm; ^{13}C NMR (176 MHz, Benzene-d_6): δ = 142.7, 142.2, 141.1, 132.2, 131.0, 129.9, 125.8, 119.6, 111.4, 95.5 (Cp), 86.6 (Cp), 73.6 (Cp), 72.4 (Cp), 72.3 (Cp), 70.3 (Cp), 21.5 (CH_3) ppm; HR-MS (ESI): calcd. for $C_{23}H_{19}FeNOS$ ($[M+H]^+$): 426.0610, found: 426.0635.

5.4.2.4 Synthesis of 1-(4-cyanophenyl)-2-(*p*-tolylsulfinyl)ferrocene ±4a from 4-bromobenzonitrile

The quantities involved are as follows. Compound **(±)3** (0.150 g, 0.27 mmol), 4-bromobenzonitrile (0.122 g, 0.67 mmol), sodium iodide (0.161 g, 1.07 mmol) and $Pd(PPh_3)_4$ (0.006 g, 2.0 mol %). After refluxing for 2 h the title compound was purified by flash column chromatography (*n*-hexane: EtOAc 4:1). Yield = 0.055 g (48%).

5.4.2.5 (S_p,*S*)-1-(4-Cyanophenyl)-2-(*p*-tolylsulfinyl)ferrocene 4a

The quantities involved are as follows: Compound **3** (0.280 g, 0.5 mmol), 4-iodobenzonitrile (0.290 g, 1.25 mmol), sodium iodide (0.300 g, 2.0 mmol) and $Pd(PPh_3)_4$ (0.012 g, 2.0 mol %). After refluxing for 2 h the title compound was

purified by flash column chromatography (*n*-hexane: EtOAc 4:1). Yield = 0.200 g (95%, de 97%), $[\alpha]^{22}_{D}$ = +362 (c =0.05, $CHCl_3$), mp = 197-198 °C. The diastereomeric excess was determined by Daicel chiralpak OD-H (4.6mm Φ X 250 mmL), *n*-hexane / IPA = 9.2/0.8, 1 mL/min, λ = 254 nm, t (minor) = 12.28 min, t (major) = 18.75 min.

5.4.2.6 1-(Phenyl)-2-(*p*-tolylsulfinyl)ferrocene ±4b

The quantities involved are as follows. Compound **(±)3** (0.200 g, 0.36 mmol), iodobenzene (0.182 g, 0.89 mmol), sodium iodide (0.214 g, 1.43 mmol) and $Pd(PPh_3)_4$ (0.009 g, 2.0 mol %). After refluxing for 12 h the title compound was purified by flash column chromatography *(n*-hexane: EtOAc 4:1). Yield = 0.110 g (76%), mp = 163-164 °C; ^{1}H NMR (700 MHz, Benzene-d_6): δ = 8.01 (m, 2H, ArH), 7.63 (d, *J* = 8.1 Hz, 2H, ArH), 7.18 (d, *J* = 8.1 Hz, 2H, ArH), 7.06 (m, 1H, ArH), 6.79 (d, *J* = 8.1 Hz, 2H, ArH), 4.37 (dd, *J* = 2.6,1.5 Hz, 1H, Cp), 4.12 (dd, *J* = 2.7, 1.5 Hz, 1H, Cp), 4.01 (s, 5H, Cp), 3.96 (t, *J* = 2.6 Hz, 1H, Cp),1.91 (s, 3H, CH_3) ppm; ^{13}C NMR (176 MHz, Benzene-d_6) d = 142.6, 140.9, 137.3, 131.0, 129.8, 128.9, 127.9, 126.3, 94.6 (Cp), 90.0 (Cp), 72.6 (Cp), 72.1 (Cp), 71.7 (Cp), 69.6 (Cp), 21.6 (CH_3) ppm; HR-MS (ESI): calcd. for $C_{23}H_{20}FeOS$ ($[M+H]^+$): 401.0657, found: 401.0672.

5.4.2.7 (S_p,*S*)-1-(Phenyl)-2-(*p*-tolylsulfinyl)ferrocene 4b

The quantities involved are as follows: Compound **3** (0.220 g, 0.4 mmol), iodobenzene (0.200 g, 1.0 mmol), sodium iodide (0.240 g, 1.6 mmol) and $Pd(PPh_3)_4$ (0.090 g, 2.0 mol %). After refluxing for 12 h the title compound was purified by flash column chromatography (*n*-hexane: EtOAc 4:1). Yield = 0.110 g (69%, de 91%), $[\alpha]^{22}_{D}$ = -48 (c = 0.05, $CHCl_3$), mp = 159-160 °C. The diastereomeric excess was determined by Daicel chiralpak OD-H (4.6mm Φ X 250 mmL), *n*-hexane / IPA = 4/1, 1 mL/min, λ = 254 nm, t (minor) = 10.69 min, t (major) = 17.76 min.

5.4.2.8 1-(4-Florophenyl)-2-(*p*-tolylsulfinyl)ferrocene ±4c

The quantities involved are as follows. Compound **(±)3** (0.280 g, 0.5 mmol), 1-fluoro-4-iodobenzene (0.280 g, 1.25 mmol), sodium iodide (0.300 g, 2.0 mmol) and $Pd(PPh_3)_4$ (0.012 g, 2.0 mol %). After refluxing for 4 h the title compound was purified by flash column chromatography (*n*-hexane: EtOAc 4:1). Yield = 0.160 g (76%); mp = 148-149 °C; ^{1}H NMR (700 MHz, Benzene-d_6); δ = 7.80 (d, *J* = 8.4 Hz, 2H, ArH), 7.54 (d, *J* = 7.7 Hz, 2H, ArH), 6.80 (d, *J* = 8.4 Hz, 2H, ArH), 6.76 (d, *J* = 7.7 Hz, 2H, ArH), 4.24 (s, 1H, Cp), 4.15 (s, 1H, Cp), 4.03 (s, 5H, Cp), 3.94 (s, 1H, Cp), 1.88 (s, 3H, CH_3) ppm; ^{13}C NMR (176 MHz, Benzene-d_6): δ = 163.7 (d, *J* = 246 Hz), 142.5, 140.9, 133.2 (d, *J* = 3 Hz), 132.7 (d, *J* = 8 Hz), 129.8, 126.3, 126.0, 115.5 (d, *J* = 21 Hz), 94.6 (Cp), 88.8 (Cp), 72.4 (Cp), 72.1 (Cp), 72.1 (Cp), 69.5 (Cp), 21.6 (CH_3) ppm; HR-MS (ESI): calcd. for $C_{23}H_{19}FFeOS$ ($[M+H]^+$): 419.6452, found: 419.6469.

5.4.2.9 (S_p,*S*)-1-(4-Fluorophenyl)-2-(*p*-tolylsulfinyl)ferrocene 4c

The quantities involved are as follows: Compound **3** (0.280 g, 0.5 mmol), 1-iodo-4-fluorobenzene (0. 310 g, 1.25 mmol), sodium iodide (0.300 g, 2.0 mmol) and $Pd(PPh_3)_4$ (0.012 g, 2.0 mol %). After refluxing for 4 h the title compound was purified by flash column chromatography (*n*-hexane: EtOAc 4:1). Yield = 0.160 g (76%, de >99%), $[\alpha]^{22}_D$ = +22 (c = 0.05, $CHCl_3$), mp = 186-187 °C. The diastereomeric excess was determined by Daicel chiralpak OD-H (4.6mm Φ X 250 mmL), *n*-hexane / IPA = 4/1, 1 mL/min, λ = 254 nm, t (minor) = 10.15 min, t (major) = 13.83 min.

5.4.2.10 1-(4-bromophenyl)-2-(*p*-tolylsulfinyl)ferrocene ±4d

The quantities involved are as follows. Compound **(±)3** (0.400 g, 0.72 mmol), 1-bromo-4-iodobenzene (0.484 g, 1.78 mmol), sodium iodide (0.430 g, 2.86 mmol) and

$Pd(PPh_3)_4$ (0.017 g, 2.0 mol %). After refluxing for 4 h the title compound was purified by flash column chromatography (*n*-hexane: EtOAc 4:1). Yield = 0.291 g (85%); mp = 155-156 °C; ^{1}H NMR (700 MHz, Benzene-d_6): δ= 7.69 (d, *J* = 8.0 Hz, 2H, ArH), 7.53 (d, *J* = 7.8 Hz, 2H, ArH), 7.25 (d, *J* = 8.0 Hz, 2H, ArH), 6.75 (d, *J* = 7.8 Hz, 2H, ArH), 4.21 (s, 1H, Cp), 4.16 (s, 1H, Cp), 4.01 (s, 5H, Cp), 3.93 (s, 1H, Cp), 1.87 (s, 3H, CH_3) ppm; ^{13}C NMR (176 MHz, Benzene-d_6): δ = 141.6, 140.2, 135.7, 131.7, 131.0, 129.0, 125.2, 121.0, 94.0 (Cp), 87.3 (Cp), 71.6 (Cp), 71.4 (Cp), 71.3 (Cp), 68.9 (Cp), 20.7 (CH_3) ppm; HR-MS (ESI): calcd. for $C_{23}H_{19}BrFeOS$ ($[M+H]^+$): 478.9764, found: 478.9791.

5.4.2.11 (S_p,*S*)-1-(4-bromophenyl)-2-(*p*-tolylsulfinyl)ferrocene 4d

The quantities involved are as follows: Compound **3** (0.560 g, 1.0 mmol), of 1-bromo-4-iodobenzene (0.71 g, 2.5 mmol), sodium iodide (0.600 g, 4.0 mmol) and $Pd(PPh_3)_4$ (0.025 g, 2.0 mol %). After refluxing for 4 hours the title compound was purified by flash column chromatography (*n*-hexane: EtOAc 4:1). Yield = 0.420 g (88%, de 95%), $[\alpha]^{22}_D$ = +98 (c = 0.05, $CHCl_3$), mp = 183-184 °C. The diastereomeric excess was determined by Daicel chiralpak OD-H (4.6mm Φ X 250 mmL), *n*-hexane / IPA = 7.5/2.5, 1 mL/min, λ = 254 nm, t (minor) = 8.18 min, t (major) = 10.49 min.

5.4.2.12 1-(4-Trifluoromethylphenyl)-2-(*p*-tolylsulfinyl)ferrocene ±4e

The quantities involved are as follows. Compound **(±)3** (0.200 g,0.36 mmol), 4-iodobenzotrifluoride (0.240 g, 0.89 mmol), sodiumiodide (0.214 g, 1.43 mmol) and $Pd(PPh_3)_4$ (0.012 g, 2.0 mol %). After refluxing for 4 h the title compound was purified by flash column chromatography (*n*-hexane: EtOAc 4:1). Yield = 0.143 g (86%); mp = 135-136 °C; ^{1}H NMR (700 MHz, Benzene-d_6): δ = 7.86 (d,*J* = 8.1 Hz, 2H), 7.50 (d, *J* = 8.0 Hz, 2H), 7.32 (d, *J* = 8.1 Hz, 2H), 6.73(d, *J* = 8.0 Hz, 2H), 4.23 (dd, *J* = 2.6, 1.5 Hz, 1H, Cp), 4.21 (dd, *J* = 2.6,1.5 Hz, 1H, Cp), 4.02 (s, 5H, Cp), 3.96

(t, *J* = 2.6 Hz, 1H, Cp), 1.85 (s, 3H,CH_3) ppm; ^{13}C NMR (176 MHz, Benzene-d_6): δ = 142.4, 141.8, 141.0, 131.1,129.8, 129.6, 129.4, 126.4, 125.9, 125.6 (q, *J* = 3 Hz), 124.9, 95.3 (Cp),87.4 (Cp), 73.0 (Cp), 72.5 (Cp), 72.3 (Cp), 70.0 (Cp), 21.5 (CH_3) ppm. HRMS (ESI): calcd. for $C_{24}H_{19}F_3FeOS$ ($[M+H]^+$): 469.0531, found: 469.0521.

5.4.2.13 Synthesis of 1-(4-trifluoromethylphenyl)-2-(*p*-tolylsulfinyl) ferrocene ±4e from 4-bromobenzotrifluoride

The quantities involved are as follows. Compound **(±)3** (0.150 g, 0.27 mmol), 4-bromobenzotrifluoride (0.151 g, 0.67 mmol), sodium iodide(0.161 g, 1.07 mmol) and $Pd(PPh_3)_4$ (0.006 g, 2.0 mol %). After refluxing for 4 h the title compound was purified by flash column chromatography (*n*-hexane: EtOAc 4:1). Yield = 0.036 g (28%).

5.4.2.14 (S_p,*S*)-1-(4-Trifluoromethylphenyl)-2-(*p*-tolylsulfinyl)ferrocene 4e

The quantities involved are as follows: Compound **3** (0.280 g,0.5 mmol), 4-iodobenzotrifluoride (0.340 g, 1.25 mmol), sodiumiodide (0.300 g, 2.0 mmol) and $Pd(PPh_3)_4$ (0.012 g, 2.0 mol %). After refluxing for 4 hours the title compound was purified by flash column chromatography (*n*-hexane: EtOAc 4:1). Yield = 0.200 g (86%, de>99%), $[\alpha]^{22}_D$ = +100 (c = 0.05, $CHCl_3$), mp = 164-165 °C.The diastereomeric excess was determined by Daicel chiralpak OD-H(4.6mm Φ X 250 mmL), *n*-hexane / IPA = 9/1, 1 mL/min, λ = 254nm, t (minor) = 17.92 min, t (major) = 19.23 min.

5.4.2.15 1-(3-Trifluoromethylphenyl)-2-(*p*-tolylsulfinyl)ferrocene ±4f

The quantities involved are as follows. Compound **(±)3** (0.200 g, 0.36 mmol), 3-iodobenzotrifluoride (0.240 g, 0.89 mmol), sodium iodide (0.240 g, 1.4 mmol) and $Pd(PPh_3)_4$ (0.012 g, 2.0 mol %). After refluxing for 12 h the title compound was purified by flash column chromatography (*n*-hexane: EtOAc 4:1). Yield = 0.125 g

(75%); mp = 138-140 °C; ^{1}H NMR (700 MHz, Benzene-d_6): δ = 8.16 (s, 1H, ArH), 8.12 (d, *J* = 7.8 Hz, 1H, ArH), 7.47 (d, *J* = 7.2 Hz, 2H, ArH), 7.20 (d, *J* = 7.8 Hz, 1H, ArH), 6.95 (t, *J* = 7.8 Hz, 1H, ArH), 6.73 (d, *J* = 7.2 Hz, 2H, ArH), 4.26 (dd, *J* = 2.8,1.6 Hz, 1H, Cp), 4.19 (dd, *J* = 2.8, 1.6 Hz, 1H, Cp), 4.05 (s, 5H, Cp), 3.95 (t, *J* = 2.8, 1H, Cp), 1.86 (s, 3H, CH_3) ppm; ^{13}C NMR (176 MHz, Benzene-d_6): δ = 142.0, 140.4, 138.3, 134.0, 130.7,130.6, 130.4, 129.4, 127.5, 127.1 (q, *J* = 4 Hz), 126.0, 125.3, 123.9 (q, *J* = 3 Hz), 94.4 (Cp), 86.7 (Cp), 72.3 (Cp), 71.4 (Cp), 71.4 (Cp), 69.0 (Cp), 20.6 (CH_3) ppm; HR-MS (ESI): calcd. for $C_{24}H_{19}F_3FeOS$ ($[M+H]^+$): 469.0531, found: 469.0599.

5.4.2.16 (*S*$_p$,*S*)-1-(3-Trifluoromethylphenyl)-2-(*p*-tolylsulfinyl)ferrocene 4f

The quantities involved are as follows: Compound **3** (0.280 g,0.5 mmol), 3-iodobenzotrifluoride (0.340 g, 1.25 mmol), sodiumiodide (0.300 g, 1.4 mmol) and $Pd(PPh_3)_4$ (0.012 g, 2.0 mol %). After refluxing for 12 hours the title compound was purified by flash column chromatography (*n*-hexane: EtOAc 4:1). Yield = 0.150 g (64%,de = 82%), $[\alpha]^{22}_D$ = +96 (c = 0.05, $CHCl_3$), mp = 138-140 °C. The diastereomeric excess was determined by Daicel chiralpakOD-H (4.6mm Φ X 250 mmL), *n*-hexane / IPA = 8/2, 1mL/min, λ = 254 nm, t (minor) = 8.16 min, t (major) = 9.45 min.

5.4.2.17 1-(2-Trifluoromethylphenyl)-2-(*p*-tolylsulfinyl)ferrocene ±4g

The quantities involved are as follows. Compound **(±)3** (0.200 g,0.36 mmol), 2-iodobenzotrifluoride (0.240 g, 0.89 mmol), sodiumiodide (0.214 g, 1.4 mmol) and $Pd(PPh_3)_4$ (0.012 g, 2.0 mol %). After refluxing for 12 h the title compound was purified by flash column chromatography (*n*-hexane: EtOAc 4:1). Yield = 0.040 g (27%), mp = 135-136 °C; ^{1}H NMR (700 MHz, Benzene-d_6): δ = 8.70 (d, *J* = 7.8 Hz, 1H, ArH), 7.24 (t, *J* = 7.7 Hz, 1H, ArH), 7.20 (d, *J* = 7.9 Hz, 1H, ArH), 7.10 (d, *J* =

7.9 Hz, 2H, ArH), 6.88 (t, *J* = 7.7 Hz, 1H, ArH), 6.66 (d, *J* = 7.9 Hz, 2H, ArH), 4.46 (dd, *J* = 2.6 Hz, 1H, Cp), 4.37 (dd, *J* = 2.6 Hz, 1.5 Hz, 1H, Cp), 4.26 (s, 5H, Cp), 3.96 (t, *J* = 2.6 Hz, 1H, Cp), 1.89 (s, 3H, CH_3) ppm; ^{13}C NMR (176 MHz, Benzene-d_6): δ = 141.7, 139.7,138.3, 134.1, 130.6, 130.1, 128.9, 127.7, 125.0 (q, *J* = 6 Hz), 124.3, 123.9, 96.8 (Cp), 87.9 (Cp), 73.1 (Cp), 71.8 (Cp), 71.6 (Cp), 68.3 (Cp), 21.0 (CH_3) ppm; HR-MS (ESI): calcd. for $C_{24}H_{19}F_3FeOS$ ($[M+H]^+$): 469.0531, found: 469.0477.

5.4.2.18 (*S*$_p$,*S*)-1-(2-Trifluoromethylphenyl)-2-(*p*-tolylsulfinyl)ferrocene 4g

The quantities involved are as follows: Compound **3** (0.220 g, 0.4 mmol), 2-iodobenzotrifluoride (0.270 g, 1.0 mmol), sodium iodide (0.240 g, 1.6 mmol) and $Pd(PPh_3)_4$ (0.010 g, 2.0 mol %). After refluxing for 12 hours the title compound was purified by flash column chromatography (*n*-hexane: EtOAc 4:1). Yield = 0.050 g (27%, de 96%), $[\alpha]^{22}_D$ = +192 (c = 0.05, $CHCl_3$), mp = 103-104 °C. The diastereomeric excess was determined by Daicel chiralpakOD-H (4.6mm Φ X 250 mmL), *n*-hexane / IPA = 8/2, 1 mL/min, λ = 254 nm, t (minor) = 6.12 min, t (major) = 7.82 min.

5.4.2.19 1-(4-Nitrophenyl)-2-(*p*-tolylsulfinyl)ferrocene ±4h

The quantities involved are as follows. Compound **(±)3** (0.280 g, 0.5 mmol), 1-iodo-4-nitrobenzene (0.310 g, 1.25 mmol), sodium iodide (0.300 g, 2.0 mmol) and $Pd(PPh_3)_4$ (0.012 g, 2.0 mol %). After refluxing for 4 h the title compound was purified by flash column chromatography (*n*-hexane: EtOAc 3:1). Yield = 0.170 g (76%); mp = 205-206 °C; ^{1}H NMR (700 MHz, Benzene-d_6): δ = 7.84 (d, *J* = 8.7 Hz, 2H, ArH), 7.74 (d, *J* = 8.7 Hz, 2H, ArH), 7.46 (d, *J* = 7.9 Hz, 2H, ArH), 6.72 (d, *J* = 7.9 Hz, 2H, ArH), 4.26 (s, 1H, Cp), 4.18 (s, 1H, Cp), 4.02 (s, 5H, Cp), 3.97 (s, 1H, Cp), 1.83 (s, 3H, CH_3). ^{13}C NMR (176 MHz, Benzene-d_6): δ = 146.5, 144.2, 141.4, 140.3, 130.1, 129.1, 127.9, 124.9, 122.9, 95.0 (Cp), 85.0 (Cp), 73.2 (Cp), 71.7 (Cp),

71.5 (Cp), 69.5 (Cp), 20.6 (CH_3) ppm; HR-MS (ESI): calcd. for $C_{23}H_{19}FeNO_3S$ ($[M+H]^+$): 446.0508, found: 446.0518.

5.4.2.20 (S_p,*S*)-1-(4-Nitrophenyl)-2-(*p*-tolylsulfinyl)ferrocene 4h

The quantities involved are as follows: Compound **3** (0.280 g, 0.5 mmol), 1-iodo-4-nitrobenzene (0.310 g, 1.25 mmol), sodium iodide (0.300 g, 2.0 mmol) and $Pd(PPh_3)_4$ (0.012 g, 2.0 mol %). After refluxing for 4 hours the title compound was purified by flash column chromatography (*n*-hexane: EtOAc 3:1). Yield = 0.170 g (76%, de 96%), $[\alpha]^{22}_D$ = +294 (c = 0.05, $CHCl_3$), mp = 154-155 °C. The diastereomeric excess was determined by Daicel chiralpak OD-H (4.6mm Φ X 250 mmL), *n*-hexane / IPA = 7/3, 1 mL/min, λ = 254 nm, t (minor) = 15.42 min, t (major) = 23.13 min.

5.4.2.21 General synthetic procedure for Control Experiment (Synthesis of compound 6)

In a Schlenk tube, 0.28 g (0.5 mmol) of compound **3** and 0.30 g (2.0 mmol) of NaI were placed. Subsequently, 3 mL of dry THF and 2 ml of dry acetone were added and the reaction mixture was refluxed for 12 h. The reaction mixture was filtered through a pad of silica, washed with 2x20 mL of THF and the resultant filtrate was concentrated. The crude product was purified by flash column chromatography using a *n*-hexane and ethyl acetate as an eluent to afford the desired product in 85% yield (0.23 g); mp.= > 230 °C (decomposes); ^{1}H NMR (400 MHz, C_6D_6): δ = 7.58 (d, *J* = 8Hz, 2H, ArH), 6.84 (d, *J* = 8Hz,2H, ArH), 4.77 (s, 5H), 4.60 (s, 1H), 4.39 (s, 1H), 4.29 (s, 1H), 4.05 (ferrocene), 1.90 (s, 3H, CH_3) ppm; ^{13}C NMR (100 MHz, C_6D_6): δ = 146.21, 140.15, 129.77, 124.21, 102.71, 95.42, 77.50, 72.68, 70.62, 69.79, 21.06 (CH_3) ppm; HR-MS (ESI): calcd. for $C_{34}H_{30}Fe_2HgO_2S_2$ ($[M+H]^+$): 849.0169, found: 849.0157.

5.5 References

(1) Stepnicka, P. *Ferrocenes: Ligands, materials and biomolecules*; Wiley-Blackwell, **2008**.

(2) Togni, A.; Hayashi, T. *Ferrocenes: Homogeneous catalysis, organic synthesis, materials science*; VCH, **1994**.

(3) Chivers, T.; Manners, I. *Inorganic Rings and Polymers of the P-Block Elements: From Fundamentals to Applications*; RSC, **2009**.

(4) Heilmann, J. B.; Scheibitz, M.; Qin, Y.; Sundararaman, A.; Jakle, F.; Kretz, T.; Bolte, M.; Lerner, H.-W.; Holthausen, M. C.; Wagner, M. *Angew. Chem., Int. Ed.* **2006**, *45*, 920.

(5) Manners, I. *Adv. Organomet Chem.* **1995**, *37*, 131.

(6) Bhattacharjee, H.; Muller, J. *Coord. Chem. Rev.* **2016**, *314*, 114.

(7) Marquarding, D.; Klusacek, H.; Gokel, G.; Hoffmann, P.; Ugi, I. *J. Am. Chem., Soc.* **1970**, *92*, 5389.

(8) Nishibayashi, Y.; Uemura, S. *Synlett.* **1995**, *1995*, 79.

(9) Richards, C. J.; Damalidis, T.; Hibbs, D. E.; Hursthouse, M. B. *Synlett.* **1995**, *1995*, 74.

(10) Enders, D.; Peters, R.; Lochtman, R.; Raabe, G. *Angew. Chem., Int. Ed.* **1999**, *38*, 2421.

(11) Enders, D.; Peters, R.; Lochtman, R.; Runsink, J. *Eur. J. Org. Chem.* **2000**, *2000*, 2839.

(12) Ferber, B.; Kagan, H. B. *Adv. Synth. Catal.* **2007**, *349*, 493.

(13) Bolm, C.; Kesselgruber, M.; Muniz, K.; Raabe, G. *Organometallics.* **2000**, *19*, 1648.

(14) Ganter, C.; Wagner, T. *Chem. Ber.* **1995**, *128*, 1157.

(15) Rebiere, F.; Riant, O.; Ricard, L.; Kagan, H. B. *Angew. Chem., Int. Ed.* **1993**, *32*, 568.

(16) Riant, O.; Samuel, O.; Flessner, T.; Taudien, S.; Kagan, H. B.*J. Org. Chem.* **1997**, *62*, 6733.

(17) Riant, O.; Argouarch, G.; Guillaneux, D.; Samuel, O.; Kagan, H. B. *J. Org. Chem.* **1998**, *63*, 3511.

(18) Kloetzing, R. J.; Knochel, P. *Tetrahedron: Asymmetry.* **2006**, *17*, 116.

(19) Venkatasubbaiah, K.; Bats, J. W.; Rheingold, A. L.; Jakle, F. *Organometallics.* **2005**, *24*, 6043.

(20) Butler, I. R.; Drew, M. G. B. *Inorg. Chem. Commun.* **1999**, *2*, 234.

(21) Gomez Arrayas, R.; Adrio, J.; Carretero, J. C. *Angew. Chem., Int. Ed.* **2006**, *45*, 7674.

(22) Lotz, M.; Kramer, G.; Knochel, P. *Chem. Commun.* **2002**, 2546.

(23) Venkatasubbaiah, K.; DiPasquale, A. G.; Bolte, M.; Rheingold, A. L.; Jakle, F. *Angew. Chem., Int. Ed.* **2006**, *45*, 6838.

(24) Chen, J.; Venkatasubbaiah, K.; Pakkirisamy, T.; Doshi, A.; Yusupov, A.; Patel, Y.; Lalancette, R. A.; Jakle, F. *Chem. Eur. J.* **2010**, *16*, 8861.

(25) Guillaneux, D.; Kagan, Henri, B. *J. Org. Chem.* **1994**, *60*, 2502.

(26) Wu, Y.; Huo, S.; Gong, J.; Cui, X.; Ding, L.; Ding, K.; Du, C.; Liu, Y.; Song, M. *J. Organomet. Chem.* **2001**, *637-639*, 27.

(27) Beletskaya, I. P.; Tsvetkov, A. V.; Latyshev, G. V.; Tafeenko, V. A.; Lukashev, N. V. *J. Organomet. Chem.* **2001**, *637-639*, 653.

(28) Canty, A. J.; Deacon, G. B. *Inorg. Chim. Acta.* **1980**, *45*, L225.

(29) Nyburg, S. C.; Faerman, C. H. *Acta Cryst. B.* **1985**, *41*, 274.

(30) Schmidbaur, H.; Oller, H.-J.; Wilkinson, D. L.; Huber, B.; Muller, G. *Chem. Ber*. **1989**, *122*, 31.

(31) Tschinkl, M.; Schier, A.; Riede, J.; Gabbai, F. P. *Angew. Chem., Int. Ed.* **1999**, *38*, 3547.

(32) Beauchamp, A. L.; Olivier, M. J.; Wuest, J. D.; Zacharie, B. *Organometallics.* **1987**, *6*, 153.

(33) Rausch, M. D. *J. Org. Chem.* **1963**, *28*, 3337.

Conclusion

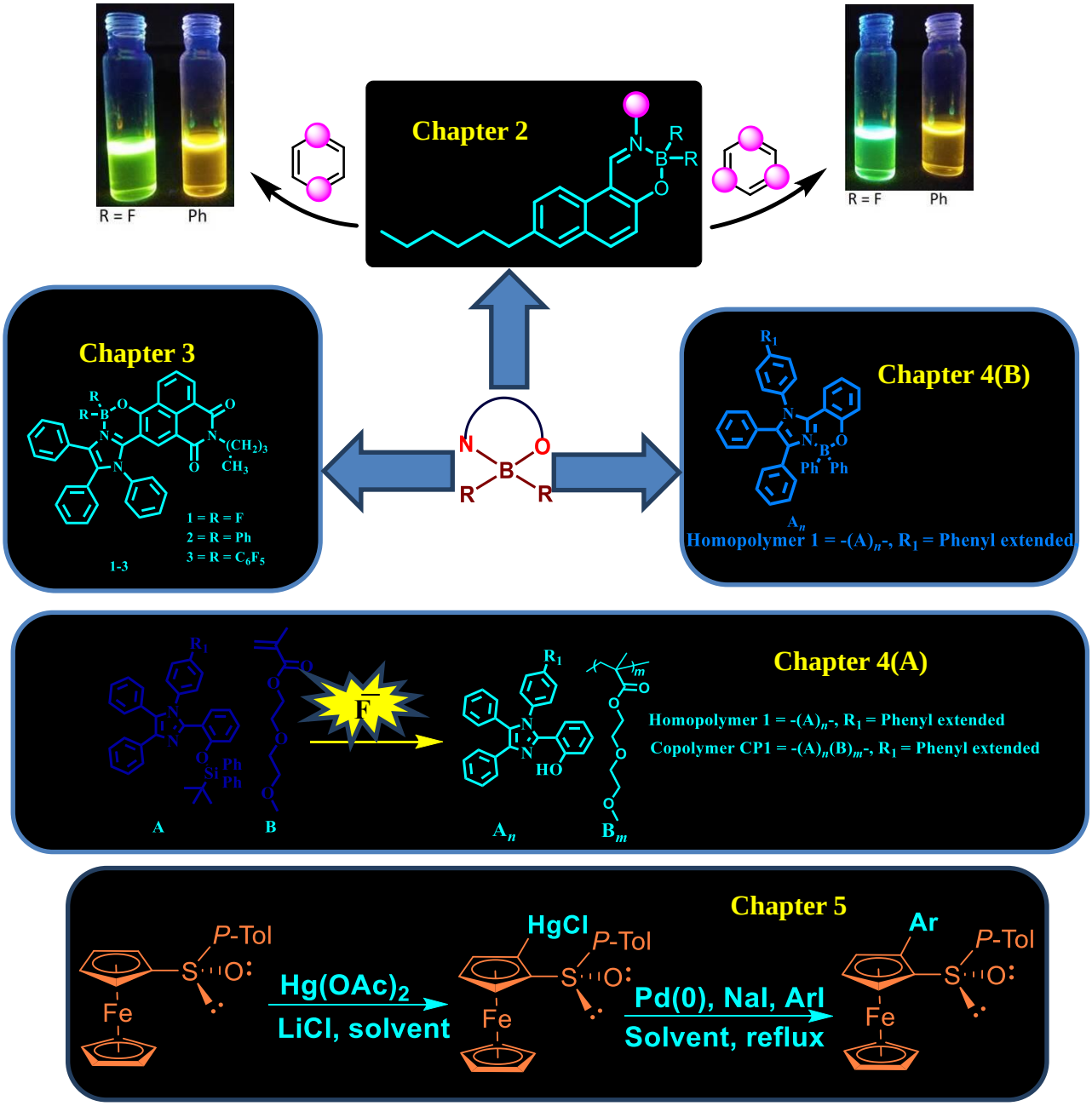
R = F
Ph
Chapter 2
R = F
Ph
Chapter 3
1 = R = F
2 = R = Ph
3 = R = C6F5
1-3
Chapter 4(B)
Homopolymer 1 = -(A)n-, R1 = Phenyl extended
Chapter 4(A)
Homopolymer 1 = -(A)n-, R1 = Phenyl extended
Copolymer CP1 = -(A)n(B)m-, R1 = Phenyl extended
A
B
Chapter 5
P-Tol
Hg(OAc)2
LiCl, solvent
HgCl
Pd(0), NaI, ArI
Solvent, reflux
Ar
Fe

List of Abbreviations

^{1}H NMR	Proton nuclear magnetic resonance
^{13}C NMR	Carbon-13 nuclear magnetic resonance
^{11}B NMR	Boron-11 nuclear magnetic resonance
^{19}F NMR	Fluorine-19 nuclear magnetic resonance
^{29}Si NMR	Silicon-29 nuclear magnetic resonance
FT-IR	Fourier-transform infrared spectroscopy
UV-Vis	Ultraviolet–Visible
ESI	Electrospray ionization
DFT	Density functional theory
TGA	Thermogravimetric analysis
DSC	Differential scanning calorimetry
HRMS	High-resolution mass spectrometry
ICT	Intramolecular charge transfer
GPC	Gel permeation chromatography
HPLC	High Performance Liquid Chromatography
XRD	X-ray diffraction
GOF	Goodness of fit
PDI	Polydispersity index
OLEDs	Organic light emitting diodes
HOMO	Highest occupied molecular orbital
LUMO	Lowest unoccupied molecular orbital
eV	Electronvolt
EL	Electroluminescence
ACQ	Aggregation caused quenching
ESIPT	Excited state intramolecular proton transfer
BODIPY	Boron dipyrromethene
M_n	Number average molecular weight
M_w	Weight average molecular weight
T_g	Glass Transition Temperature
ppm	Parts per million
CH_2Cl_2	Dichloromethane

$CHCl_3$	Chloroform
DCE	1,2-Dichloroethane
DME	1,2-Dimethoxyethane
CH_3CN	Acetonitrile
EtOH	Ethanol
DMSO	Dimethyl sulfoxide
THF	Tetrahydrofuran
DMF	Dimethylformamide
$CDCl_3$	Deuterated chloroform
C_6D_6	Deuterated benzene
NH_4OAc	Ammonium acetate
AcOH	Acetic acid
Na_2CO_3	Sodium carbonate
K_2CO_3	Potassium carbonate
Na_2SO_4	Sodium sulfate
CaH_2	Calcium hydride
KBr	Potassium bromide
$AlCl_3$	Aluminium chloride
Bu_4NPF_6	Tetrabutylammonium hexafluorophosphate
CuO	Copper(II) Oxide
n-BuLi	*n*-Butyllithium
i-Pr_2NEt	N,N-Diisopropylethylamine
H_3PO_4	Phosphoric acid
AIBN	Azobisisobutyronitrile
NaH	Sodium hydride
NaI	Sodium Iodide
$Pd(PPh_3)_4$	Tetrakis(triphenylphosphine)palladium(0)
$PdCl_2$(dppf)	1,1'-Bis(diphenylphosphino)ferrocene-palladium(II)dichloride
$Pd(dba)_2$	Bis(dibenzylideneacetone)palladium(0)
$ZnCl_2$	Zink(II) Chloride
Mes	Mesityl
PMMA	Poly(methyl methacrylate)